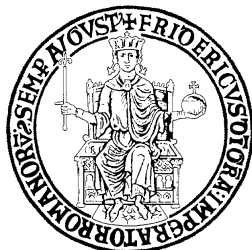


UNIVERSITA' DEGLI STUDI DI NAPOLI 'FEDERICO II'

FACOLTA' DI MEDICINA & CHIRURGIA



DOTTORATO DI RICERCA

IN FISIOPATOLOGIA CLINICA E MEDICINA SPERIMENTALE

PhD Program

XXV CICLO

INDIRIZZO: SCIENZE CARDIOVASCOLARI

INVECCHIAMENTO E DISFUNZIONE BETA CELLULARE:

IL RUOLO FISIOPATOLOGICO

DEL RECETTORE BETA 2 ADRENERGICO

Relatore

Ch.mo Prof. Bruno Trimarco, MD

Candidato

Dr. Gaetano Santulli, MD

ANNO ACCADEMICO 2011-2012

Indice

Abstract	3
Introduzione	4
Materiali e Metodi	5
▪ Studi <i>in vivo</i>	
✓ Animali	5
✓ Test di tolleranza al glucosio (GTT) e valutazione della secrezione di insulina	5
✓ Determinazione della sensibilità insulinica (clamp)	5
▪ Studi <i>ex vivo</i>	
✓ Analisi istologica	7
✓ Isolamento di insulae pancreatiche e valutazione della secrezione di insulina	7
✓ Reinstallazione di β_2AR <i>in vivo</i> ed <i>ex vivo</i> (gene delivery)	7
▪ Studi <i>in vitro</i>	
✓ Short hairpin RNA (shRNA): progettazione, produzione e trasfezione	9
✓ Radioligand binding assay	9
✓ Quantitative real-time RT-PCR e immunoblotting	9
✓ Analisi statistica	10
Risultati	10
▪ Fenotipo metabolico di animali privi del $\beta_2AR^{-/-}$	11
▪ Profilo di espressione genica nelle β -cellule con delezione del $\beta_2AR^{-/-}$	15
▪ L'overespressione del β_2AR ripristina l'alterato rilascio di insulina età-dipendente	19
Discussione	24
Conclusioni	25
Bibliografia	26
Pubblicazioni del candidato (2010-2012) e allegati selezionati	32

Abstract

L'invecchiamento è associato ad una progressiva diminuzione della capacità delle β -cellule del pancreas a secernere insulina. Con l'invecchiamento, inoltre, la densità dei recettori adrenergici β (β ARs), in particolare il β_2 AR, diminuisce. Per valutare il ruolo dei β_2 AR nel rilascio di insulina e nell'omeostasi del glucosio sono stati condotti degli esperimenti *in vivo*, in topi con delezione del β_2 AR (β_2 AR^{-/-}) a diverse età, *ex vivo*, in insulae isolate e *in vitro*, in β -cellule di insulinoma di ratto silenziate (shRNA) per il β_2 AR.

Si è dimostrato per la prima volta che la densità del β_2 AR a livello del pancreas diminuisce nel tempo negli animali wild-type (β_2 AR^{+/+}). Inoltre, gli animali β_2 AR^{-/-} a 6 mesi di età evidenziano una ridotta produzione di insulina ed un'intolleranza al glucosio. Tali caratteristiche sono evidenziabili anche in β_2 AR^{+/+} anziani (20 mesi). Questi risultati sono stati confermati anche *ex vivo* ed *in vitro*. È interessante notare inoltre, che l'infezione adenovirale di β_2 AR in animali knock-out per il β_2 AR è in grado di ripristinare il normale rilascio di insulina. È evidente, quindi, che i risultati ottenuti indicano che il β_2 AR gioca un ruolo fondamentale nel rilascio di insulina. I topi β_2 AR^{-/-}, riproducendo le caratteristiche metaboliche degli animali β_2 AR^{+/+} anziani, rappresentano un modello di invecchiamento utile per lo studio del diabete mellito.

Introduzione

La compromissione del metabolismo del glucosio e l'invecchiamento rappresentano fattori determinanti per lo sviluppo del diabete mellito. Sebbene i processi fisiopatologici alla base di questo fenomeno non siano ancora completamente noti, si ipotizza che alla base vi sia una concomitanza di cause piuttosto che un unico meccanismo coinvolto (1; 2). L'invecchiamento è già di per sé associato ad una diminuzione del rilascio di insulina (3; 4). Infatti, l'incidenza dell'età sul rilascio dell'insulina è tale da aumentare la probabilità di intolleranza al glucosio ed infine di diabete (2; 5). Questo fenomeno è comune a diverse specie, in quanto è stato osservato sia nel ratto (6; 7) che negli esseri umani (5; 8; 9). Nonostante ciò, il motivo di una ridotta secrezione insulinica da parte delle cellule β -pancreatiche, legata all'avanzare dell'età, non è ancora noto.

Le catecolamine rappresentano un fine regolatore dell'attività del pancreas endocrino, mediante i recettori α e β adrenergici (ARs) (10; 11). Per di più, la stretta connessione tra il sistema adrenergico e l'insulina è testimoniata da numerosi studi che mostrano la regolazione reciproca di questi due sistemi (12-14). Questa ipotesi è supportata da recenti lavori che mostrano che i topi con delezione dei tre geni conosciuti per i β ARs, vale a dire β_1 , β_2 e β_3 AR, presentano un fenotipo caratterizzato da ridotta tolleranza al glucosio (15). Studi con agonisti del β_2 AR suggeriscono, inoltre, che esso possa svolgere un ruolo importante nella regolazione della secrezione insulinica (16). Diversi polimorfismi del gene umano β_2 AR sono stati associati ad alti livelli di insulina a digiuno (17). Tuttavia, l'impatto del sottotipo β_2 AR sulla tolleranza al glucosio e la secrezione insulinica non è del tutto chiaro.

È interessante notare che anche il signaling AR è influenzato negativamente dall'invecchiamento (18-21), ma i precisi meccanismi coinvolti sono tuttora sconosciuti. In particolar modo il signaling β AR appare alterato con l'avanzare dell'età, con dei cambiamenti nell'espressione dei componenti molecolari coinvolti nel signaling (22-25). Si è quindi ipotizzato che le alterazioni dovute all'invecchiamento abbiano un ruolo negativo sul β AR ed il rilascio dell'insulina. Per verificare tale ipotesi si è analizzata la secrezione insulinica in animali β_2 AR knock-out e si è indagato il ruolo dell'invecchiamento sulla tolleranza al glucosio.

Materiali e metodi

Studi *in vivo*

Animali

Sono stati studiati topi maschi C57BL/6J con delezione omozigote del gene β_2AR ($\beta_2AR^{-/-}$). I founders di tali animali sono stati gentilmente forniti da Brian Kent Kobilka, Stanford University, Stanford, CA, USA (26). I wild-type ($\beta_2AR^{+/+}$) sono stati utilizzati come controlli. Gli animali sono stati collocati in una stanza ad una temperatura di 22°C con un ciclo luce/buio 12/12h in conformità con la Guida per la Cura di animali da laboratorio pubblicato dal National Institute of Health negli Stati Uniti (NIH Publication N. 85 - 23, riveduta nel 1996) e approvato dal Comitato Etico dell'Università "Federico II" di Napoli. I pancreas sono stati asportati rapidamente dopo eutanasia degli animali. I campioni sono stati processati, fissati per immersione in paraformaldeide al 4% per l'istologia, omogeneizzati per la determinazione del contenuto totale di insulina e glucagone o congelati in azoto liquido e conservati a -80°C per successive analisi (10; 27).

Test di tolleranza al glucosio (GTT) e valutazione della secrezione di insulina

Il GTT è stato eseguito come descritto in precedenza (28). I topi sono stati tenuti a digiuno durante la notte e al mattino è stata effettuata un'iniezione intraperitoneale di glucosio (2 g/kg). La glicemia è stata misurata mediante prelievo di sangue dalla coda (Glucose Analyzer II, Beckman Coulter, Brea, CA, USA) ai tempi indicati. La valutazione della secrezione di insulina è stata eseguita come descritto in precedenza (27; 28). L'insulina nel siero è stata valutata su sangue prelevato dalla vena mandibolare mediante test radio-immunologici (RIA, Millipore, Billerica, MA, USA).

Determinazione della sensibilità insulinica (clamp)

Il clamp euglicemico-iperinsulinemico è stato eseguito mediante infusione endovenosa (catetere impiantato in giugulare) di insulina (velocità costante) e di glucosio (velocità variabile) in modo da mantenere costanti (clampare) livelli euglicemici. L'infusione di insulina consente di raggiungere elevate concentrazioni ematiche dell'ormone in grado di sopprimere la produzione epatica di glucosio; in tali condizioni l'unica fonte di glucosio è rappresentata dall'infusione esogena, che viene regolata sulla base di frequenti determinazioni glicemiche, in modo da mantenere costante la glicemia. Le misurazioni dei livelli ematici di glucosio e traccianti sono

state eseguite su sangue arterioso prelevato da una cannula precedentemente impiantata in carotide destra. Gli interventi chirurgici di cateterizzazione di giugulare sinistra e carotide destra, con successiva dorsalizzazione subcutanea delle cannule, sono stati eseguiti almeno cinque giorni prima dell'effettuazione del clamp. Abbiamo quindi misurato i seguenti parametri: produzione epatica di glucosio (PEG), velocità di infusione del glucosio (VIG), indicativa dell'azione dell'insulina sull'intero organismo, velocità di eliminazione del glucosio (VEG), essenzialmente legato all'uptake periferico.

Studi *ex vivo*

Analisi istologica

L'immunoistochimica è stata effettuata su sezioni in paraffina probate con anticorpi specifici per insulina (H38 rabbit) e glucagone (N-17 goat) (entrambi da Santa Cruz Biotechnology, Santa Cruz, CA, USA; diluizione 1:200). L'anti-rabbit (made in goat) legato a perossidasi (Immunotech, Marsiglia, Francia) è stato usato come anticorpo secondario. Dopo l'esposizione all'anticorpo primario, le sezioni sono state incubate con immunoglobuline G anti-rabbit e anti-goat biotinilate e con perossidasi-streptavidina (Dako Corporation; Danimarca). Tutte le reazioni sono state rivelate con diaminobenzidina (29). Le sezioni sono state colorate con ematossilina e montate (30).

Isolamento di insulae pancreatiche e valutazione della secrezione di insulina.

L'isolamento di insulae pancreatiche murine è stato ottenuto mediante digestione con collagenasi P (Roche Applied Sciences, Penzberg, Germania) a 37°C agitando la preparazione per 5-8 minuti (27; 31; 32). Le insulae sono state raccolte e poi coltivate a 37°C con 95% di O₂ e il 5% di CO₂ in mezzo Roswell Park Memorial Institute (RPMI 1640), integrato con 5% di siero fetale bovino, 1 mmol/L di sodio piruvato, 50 µmol/L 2-mercaptoetanololo, 2mMol/L glutammina, 10mmol/L HEPES, 100 U/ml penicillina e 100 µg/ml di streptomina (tutti da Sigma-Aldrich, Milano, Italia), come descritto (28; 32).

Le insulae isolate sono state preincubate a 37°C per 30 minuti in Krebs-Ringer bicarbonato (KRBB: 120mMol/L di NaCl, 4.7 mmol/L di KCl, 1.2 mmol/L MgSO₄, 1.2 mmol/L KH₂PO₄, 2.4 mMol/L CaCl₂, 20 mMol/L NaHCO₃) integrate con 10 mmol/L HEPES e 0,2% di albumina sierica bovina e ossigenate con una miscela di 95% O₂ e 5% CO₂ contenente 2 mmol/L di glucosio. Le insulae sono state incubate per 1 ora a 37°C con 500 µl di KRBB contenente glucosio 2,8 mmol/L o 16,7 mmol o 33mMol/L KCl. Le insulae sono state poi centrifugate (9000g, 2 minuti, 4°C) per valutare la secrezione di insulina (32).

Reinstallazione di β₂AR *in vivo* ed *ex vivo* (gene delivery)

I topi β₂AR^{+/+} di 20 mesi sono stati anestetizzati con isoflurano (4%) e mantenuti in anestesia mediante ventilazione in maschera (isoflurano 1,8%) (29). In seguito a minima laparotomia, si è identificato e immobilizzato il pancreas ed è stata effettuata una iniezione intraduttale di adenovirus (7 × 10¹⁰ pfu) utilizzando un ago 33 Gauge. Sono stati impiegati

adenovirus esprimenti il β_2 AR umano (Ad β_2 AR) o, come controllo, una cassetta di espressione vuota derivata da pcDNA3.2/V5/GW/D-mouse (AdEmpty), per gentile dono di Walter J. Koch, Temple University, Philadelphia, PA, USA (33; 34). Infine, l'incisione addominale è stata chiusa a strati utilizzando fili di sutura di seta 3/0 e gli animali sono stati osservati e monitorati fino al recupero.

Le insulae isolate sono state infettate con Ad β_2 AR o AdEmpty. A seguito di tre ore di incubazione con l'adenovirus (12×10^4 pfu/insula), le insulae pancreatiche sono state poste in mezzo fresco in condizioni normossiche (95% di O₂, 5% CO₂) a 37°C per 24 ore.

Studi *in vitro*

Le cellule INS-1E, derivate e selezionate dalla linea parentale di insulinoma di ratto INS-1, sono state poste in coltura monostrato in RPMI-1640 come sopra descritto per gli esperimenti *ex vivo*. Per i test di secrezione di insulina, le cellule sono state piastrate ad una densità di 5×10^5 cellule/cm² almeno 96 ore prima dell'uso (28). La trasfezione del cDNA codificante per PPAR γ e il plasmide di controllo vuoto sono state eseguite utilizzando Lipofectamine 2000 (Life Technologies, Norwalk, CT, USA), come descritto (33).

Short hairpin RNA (shRNA): progettazione, produzione e trasfezione

Sono stati disegnati degli shRNA specifici per il β_2 AR, poi sintetizzati da Life Technologies (Norwalk, CT, USA). Le cellule INS-1E sono state transfettate con 100 nmol/L sh-RNA β_2 AR o sh-RNA scramble utilizzando Lipofectamine 2000 secondo le istruzioni del produttore (Life Technologies, Norwalk, CT, USA). Dopo 20 minuti di incubazione, la miscela di trasfezione è stata aggiunta alle cellule in 6 piastre contenenti 2 ml di mezzo RPMI-1640 fresco, privo di siero. Le cellule sono state quindi incubate per 5 ore a 37°C, 5% CO₂, ed il mezzo di trasfezione è stato sostituito con il mezzo condizionato. Tutti i test successivi sono stati effettuati almeno 3 giorni dopo la trasfezione del shRNA.

Radioligand binding assay

Su frazioni di membrana di tessuto pancreatico, insulae isolate e cellule INS-1E sono stati utilizzati radioligandi per studi di binding utilizzando una quantità saturante dell'antagonista β AR [125I]-Cyanopindolol (PerkinElmer, Monza, Italia), come descritto in precedenza (35; 36).

Quantitative real-time RT-PCR e immunoblotting

L'RNA cellulare totale è stato isolato da insulae pancreatiche e campioni di tessuto, utilizzando il kit RNasy (Qiagen, Hilden, Germania) in base alle istruzioni del produttore (28). I valori di PCR sono stati analizzati utilizzando platinum SYBR green (Life Technologies, Norwalk, CT, USA). Le reazioni sono state eseguite in triplicato (30) utilizzando iCycler IQ Real Time PCR Detection System (Biorad, Hercules, CA, USA). La ciclofilina è stata utilizzata come standard interno (32; 37). Il western blot è stato effettuato come descritto in precedenza (35; 36).

Analisi statistica

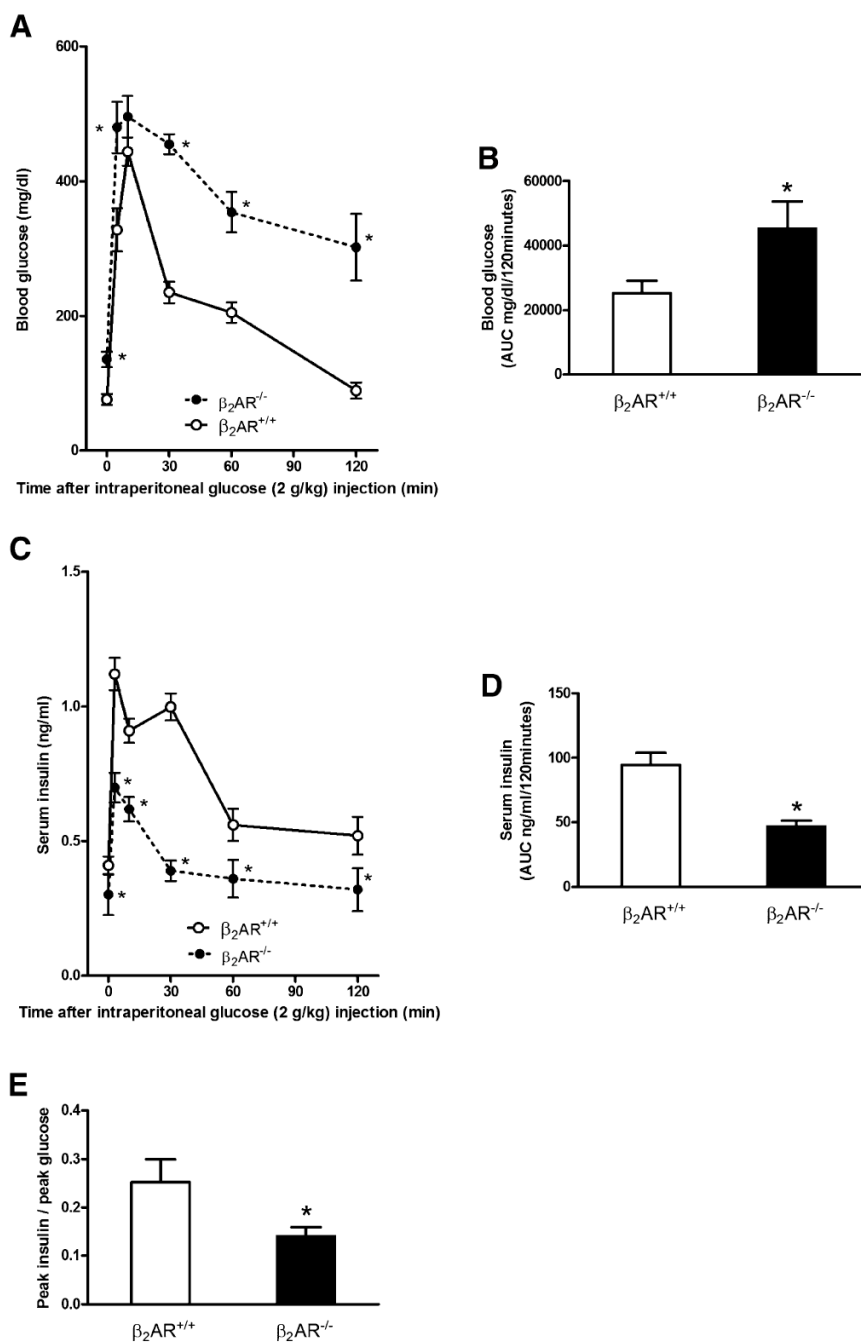
Tutti i dati sono presentati come $\text{media} \pm \text{errore standard (ES)}$. Le differenze statistiche sono state determinate mediante test ANOVA a una o due vie, seguito da test di Bonferroni ove applicabile. Un valore di p inferiore a 0,05 è stato considerato significativo. Tutte le analisi statistiche e la valutazione dei dati sono state eseguite utilizzando GraphPad Prism versione 6.00 (GraphPad Software, San Diego, CA, USA).

Risultati

Fenotipo metabolico di animali privi del $\beta_2AR^{-/-}$

Per studiare *in vivo* il ruolo del gene codificante per il β_2AR nella regolazione della secrezione di insulina, si sono confrontati i fenotipi metabolici di topi adulti (6-mesi) $\beta_2AR^{-/-}$ e $\beta_2AR^{+/+}$. Da questa comparazione si è evinto che la concentrazione di glucosio nel sangue è significativamente più alta nei topi in cui il gene è deletato rispetto ai wild type, sia a digiuno che in condizioni di alimentazione random. Inoltre, nei topi $\beta_2AR^{-/-}$ i livelli di insulina plasmatica a digiuno sono significativamente ridotti. I dati dagli esperimenti di carico di glucosio (GTT) riportano che i topi $\beta_2AR^{-/-}$ mostrano una marcata riduzione della tolleranza al glucosio e dei livelli sierici di insulina (Fig. 1A-D). Inoltre è ridotto il rapporto tra picco di insulina/picco di glucosio (Fig. 1E), ciò indica un'alterata funzione β -cellulare. Il clamp iperinsulinemico euglicemico mostra che l'animale KO ha un'elevata sensibilità all'insulina (VIG: $\beta_2AR^{+/+}$ 12 ± 4 mg/kg/min vs $\beta_2AR^{-/-}$ 31 ± 6 mg/kg/min; VEG: $\beta_2AR^{+/+}$ 92 ± 7 mg/kg/min vs $\beta_2AR^{-/-}$ 66 ± 5 mg/kg/min). I valori registrati a livello epatico (PEG: $\beta_2AR^{+/+}$ 74 ± 5 mg/kg/min vs $\beta_2AR^{-/-}$ 45 ± 3 mg/kg/min) suggeriscono un ruolo chiave per il β_2AR anche nel fegato. Ulteriori studi sono attualmente in corso nei nostri laboratori per approfondire questo aspetto.

Figura 1

FIG. 1. Profilo metabolico di topi $\beta_2AR^{-/-}$.

Topi di sei mesi $\beta_2AR^{-/-}$ e $\beta_2AR^{+/+}$ a seguito di 16 ore di digiuno, sono stati sottoposti a carico di glucosio intraperitoneale (2g/kg peso corporeo). AD: I livelli di glicemia (A, B) e i livelli sierici di insulina (C, D) sono stati monitorati per 120 e 30 minuti, rispettivamente, dopo somministrazione di glucosio (n = 12-16 animali per gruppo). Visualizzazione dell'intolleranza al glucosio (A) e della ridotta secrezione di insulina (C) nei topi $\beta_2AR^{-/-}$. Abbiamo calcolato l'AUC dal glucosio (B), e le curve di escursione insulinica (D). E: il rapporto picco di insulina/picco di glucosio rappresenta la funzione β -cellulare. *: $P < 0,05$ vs $\beta_2AR^{+/+}$; le barre rappresentano la media \pm ES; AUC indica l'area sotto la curva.

L'istologia delle insulae pancreatiche non ha mostrato alcuna differenza significativa tra questi topi (Fig. 2A), e la concentrazione di insulina e glucagone è simile negli animali wild-type e nei knock-out (Fig. 2B-C).

Un ulteriore quesito è se l'ulteriore riduzione della secrezione di insulina che si osserva nei topi $\beta_2AR^{-/-}$ *in vivo* sia dovuta ad una conseguenza diretta della mancanza del β_2AR a livello delle β -cellule pancreatiche o se sia indirettamente mediato da altri fattori di regolazione. Per rispondere a questa domanda, si è analizzato *ex vivo* l'effetto del glucosio su insulae pancreatiche isolate dai topi $\beta_2AR^{-/-}$. Come mostrato in fig. 2D, queste insulae rispondono in maniera non ottimale al glucosio rispetto alle insulae prelevate dai topi wild-type, ma restano sensibili alla depolarizzazione KCl-mediata.

Figura 2

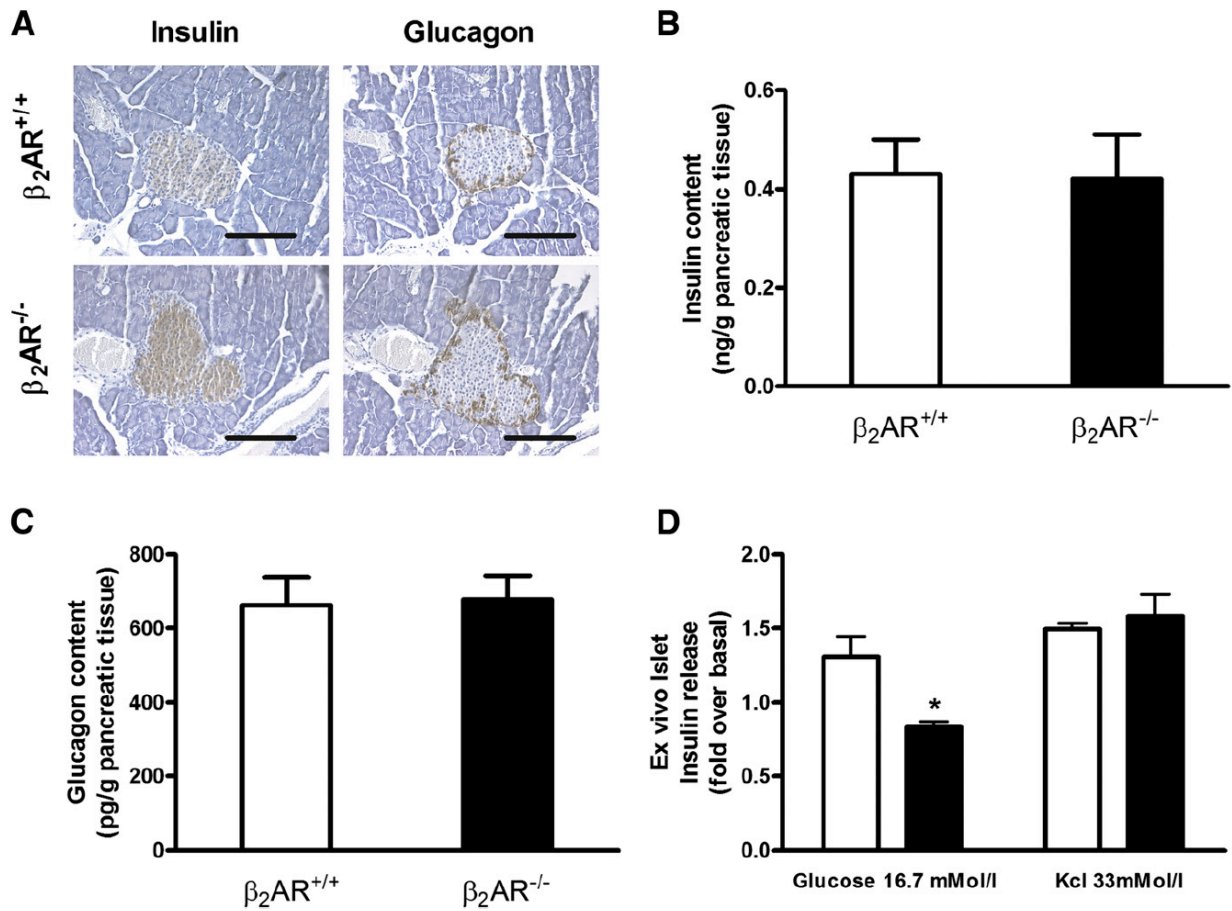


FIG. 2. Morfologia e funzionalità di isole pancreatiche $\beta_2AR^{+/+}$ e $\beta_2AR^{-/-}$

A: L'analisi Immunoistochimica delle isole è stata effettuata su sezioni di paraffina con insulina (colonna a sinistra) o glucagone (colonna di destra). Le microfotografie sono rappresentative di immagini ottenute da sezioni di pancreas di cinque topi $\beta_2AR^{+/+}$ (riga superiore) o $\beta_2AR^{-/-}$ (fila inferiore). B, C: contenuto di insulina (B) e glucagone (C) in insulae da topi $\beta_2AR^{+/+}$ (n = 10) o $\beta_2AR^{-/-}$ (n = 13). D: La secrezione di insulina in risposta a glucosio (16,7 mmol/L) o KCl (33 mmol/L) è stata misurata in insulae da topi $\beta_2AR^{+/+}$ (barre bianche) e $\beta_2AR^{-/-}$ (barre nere). Le barre rappresentano la media \pm ES di dati provenienti da dieci topi per gruppo. *: P <0,05 vs $\beta_2AR^{+/+}$; test di Bonferroni *post hoc*.

Profilo di espressione genica nelle β -cellule con delezione del $\beta_2AR^{-/-}$

Per ottenere una visione più completa del meccanismo alla base della ridotta secrezione insulinica in topi privi del β_2AR , si sono valutati i profili di espressione di diversi geni rilevanti per la regolazione delle β -cellule pancreatiche mediante real-time RT-PCR (mRNA) e western-blot (proteine). Come mostrato in Fig. 3, i livelli PDX-1 e di GLUT2, due geni coinvolti nella funzione delle β cellule, sono diminuiti del 75 e del 60% nelle insulae dei topi $\beta_2AR^{-/-}$. Inoltre, i livelli di PPAR γ sono diminuiti del 54% rispetto ai topi wild-type.

Figura 3

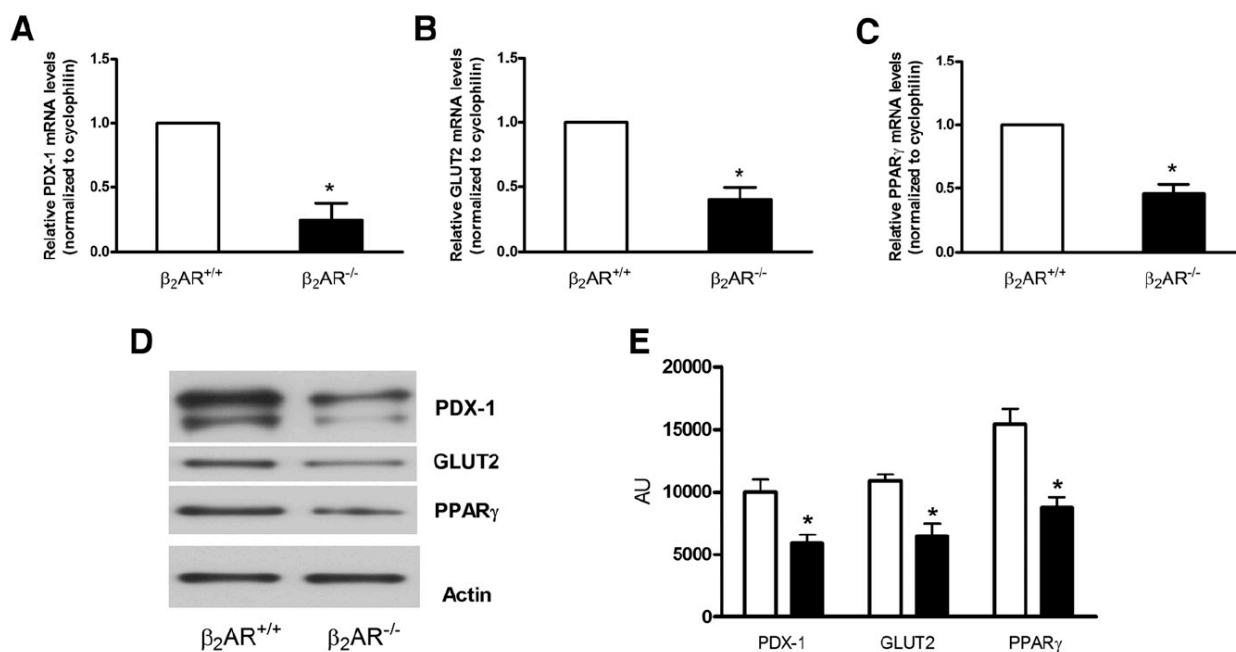


FIG.3 Profilo di espressione genica in insulae isolate da topi $\beta_2AR^{+/+}$ e $\beta_2AR^{-/-}$.

Livelli di mRNA (A-C) e proteine (D, E) per PDX-1, GLUT 2 e PPAR γ . L'abbondanza di mRNA è stata determinata mediante real-time RT-PCR di RNA totale, utilizzando ciclofilina come standard interno. I livelli di mRNA in topi $\beta_2AR^{-/-}$ sono relativi a quelli degli animali di controllo. Ogni banda rappresenta la media \pm ES di quattro esperimenti indipendenti in ciascuno dei quali le reazioni sono state eseguite in triplicato utilizzando il pool di RNA totale da cinque topi/genotipo. *: P <0,05 vs $\beta_2AR^{+/+}$; AU rappresenta unità arbitrarie.

Si è quindi cercato di comprendere se queste anomalie nell'espressione genica siano direttamente causate dall'assenza del β_2 AR. Per perseguire questo obiettivo, si è silenziato con uno specifico shRNA il gene β_2 AR in linee cellulari INS-1E (INS-1E_{sh β_2 AR}, Fig. 4A and B). Come mostrato in fig. 4C, la secrezione insulinica glucosio-indotta è ridotta del 58% nelle cellule silenziate rispetto alle cellule di controllo. Coerentemente con i nostri risultati *ex vivo*, le cellule INS-1E_{sh β_2 AR} mostrano una riduzione dei livelli di mRNA dei geni PDX-1, GLUT2 e PPAR γ (Fig. 4D-F). È interessante notare che le cellule INS-1E_{sh β_2 AR} trasfettate in seguito con cDNA codificante per PPAR γ aumentano transitoriamente la secrezione insulinica glucosio-indotta rispetto alle cellule di controllo (Fig. 4C). Inoltre, l'overespressione di PPAR γ evita la down-regulation di PDX-1 e GLUT2 in cellule INS-1E_{sh β_2 AR} (Fig. 4D ed E).

Figura 4

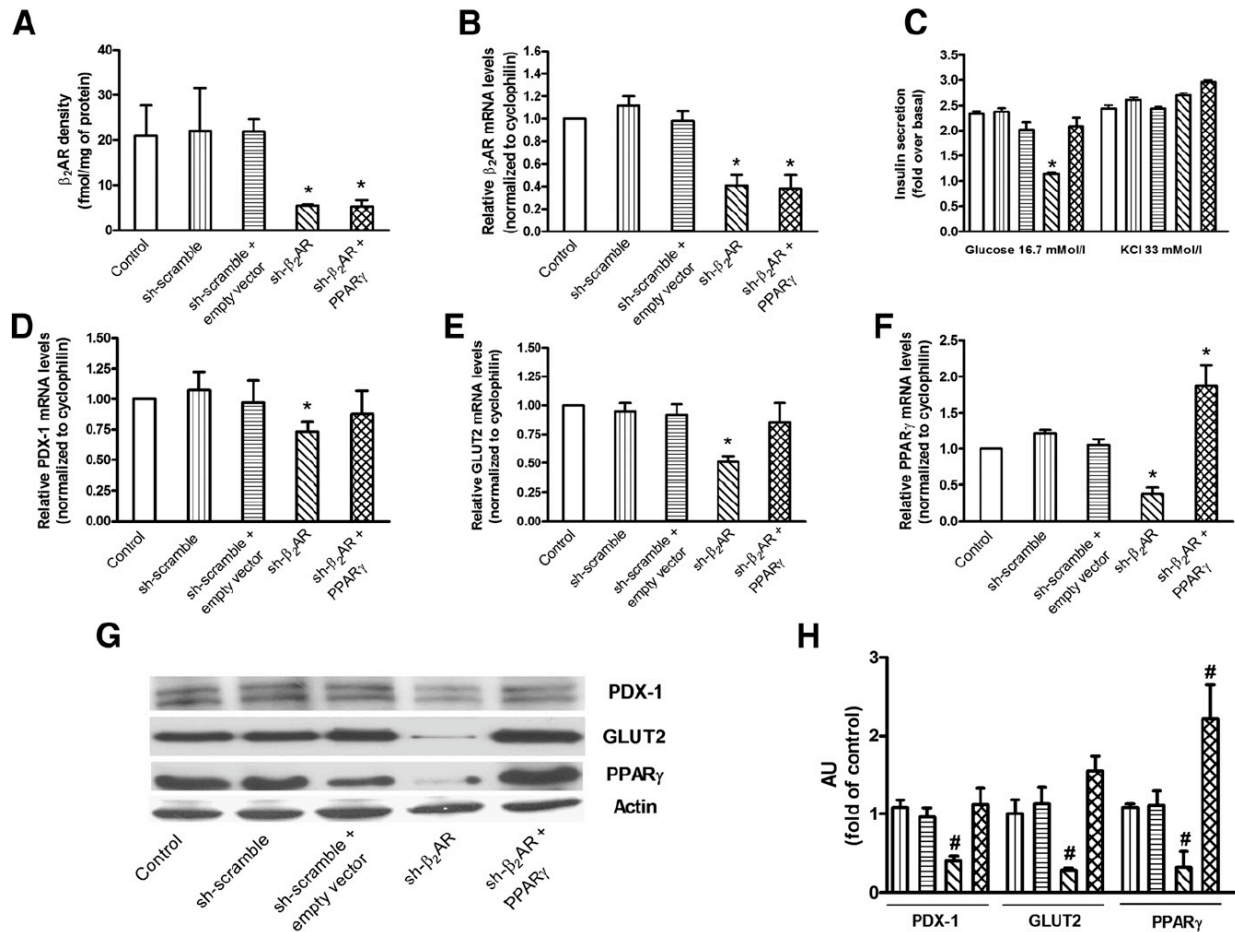


FIG. 4. Livelli del β_2 AR, secrezione insulinica glucosio-indotta e profilo di espressione genica in β -cellule β_2 AR silenziate.

Il trattamento con uno specifico β_2 AR-shRNA diminuisce significativamente la densità (da 73,7%, A) e i livelli di mRNA (da 59,1%, B) di β_2 AR in β -cellule INS-1E. β_2 AR-shRNA inibisce la risposta secretoria insulinica a 16,7 mmol/L di glucosio, che viene ripristinata dalla overespressione di PPAR γ (C). Il rilascio di insulina KCl indotto (C) non è significativamente differente tra i gruppi studiati. β_2 AR-shRNA determina anche una significativa riduzione del livello di mRNA di PDX-1 (D), GLUT2 (E) e PPAR (F), che non è più presente dopo overespressione di PPAR γ . L'espressione genica è stata inoltre valutata a livello proteico (G, H). Le barre rappresentano la media \pm ES. 4-5 esperimenti indipendenti in ciascuno dei quali le reazioni sono state effettuate in triplicato (□ : controllo, *i.e.* cellule INS-1E non trattate; ▨ : sh-scramble; ▩ : sh-scramble+empty vector; ▧ : sh- β_2 AR; ▦ : sh- β_2 AR+PPAR γ ; *: $p < 0,05$ vs controllo; # indica glucosio 2,8 mmol/L).

Questi risultati mostrano che l'assenza del β_2 AR è responsabile, attraverso un meccanismo mediato almeno in parte da PPAR γ , della diminuita secrezione di insulina età-dipendente (Fig. 4D-F).

L'overespressione del β_2 AR *ex vivo* ripristina l'alterato rilascio di insulina

L'espressione del β_2 AR risulta significativamente diminuita nelle insulae di topi β_2 AR^{+/+} di 20 mesi rispetto a quelle isolate da topi di 6 mesi sia in esperimenti di binding recettoriale che alla real-time RT-PCR (Fig. 5A and B). A livello delle insulae pancreatiche di topi β_2 AR^{+/+} anziani i livelli di espressione di PDX-1, GLUT2 and PPAR γ sono ridotti così come è ridotta la secrezione insulinica glucosio-indotta, mentre non è ridotta quella mediata dalla depolarizzazione indotta dal KCl (Fig. 5C-F).

Questi dati suggeriscono una ridotta espressione del β_2 AR a livello delle insulae pancreatiche in questi animali. Per dimostrare questa ipotesi, le insule sono state trattate *ex vivo* con un adenovirus esprime il β_2 AR umano (Ad β_2 AR). In questo modo, si ottiene un miglioramento significativo della secrezione di insulina glucosio-indotta, fino a livelli paragonabili a quelli di insulae di animali adulti di 6 mesi (Fig. 5C), così come sono ripristinate le espressioni di PDX-1, GLUT2 e PPAR γ (Fig. 5D-F).

Figura 5

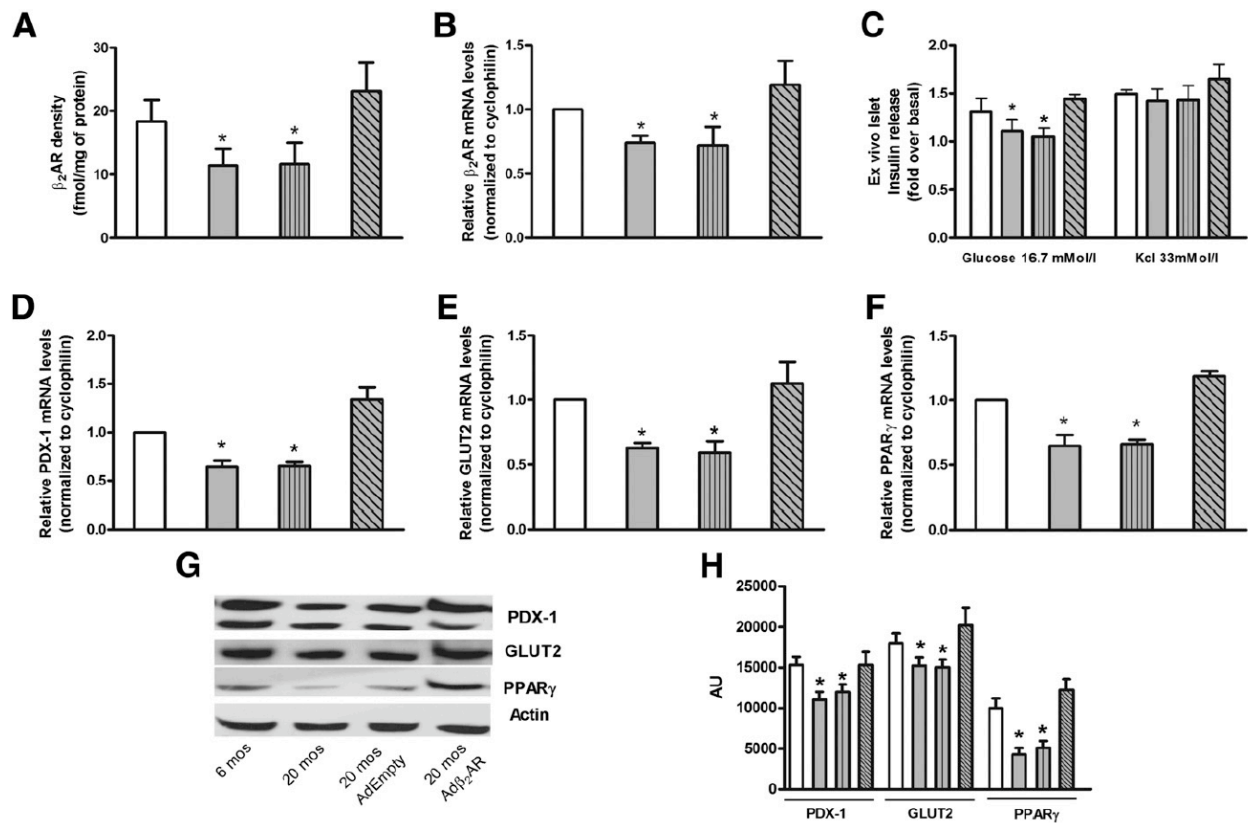


FIG. 5. Il gene delivery del β_2 AR ripristina il deterioramento età-dipendente della funzione β -cellulare.

Densità (A) e livelli di mRNA (B) di β_2 AR sono stati valutati sulle membrane delle cellule di isole isolate da topi β_2 AR^{+/+}. Il rilascio di insulina (C) è stato determinato a seguito di esposizione alla concentrazione indicata di glucosio o di KCl. I livelli di mRNA di PDX-1 (D), GLUT2 (E) e PPAR (F) sono stati determinati mediante Real-time RT-PCR utilizzando il pool di RNA totale da cinque topi/gruppo con ciclofilina come standard interno. L'espressione genica è stata inoltre valutata a livello proteico (G, H). AdEmpty: insulae infettate con un adenovirus di controllo; Ad β_2 AR: insulae infettate con un adenovirus che codifica per il gene β_2 AR umano. Ogni barra rappresenta la media \pm ES di cinque esperimenti indipendenti in ciascuno dei quali le reazioni sono state eseguite in triplicato. (□ : 6 mesi; ■ : 20 mesi; ▨ : 20 mesi AdEmpty; ▩ : 20 mesi Ad β_2 AR; *: p <0,05 vs 6 mesi; basale indica glucosio 2,8 mmol/L).*: p <0,05 vs β_2 AR^{+/+}6 mos; mos indica mesi di età.

Effetti dell'iniezione intrapancreatica dell'Adenovirus Ad β_2 AR sull'omeostasi del glucosio

I topi β_2 AR^{+/+} di 20 mesi di età mostrano una significativa riduzione dei livelli sierici di insulina a digiuno accompagnata da ridotta tolleranza al glucosio e ridotta risposta insulinica dopo GTT (Fig. 6A-E). Si è quindi ideato un protocollo di terapia genica per dimostrare il concetto che queste anomalie possano essere corrette mediante il ripristino della densità β_2 AR. Di conseguenza, dopo aver infettato il pancreas di topi mediante iniezione intraduttale di Ad β_2 AR, si è ripristinata l'espressione di β_2 AR nel tessuto pancreatico, che è tornata a livelli paragonabili a quella di topi di 6 mesi. L'effetto è evidenziabile anche con un significativo miglioramento della tolleranza al glucosio e della secrezione di insulina a seguito di GTT (Fig. 6A-E).

Figura 6

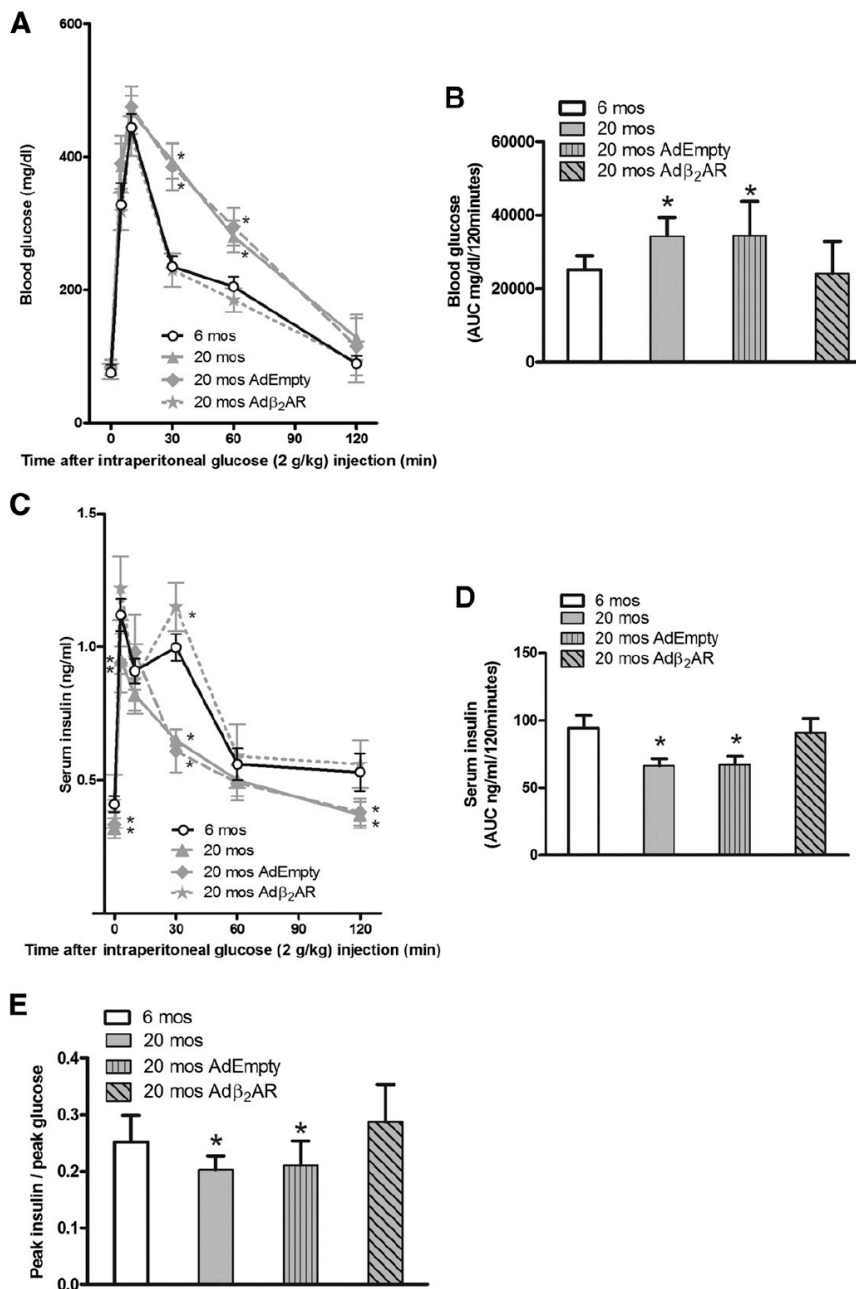


FIG. 6. Il trasferimento genico del β_2 AR adenovirus-mediato nel pancreas ripristina la riduzione della tolleranza al glucosio legata all'età.

Livelli di glucosio nel sangue (A) e livelli sierici di insulina (C) dopo 120 e 30 minuti dalla somministrazione di glucosio, rispettivamente (n = 12-16 animali per gruppo). Sono state calcolate le AUC del glucosio (B) e dell'insulina (D); i topi β_2 AR^{+/+} di 20 mesi di età hanno mostrato intolleranza al glucosio (A, B), ridotta secrezione di insulina (C, D) e anche un'alterata funzione β -cellulare, valutata misurando il rapporto picco di insulina / picco di glucosio (E). Tutti questi parametri sono stati ripristinati dopo infezione del Ad β_2 AR *in vivo*. *: p < 0,05 vs β_2 AR^{+/+} 6 mos; mos indica mesi di età; AUC indica l'area sotto la curva.

I livelli di insulina a digiuno sono aumentati, raggiungendo valori simili a quelli misurati in topi di 6 mesi, sottolineando ulteriormente l'importanza della funzione del β_2 AR per consentire un'adeguata risposta all'iperglicemia a livello delle β -cellule pancreatiche.

Discussione

Nel presente elaborato di tesi, si mostra che l'assenza del gene β_2AR provoca la riduzione del rilascio di insulina glucosio-indotta da parte delle β -cellule pancreatiche. Questo fenotipo ricorda quello osservato nei topi con delezione del gene Ga_s a livello delle β -cellule pancreatiche (27). In questi topi, però, sono evidenti gravi anomalie delle insulae pancreatiche. È interessante notare che, a livello delle insulae di $\beta_2AR^{-/-}$, i livelli di espressione di PPAR γ sono significativamente down-regolati insieme ad una ridotta espressione di PDX-1 e GLUT2, due geni fondamentali per la funzionalità delle β -cellule pancreatiche (31; 38; 39). Questi meccanismi, oltre ad essere stati dimostrati nell'animale KO per il gene β_2AR sono stati supportati anche da studi *in vitro* condotti sulle β -cellule pancreatiche INS-1E. Tali studi mostrano che il silenziamento del β_2AR altera la risposta al glucosio e inibisce l'espressione di PPAR γ riducendo anche i livelli di PDX-1 e GLUT2. Questi dati indicano che β_2AR controlla la secrezione di insulina, almeno in parte attraverso questo pathway. A riprova di ciò, in questa tesi si è dimostrato che l'overespressione di PPAR γ nelle β -cellule INS-1E silenziate per il β_2AR porta al recupero dei livelli di PDX-1/GLUT2 e della secrezione di insulina stimolata dal glucosio. A supporto di questa visione, numerose evidenze suggeriscono un'interconnessione tra β_2AR e PPAR γ (38; 40-42), un elemento chiave nel processo di secrezione di insulina, recentemente studiato anche nell'invecchiamento (39; 43).

Se e in che misura il knock-out del gene β_2AR nel fegato e nei tessuti periferici colpisca l'omeostasi del glucosio deve essere ancora approfondito. Infatti, variazioni a livello del locus β_2AR sono state associate a resistenza insulinica nei pazienti diabetici tipo 2 (17). Tuttavia, come mostrato in questo elaborato di tesi, l'alterata tolleranza al glucosio degli animali $\beta_2AR^{-/-}$ appare essere essenzialmente dovuta a una disfunzione delle β -cellule.

Negli esseri umani, la tolleranza al glucosio diminuisce con l'età, con una conseguente elevata prevalenza di diabete mellito e di ridotta tolleranza al glucosio nella popolazione anziana (2; 9). Come la tolleranza al glucosio peggiori nel tempo a livello individuale rimane poco chiaro, ma è probabilmente determinato da molteplici fattori tra cui la diminuzione della secrezione di insulina (3; 4; 8). Nei modelli animali e nell'uomo, è stato documentato un progressivo deterioramento della funzione β -cellulare con l'età (5; 6). Similmente a risultati evidenziati in diversi tessuti umani (19-22; 44-46), a questi cambiamenti si accompagnano livelli ridotti del β_2AR in insulae pancreatiche murine da noi riscontrati.

La diminuzione dell'espressione del β_2 AR in insulae di animali anziani ricapitola gli stessi meccanismi che portano alla compromissione della secrezione insulinica registrata in roditori privi del β_2 AR. Ciò indica ancora una volta che vi è una correlazione tra l'invecchiamento e la compromissione della tolleranza al glucosio. Infatti, esperimenti sia *in vivo* che *ex vivo* di terapia genica attuata mediante trasferimento del β_2 AR hanno rivelato che il recupero di livelli normali del β_2 AR ripristina il rilascio di insulina e la tolleranza al glucosio negli animali anziani. Così, nel modello murino il progressivo declino dell'espressione del β_2 AR a livello delle insulae sembra contribuire alla riduzione della tolleranza al glucosio che accompagna l'invecchiamento. Se lo stesso meccanismo sia applicabile anche negli esseri umani è attualmente in corso di studio.

Conclusioni

Il β_2 AR regola fisiologicamente la secrezione di insulina da parte delle β -cellule pancreatiche modulando la funzione PPAR γ /PDX-1/GLUT2. L'espressione ridotta del β_2 AR contribuisce all'alterazione età-dipendente della tolleranza al glucosio.

Bibliografia

1. DeFronzo RA: Banting Lecture. From the triumvirate to the ominous octet: a new paradigm for the treatment of type 2 diabetes mellitus. *Diabetes* 58:773-795, 2009
2. Basu R, Breda E, Oberg AL, Powell CC, Dalla Man C, Basu A, Vittone JL, Klee GG, Arora P, Jensen MD, Toffolo G, Cobelli C, Rizza RA: Mechanisms of the age-associated deterioration in glucose tolerance: contribution of alterations in insulin secretion, action, and clearance. *Diabetes* 52:1738-1748, 2003
3. Gumbiner B, Polonsky KS, Beltz WF, Wallace P, Brechtel G, Fink RI: Effects of aging on insulin secretion. *Diabetes* 38:1549-1556, 1989
4. Chang AM, Halter JB: Aging and insulin secretion. *Am J Physiol Endocrinol Metab* 284:E7-12, 2003
5. Ma X, Becker D, Arena VC, Vicini P, Greenbaum C: The effect of age on insulin sensitivity and insulin secretion in first-degree relatives of type 1 diabetic patients: a population analysis. *J Clin Endocrinol Metab* 94:2446-2451, 2009
6. Perfetti R, Rafizadeh CM, Liotta AS, Egan JM: Age-dependent reduction in insulin secretion and insulin mRNA in isolated islets from rats. *Am J Physiol* 269:E983-990, 1995
7. Reaven E, Wright D, Mondon CE, Solomon R, Ho H, Reaven GM: Effect of age and diet on insulin secretion and insulin action in the rat. *Diabetes* 32:175-180, 1983
8. Ihm SH, Matsumoto I, Sawada T, Nakano M, Zhang HJ, Ansite JD, Sutherland DE, Hering BJ: Effect of donor age on function of isolated human islets. *Diabetes* 55:1361-1368, 2006
9. Iozzo P, Beck-Nielsen H, Laakso M, Smith U, Yki-Jarvinen H, Ferrannini E: Independent influence of age on basal insulin secretion in nondiabetic humans. European Group for the Study of Insulin Resistance. *J Clin Endocrinol Metab* 84:863-868, 1999
10. Rosengren AH, Jokubka R, Tojjar D, Granhall C, Hansson O, Li DQ, Nagaraj V, Reinbothe TM, Tuncel J, Eliasson L, Groop L, Rorsman P, Salehi A, Lyssenko V, Luthman H, Renstrom E:

Overexpression of alpha2A-adrenergic receptors contributes to type 2 diabetes. *Science* 327:217-220, 2010

11. Doyle ME, Egan JM: Pharmacological agents that directly modulate insulin secretion. *Pharmacol Rev* 55:105-131, 2003

12. Lembo G, Napoli R, Capaldo B, Rendina V, Iaccarino G, Volpe M, Trimarco B, Saccà L: Abnormal sympathetic overactivity evoked by insulin in the skeletal muscle of patients with essential hypertension. *J Clin Invest* 90:24-29, 1992

13. Seals DR, Esler MD: Human ageing and the sympathoadrenal system. *J Physiol* 528:407-417, 2000

14. Lembo G, Capaldo B, Rendina V, Iaccarino G, Napoli R, Guida R, Trimarco B, Saccà L: Acute noradrenergic activation induces insulin resistance in human skeletal muscle. *Am J Physiol* 266:E242-247, 1994

15. Asensio C, Jimenez M, Kuhne F, Rohner-Jeanrenaud F, Muzzin P: The lack of beta-adrenoceptors results in enhanced insulin sensitivity in mice exhibiting increased adiposity and glucose intolerance. *Diabetes* 54:3490-3495, 2005

16. Haffner CA, Kendall MJ: Metabolic effects of beta 2-agonists. *J Clin Pharm Ther* 17:155-164, 1992

17. Ikarashi T, Hanyu O, Maruyama S, Souda S, Kobayashi C, Abe E, Ukisu J, Naganuma K, Suzuki A, Toya M, Kaneko S, Suzuki K, Nakagawa O, Aizawa Y: Genotype Gly/Gly of the Arg16Gly polymorphism of the beta2-adrenergic receptor is associated with elevated fasting serum insulin concentrations, but not with acute insulin response to glucose, in type 2 diabetic patients. *Diabetes Res Clin Pract* 63:11-18, 2004

18. Scarpace PJ, Mooradian AD, Morley JE: Age-associated decrease in beta-adrenergic receptors and adenylate cyclase activity in rat brown adipose tissue. *J Gerontol* 43:B65-70, 1988

19. Xiao RP, Tomhave ED, Wang DJ, Ji X, Boluyt MO, Cheng H, Lakatta EG, Koch WJ: Age-associated reductions in cardiac beta1- and beta2-adrenergic responses without changes in inhibitory G proteins or receptor kinases. *J Clin Invest* 101:1273-1282, 1998
20. Schocken DD, Roth GS: Reduced beta-adrenergic receptor concentrations in ageing man. *Nature* 267:856-858, 1977
21. Feldman RD, Limbird LE, Nadeau J, Robertson D, Wood AJ: Alterations in leukocyte beta-receptor affinity with aging. A potential explanation for altered beta-adrenergic sensitivity in the elderly. *N Engl J Med* 310:815-819, 1984
22. Bao X, Mills PJ, Rana BK, Dimsdale JE, Schork NJ, Smith DW, Rao F, Milic M, O'Connor DT, Ziegler MG: Interactive effects of common beta2-adrenoceptor haplotypes and age on susceptibility to hypertension and receptor function. *Hypertension* 46:301-307, 2005
23. Ho D, Yan L, Iwatsubo K, Vatner DE, Vatner SF: Modulation of beta-adrenergic receptor signaling in heart failure and longevity: targeting adenylyl cyclase type 5. *Heart Fail Rev* 15:495-512, 2010
24. Kang KB, Rajanayagam MA, van der Zyppe A, Majewski H: A role for cyclooxygenase in aging-related changes of beta-adrenoceptor-mediated relaxation in rat aortas. *Naunyn Schmiedebergs Arch Pharmacol* 375:273-281, 2007
25. Ryall JG, Plant DR, Gregorevic P, Sillence MN, Lynch GS: Beta 2-agonist administration reverses muscle wasting and improves muscle function in aged rats. *J Physiol* 555:175-188, 2004
26. Chruscinski AJ, Rohrer DK, Schauble E, Desai KH, Bernstein D, Kobilka BK: Targeted disruption of the beta2 adrenergic receptor gene. *J Biol Chem* 274:16694-16700, 1999
27. Xie T, Chen M, Zhang QH, Ma Z, Weinstein LS: Beta cell-specific deficiency of the stimulatory G protein alpha-subunit Gsalpha leads to reduced beta cell mass and insulin-deficient diabetes. *Proc Natl Acad Sci U S A* 104:19601-19606, 2007

28. Vigliotta G, Miele C, Santopietro S, Portella G, Perfetti A, Maitan MA, Cassese A, Oriente F, Trencia A, Fiory F, Romano C, Tiveron C, Tatangelo L, Troncone G, Formisano P, Béguinot F: Overexpression of the ped/pea-15 gene causes diabetes by impairing glucose-stimulated insulin secretion in addition to insulin action. *Mol Cell Biol* 24:5005-5015, 2004
29. Santulli G, Basilicata MF, De Simone M, Del Giudice C, Anastasio A, Sorriento D, Saviano M, Del Gatto A, Trimarco B, Pedone C, Zaccaro L, Iaccarino G: Evaluation of the anti-angiogenic properties of the new selective alpha(V)beta(3) integrin antagonist RGDechiHCit. *Journal of Translational Medicine* 9, 2011
30. Sorriento D, Santulli G, Fusco A, Anastasio A, Trimarco B, Iaccarino G: Intracardiac injection of AdGRK5-NT reduces left ventricular hypertrophy by inhibiting NF-kappaB-dependent hypertrophic gene expression. *Hypertension* 56:696-704, 2010
31. Evans-Molina C, Robbins RD, Kono T, Tersey SA, Vestermark GL, Nunemaker CS, Garmey JC, Deering TG, Keller SR, Maier B, Mirmira RG: Peroxisome proliferator-activated receptor gamma activation restores islet function in diabetic mice through reduction of endoplasmic reticulum stress and maintenance of euchromatin structure. *Mol Cell Biol* 29:2053-2067, 2009
32. Lombardi A, Ulianich L, Treglia A, Nigro C, Parrillo L, Lofrumento D, Nicolardi G, Garbi C, Béguinot F, Miele C, Di Jeso B: Increased hexosamine biosynthetic pathway flux dedifferentiates INS-1E cells and murine islets by an extracellular signal-regulated kinase (ERK)1/2-mediated signal transmission pathway. *Diabetologia* In press, 2011
33. Iaccarino G, Ciccarelli M, Sorriento D, Galasso G, Campanile A, Santulli G, Cipolletta E, Cerullo V, Cimini V, Altobelli GG, Piscione F, Priante O, Pastore L, Chiariello M, Salvatore F, Koch WJ, Trimarco B: Ischemic neoangiogenesis enhanced by beta2-adrenergic receptor overexpression: a novel role for the endothelial adrenergic system. *Circ Res* 97:1182-1189, 2005

34. Ciccarelli M, Sorriento D, Cipolletta E, Santulli G, Fusco A, Zhou RH, Eckhart AD, Peppel K, Koch WJ, Trimarco B, Iaccarino G: Impaired neoangiogenesis in beta-adrenoceptor gene-deficient mice: restoration by intravascular human beta-adrenoceptor gene transfer and role of NFkappaB and CREB transcription factors. *Br J Pharmacol* 162:712-721, 2011
35. Perino A, Ghigo A, Ferrero E, Morello F, Santulli G, Baillie GS, Damilano F, Dunlop AJ, Pawson C, Walser R, Levi R, Altruda F, Silengo L, Langeberg LK, Neubauer G, Heymans S, Lembo G, Wymann MP, Wetzker R, Houslay MD, Iaccarino G, Scott JD, Hirsch E: Integrating Cardiac PIP(3) and cAMP Signaling through a PKA Anchoring Function of p110gamma. *Mol Cell* 42:84-95, 2011
36. Ciccarelli M, Santulli G, Campanile A, Galasso G, Cervero P, Altobelli GG, Cimini V, Pastore L, Piscione F, Trimarco B, Iaccarino G: Endothelial alpha1-adrenoceptors regulate neoangiogenesis. *Br J Pharmacol* 153:936-946, 2008
37. Fiory F, Lombardi A, Miele C, Giudicelli J, Béguinot F, Van Obberghen E: Methylglyoxal impairs insulin signalling and insulin action on glucose-induced insulin secretion in the pancreatic beta cell line INS-1E. *Diabetologia* 54:2941-2952, 2011
38. Faisy C, Pinto FM, Blouquit-Laye S, Danel C, Naline E, Buenestado A, Grassin Delyle S, Burgel PR, Chapelier A, Advenier C, Candenas ML, Devillier P: beta2-Agonist modulates epithelial gene expression involved in the T- and B-cell chemotaxis and induces airway sensitization in human isolated bronchi. *Pharmacol Res* 61:121-128, 2010
39. Blalock EM, Phelps JT, Pancani T, Searcy JL, Anderson KL, Gant JC, Popovic J, Avdiushko MG, Cohen DA, Chen KC, Porter NM, Thibault O: Effects of long-term pioglitazone treatment on peripheral and central markers of aging. *PLoS One* 5:e10405, 2010

40. Collins S, Yehuda-Shnaidman E, Wang H: Positive and negative control of Ucp1 gene transcription and the role of beta-adrenergic signaling networks. *Int J Obes (Lond)* 34 Suppl 1:S28-33, 2010
41. Fan X, Gabbi C, Kim HJ, Cheng G, Andersson LC, Warner M, Gustafsson JA: Gonadotropin-positive pituitary tumors accompanied by ovarian tumors in aging female ERbeta-/- mice. *Proc Natl Acad Sci U S A* 107:6453-6458, 2010
42. Tadaishi M, Miura S, Kai Y, Kawasaki E, Koshinaka K, Kawanaka K, Nagata J, Oishi Y, Ezaki O: Effect of exercise intensity and AICAR on isoform-specific expressions of murine skeletal muscle PGC-1alpha mRNA: a role of beta-adrenergic receptor activation. *Am J Physiol Endocrinol Metab* 300:E341-349, 2011
43. Sung B, Park S, Yu BP, Chung HY: Modulation of PPAR in aging, inflammation, and calorie restriction. *J Gerontol A Biol Sci Med Sci* 59:997-1006, 2004
44. White M, Roden R, Minobe W, Khan MF, Larrabee P, Wollmering M, Port JD, Anderson F, Campbell D, Feldman AM, et al.: Age-related changes in beta-adrenergic neuroeffector systems in the human heart. *Circulation* 90:1225-1238, 1994
45. Santulli G, Iaccarino G: Pinpointing beta 2 adrenergic receptor in ageing pathophysiology: victim or executioner? Evidence from crime scenes. *Immunity & Ageing* 2013;in press
46. Santulli G, Trimarco B, Iaccarino G: G-Protein-Coupled Receptor Kinase 2 and Hypertension: Molecular Insights and Pathophysiological Mechanisms. *High Blood Pressure & Cardiovascular Prevention* 2013;in press

Selezione di lavori pubblicati dal candidato durante il periodo di Dottorato (2010-2012)

1. Santulli G: Coronary Heart Disease Risk Factors and Mortality. *JAMA-Journal of the American Medical Association* 307:1137-1137, 2012
2. Santulli G. et al: CaMK4 Gene Deletion Induces Hypertension. *JAHA, Journal of the American Heart Association* 2012;1:e001081
3. Santulli G, Thrombolysis outcomes in acute ischemic stroke patients with prior stroke and diabetes mellitus. *Neurology* 2012;78:840
4. Sorriento D, Santulli G, Del Giudice C, Anastasio A, Trimarco B, Iaccarino G: Endothelial cells are able to synthesize and release catecholamines both in vitro and in vivo. *Hypertension* 2012;60:129-136
5. Matarese A. Santulli G: Angiogenesis in Chronic Obstructive Pulmonary Disease: A Translational Appraisal. *Translational Medicine @ UniSa* 3(6): 49-56,2012
6. Santulli G, D'Ascia S, D'Ascia C: Regarding the impact of left ventricular size on response to cardiac resynchronization therapy. *American Heart Journal* 163:E11-E11, 2012
7. Del Giudice C, Cipolletta E, Anastasio A, Santulli G, Rusciano M, Maione AS, Campiglia P, Illario M, Trimarco B, Iaccarino G: A novel CaMKII/ERK interaction in the heart sustains cardiac hypertrophy in spontaneously hypertensive rats. *Cardiovascular Research* 93:S12-S12, 2012
8. Fusco A, Sorriento D, Santulli G, Trimarco B, Iaccarino G: GRK5-NT regulates the activity of calcium-calmodulin dependent transcription factors. *Cardiovascular Research* 93:S55-S55, 2012
9. Sorriento D, Santulli G, Del Giudice C, Anastasio A, Trimarco B, Iaccarino G: Endothelial cells are able to synthesize and release catecholamines both in vitro and in vivo. *Cardiovascular Research* 93:S61-S61, 2012
10. Matarese A. Santulli G: Angiogenesis in Chronic Obstructive Pulmonary Disease: A Translational Appraisal. *Nature Preceedings*; 7112.1,2012
11. Santulli G, D'ascia SL, D'ascia C: Development of Atrial Fibrillation in Recipients of Cardiac Resynchronization Therapy: The Role of Atrial Reverse Remodelling. *Canadian Journal of Cardiology* 28, 2012
12. Santulli G, D'ascia C: Atrial remodelling in echocardiographic super-responders to cardiac resynchronization therapy. *Heart* 98:517-517, 2012

13. Santulli G: The Ten Commandments of Ethical Publishing. *Cell & Developmental Biology* 1:1, 2012
14. Santulli G, Lombardi A, Sorriento D, Anastasio A, Del Giudice C, Formisano P, Beguinot F, Trimarco B, Miele C, Iaccarino G: Age-Related Impairment in Insulin Release The Essential Role of beta(2)-Adrenergic Receptor. *Diabetes* 61:692-701, 2012
15. Fusco A, Santulli G, Sorriento D, Cipolletta E, Garbi C, Dorn GW, Trimarco B, Feliciello A, Iaccarino G: Mitochondrial localization unveils a novel role for GRK2 in organelle biogenesis. *Cellular Signalling* 24:468-475, 2012
16. Santulli G, D'Ascia S, Marino V, D'Ascia C: Atrial Function in Patients Undergoing CRT. *JACC-Cardiovascular Imaging* 5:124-125, 2012
17. Marino V, D'Ascia C, D'Ascia S, G. Santulli: Development of atrial fibrillation in recipients of cardiac resynchronization therapy: the role of atrial reverse remodelling. *European Journal of Heart Failure* 2012;11(S1)
18. Santulli G, Campanile A, Spinelli L, di Panzillo EA, Ciccarelli M, Trimarco B, Iaccarino G: G Protein-Coupled Receptor Kinase 2 in Patients With Acute Myocardial Infarction. *American Journal of Cardiology* 107:1125-1130, 2011
19. Perino A, Ghigo A, Ferrero E, More F, Santulli G, Baillie GS, Damilano F, Dunlop AJ, Pawson C, Walser R, Levi R, Altruda F, Silengo L, Langeberg LK, Neubauer G, Heymans S, Lembo G, Wymann MP, Wetzker R, Houslay MD, Iaccarino G, Scott JD, Hirsch E: Integrating Cardiac PIP3 and cAMP Signaling through a PKA Anchoring Function of p110 gamma. *Molecular Cell* 42:84-95, 2011
20. Ciccarelli M, Sorriento D, Cipolletta E, Santulli G, Fusco A, Zhou RH, Eckhart AD, Peppel K, Koch WJ, Trimarco B, Iaccarino G: Impaired neoangiogenesis in beta(2)-adrenoceptor gene-deficient mice: restoration by intravascular human beta(2)-adrenoceptor gene transfer and role of NF kappa B and CREB transcription factors. *British Journal of Pharmacology* 162:712-721, 2011
21. Santulli G, Basilicata MF, De Simone M, Del Giudice C, Anastasio A, Sorriento D, Saviano M, Del Gatto A, Trimarco B, Pedone C, Zaccaro L, Iaccarino G: Evaluation of the anti-angiogenic properties of the new selective alpha(V)beta(3) integrin antagonist RGDechiHCit. *Journal of Translational Medicine* 9, 2011
22. Cipolletta E, Santulli G, Rusciano MR, Anastasio A, Maione AS, del Giudice C, Campiglia P, Illario M, Iaccarino G: A Novel CaMKII/ERK Interaction in the Heart Sustains Cardiac Hypertrophy in Spontaneously Hypertensive Rats. *Circulation* 122, 2010
23. Fusco A, Santulli G, Sorriento D, Cipolletta E, Garbi C, Dorn GW, Trimarco B, Feliciello A, Iaccarino G: Mitochondrial Localization Unveils a Novel Role for Grk2 in the Regulation of Oxidative Metabolism. *Circulation* 122, 2010

24. Santulli G, Lombardi A, Sorriento D, Anastasio A, Del Giudice C, Miele C, Iovino S, Formisano P, Trimarco B, Beguinot F, Iaccarino G: Decreased Insulin Secretion and Insulin Resistance in Beta 2 Adrenergic Receptor Knock-out Mice. *Circulation* 122, 2010
25. Campanie A, Spinelli L, Santulli G, Ciccarelli M, De Gennaro S, Di Panzillo EA, Trimarco B, Iaccarino G: Elevated g protein-coupled receptor kinases 2 (GRK2) levels in lymphocytes associate with worse cardiac function in acute ST segment elevation myocardial infarction (STEMI). *European Heart Journal Supplements* 12:F19-F19, 2010
26. Sorriento D, Santulli G, Fusco A, Anastasio A, Trimarco B, Iaccarino G: Intracardiac Injection of AdGRK5-NT Reduces Left Ventricular Hypertrophy by Inhibiting NF-kappa B-Dependent Hypertrophic Gene Expression. *Hypertension* 56:696-704, 2010
27. Galasso G, Santulli G, Piscione F, De Rosa R, Trimarco V, Piccolo R, Cassese S, Iaccarino G, Trimarco B, Chiariello M: The GPIIIA PIA2 polymorphism is associated with an increased risk of cardiovascular adverse events. *Bmc Cardiovascular Disorders* 10, 2010
28. Cipoletta E, Santulli G, Illario M, Campiglia P, Iaccarino G: A novel CaMKII/ERK interaction in the heart sustain cardiac hypertrophy in spontaneously hypertensive rats. *European Heart Journal* 31:307-307, 2010
29. Lombardi A, Santulli G, Sorriento D, Anastasio A, Iovino S, Del Giudice C, Trimarco B, Beguinot F, Formisano P, Miele C, Iaccarino G: The lack of beta 2 adrenoceptors in mice results in glucose intolerance and impaired insulin secretion. *Diabetologia* 53, 2010
30. Santulli G, Lombardi A, Sorriento D, Anastasio A, Iovino S, Del Giudice C, Miele C, Formisano P, Iaccarino G: Beta 2 adrenergic receptor knock out mice develop insulin-resistance. *European Heart Journal* 31:936-936, 2010
31. Sorriento D, Santulli G, Fusco A, Trimarco B, Iaccarino G: The RH domain of GRK5 regulates cardiac hypertrophy in vivo. *European Heart Journal* 31:306-306, 2010
32. Campanie A, Spinelli L, Santulli G, Ciccarelli M, De Gennaro S, Di Panzillo EA, Trimarco B, Iaccarino G: Elevated g protein-coupled receptor kinases 2 (GRK2) levels in lymphocytes associate with worse cardiac function in acute ST segment elevation myocardial infarction (STEMI). *Cardiovascular Research* 87:S77-S77, 2010
33. Cipoletta E, Santulli G, Attanasio A, Del Giudice C, Campiglia P, Illario M, Iaccarino G: A novel CaMKII/ERK interaction in the heart sustains cardiac hypertrophy in spontaneously hypertensive rats. *Cardiovascular Research* 87:S78-S79, 2010
34. De Rosa R, Galasso G, Piscione F, Santulli G, Iaccarino G, Piccolo R, Luciano R, Chiariello M: Increased risk of cardiovascular events associated with the GPIIIA PIA2 polymorphism. *Cardiovascular Research* 87:S74-S75, 2010
35. Fusco A, Santulli G, Cipoletta E, Sorriento D, Cervero P, Trimarco B, Feliciello A, Iaccarino G: Mitochondrial localization unveils a novel role for GRK2 in the regulation of oxidative metabolism. *Cardiovascular Research* 87:S87-S87, 2010

36. Sorriento D, Santulli G, Fusco A, Trimarco B, Iaccarino G: The RH domain of GRK5 regulates cardiac hypertrophy in vivo. *Cardiovascular Research* 87:S122-S123, 2010
37. D'Ascia SL, Santulli G, Liguori V, Marino V, Arturo C, Chiariello M, D'Ascia C: Advanced algorithms can lead to electrocardiographic misinterpretations. *International Journal of Cardiology* 141:E34-E36, 2010
38. Santulli G, Illario M, Cipolletta E, Sorriento D, Del Giudice C, Anastasio A, Trimarco B, Iaccarino G: Deletion of the CaMK4 gene in mice determines a hypertensive phenotype. *Cardiovascular Research* 87:S89-S89, 2010

Age-Related Impairment in Insulin Release

The Essential Role of β_2 -Adrenergic Receptor

Gaetano Santulli,^{1,2} Angela Lombardi,^{3,4} Daniela Sorriento,¹ Antonio Anastasio,¹ Carmine Del Giudice,¹ Pietro Formisano,⁴ Francesco Béguinot,⁴ Bruno Trimarco,¹ Claudia Miele,⁴ and Guido Iaccarino⁵

In this study, we investigated the significance of β_2 -adrenergic receptor (β_2 AR) in age-related impaired insulin secretion and glucose homeostasis. We characterized the metabolic phenotype of β_2 AR-null C57Bl/6N mice (β_2 AR^{-/-}) by performing in vivo and ex vivo experiments. In vitro assays in cultured INS-1E β -cells were carried out in order to clarify the mechanism by which β_2 AR deficiency affects glucose metabolism. Adult β_2 AR^{-/-} mice featured glucose intolerance, and pancreatic islets isolated from these animals displayed impaired glucose-induced insulin release, accompanied by reduced expression of peroxisome proliferator-activated receptor (PPAR) γ , pancreatic duodenal homeobox-1 (PDX-1), and GLUT2. Adenovirus-mediated gene transfer of human β_2 AR rescued these defects. Consistent effects were evoked in vitro both upon β_2 AR knockdown and pharmacologic treatment. Interestingly, with aging, wild-type (β_2 AR^{+/+}) littermates developed impaired insulin secretion and glucose tolerance. Moreover, islets from 20-month-old β_2 AR^{+/+} mice exhibited reduced density of β_2 AR compared with those from younger animals, paralleled by decreased levels of PPAR γ , PDX-1, and GLUT2. Overexpression of β_2 AR in aged mice rescued glucose intolerance and insulin release both in vivo and ex vivo, restoring PPAR γ /PDX-1/GLUT2 levels. Our data indicate that reduced β_2 AR expression contributes to the age-related decline of glucose tolerance in mice. *Diabetes* 61:692–701, 2012

Impairment of glucose metabolism with age represents a major determinant of type 2 diabetes epidemics within the elderly population. The molecular mechanisms underlying these changes have not been fully elucidated and are likely attributable to multiple causes (1,2). Aging per se is associated with a continuous decrease in basal insulin release (3). The size of this effect is sufficient to increase the likelihood of developing abnormalities in glucose tolerance and even overt diabetes (2,4). The consequence of aging on glucose tolerance occurs in different species, having been identified in rats

(5,6) as well as in humans (4,7,8). However, why insulin secretion deteriorates with aging remains a moot point.

The noradrenergic system provides fine-tuning to the endocrine pancreas activity through the function of α - and β -adrenergic receptors (ARs) (9,10). The reciprocal regulation exerted by insulin and the adrenergic system has been well documented through a large number of studies (11–13). More recent evidence shows that mice with simultaneous deletion of the three known genes encoding the β ARs (β_1 , β_2 , and β_3) present a phenotype characterized by impaired glucose tolerance (14). Studies with β_2 AR agonists further suggest that the β_2 AR may play an important role in regulating insulin secretion (15). In addition, different human polymorphisms in the β_2 AR gene have been associated with higher fasting insulin levels (16). Nevertheless, the impact of the β_2 AR subtype on glucose tolerance and insulin secretion is still unclear.

Similar to glucose tolerance, β AR function and responsiveness deteriorate with aging (17–20), but the precise mechanisms involved are unknown. However, current evidence indicates that aging may downregulate β AR signaling, β_2 AR in particular, by decreasing the expression of molecular components of the adrenergic signaling machinery (21–24). We have therefore hypothesized that age-dependent alterations in β AR function impair glucose-regulated insulin release by the pancreatic β -cells and may contribute to deterioration of glucose tolerance. To test this hypothesis, we explored the consequences of β_2 AR knockout on insulin secretion in mice and investigated the significance of the age-related changes in β_2 AR function with regard to glucose tolerance.

RESEARCH DESIGN AND METHODS

In vivo studies. We studied male mice with a homozygous deletion of the β_2 AR gene (β_2 AR^{-/-}) and backcrossed >12 generations onto C57Bl/6N background. Founders were provided by Brian Kobilka (Stanford University, Stanford, CA) (25). Wild-type littermates (β_2 AR^{+/+}) were used as controls. The animals were housed in a temperature-controlled (22°C) room with a 12-h light/dark cycle in accordance with the *Guide for the Care and Use of Laboratory Animals* published by the National Institutes of Health (NIH publication no. 85-23, revised 1996), and experiments were approved by the ethics committee of the Federico II University. Mice were killed by cervical dislocation. Pancreata were excised and collected rapidly after mice were killed. Samples were weighted, fixed by immersion in 4% paraformaldehyde for histology, homogenized for determination of total insulin content, or snap-frozen in liquid nitrogen and stored at -80°C for subsequent analyses. For determination of insulin or glucagon content, pancreatic tissue was homogenized in acid ethanol and extracted at 4°C overnight. The acidic extracts were dried by vacuum, reconstituted, and subjected to insulin and glucagon measurements.

Glucose tolerance test and assessment of insulin secretion. Glucose tolerance test (GTT) was performed as previously described (9,26). Briefly, mice were fasted overnight and then injected with glucose (2 g/kg i.p.). Blood glucose was measured by tail bleeding (Glucose Analyzer II; Beckman Coulter, Brea, CA) at indicated time points. The assessment of insulin secretion before

From the ¹Department of Clinical Medicine, Cardiovascular & Immunologic Sciences, “Federico II” University of Naples, Naples, Italy; ²Columbia-Presbyterian Medical Center, College of Physicians & Surgeons, Columbia University, New York, New York; ³Columbia University Medical Center, Columbia University, New York, New York; the ⁴Department of Cellular and Molecular Biology and Pathology and Institute of Experimental Endocrinology and Oncology “Gaetano Salvatore,” “Federico II” University of Naples, Naples, Italy; and the ⁵School of Medicine, University of Salerno, Salerno, Italy.

Corresponding authors: Guido Iaccarino, giaccarino@unisa.it, and Claudia Miele, c.miele@ieos.cnr.it.

Received 21 July 2011 and accepted 3 December 2011.

DOI: 10.2337/db11-1027

This article contains Supplementary Data online at <http://diabetes.diabetesjournals.org/lookup/suppl/doi:10.2337/db11-1027/-/DC1>.

G.S. and A.L. contributed equally to this work.

© 2012 by the American Diabetes Association. Readers may use this article as long as the work is properly cited, the use is educational and not for profit, and the work is not altered. See <http://creativecommons.org/licenses/by-nc-nd/3.0/> for details.

and during glucose challenge was performed as previously described (9,27). Blood from the mandibular vein of overnight-fasted mice was collected at the indicated time for serum insulin assessment. The evaluation of glucagon secretion was performed by collecting blood from the mandibular vein of randomized mice before and after injection of insulin (0.75 IU/kg i.p.). Serum insulin and plasma glucagon were assayed by radioimmunoassay (Millipore, Billerica, MA).

Histological analysis. Immunohistochemistry was carried out on paraffin sections using the H38 rabbit insulin antibody or the N-17 goat glucagon antibody (1:200 dilution; both from Santa Cruz Biotechnology, Santa Cruz, CA). Goat anti-rabbit serum coupled with peroxidase (Immunotech, Marseille, France) was used as secondary antibody. After primary antibody exposure, slides were incubated with biotinylated anti-rabbit or anti-goat IgG and peroxidase-labeled streptavidin (Dako Corporation). All reactions were revealed with diaminobenzidine. Sections were counterstained with hematoxylin and mounted (28,29).

Ex vivo studies

Isolation of mouse pancreatic islets. Islets of Langerhans were isolated by collagenase digestion (26,30). In brief, mice were killed as described above, the fur was soaked with ethanol, and the abdomen was opened to locate and excise the pancreas. Digestion was completed with collagenase P (Roche Applied Sciences, Penzberg, Germany) in a shaking water bath (37°C) for 5–8 min. The digested pancreas was treated with DNase I (New England Biolabs, Ipswich, MA). The islets were hand-picked under a stereomicroscope using a syringe with a 25-gauge needle and cultured at 37°C with 95% air and 5% CO₂ in complete RPMI-1640 supplemented with 5% heat-inactivated FBS, 1 mmol/L sodium pyruvate, 50 μmol/L 2-mercaptoethanol, 2 mmol/L glutamine, 10 mmol/L HEPES, 100 units/mL penicillin, and 100 μg/mL streptomycin (all from Sigma-Aldrich, Saint Louis, MO) as previously described (31,32).

Evaluation of insulin secretion. Isolated islets were preincubated at 37°C for 30 min in Krebs-Ringer bicarbonate buffer (120 mmol/L NaCl, 4.7 mmol/L KCl, 1.2 mmol/L MgSO₄, 1.2 mmol/L KH₂PO₄, 2.4 mmol/L CaCl₂, and 20 mmol/L NaHCO₃) supplemented with 10 mmol/L HEPES and 0.2% BSA and gassed with a mixture of 95% O₂ and 5% CO₂ containing 2 mmol/L glucose. Twenty size-matched islets collected in each tube were incubated for 1 h in a 37°C water bath with 500 μL Krebs-Ringer bicarbonate buffer medium containing 2.8 mmol/L glucose, 16.7 mmol/L glucose, or 2.8 mmol/L glucose plus 33 mmol/L KCl. Islets were then pelleted by centrifugation (9,000g, 2 min, 4°C), and supernatants were collected for insulin secretion. Insulin concentrations were determined using radioimmunoassay (31).

Adenovirus-mediated reinstallation of β₂AR in vivo and ex vivo.

Twenty-month-old β₂AR^{+/+} mice were anesthetized by isoflurane (4%) inhalation and maintained by mask ventilation (isoflurane 1.8%) (28). After laparotomy, we identified and mobilized the distal pancreas and we performed two injections (50 μL each) of adenovirus (7 × 10¹⁰ plaque-forming units [pfu]/mouse) using a 30-gauge needle. Given the high homology between the human and mouse β₂AR (33) and the validated use of the adenoviruses expressing the human β₂AR (Adβ₂AR) for in vivo gene transfer (34–36), we used the human Adβ₂AR or, as control, an empty expression cassette derived from pcDNA3.2/V5/GW/D-TOPO (AdEmpty), kindly provided by Walter J. Koch, Jefferson University (Philadelphia, PA). Finally, abdominal incision was quickly closed in layers using 3–0 silk suture, and animals were observed and monitored until recovery. Isolated islets were infected (12 × 10⁴ pfu/islet) with Adβ₂AR or AdEmpty. After 3 h incubation with the adenoviruses, pancreatic islets were incubated with fresh medium and under normoxic conditions (95% air, 5% CO₂) at 37°C for 24 h.

In vitro studies. The INS-1E β-cells (provided by P. Maechler, University of Geneva, Geneva, Switzerland), derived and selected from the parental rat insulinoma INS-1 β-cell line, were maintained in monolayer culture in RPMI-1640 medium as described above for the ex vivo experiments. For the insulin secretion assays, cells were seeded at a density of 5 × 10⁵ cells/cm² for at least 96 h before use (31). Transient transfection of the PPARγ cDNA and control empty plasmid was performed using Lipofectamine 2000 (Invitrogen, Carlsbad, CA) (37). We also tested the effects of the specific pharmacological β₂AR antagonist ICI 118,551 (0.1 μmol/L) or agonist (1 μmol/L fenoterol) (both from Sigma-Aldrich) (36).

Short hairpin RNA design, generation, and transfection and radioligand-binding assay.

Stealth short hairpin (sh)RNA oligoribonucleotides against β₂AR and scramble were designed (sequences and efficiency shown in Supplementary Table 1 and Supplementary Fig. 2, respectively) and then synthesized by Invitrogen. The shRNA hairpin configuration is cleaved by the cellular machinery into small interfering RNA, which is then bound to the RNA-induced silencing complex. This complex binds to and cleaves mRNAs that match the small interfering RNA that is bound to it. We transfected INS-1E β-cells with 100 nmol/L sh-β₂AR RNA or sh-scramble RNA using Lipofectamine 2000 (Invitrogen) according to the manufacturer's instructions. Assays were performed at least 3 days after shRNA transfection. Membrane fractions from pancreatic tissue, isolated islets, and INS-1E β-cells were used for

radioligand-binding studies to assess the density of ARs as previously described and validated (35,36,38,39).

Real-time RT-PCR analysis. Total cellular RNA was isolated from INS-1E β-cells, isolated islets, and pancreatic tissue samples with the RNeasy kit (Qiagen, Germantown, MD), according to the manufacturer's instructions, as previously described (31,40). PCRs were analyzed using SYBR Green mix (Invitrogen). Reactions were performed in triplicate using Platinum SYBR Green qPCR Super-UDG by means of an iCycler IQ multicolor Real Time PCR Detection system (Bio-Rad, Hercules, CA). Cyclophilin was used as an internal standard. Primer sequences are reported in Supplementary Table 2.

Immunoblotting. Immunoblot analysis was performed as previously described (31,37). Blots were probed with mouse monoclonal antibodies against adenylate cyclase type VI (AC-VI) (Abcam, Cambridge, MA), pancreatic and duodenal homeobox (PDX)-1, GLUT2, peroxisome proliferator-activated receptor (PPAR)γ, G-protein-coupled receptor (GRK)2, G protein α_s (Gα_s), clathrin heavy chain, and actin (Santa Cruz Biotechnology). Experiments were performed in triplicate to ensure reproducibility. Membrane extracts were obtained as previously described (29,38). Data are presented as arbitrary units using actin as internal control (clathrin heavy chain for membrane extracts) as indicated.

Measurement of cAMP production in vitro and ex vivo. Intracellular content of cAMP was determined using a cAMP^{125I}-scintillation proximity assay (GE Healthcare, Piscataway, NJ) according to the manufacturer's instructions. Briefly, we used 20 size-matched islets (for the ex vivo assays) and 4,000 cells/well INS-1E (for the in vitro assays). Islets and β-cells were washed once and preincubated at 37°C in HEPES-buffered Krebs-Ringer solution containing 1 mmol/L glucose and 0.5 mmol/L isobutylmethylxanthine (a phosphodiesterase inhibitor) for 1 h and incubated for another 15 min in the same buffer with or without 100 μmol/L forskolin (MP Biomedicals, Solon, OH), 3 mmol/L NaF (Thermo Fisher Scientific, Pittsburgh, PA), or 1 μmol/L isoproterenol (Tocris Bioscience, Ellisville, MO). The reaction was stopped by addition of 50 mmol/L HCl and neutralized with NaOH. The cAMP levels were normalized to the protein concentration.

Statistical analysis. All data are presented as means ± SE. Statistical differences were determined by one-way or two-way ANOVA as appropriate, and Bonferroni post hoc testing was performed when applicable. A *P* value <0.05 was considered significant. Statistical analysis was performed using GraphPad Prism (version 5.01; GraphPad Software Inc., San Diego, CA).

RESULTS

Metabolic phenotype of β₂AR^{-/-} mouse. To investigate in vivo the relevance of the β₂AR gene in the regulation of insulin secretion, we compared the metabolic phenotype of adult (6 months old) β₂AR^{-/-} and β₂AR^{+/+} mice. Blood glucose was significantly higher in the null mice compared with that in their wild-type littermates both upon fasting and under random feeding conditions (Table 1). In addition, their fasting serum insulin levels were significantly reduced (Table 1). Upon glucose loading (GTT), the β₂AR^{-/-} mice displayed a marked reduction in glucose tolerance (Fig. 1A and B). In β₂AR^{+/+} mice, we observed a threefold increase in insulin secretion 3 min after intraperitoneal glucose injection, presumably corresponding with the peak of first-phase insulin release. This was followed by a decrease at 10

TABLE 1
Metabolic characteristics of adult (6 months old) wild-type and knockout mice

	β ₂ AR ^{+/+}	β ₂ AR ^{-/-}
<i>n</i>	15	14
Body weight (g)	29.6 ± 1.1	28.2 ± 0.7
Food intake (g/day)	3.1 ± 0.6	3.1 ± 0.8
Water intake (mL/day)	5.8 ± 0.6	6.3 ± 0.9*
Random-fed blood glucose (mg/dL)	170.1 ± 12.3	198.4 ± 11.1*
Fasting blood glucose (mg/dL)	75.7 ± 8.2	135.3 ± 11.5*
Fasting serum insulin (ng/mL)	0.41 ± 0.03	0.30 ± 0.07*

Data are means ± SE unless otherwise indicated. **P* < 0.05 vs. β₂AR^{+/+}.

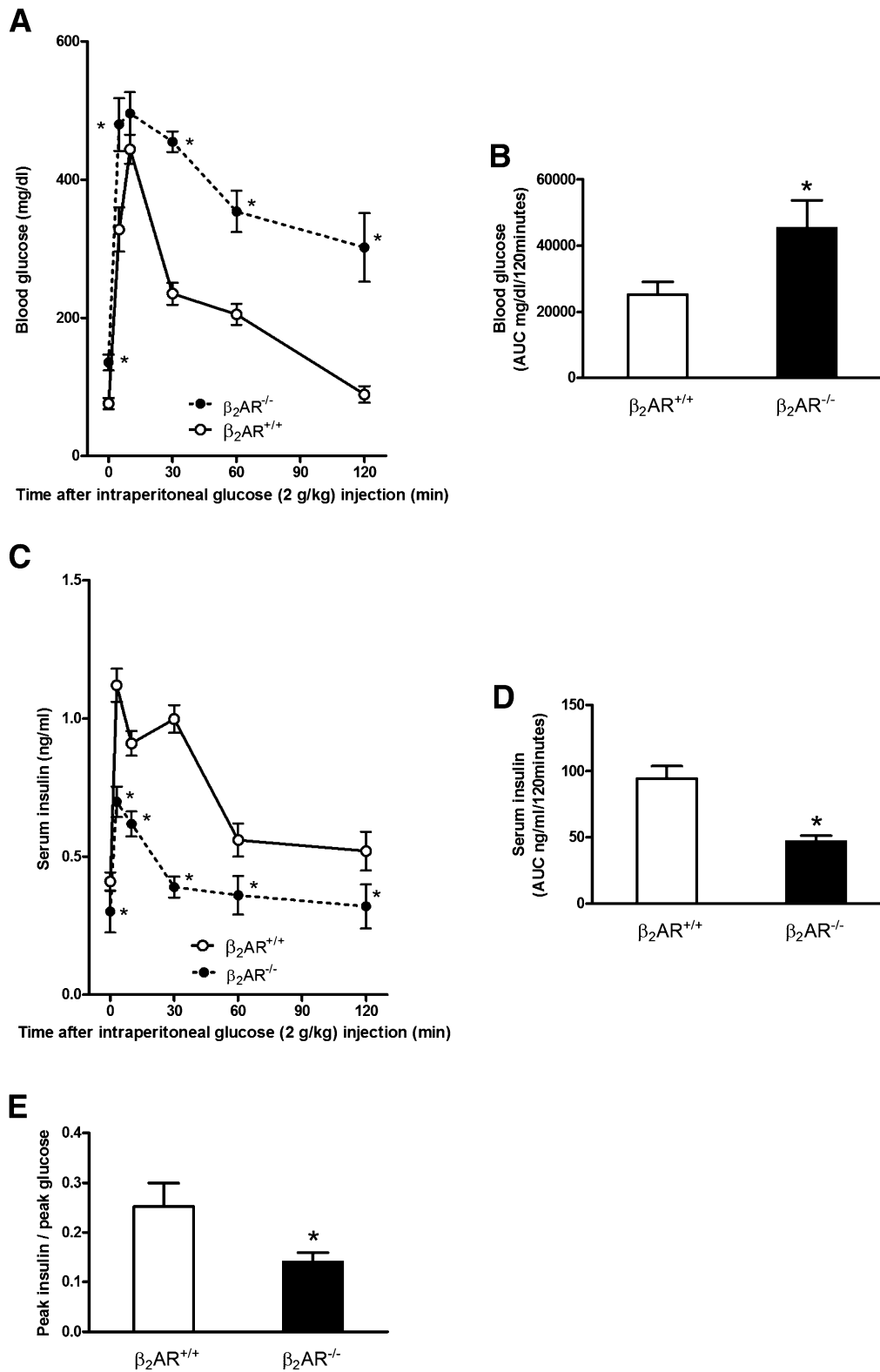


FIG. 1. Metabolic profile of $\beta_2AR^{-/-}$ mice. Six-month-old $\beta_2AR^{-/-}$ mice and their wild-type littermates ($\beta_2AR^{+/+}$) were fasted for 16 h and subjected to intraperitoneal glucose loading (2 g/kg body weight). Blood glucose (A and B) and serum insulin (C and D) were monitored for 120 min after glucose administration ($n = 14-18$ animals per group). $\beta_2AR^{-/-}$ mice displayed glucose intolerance (A) and impaired insulin secretion (C). We calculated the AUC from glucose (B) and insulin excursion (D) curves. Peak insulin-to-peak glucose ratio (E) represents β -cell function, as better described in RESEARCH DESIGN AND METHODS. Bars represent means \pm SE. * $P < 0.05$ vs. $\beta_2AR^{+/+}$, Bonferroni post hoc test. AUC, area under the curve.

min and then a gradual increase over 30 min that may indicate a second-phase response (27,41).

In $\beta_2AR^{-/-}$ mice, the early phase of insulin secretory response to glucose was reduced by more than twofold. The late response was also significantly impaired in the $\beta_2AR^{-/-}$ compared with $\beta_2AR^{+/+}$ mice (Fig. 1C and D). The peak insulin-to-peak glucose ratio was also decreased (Fig. 1E), further indicating impaired insulin response to hyperglycemia in the null mice.

To investigate whether the alterations in glucose tolerance identified in the $\beta_2AR^{-/-}$ mice were contributed by deranged glucagon release, we further measured blood glucose and plasma glucagon levels 30 min after insulin administration. Indeed, insulin administration determines a fall in blood glucose and a counterregulatory rise in plasma glucagon (2,30). However, $\beta_2AR^{-/-}$ and $\beta_2AR^{+/+}$ mice exhibited comparable glucose and glucagon responses to insulin administration (Supplementary Fig. 1A and B). Pancreatic islet histology also did not show any significant difference in these mice (Fig. 2A), similar to total insulin and glucagon pancreatic content (Fig. 2B and C).

We then posed the further question of whether the reduced glucose insulin secretion observed in the $\beta_2AR^{-/-}$ mice in vivo may represent the direct consequence of the $\beta_2AR^{-/-}$ lack in the β -cells or whether it is indirectly mediated by other regulatory factors. To answer this question, we analyzed glucose effect on islets isolated from the null mice. As shown in Fig. 2D, these islets responded poorly to increased glucose concentration in the culture medium compared with the islets from their wild-type littermates but were fully responsive to KCl depolarization.

Islets and β -cell profiling after β_2AR deletion. To gain further insight into the mechanism leading to impaired insulin secretion in mice lacking β_2AR , we profiled the expression of different genes relevant to β -cell regulation by real-time RT-PCR of islet mRNA. As shown in Fig. 3A and B, mRNA levels of both *PDX-1* and *GLUT2*, two major genes involved in β -cell function, were decreased in islets from $\beta_2AR^{-/-}$ mice by 75 and 60%, respectively. Also, mRNA levels of the *PDX-1/GLUT2* upstream regulator *PPAR γ* were decreased by 54% compared with islets from wild-type mice (Fig. 3C). Reliable results were obtained in

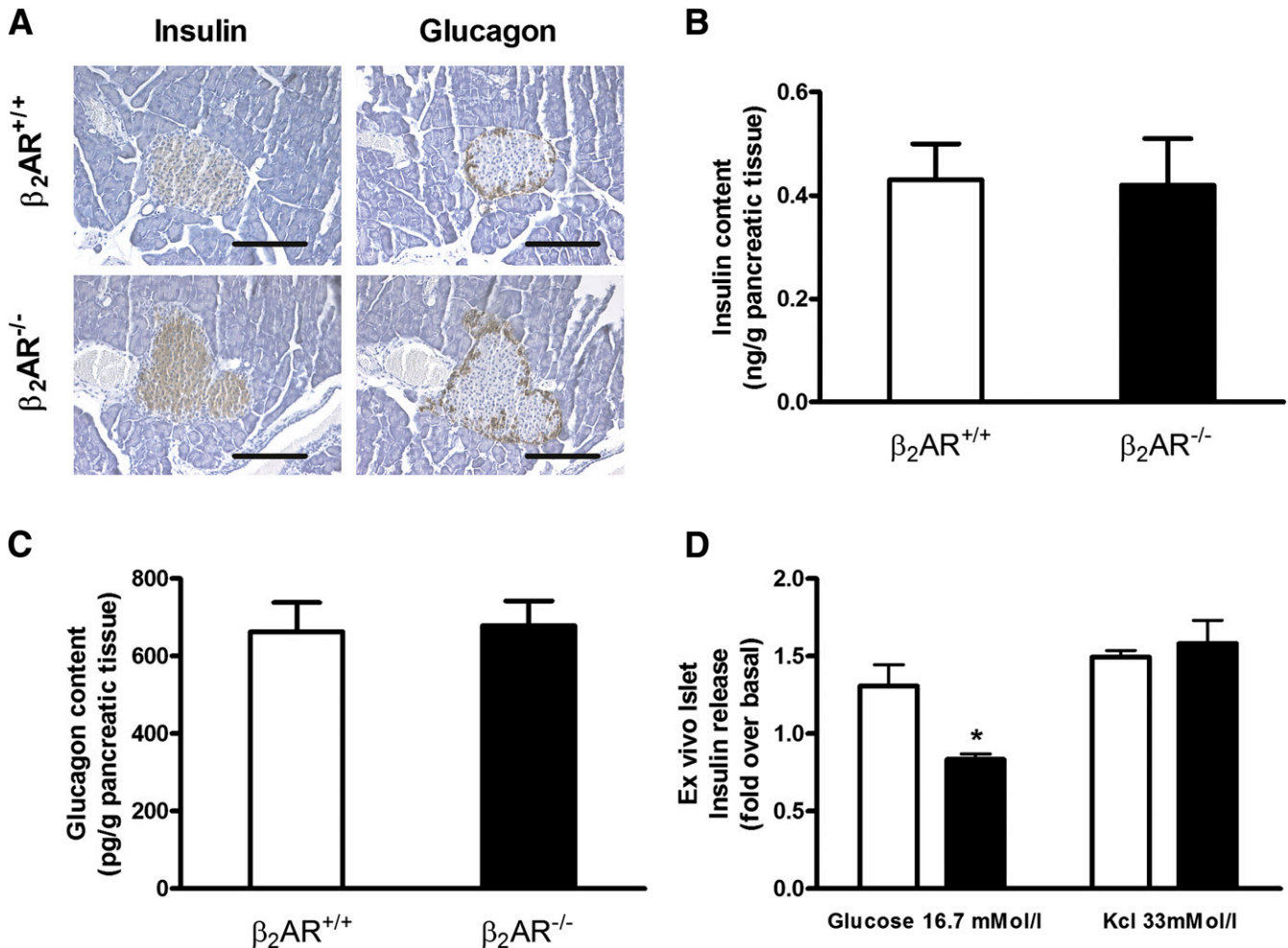


FIG. 2. Comparison of $\beta_2AR^{+/+}$ and $\beta_2AR^{-/-}$ pancreatic islets. Immunohistochemical analysis (A) of the islets was carried out on paraffin sections using insulin (left panel) or glucagon (right panel) antibodies. Microphotographs are representative of images obtained from pancreas sections of five 6-month-old $\beta_2AR^{+/+}$ (upper panel) or $\beta_2AR^{-/-}$ (lower panel) mice. Insulin (B) and glucagon (C) content in isolated islets from $\beta_2AR^{+/+}$ ($n = 10$) or $\beta_2AR^{-/-}$ ($n = 13$) mice. Insulin secretion in response to basal (2.8 mmol/L) or high (16.7 mmol/L) glucose concentration and to KCl (33 mmol/L) was measured in isolated islets from $\beta_2AR^{+/+}$ (□) and $\beta_2AR^{-/-}$ (■) mice (D). Bars represent means \pm SE of data from 10 mice per group. * $P < 0.05$ vs. $\beta_2AR^{+/+}$, Bonferroni post hoc test. (See also Supplementary Fig. 1.) (A high-quality digital representation of this figure is available in the online issue.)

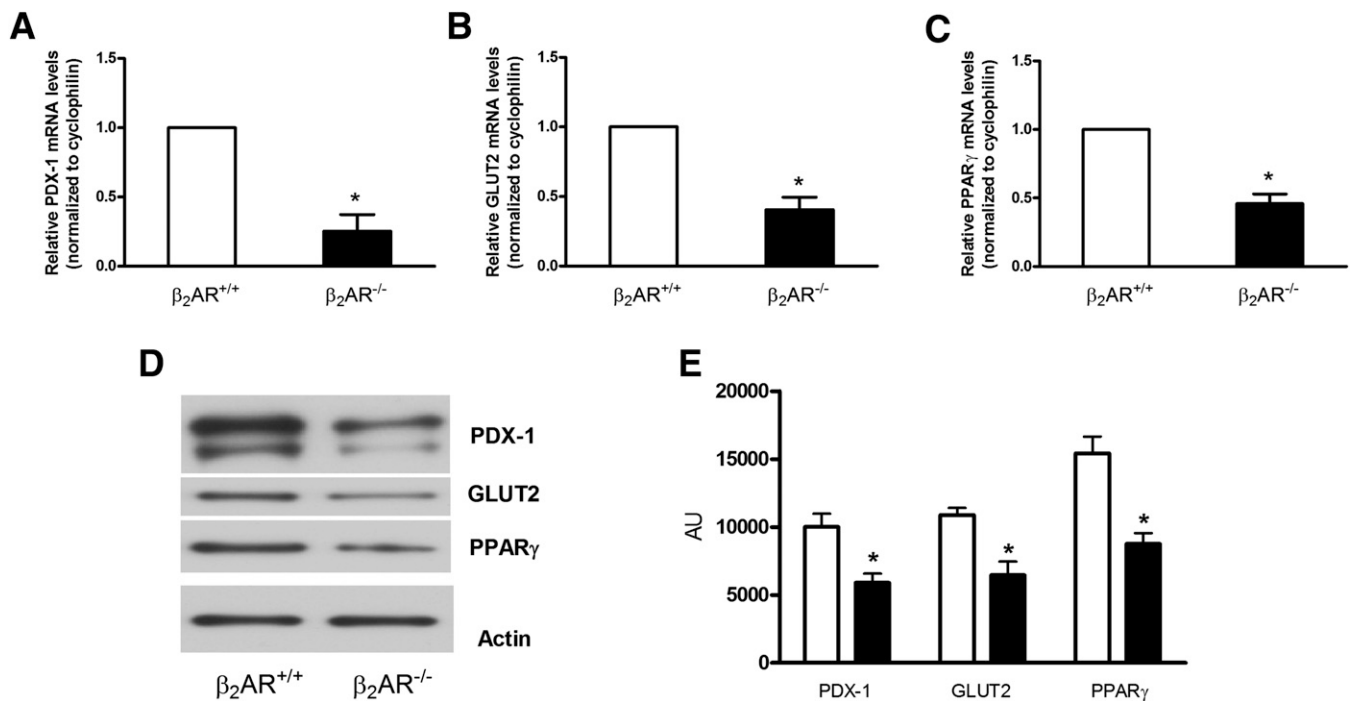


FIG. 3. Gene expression profile in isolated Langerhans islets from $\beta_2AR^{+/+}$ and $\beta_2AR^{-/-}$ mice. The abundance of mRNAs for PDX-1 (A), GLUT2 (B), and PPAR γ (C) was determined by real-time RT-PCR analysis of total RNA, using cyclophilin as internal standard. The mRNA levels in $\beta_2AR^{-/-}$ mice are relative to those in control animals. Each bar represents means \pm SE of four independent experiments in each of which reactions were performed in triplicate using the pooled total RNAs from five mice/genotype. Proteins from a Western blot representative of three independent experiments were quantified by densitometry (D and E). * $P < 0.05$ vs. $\beta_2AR^{+/+}$, Bonferroni post hoc test. AU, arbitrary units.

immunoblotting experiments (Fig. 3D and E). PDX-1 and GLUT2 mRNAs were also reduced to a similar extent in total pancreatic tissue from the $\beta_2AR^{-/-}$ mice (data not shown).

We then sought to demonstrate whether these abnormalities in gene expression were directly caused by β_2AR silencing. To pursue this objective, we silenced with a specific shRNA (Supplementary Fig. 2) the β_2AR gene in the glucose-responsive INS-1E β -cell line (INS-1E $_{sh\beta_2AR}$) (Fig. 4A and B). As shown in Fig. 4C, this specific knock-down impaired glucose-induced insulin secretion by 58% in these cells. A similarly sized effect was achieved by treatment with the specific β_2AR antagonist ICI, while the β_2AR agonist fenoterol showed an opposite action (Supplementary Fig. 3A). Consistent with our ex vivo results, the INS-1E $_{sh\beta_2AR}$ displayed a reduction in PDX-1, GLUT2, and PPAR γ mRNA (Fig. 4D–F) and protein levels (Fig. 4G and H). Interestingly, transient transfection of a PPAR γ cDNA in INS-1E $_{sh\beta_2AR}$ β -cells increased glucose-induced insulin secretion compared with the wild-type INS1-E control β -cells (Fig. 4C). In addition, overexpression of PPAR γ prevented the downregulation of both PDX-1 and GLUT2 occurring in the INS-1E $_{sh\beta_2AR}$ β -cells (Fig. 4D–H). Consistently, treatment of INS-1E β -cells with ICI decreased PDX-1 and GLUT2 mRNA and protein levels, while PPAR γ overexpression completely prevented the effect of ICI (Supplementary Fig. 3B–D), suggesting that β_2AR controls insulin secretion through a PPAR γ /PDX-1-mediated mechanism.

To better define the β_2AR downstream mechanism leading to PPAR γ activation, we assessed the cAMP levels in these cells, observing an impaired production of cAMP in INS-1E $_{sh\beta_2AR}$ β -cells both in basal condition and after stimulation with the βAR agonist isoproterenol (Supplementary

Fig. 4A). Accordingly, to rule out possible involvement of other components of β_2AR signaling machinery, we assessed the protein level of AC-VI, GRK2, and G α_s , and we found no significant difference (Supplementary Fig. 4B and C). Parallel results were obtained in ex vivo experiments, performed to investigate the possible age-related alterations in the β_2AR transduction pathway, comparing pancreatic islets isolated from adult (6 months old) and old (20 months old) $\beta_2AR^{+/+}$ mice (Supplementary Fig. 4D and E).

β_2AR overexpression rescued the age-related impairment in insulin release. Based on radioligand binding and real-time RT-PCR analysis, the expression of both β_2AR protein and mRNA was significantly decreased in islets from aged (20 months old) $\beta_2AR^{+/+}$ mice compared with those isolated from adult (6 months old) mice (Fig. 5A and B). PDX-1, GLUT2, and PPAR γ expression (both in terms of mRNA and protein level) was also reduced, and insulin release in response to glucose, though not that evoked by KCl depolarization, was impaired in islets from the aged mice (Fig. 5C–H), suggesting that the reduced β_2AR density constrains islet glucose response in these animals. To prove this hypothesis, we used an adenoviral construct driving overexpression of human β_2AR in mouse islets. Interestingly, infection of islets isolated from wild-type old mice with this construct induced a twofold increase in β_2AR expression (Fig. 5A and B) and returned glucose-induced insulin secretion to levels comparable with those of islets from 6-month-old mice (Fig. 5C) accompanied by restored expression of PDX-1, GLUT2, and PPAR γ (Fig. 5D–H).

In the in vivo setup, 20-month-old $\beta_2AR^{+/+}$ mice exhibited a significant reduction in fasting serum insulin levels (Table 2) accompanied by impaired glucose tolerance and

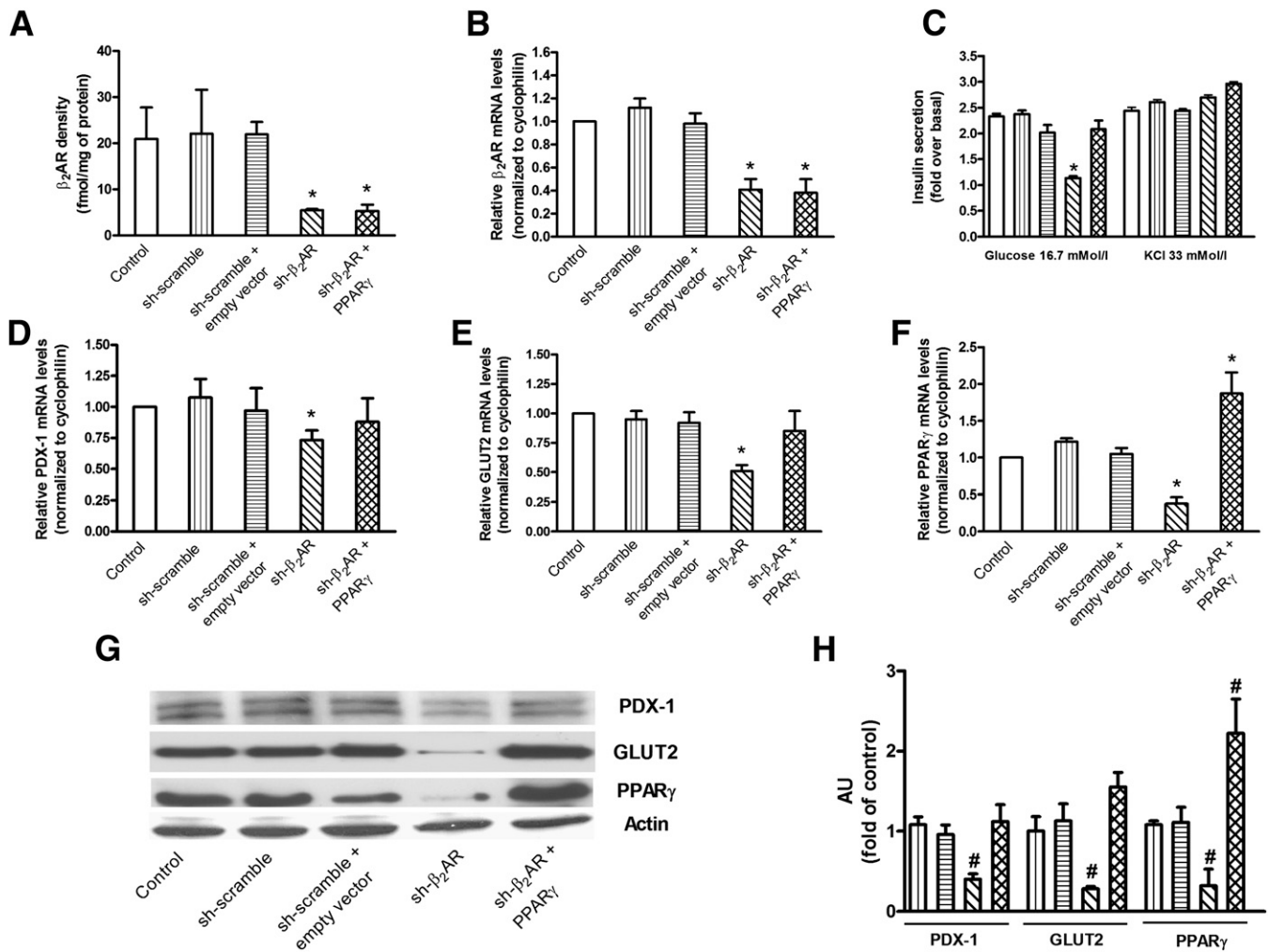


FIG. 4. β_2 AR levels, glucose-stimulated insulin secretion, and gene expression profile in silenced INS-1E β -cells. Treatment with a specific β_2 AR-shRNA significantly decreased the density (by 73.7% [A]) and mRNA levels (by 59.1% [B]) of β_2 AR in INS-1E β -cells. β_2 AR-shRNA inhibited the insulin secretory response to 16.7 mmol/L glucose, which was rescued by the overexpression of PPAR γ (C). KCl-induced insulin release (C) was not significantly different among the studied groups. β_2 AR-shRNA also determined a significant reduction in mRNA level of PDX-1 (D), GLUT2 (E), and PPAR γ (F) that was prevented by the overexpression of PPAR γ . Bars represent means \pm SE from four to five independent experiments in each of which reactions were performed in triplicate (□, control, i.e. untreated INS-1E β -cells; ▨, sh-scramble; ▩, sh-scramble+empty vector; ▤, sh- β_2 AR; ▥, sh- β_2 AR+PPAR γ ; * P < 0.05 vs. control, Bonferroni post hoc test; basal is glucose 2.8 mmol/L. Equal amount of proteins from three independent experiments was analyzed by Western blotting and quantified by densitometry (G and H). * P < 0.05 vs. sh-scramble. AU, arbitrary units. (See also Supplementary Figs. 2–4.)

insulin response upon GTT (Fig. 6A–E). We have therefore designed a gene therapy protocol aimed to prove that these abnormalities can be corrected by restoring β_2 AR density. Accordingly, we infected the pancreas of aged mice by Ad β_2 AR injection. This injection effectively rescued β_2 AR expression in the pancreatic tissue, returning it to levels comparable with those of 6-month-old mice (Supplementary Fig. 5A and B), and restored the expression of PDX-1, GLUT2, and PPAR γ (Supplementary Fig. 5C–E). Injections in the distal pancreas did not induce β_2 AR expression in other tissues, such as the liver (Supplementary Fig. 6A and B) or the skeletal muscle (Supplementary Fig. 6C and D).

These effects were paralleled by significant improvement in glucose tolerance and insulin secretion during GTT (Fig. 6A–E). Fasting insulin levels also increased, reaching values similar to those measured in 6-month-old mice (Table 2), further underlining the relevance of β_2 AR function in enabling adequate pancreatic β -cell response to hyperglycemia.

DISCUSSION

In the present work, we provide evidence that β_2 AR gene deletion in mice causes reduction of glucose-stimulated insulin release by pancreatic β -cells. This phenotype is reminiscent of that observed in mice with targeted β -cell disruption of the $G\alpha_s$ gene (30). In these mice, however, the impairment of $G\alpha_s$ prevented response to multiple $G\alpha_s$ -related receptors, causing a severe phenotype, with gross abnormalities in pancreatic islets. Interestingly, in islets from β_2 AR $^{-/-}$ mice, PPAR γ expression was reduced by 50%, leading to repression of the PPAR γ downstream molecules PDX-1 and GLUT2, two key effectors of β -cell function (26,42,43). This downregulation resulted in a clear impairment in insulin release, though islet architecture and insulin content were not affected by the β_2 AR gene deletion.

Rosen et al. (44) showed that islets from mice with targeted elimination of PPAR γ in β -cells were approximately twice as large as those from control mice. Thus, we can speculate that in our model the 50% reduction in

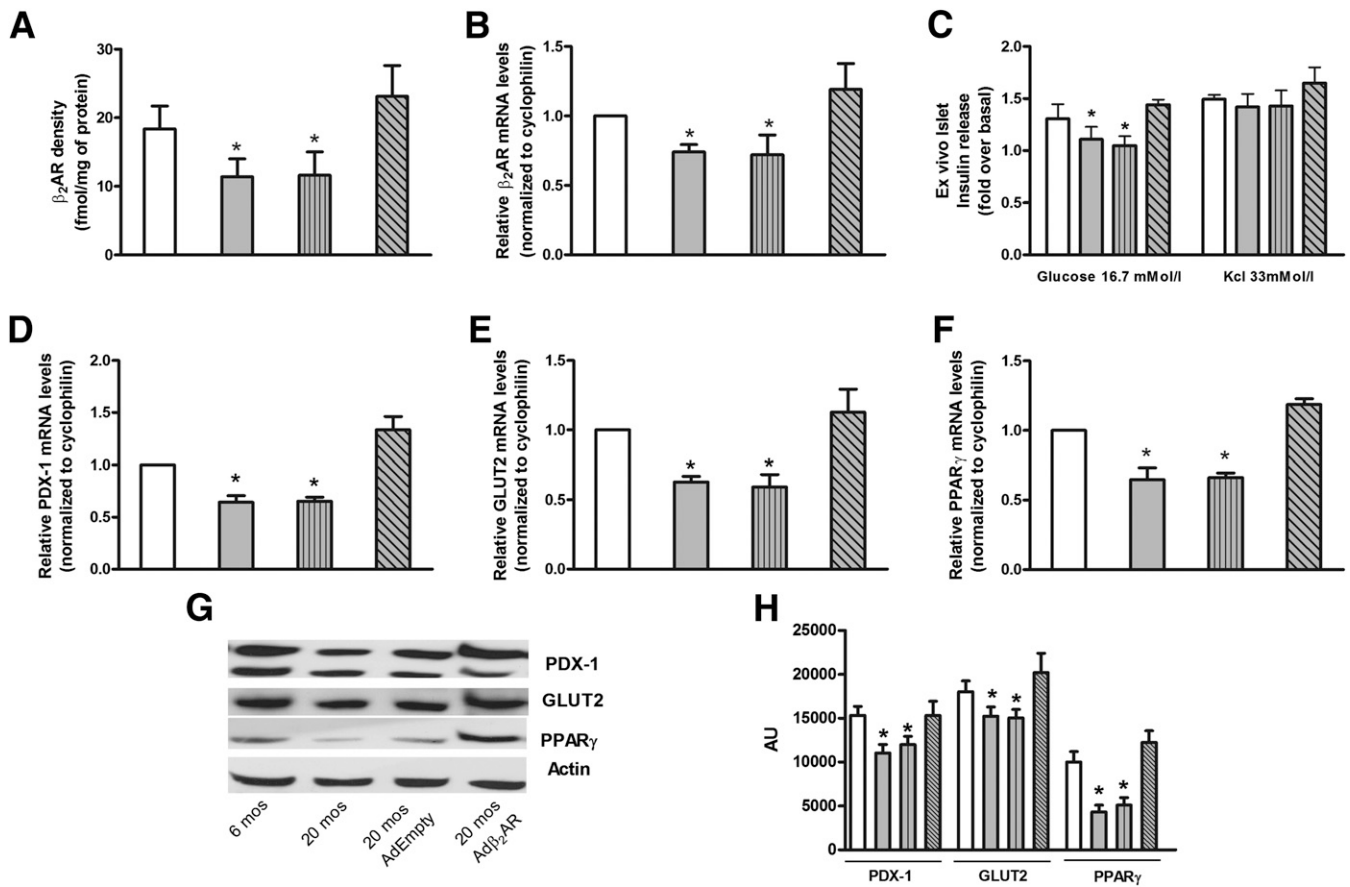


FIG. 5. β_2AR ex vivo infection rescued age-dependent impairment of β -cell function. Density (A) and mRNA levels (B) of β_2AR were evaluated on cell membranes of islets isolated from $\beta_2AR^{+/+}$ mice. Insulin release (C) was determined upon exposure to the indicated concentration of glucose or KCl as described in RESEARCH DESIGN AND METHODS. mRNA levels of PDX-1 (D), GLUT2 (E), and PPAR γ (F) were determined by real-time RT-PCR using the pooled total RNAs from five mice/group with cyclophilin as internal standard. Each bar represents means \pm SE of five independent experiments in each of which reactions were performed in triplicate. Islets isolated from $\beta_2AR^{+/+}$ mice were solubilized and aliquots of the lysates were blotted with PDX-1, GLUT2, and PPAR γ antibodies. Actin was used as loading control. The autoradiographs shown (G) are representative of three independent experiments, which are quantified in H. \square , age 6 months (mos); \blacksquare , 20 months; ▨ , 20 months AdEmpty; ▩ , 20 months Ad β_2AR . * $P < 0.05$ vs. $\beta_2AR^{+/+}$ 6 months, Bonferroni post hoc test.

PPAR γ levels is sufficient to restrain β -cell function without altering islet mass.

The mechanistic significance of β_2AR gene knockout was further sustained by in vitro studies in the INS-1E pancreatic β -cells, showing that the silencing of the β_2AR as well as the pharmacological treatment with a specific β_2AR antagonist impaired glucose response and down-regulated PPAR γ expression, reducing both PDX-1 and GLUT2 levels. No alteration of αARs was observed instead

(data not shown). In addition, treatment with the β_2AR agonist fenoterol activated PPAR γ /PDX-1/GLUT2 signaling, indicating that, at least in part, β_2AR controls insulin secretion through this pathway. Indeed, in this study we show that exogenous PPAR γ expression in INS-1E β -cells silenced for β_2AR led to recovery of PDX-1/GLUT2 levels and glucose-stimulated insulin secretion. This finding is supported by recent evidence that directly relates β_2AR to PPAR γ (42,45–47), a key element in the process of insulin

TABLE 2
Metabolic effects of β_2AR overexpression in aged (20 months old) $\beta_2AR^{+/+}$ mice

	20 months old			6 months old
	Untreated	AdEmpty	Ad β_2AR	Untreated
<i>n</i>	10	6	8	15
Body weight (g)	38.4 \pm 1.7*	38.1 \pm 2.4*	38.6 \pm 2.1*	29.6 \pm 1.1
Food intake (g/day)	4.0 \pm 1.1*	4.2 \pm 1.8*	3.9 \pm 1.5*	3.1 \pm 0.6
Water intake (mL/day)	6.8 \pm 1.2*	6.9 \pm 1.7*	6.6 \pm 1.8*	5.8 \pm 0.6
Random-fed blood glucose (mg/dL)	176.5 \pm 8.6	178.4 \pm 12.7	173.2 \pm 10.4	170.1 \pm 12.3
Fasting blood glucose (mg/dL)	84.2 \pm 10.4	83.6 \pm 11.9	77.7 \pm 11.7	75.7 \pm 8.2
Fasting serum insulin (ng/mL)	0.32 \pm 0.04*	0.33 \pm 0.05*	0.42 \pm 0.1	0.41 \pm 0.03

Data are means \pm SE unless otherwise indicated. * $P < 0.05$ vs. adult (6 months old) $\beta_2AR^{+/+}$ mice.

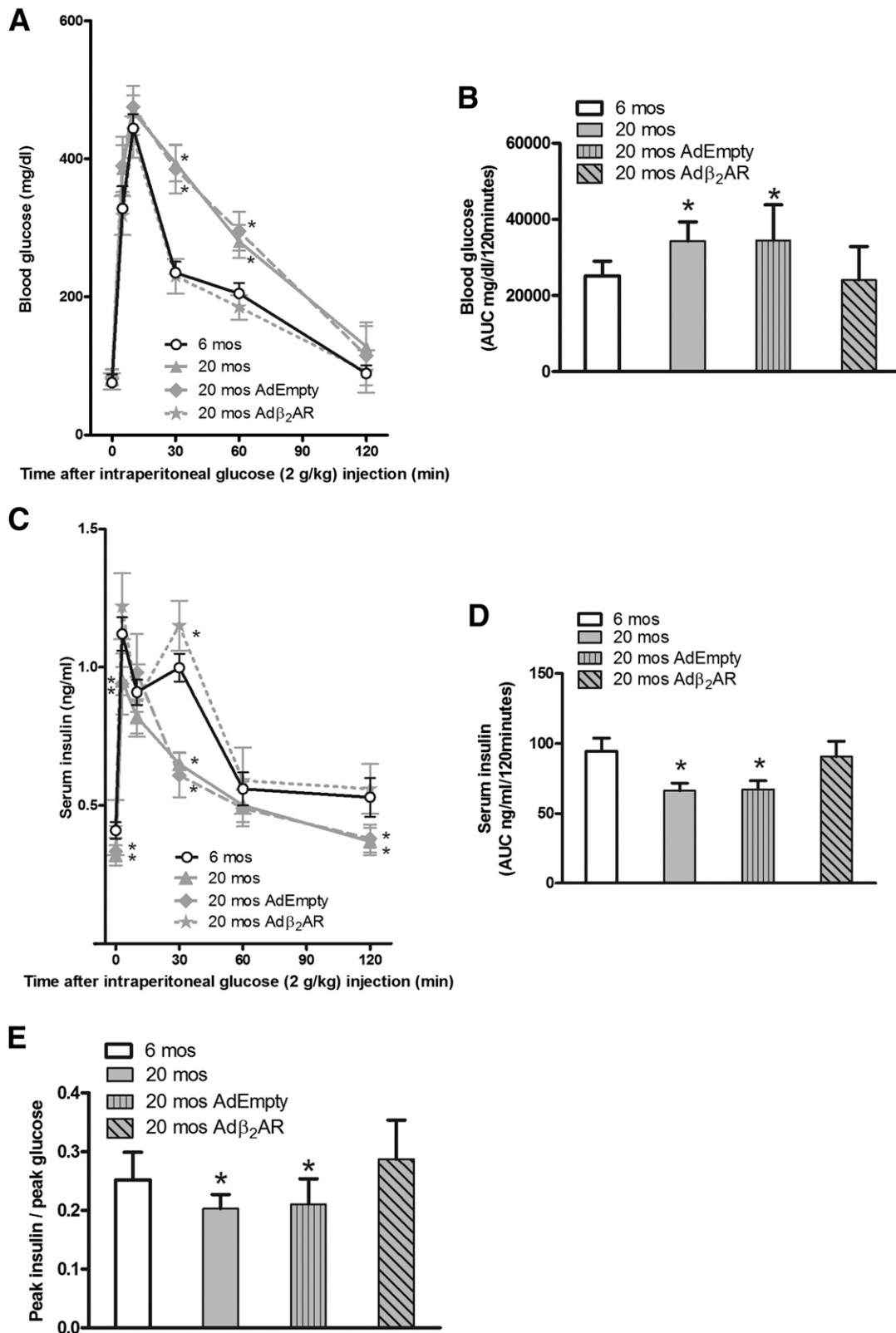


FIG. 6. Adenoviral vector-mediated β_2 AR gene transfer in the mouse pancreas rescued age-related reduction in glucose tolerance. Blood glucose levels (A) and serum insulin (C) after 120 min of glucose administration ($n = 14$ – 18 animals per group). We calculated the AUC from glucose (B) and insulin excursion (D) curves. Twenty-month-old β_2 AR $^{+/+}$ mice showed glucose intolerance (A and B), impaired insulin secretion (C and D), and also an impairment in β -cell function, evaluated measuring the peak insulin-to-peak glucose ratio (E). All of these parameters were restored after Ad β_2 AR in vivo infection. * $P < 0.05$ vs. β_2 AR $^{+/+}$ at 6 months (mos) of age, Bonferroni post hoc test. (See also Supplementary Figs. 5 and 6.)

secretion that has also recently been investigated in aging (43,48). Our results are consistent with these observations, sustaining also the hypothesis that cAMP levels could act as a connecting link through which β_2 AR signaling leads to activation of PPAR γ (49,50). Moreover, the cAMP assays, performed both in INS-1E_{sh β_2 AR} pancreatic β -cells and in islets isolated from aged mice, showed an impairment in basal conditions and after stimulation with isoproterenol, while the responses to NaF and forskolin were not affected. Also, G α_s and AC-VI protein levels were not significantly different among the explored settings. This combination of events is usually observed in models of β_2 AR gene deletion or impaired β_2 AR signaling (18,34).

Whether and to what extent β_2 AR gene knockout in liver and peripheral tissues affects glucose homeostasis in the β_2 AR^{-/-} mice remain to be conclusively addressed. Indeed, variations at the β_2 AR locus have also been reported to associate with insulin resistance in type 2 diabetic patients (16). However, as shown in this work, the impaired glucose tolerance of β_2 AR^{-/-} mice is likely contributed by the defective β -cell function, as indicated by the major effect of β_2 AR lack on glucose-evoked insulin secretion.

In humans, glucose tolerance declines with age, resulting in a high prevalence of type 2 diabetes and impaired glucose tolerance in the elderly population (2,8). How, at the individual level, glucose tolerance declines remains unclear, but it is likely determined by multiple factors including diminished insulin secretion (3,7). In rat models and in humans, a progressive decline in β -cell activity with age has been documented (4,6). In the present work, we show that the same occurs in the C57Bl/6N mouse and is paralleled by the development of abnormal glucose tolerance. Similar to previous findings in several human tissues (18–21,24), our results show that these changes are accompanied by reduced β_2 AR levels in mouse pancreatic islets. The decreased β_2 AR density in islets from aged mice recapitulates the mechanisms leading to the insulin secretory defect occurring in β_2 AR-null mice, indicating that it may contribute to the age-related impairment in glucose tolerance. Indeed, both in vivo and ex vivo experiments of β_2 AR gene transfer revealed that recovery of normal β_2 AR levels rescued insulin release and glucose tolerance in aged mice. Thus, in the mouse model progressive decline of islet β_2 AR density appears to contribute to the reduction in glucose tolerance that accompanies aging. Whether the same also occurs in humans needs to be clarified and is currently under investigation in our laboratory.

In conclusion, we have shown that β_2 AR physiologically regulates pancreatic β -cell insulin secretion by modulating PPAR γ /PDX-1/GLUT2 function. Reduced β_2 AR expression contributes to the age-dependent deterioration of glucose tolerance.

ACKNOWLEDGMENTS

The financial support of Telethon and Fondazione Veronesi is gratefully acknowledged.

No potential conflicts of interest relevant to this article were reported.

G.S. conceived the project, performed experiments, analyzed data, and wrote the manuscript. A.L. performed experiments, analyzed data, and wrote the manuscript. D.S. performed experiments and contributed to discussion. A.A. performed experiments. C.D.G. performed experiments. P.F. analyzed data and contributed to discussion. F.B. analyzed data and wrote the manuscript. B.T. designed

research and supervised the project. C.M. analyzed data and wrote the manuscript. G.I. designed research, analyzed data, and wrote the manuscript. G.S. and G.I. are the guarantors of this work and, as such, had full access to all the data in the study and take responsibility for the integrity of the data and the accuracy of the data analysis.

The authors thank Brian Kobilka (Stanford University, Stanford, CA) for providing the founders of β_2 AR^{-/-} mice, Pierre Maechler (University of Geneva, Geneva, Switzerland) for supplying INS-1E pancreatic β -cells, and Walter J. Koch (Center for Translational Medicine, and Thomas Jefferson University, Philadelphia, PA) for providing the Ad β_2 AR. The valuable technical assistance of Alfonso Anastasio ("San Giovanni di Dio" Hospital, Frattaminore, Italy) is also acknowledged.

REFERENCES

- Defronzo RA. Banting Lecture. From the triumvirate to the ominous octet: a new paradigm for the treatment of type 2 diabetes mellitus. *Diabetes* 2009;58:773–795
- Basu R, Breda E, Oberg AL, et al. Mechanisms of the age-associated deterioration in glucose tolerance: contribution of alterations in insulin secretion, action, and clearance. *Diabetes* 2003;52:1738–1748
- Gumbiner B, Polonsky KS, Beltz WF, Wallace P, Brechtel G, Fink RI. Effects of aging on insulin secretion. *Diabetes* 1989;38:1549–1556
- Ma X, Becker D, Arena VC, Vicini P, Greenbaum C. The effect of age on insulin sensitivity and insulin secretion in first-degree relatives of type 1 diabetic patients: a population analysis. *J Clin Endocrinol Metab* 2009;94:2446–2451
- Reaven E, Wright D, Mondon CE, Solomon R, Ho H, Reaven GM. Effect of age and diet on insulin secretion and insulin action in the rat. *Diabetes* 1983;32:175–180
- Perfetti R, Rafizadeh CM, Liotta AS, Egan JM. Age-dependent reduction in insulin secretion and insulin mRNA in isolated islets from rats. *Am J Physiol* 1995;269:E983–E990
- Ihm SH, Matsumoto I, Sawada T, et al. Effect of donor age on function of isolated human islets. *Diabetes* 2006;55:1361–1368
- Iozzo P, Beck-Nielsen H, Laakso M, Smith U, Yki-Järvinen H, Ferrannini E; European Group for the Study of Insulin Resistance. Independent influence of age on basal insulin secretion in nondiabetic humans. *J Clin Endocrinol Metab* 1999;84:863–868
- Rosengren AH, Jokubka R, Tojjar D, et al. Overexpression of alpha2A-adrenergic receptors contributes to type 2 diabetes. *Science* 2010;327:217–220
- Doyle ME, Egan JM. Pharmacological agents that directly modulate insulin secretion. *Pharmacol Rev* 2003;55:105–131
- Lembo G, Napoli R, Capaldo B, et al. Abnormal sympathetic overactivity evoked by insulin in the skeletal muscle of patients with essential hypertension. *J Clin Invest* 1992;90:24–29
- Seals DR, Esler MD. Human ageing and the sympathoadrenal system. *J Physiol* 2000;528:407–417
- Lembo G, Capaldo B, Rendina V, et al. Acute noradrenergic activation induces insulin resistance in human skeletal muscle. *Am J Physiol* 1994;266:E242–E247
- Asensio C, Jimenez M, Kühne F, Rohner-Jeanraud F, Muzzin P. The lack of beta-adrenoceptors results in enhanced insulin sensitivity in mice exhibiting increased adiposity and glucose intolerance. *Diabetes* 2005;54:3490–3495
- Haffner CA, Kendall MJ. Metabolic effects of beta 2-agonists. *J Clin Pharm Ther* 1992;17:155–164
- Ikarashi T, Hanyu O, Maruyama S, et al. Genotype Gly/Gly of the Arg16Gly polymorphism of the beta2-adrenergic receptor is associated with elevated fasting serum insulin concentrations, but not with acute insulin response to glucose, in type 2 diabetic patients. *Diabetes Res Clin Pract* 2004;63:11–18
- Scarpace PJ, Mooradian AD, Morley JE. Age-associated decrease in beta-adrenergic receptors and adenylate cyclase activity in rat brown adipose tissue. *J Gerontol* 1988;43:B65–B70
- Xiao RP, Tomhave ED, Wang DJ, et al. Age-associated reductions in cardiac beta1- and beta2-adrenergic responses without changes in inhibitory G proteins or receptor kinases. *J Clin Invest* 1998;101:1273–1282
- Schocken DD, Roth GS. Reduced beta-adrenergic receptor concentrations in aging man. *Nature* 1977;267:856–858

20. Feldman RD, Limbird LE, Nadeau J, Robertson D, Wood AJ. Alterations in leukocyte beta-receptor affinity with aging. A potential explanation for altered beta-adrenergic sensitivity in the elderly. *N Engl J Med* 1984;310: 815–819
21. Bao X, Mills PJ, Rana BK, et al. Interactive effects of common beta2-adrenoceptor haplotypes and age on susceptibility to hypertension and receptor function. *Hypertension* 2005;46:301–307
22. Kang KB, Rajanayagam MA, van der Zyppe A, Majewski H. A role for cyclooxygenase in aging-related changes of beta-adrenoceptor-mediated relaxation in rat aortas. *Naunyn Schmiedeberg Arch Pharmacol* 2007;375: 273–281
23. Ryall JG, Plant DR, Gregorevic P, Sillence MN, Lynch GS. Beta 2-agonist administration reverses muscle wasting and improves muscle function in aged rats. *J Physiol* 2004;555:175–188
24. White M, Roden R, Minobe W, et al. Age-related changes in beta-adrenergic neuroeffector systems in the human heart. *Circulation* 1994;90:1225–1238
25. Chruscinski AJ, Rohrer DK, Schauble E, Desai KH, Bernstein D, Kobilka BK. Targeted disruption of the beta2 adrenergic receptor gene. *J Biol Chem* 1999;274:16694–16700
26. Evans-Molina C, Robbins RD, Kono T, et al. Peroxisome proliferator-activated receptor gamma activation restores islet function in diabetic mice through reduction of endoplasmic reticulum stress and maintenance of euchromatin structure. *Mol Cell Biol* 2009;29:2053–2067
27. Vigliotta G, Miele C, Santopietro S, et al. Overexpression of the ped/pea-15 gene causes diabetes by impairing glucose-stimulated insulin secretion in addition to insulin action. *Mol Cell Biol* 2004;24:5005–5015
28. Santulli G, Basilicata MF, De Simone M, et al. Evaluation of the anti-angiogenic properties of the new selective $\alpha v \beta 3$ integrin antagonist RGDechiHCit. *J Transl Med* 2011;9:7
29. Sorriento D, Santulli G, Fusco A, Anastasio A, Trimarco B, Iaccarino G. Intracardiac injection of AdGRK5-NT reduces left ventricular hypertrophy by inhibiting NF-kappaB-dependent hypertrophic gene expression. *Hypertension* 2010;56:696–704
30. Xie T, Chen M, Zhang QH, Ma Z, Weinstein LS. Beta cell-specific deficiency of the stimulatory G protein alpha-subunit Gsalpha leads to reduced beta cell mass and insulin-deficient diabetes. *Proc Natl Acad Sci USA* 2007;104: 19601–19606
31. Lombardi A, Ulianich L, Treglia AS, et al. Increased hexosamine biosynthetic pathway flux dedifferentiates INS-1E cells and murine islets by an extracellular signal-regulated kinase (ERK)1/2-mediated signal transmission pathway. *Diabetologia* 2012;55:141–153
32. Fiory F, Lombardi A, Miele C, Giudicelli J, Béguinot F, Van Obberghen E. Methylglyoxal impairs insulin signalling and insulin action on glucose-induced insulin secretion in the pancreatic beta cell line INS-1E. *Diabetologia* 2011; 54:2941–2952
33. McGraw DW, Forbes SL, Mak JC, et al. Transgenic overexpression of beta (2)-adrenergic receptors in airway epithelial cells decreases bronchoconstriction. *Am J Physiol Lung Cell Mol Physiol* 2000;279:L379–L389
34. Mutlu GM, Dumasius V, Burhop J, et al. Upregulation of alveolar epithelial active Na⁺ transport is dependent on beta2-adrenergic receptor signaling. *Circ Res* 2004;94:1091–1100
35. Ciccarelli M, Sorriento D, Cipolletta E, et al. Impaired neoangiogenesis in $\beta 2$ -adrenoceptor gene-deficient mice: restoration by intravascular human $\beta 2$ -adrenoceptor gene transfer and role of NF κ B and CREB transcription factors. *Br J Pharmacol* 2011;162:712–721
36. Iaccarino G, Ciccarelli M, Sorriento D, et al. Ischemic neoangiogenesis enhanced by beta2-adrenergic receptor overexpression: a novel role for the endothelial adrenergic system. *Circ Res* 2005;97:1182–1189
37. Sorriento D, Ciccarelli M, Santulli G, et al. The G-protein-coupled receptor kinase 5 inhibits NFkappaB transcriptional activity by inducing nuclear accumulation of IkappaB alpha. *Proc Natl Acad Sci USA* 2008;105:17818–17823
38. Perino A, Ghigo A, Ferrero E, et al. Integrating cardiac PIP3 and cAMP signaling through a PKA anchoring function of p110 γ . *Mol Cell* 2011;42: 84–95
39. Ciccarelli M, Santulli G, Campanile A, et al. Endothelial alpha1-adrenoceptors regulate neo-angiogenesis. *Br J Pharmacol* 2008;153:936–946
40. Oriente F, Iovino S, Cassese A, et al. Overproduction of phosphoprotein enriched in diabetes (PED) induces mesangial expansion and upregulates protein kinase C-beta activity and TGF-beta1 expression. *Diabetologia* 2009;52:2642–2652
41. Mauvais-Jarvis F, Virkamaki A, Michael MD, et al. A model to explore the interaction between muscle insulin resistance and beta-cell dysfunction in the development of type 2 diabetes. *Diabetes* 2000;49:2126–2134
42. Faisy C, Pinto FM, Blouquit-Laye S, et al. beta2-Agonist modulates epithelial gene expression involved in the T- and B-cell chemotaxis and induces airway sensitization in human isolated bronchi. *Pharmacol Res* 2010;61:121–128
43. Blalock EM, Phelps JT, Pancani T, et al. Effects of long-term pioglitazone treatment on peripheral and central markers of aging. *PLoS ONE* 2010;5: e10405
44. Rosen ED, Kulkarni RN, Sarraf P, et al. Targeted elimination of peroxisome proliferator-activated receptor gamma in beta cells leads to abnormalities in islet mass without compromising glucose homeostasis. *Mol Cell Biol* 2003;23:7222–7229
45. Collins S, Yehuda-Shnaidman E, Wang H. Positive and negative control of Ucp1 gene transcription and the role of β -adrenergic signaling networks. *Int J Obes (Lond)* 2010;34(Suppl. 1):S28–S33
46. Fogli S, Pellegrini S, Adinolfi B, et al. Rosiglitazone reverses salbutamol-induced $\beta(2)$ -adrenoceptor tolerance in airway smooth muscle. *Br J Pharmacol* 2011;162:378–391
47. Tadaishi M, Miura S, Kai Y, et al. Effect of exercise intensity and AICAR on isoform-specific expressions of murine skeletal muscle PGC-1 α mRNA: a role of β -adrenergic receptor activation. *Am J Physiol Endocrinol Metab* 2011;300:E341–E349
48. Sung B, Park S, Yu BP, Chung HY. Modulation of PPAR in aging, inflammation, and calorie restriction. *J Gerontol A Biol Sci Med Sci* 2004;59:997–1006
49. Guri AJ, Hontecillas R, Bassaganya-Riera J. Abscisic acid synergizes with rosiglitazone to improve glucose tolerance and down-modulate macrophage accumulation in adipose tissue: possible action of the cAMP/PKA/PPAR γ axis. *Clin Nutr* 2010;29:646–653
50. Kim SP, Ha JM, Yun SJ, et al. Transcriptional activation of peroxisome proliferator-activated receptor-gamma requires activation of both protein kinase A and Akt during adipocyte differentiation. *Biochem Biophys Res Commun* 2010;399:55–59

SUPPLEMENTARY DATA

Supplementary Table 1. shRNA sequences

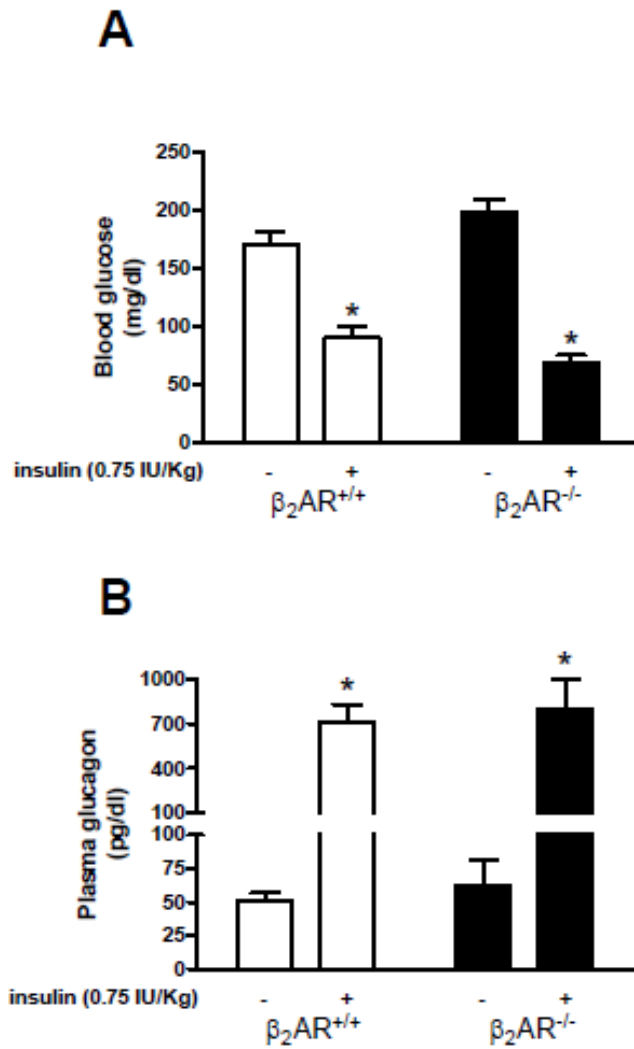
	5'- 3'
shRNA scramble	GCUGACGUAUCCUAAAUGUGUAAUA
shRNA β_2AR	CCACAAGCAAGCCAUCGACUGUUAU
shRNA β_2AR (x)	GGGAGGAAACUGUAAACACAAACGACU
shRNA β_2AR (y)	GAAGGUCCUCCAAAGUUCUGCUUGAA

Supplementary Table 2. Real Time RT-PCR primer sequences (5'- 3')

	Forward	Reverse
β_2AR (rat)	ACGAGGATGGGAGGAGCGGG	GGTTGGCCCCGGATGACGTGG
β_2AR (mouse)	GAGTGTGCAGGACGCACCCC	CTGTCGTTCCC GTGTGGCCC
PDX-1 (rat and mouse)	AAAACCGTCGCATGAAGTGG	CCCGCTACTACGTTTCTTATCT
GLUT2 (rat and mouse)	ACAGTCACACCAGCATAAC	ACCCACCAAAGAATGAGG
PPARγ (mouse)	ACGGGGTCTCGGTTGAGGGG	AGTTGGTGGGCCAGAATGGCA
PPARγ (rat)	AAGGTGCTCCAGAAGATGACA	TCAGCGACTGGGACTTTTCT
Cyclophilin (rat and mouse)	GCAGACAAAGTTCCAAAGACAG	CACCCTGGCACATGAATCC

SUPPLEMENTARY DATA

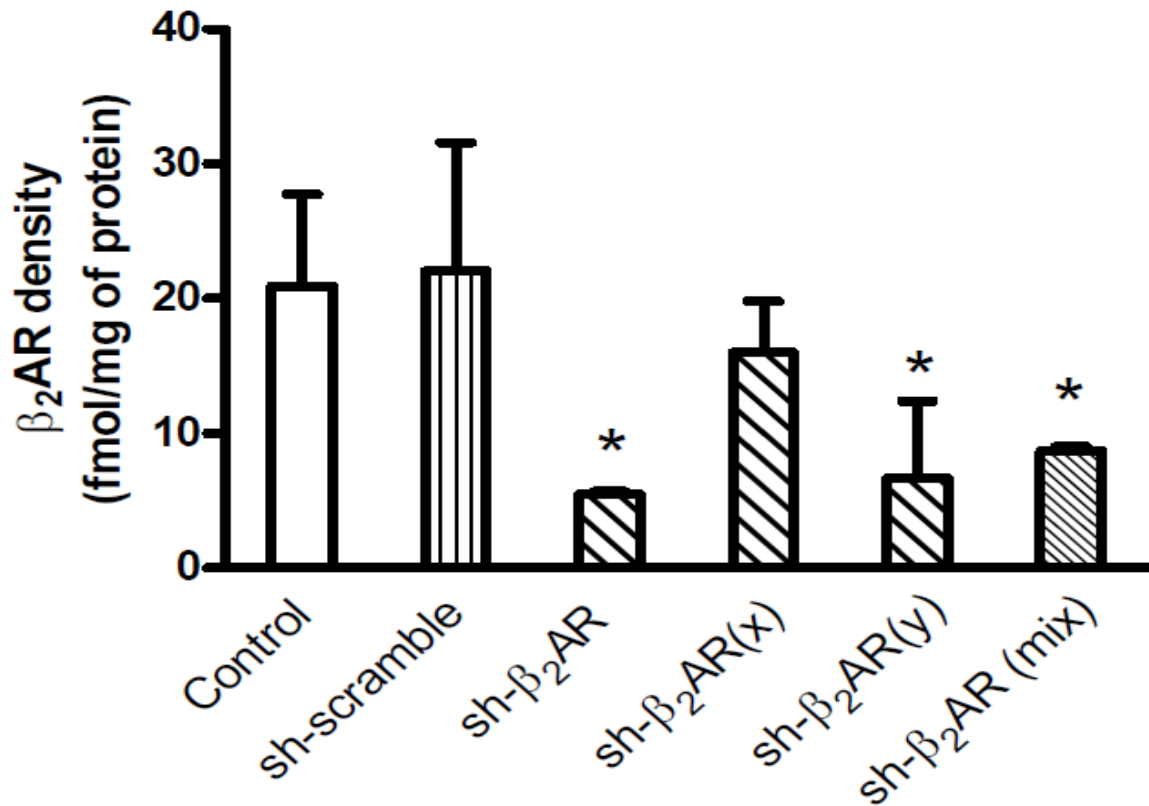
Supplementary Figure 1. Blood glucose and plasma glucagon assessed after intraperitoneal insulin administration. Blood glucose (A) and plasma glucagon (B), evaluated in basal (random fed) conditions and 30 minutes after intraperitoneal administration of insulin (0.75 IU/Kg), were not significantly different among the two studied groups of adult (6-month-old) mice. Each bar represents the mean±SE of eight independent experiments. *:p<0.05 vs basal condition; Bonferroni *post hoc* test.







SUPPLEMENTARY DATA

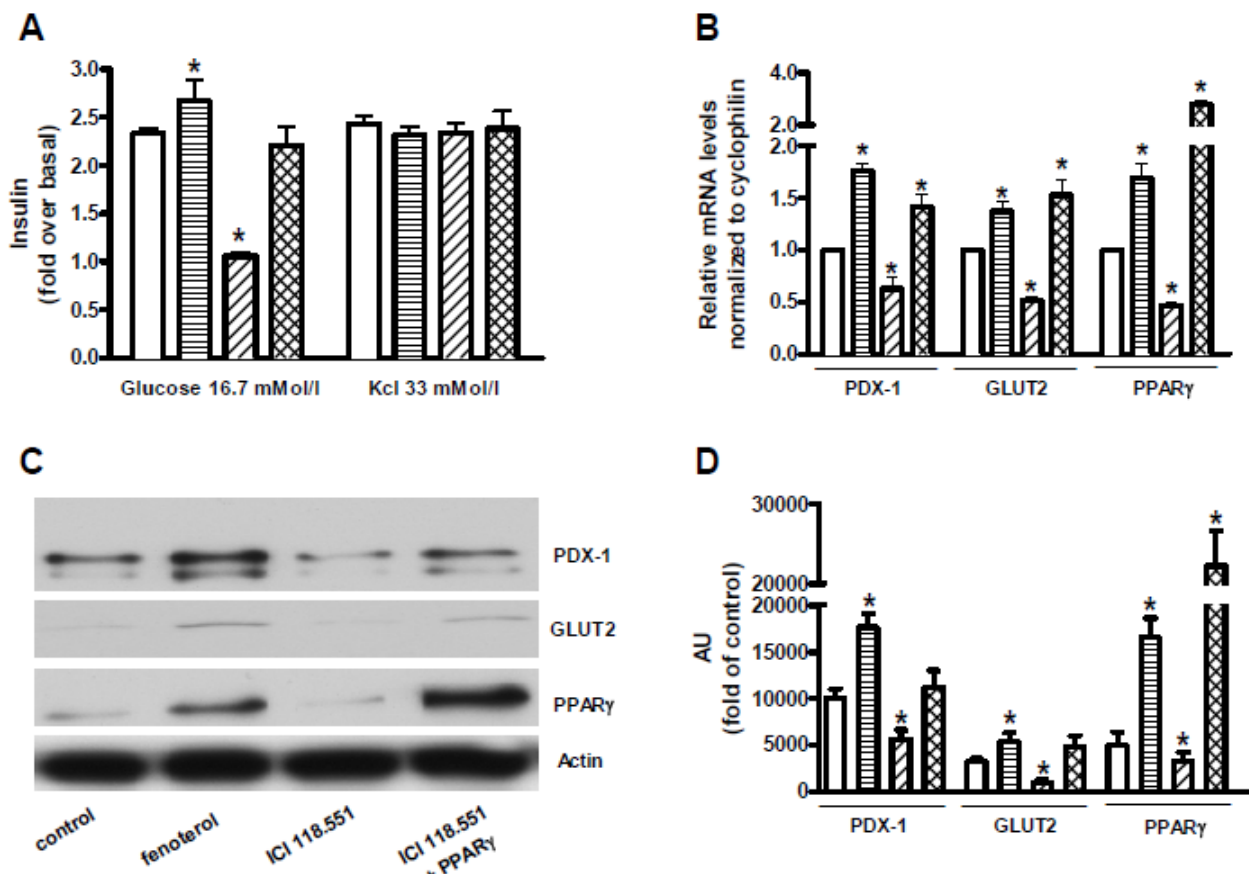
Supplementary Figure 2. β_2 AR silencing in pancreatic INS-1E β -cells.

To silence the expression of β_2 AR in INS-1E β -cells, we designed (sequences are shown in Supplementary Table 1) three shRNA, namely sh- β_2 AR, sh- β_2 AR(x), sh- β_2 AR(y). We decide to use the first one, which showed the best effectiveness, inducing a 73.7% decrease in the membrane density of β_2 AR, also better than the pooled mix of the three sh- β_2 AR. Each bar represents mean \pm SE from five independent experiments in each of whom reactions were performed in triplicate. *:p<0.05 vs control; Bonferroni *post hoc* test).



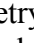
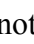


Supplementary Figure 3. Pharmacological modulation of β_2 AR.

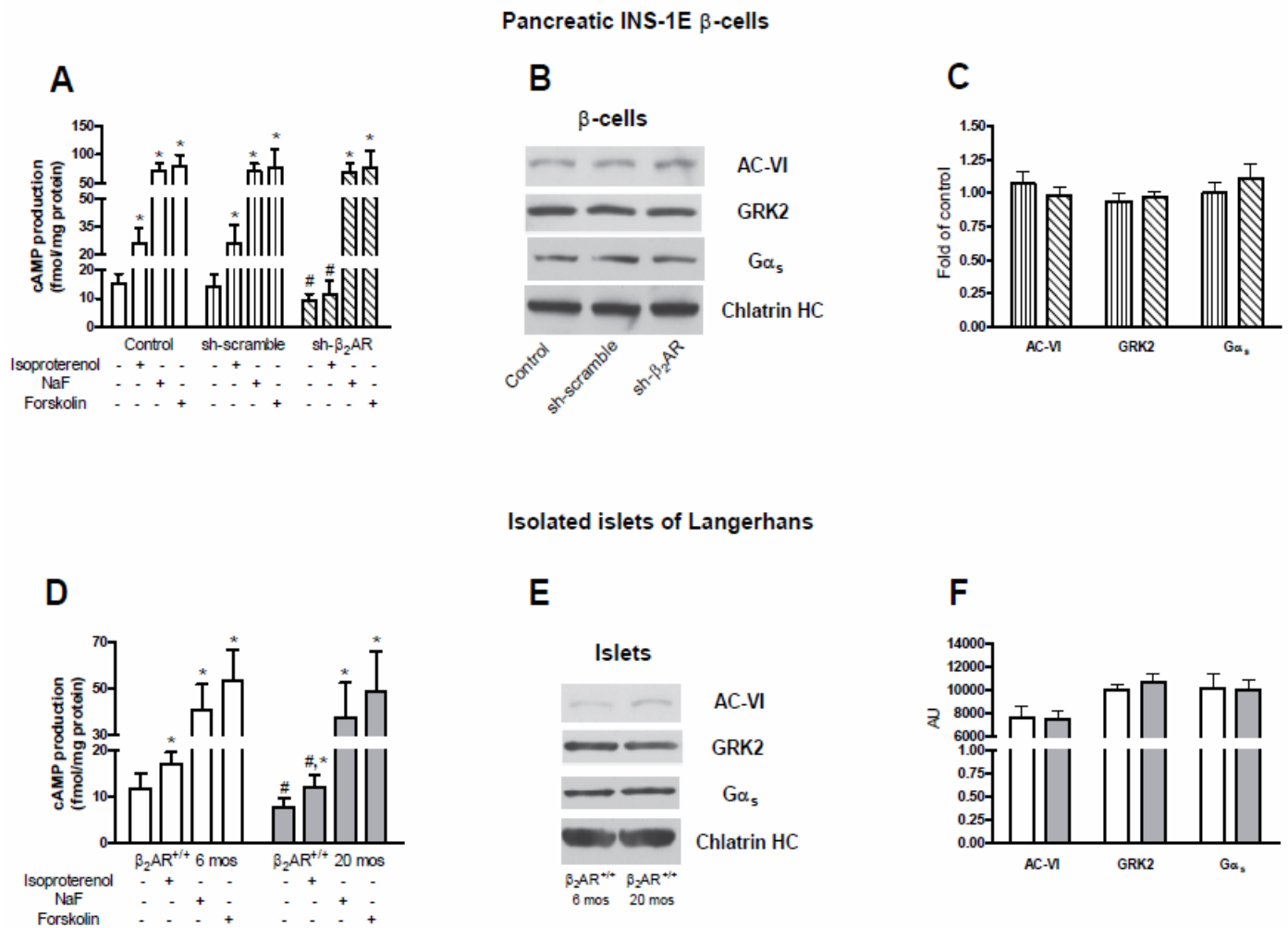
INS-1E pancreatic β -cells were incubated (1 hour) with the β_2 AR selective agonist fenoterol (1 μ Mol/l) or antagonist ICI 118.551 (ICI, 0.1 μ Mol/l). This latter inhibited the insulin secretory response to 16.7 mMol/l glucose, that was completely rescued by overexpression of PPAR γ (A). Neither fenoterol nor ICI determined significant changes in KCl-induced insulin release. Each bar represents the mean \pm SE from five independent experiments in each of whom reactions were performed in triplicate. (*:p<0.05 vs control, *i.e.* untreated INS-1E β -cells; Bonferroni *post hoc* test; basal is glucose 2.8 mMol/l). Fenoterol treatment caused a marked rise in mRNA level of PDX-1 (by 76%), GLUT2 (by 53%) and PPAR γ (by 80.5%). On the contrary, ICI determined a significant decrease in mRNA level of the same genes: PDX-1 (by 37%), GLUT2 (by 48%) and PPAR γ (by 53%), compared to untreated INS-1E β -cells (B). Bars represent the mRNA levels in treated cells and are relative to those in control cells; data are expressed as mean \pm SE of triplicate reactions for total RNA from each group in four independent experiments. Reliable results were obtained from western blot analysis (C-D); representative images (C) of triplicate experiments are shown; actin was used as loading control; bar graph in panel D show densitometry. *:p<0.05 vs control, *i.e.* untreated INS-1E cells; Bonferroni *post hoc* test; : control, *i.e.* untreated INS-1E cells; : fenoterol; : ICI 118.551; : ICI 118.551 + PPAR γ .



SUPPLEMENTARY DATA


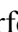


Supplementary Figure 4. Assessment of β_2AR downstream.

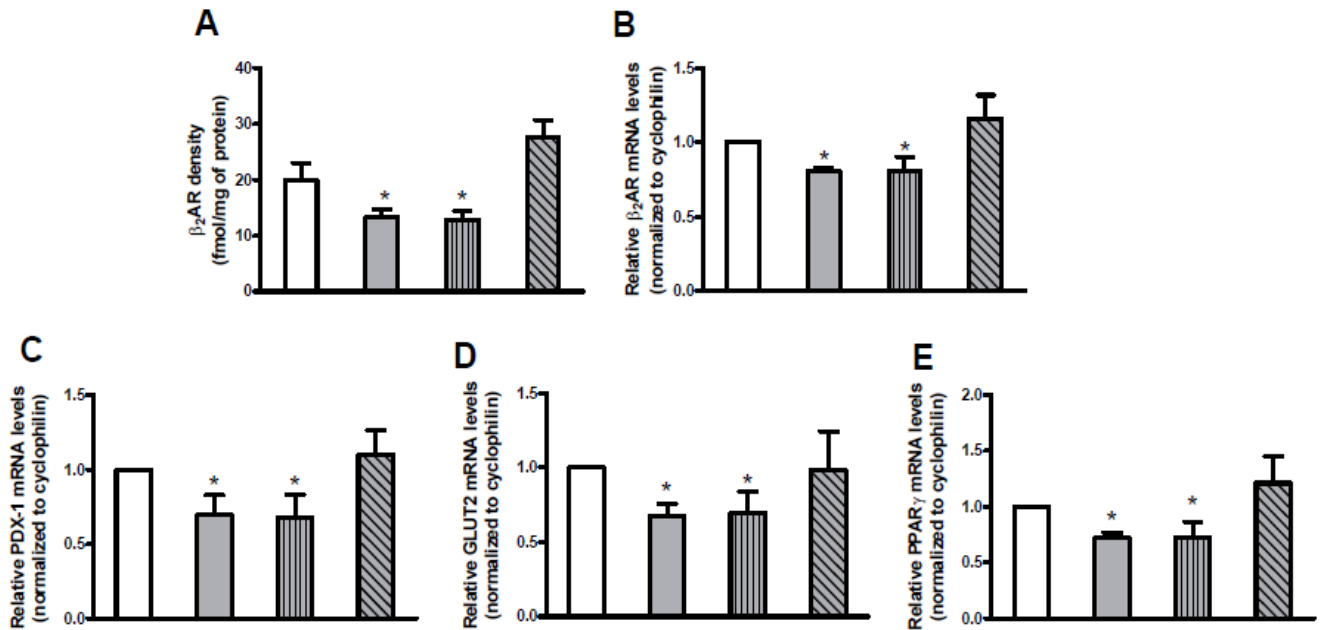
In vitro (A-C) and *ex vivo* (D-F) experiments were performed to investigate cAMP production and β_2AR downstream. cAMP levels (A, D) were measured in basal condition and after stimulation with isoproterenol (1 $\mu\text{Mol/l}$), NaF (3 mMol/l) and forskolin 100 $\mu\text{Mol/l}$, as described in RESEARCH DESIGN AND METHODS. Each bar represents the mean \pm SE of four independent experiments in each of whom reactions were performed in triplicate. We found an impaired cAMP production in basal conditions and after stimulation with isoproterenol both in INS-1E_{sh β_2AR} β -cells (A, *:p<0.05 vs unstimulated INS-1E β -cells; #:p<0.05 vs control) and in islets of Langerhans isolated from 20-month-old $\beta_2AR^{+/+}$ mice (D, *:p<0.05 vs unstimulated islets; #:p<0.05 vs $\beta_2AR^{+/+}$ 6 mos). We assessed by Western blot (B,E) protein levels of adenylate cyclase type VI (AC-VI), GRK2 and $G\alpha_s$ on membrane extracts, using chlatrin heavy chain (chlatrin HC) as loading control. Representative images of three independent experiments are shown. We quantified blots by densitometry in INS-1E pancreatic β -cells (B,  : sh-scramble;  : sh- β_2AR ; *:p<0.05 vs sh-scramble) and in isolated islets (E,  : 6 mos,  : 20 mos; *:p<0.05 vs $\beta_2AR^{+/+}$ 6 mos). Control indicates INS-1E β -cells not treated with shRNA; AU indicates arbitrary units; mos is months of age.



SUPPLEMENTARY DATA

Supplementary Figure 5. Efficacy of β_2AR *in vivo* infection.

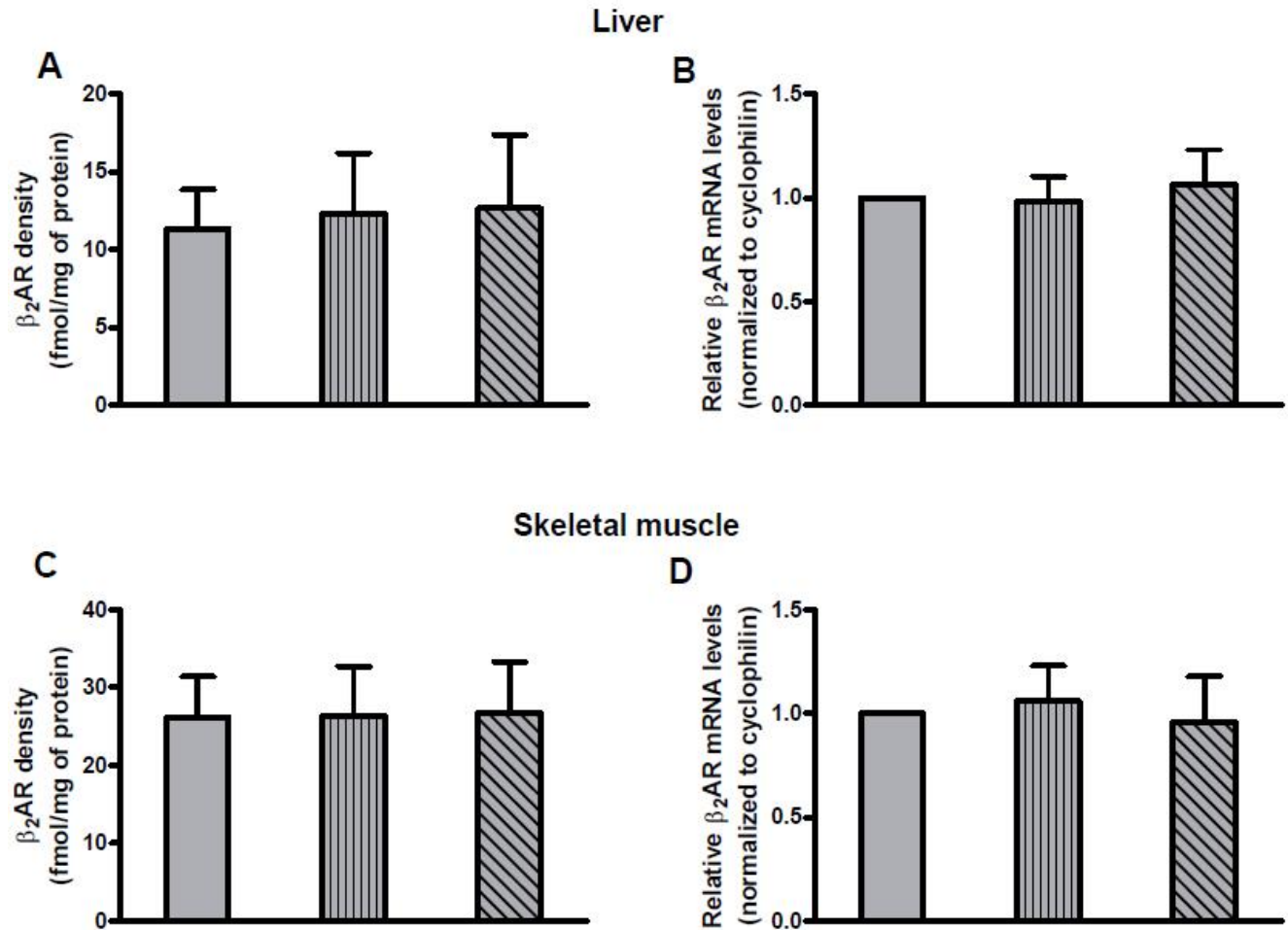
Assessment of β_2AR expression on cell membranes of pancreatic tissue from $\beta_2AR^{+/+}$ mice after β_2AR overexpression *in vivo*. β_2AR density (A) was evaluated by radioligand assay. mRNA levels of β_2AR (B), PDX-1 (C), GLUT2 (D) and PPAR γ (E) were determined by Real-time RT-PCR using the pooled total RNAs from four mice/group, using cyclophilin as internal standard. AdEmpty: Pancreata infected with a control adenovirus; Ad β_2AR : Pancreata infected with an adenovirus encoding for the human β_2AR gene. Each bar represents the mean \pm SE of four independent experiments in each of whom reactions were performed in triplicate; : 6 mos, : 20 mos, : 20 mos Adempty, : 20 mos Ad β_2AR ; *:p<0.05 vs $\beta_2AR^{+/+}$ 6 mos; Bonferroni *post hoc* test; mos is months of age.



SUPPLEMENTARY DATA

Supplementary Figure 6. Effect of Ad β_2 AR pancreatic injection on liver and muscle.

The localized injections in the distal pancreas do not induce β_2 AR expression in other tissues. Density (A, C) and mRNA levels (B, D) of β_2 AR were evaluated on cell membranes of liver and quadriceps muscle (C, D) from β_2 AR^{+/+} mice. mRNA levels were determined by Real-time RT-PCR using the pooled total RNAs from four mice/group with cyclophilin as internal standard. Each bar represents the mean \pm SE of five independent experiments in each of whom reactions were performed in triplicate. ■: 20 mos, ▨: 20 mos Adempty, ▩: 20 mos Ad β_2 AR; AdEmpty: Mice infected with a control adenovirus; Ad β_2 AR: Mice infected with an adenovirus encoding for the human β_2 AR gene; mos is months of age.



Coronary Heart Disease Risk Factors and Mortality

To the Editor: Dr Canto and colleagues¹ found that hospital mortality increased as the number of cardiovascular risk factors declined. This inverse relationship is perplexing and the potential explanations discussed by the authors appear not completely satisfactory.

The authors just considered the number of risk factors, whereas the severity of each factor was not evaluated. Blood pressure, plasma glucose, and lipids are continuous, not discrete, variables that exert a dose-dependent effect on cardiovascular risk.² It would be of interest to see the results of the analysis conducted considering these parameters, which also would help to clarify the still controversial association of the metabolic syndrome and mortality after myocardial infarction (MI).³

It also would be interesting to know if the inverse correlation is still present after correction for one of the most important predictors of mortality after acute coronary syndrome,⁴ the baseline infarct size.

Last, traditional cardiovascular risk factors do not fully explain the pathophysiological process of atherothrombosis in acute ischemic heart disease. Several studies have identified a series of emerging biomarkers reflecting thrombosis, inflammation, and oxidative stress.⁵ Do the authors have any data about this issue?

Gaetano Santulli, MD

Author Affiliation: Columbia University Medical Center, New York, New York (gs2620@columbia.edu).

Conflict of Interest Disclosures: The author has completed and submitted the ICMJE Form for Disclosure of Potential Conflicts of Interest and none were reported.

1. Canto JG, Kiefe CI, Rogers WJ, et al; NRMI Investigators. Number of coronary heart disease risk factors and mortality in patients with first myocardial infarction. *JAMA*. 2011;306(19):2120-2127.
2. D'Agostino RB Sr, Vasan RS, Pencina MJ, et al. General cardiovascular risk profile for use in primary care: the Framingham Heart Study. *Circulation*. 2008;117(6):743-753.
3. Petersen JL, Yow E, AlJaroudi W, et al. Metabolic syndrome is not associated with increased mortality or cardiovascular risk in nondiabetic patients with a new diagnosis of coronary artery disease. *Circ Cardiovasc Qual Outcomes*. 2010;3(2):165-172.
4. Wu E, Ortiz JT, Tejedor P, et al. Infarct size by contrast enhanced cardiac magnetic resonance is a stronger predictor of outcomes than left ventricular ejection fraction or end-systolic volume index: prospective cohort study. *Heart*. 2008;94(6):730-736.
5. Wang TJ, Gona P, Larson MG, et al. Multiple biomarkers for the prediction of first major cardiovascular events and death. *N Engl J Med*. 2006;355(25):2631-2639.

To the Editor: The study by Dr Canto and colleagues¹ provides an example of an epidemiological phenomenon that deserves wider recognition. Differential selection from an underlying population cohort into a study data set can reverse the direction of observed associations, making a deleterious factor appear protective. It is well-known that conditioning on a variable that is affected by both an exposure and outcome can produce a distortion

known as selection bias.² Admission into the analysis data set in this study was a function of both the exposure (number of cardiovascular risk factors) and the outcome (all-cause, in-hospital, or 30-day mortality) because deaths occurring before hospitalization and patients with existing cardiovascular disease diagnoses were excluded. Approximately 30% of MIs lead to death prior to hospitalization.³ In the study, 75% of those who were admitted to the hospital after their MI were excluded (1.62 million of 2.16 million; Figure 1 in the article).

The combined effect of these 2 selection mechanisms means that individuals with more cardiovascular risk factors were more likely to be excluded. If an increased number of risk factors accelerate mortality so that more events occur in the prehospital window rather than during hospitalization or 30-day follow-up, risk factors will appear to be protective.⁴ The study results are therefore understandable in terms of selection bias and require no elaborate speculation about pathophysiological processes¹ or "novel but as-yet uncharacterized and deadly CVD [cardiovascular disease] risk factors."⁵

Hailey R. Banack, MA
Sam Harper, PhD
Jay S. Kaufman, PhD

Author Affiliations: Department of Epidemiology, Biostatistics, and Occupational Health, McGill University, Toronto, Ontario, Canada (hailey.banack@mail.mcgill.ca).

Conflict of Interest Disclosures: The authors have completed and submitted the ICMJE Form for Disclosure of Potential Conflicts of Interest. Dr Harper reported receiving a grant to his institution from Fonds de recherche du Québec-Santé. Dr Kaufman reported holding an endowed chair from the federal government of Canada. Ms Banack reported no disclosures.

1. Canto JG, Kiefe CI, Rogers WJ, et al; NRMI Investigators. Number of coronary heart disease risk factors and mortality in patients with first myocardial infarction. *JAMA*. 2011;306(19):2120-2127.
2. Hernán MA, Hernández-Díaz S, Robins JM. A structural approach to selection bias. *Epidemiology*. 2004;15(5):615-625.
3. Chambless L, Keil U, Dobson A, et al; WHO MONICA Project. Population versus clinical view of case fatality from acute coronary heart disease: results from the WHO MONICA Project 1985-1990. *Circulation*. 1997;96(11):3849-3859.

GUIDELINES FOR LETTERS. Letters discussing a recent *JAMA* article should be submitted within 4 weeks of the article's publication in print. Letters received after 4 weeks will rarely be considered. Letters should not exceed 400 words of text and 5 references and may have no more than 3 authors. Letters reporting original research should not exceed 600 words of text and 6 references and may have no more than 5 authors. They may include up to 2 tables or figures but online supplementary material is not allowed. All letters should include a word count. Letters must not duplicate other material published or submitted for publication. Letters not meeting these specifications are generally not considered. Letters will be published at the discretion of the editors and are subject to abridgement and editing. Further instructions can be found at <http://jama.com/instructions>. A signed statement for authorship criteria and responsibility, financial disclosure, copyright transfer, and acknowledgment and the ICMJE Form for Disclosure of Potential Conflicts of Interest are required before publication. Letters should be submitted via the *JAMA* online submission and review system at <http://manuscripts.jama.com> (note: do not include "www" before the URL). For technical assistance, please contact jama-letters@jama-archives.org.

Letters Section Editor: Jody W. Zylke, MD, Senior Editor.

Table. Crude Hospital Mortality of Patients With Myocardial Infarction (MI) and Previous Cardiovascular Disease^a

	No. of Risk Factors at Presentation ^b					
	0	1	2	3	4	5
No. (%)						
MI (N = 630 210)	83 978 (13.3)	195 238 (31.0)	205 224 (32.6)	111 384 (17.7)	30 893 (4.9)	3493 (0.6)
Crude hospital mortality	15 790 (18.8)	30 825 (15.8)	25 894 (12.6)	10 336 (9.3)	2293 (7.4)	220 (6.3)

^aData are from the National Registry of Myocardial Infarction, 1994-2006. Excluded patients without prior cardiovascular disease, those who had been transferred, and those with missing data.

^bFive major risk factors: smoking, diabetes, dyslipidemia, hypertension, and family history of coronary heart disease.

4. Flanders WD, Klein M. Properties of 2 counterfactual effect definitions of a point exposure. *Epidemiology*. 2007;18(4):453-460.

5. Peterson ED, Gaziano JM. Cardiology in 2011—amazing opportunities, huge challenges. *JAMA*. 2011;306(19):2158-2159.

In Reply: Our study challenges conventional wisdom that patients with more coronary heart disease (CHD) risk factors have worse outcomes following their first MI. We found that patients with multiple CHD risk factors presented much earlier in life with MI and had lower hospital mortality than patients with fewer or no risk factors. We confirmed that the high prevalence of risk factor exposure in patients with MI was consistent with the prior literature.

Dr Santulli seeks additional information that may enhance our study, such as the influence of a dose-dependent effect of CHD risk factors, presence of the metabolic syndrome, other novel risk markers, and infarct size. Unfortunately, these factors were not available in the National Registry of Myocardial Infarction. Although baseline infarct size was not recorded, the finding of an inverse relationship between the number of CHD risk factors and mortality was consistently observed among patients with low-, intermediate-, and high-risk features using 2 well-validated measures of infarct severity (Killip classification and TIMI Risk Index).

Ms Banack and colleagues suggest that bias in the selection of our study cohort could have reversed the direction of observed associations, making a deleterious factor appear protective. An MI cohort with no previous cardiovascular disease represents a more uniform population to study given the differences in management and treatment after atherosclerosis is manifest. Excluding patients with previous cardiovascular disease simply presents findings generalizable only to patients without previous disease. When our analysis was rerun using only an MI cohort with previous cardiovascular disease (N=630 210), our results did not change appreciably (TABLE).

Banack et al also raise the possibility that patients with multiple CHD risk factors might have died disproportionately before hospitalization. This is merely speculative. No prior study has examined the relationship between the number of CHD risk factors and mortality among patients with suspected MI who died prior to hospital arrival, perhaps due to the challenges of confirming MI in the prehospital setting.

In the discussion of our findings, we devoted 4 paragraphs to methodological issues that may have limited generalizability and inferences of causality, including risk factor misclassification, bias with case ascertainment, residual confounding, healthy survivor bias, and index event bias.¹ Index event bias (also known as reverse epidemiology or collider stratification bias) may affect research that examines disease progression and severity when there are multiple risk factors for progression or for severity that are also risk factors for having the disease in the first place.¹ We also present biologically plausible alternative interpretations of our findings, including receipt of more aggressive treatments and follow-up care among patients with multiple CHD risk factors.

In summary, we report an unexpected and possibly controversial association that, like all observational findings, should be considered hypothesis-generating and further explored in terms of health care provided to patients who reach the hospital alive with first MI.

John G. Canto, MD, MSPH
 Catarina I. Kiefe, MD, PhD
 Philip Greenland, MD

Author Affiliations: Center for Cardiovascular Prevention, Research and Education, Watson Clinic LLP, Lakeland, Florida (Dr Canto) (jcanto@watsonclinic.com); Department of Quantitative Health Sciences, University of Massachusetts Medical School, Worcester (Dr Kiefe); and Clinical and Translational Sciences Institute, Northwestern University, Chicago, Illinois (Dr Greenland).

Conflict of Interest Disclosures: The authors have completed and submitted the ICMJE Form for Disclosure of Potential Conflicts of Interest. Drs Kiefe and Greenland reported receiving grants from the National Institutes of Health. Dr Greenland also reported being a consultant to the University of Pennsylvania, Ohio State University, and the National Heart, Lung, and Blood Institute; and receiving payment for lectures from the National Institutes of Health and several universities. Dr Canto reported no disclosures.

1. Dahabreh IJ, Kent DM. Index event bias as an explanation for the paradoxes of recurrence risk research. *JAMA*. 2011;305(8):822-823.

Urinary Sodium Excretion and Cardiovascular Events

To the Editor: Dr O'Donnell and colleagues, in their study on urinary sodium excretion and risk of cardiovascular events,¹ reached the counterintuitive conclusion that sodium restriction increased the risk of cardiovascular events, which runs counter to the consistent evidence that, in individuals with hypertension, decreased sodium intake reduces blood pressure and improves the effectiveness of treatment with antihypertensive agents.²⁻⁴



***CaMK4* Gene Deletion Induces Hypertension**

Gaetano Santulli, Ersilia Cipolletta, Daniela Sorriento, Carmine Del Giudice, Antonio Anastasio, Sara Monaco, Angela Serena Maione, Gianluigi Condorelli, Annibale Puca, Bruno Trimarco, Maddalena Illario and Guido Iaccarino

J Am Heart Assoc 2012, 1:

doi: 10.1161/JAHA.112.001081

Journal of the American Heart Association is published by the American Heart Association, 7272 Greenville Avenue, Dallas, TX 75214

Copyright © 2012 American Heart Association. All rights reserved. Online ISSN: 2047-9980

The online version of this article, along with updated information and services, is located on the World Wide Web at:

<http://jaha.ahajournals.org/content/1/4/e001081>

Subscriptions, Permissions, and Reprints: The Journal of the American Heart Association is an online only open access publication. Visit the Journal at <http://jaha.ahajournals.org> for more information.

CaMK4 Gene Deletion Induces Hypertension

Gaetano Santulli, MD; Ersilia Cipolletta, MD; Daniela Sorriento, PhD; Carmine Del Giudice, MS; Antonio Anastasio, MS; Sara Monaco, PhD; Angela Serena Maione, BS; Gianluigi Condorelli, MD, PhD; Annibale Puca, MD, PhD; Bruno Trimarco, MD; Maddalena Illario, MD, PhD; Guido Iaccarino, MD, PhD

Background—The expression of calcium/calmodulin-dependent kinase IV (CaMKIV) was hitherto thought to be confined to the nervous system. However, a recent genome-wide analysis indicated an association between hypertension and a single-nucleotide polymorphism (rs10491334) of the human CaMKIV gene (*CaMK4*), which suggests a role for this kinase in the regulation of vascular tone.

Methods and Results—To directly assess the role of CaMKIV in hypertension, we characterized the cardiovascular phenotype of *CaMK4*^{-/-} mice. They displayed a typical hypertensive phenotype, including high blood pressure levels, cardiac hypertrophy, vascular and kidney damage, and reduced tolerance to chronic ischemia and myocardial infarction compared with wild-type littermates. Interestingly, in vitro experiments showed the ability of this kinase to activate endothelial nitric oxide synthase. Eventually, in a population study, we found that the rs10491334 variant associates with a reduction in the expression levels of CaMKIV in lymphocytes from hypertensive patients.

Conclusions—Taken together, our results provide evidence that CaMKIV plays a pivotal role in blood pressure regulation through the control of endothelial nitric oxide synthase activity. (*J Am Heart Assoc.* 2012;1:e001081 doi: 10.1161/JAHA.112.001081)

Key Words: angiogenesis • arrhythmia • endothelium • hypertension • hypertrophy

A growing body of evidence bears out the rising interest in the function of calcium/calmodulin-dependent kinases (CaMKs) in cardiovascular pathophysiology. In particular, although it is now established that CaMKII is an important player in the regulation of cardiac responses, both in terms of electrophysiology and of cardiac myocyte hypertrophy,^{1–4} less is known about the role of other members of the CaMK family, such as CaMKIV, in the cardiovascular system.⁵

The recent genome-wide analysis of the Framingham Heart Study 100K Project⁶ showed an association between elevated diastolic blood pressure (BP) and the rs10491334 T/C

single-nucleotide polymorphism (SNP) of the human CaMKIV gene (*CaMK4*). Such a finding suggests that this kinase, the expression of which once was thought to be confined to the nervous tissue,^{7–10} has a yet unidentified role in the control of vascular tone.

We therefore hypothesized that CaMKIV could affect endothelial functions, such as the control of vascular resistance, and that changes in its level of expression or activity in endothelial cells (ECs) might alter the fine regulation of vascular responses, causing hypertension. To ascertain whether CaMKIV signaling is involved in endothelial dysfunction, a hallmark of the hypertensive state,^{11–14} we used a murine model of genetic deletion of *CaMK4*. Finally, a population study was carried out in normotensive and hypertensive patients to investigate the effects of the *CaMK4* rs10491334 SNP in humans.

Methods

In Vivo Studies

Animals

All animal procedures were performed in accordance with the policies and guidelines of the “Position of the American Heart Association on Research Animal Use”¹⁵ and were approved by

From the Department of Clinical Medicine, Cardiovascular and Immunologic Sciences (G.S., E.C., D.S., C.D.G., A.A., B.T.), Department of Cellular and Molecular Biology and Pathology (S.M., A.S.M., M.I.), “Federico II” University of Naples, Naples, Italy; Istituto clinico Humanitas IRCCS and Istituto Ricerca Genetica Biomedica, National Research Council, Rozzano, Italy (G.C.); Multi-medica Research Hospital, Milan, Italy (G.C., A.P., G.I.); Department of Medicine and Surgery, University of Salerno, Salerno, Italy (A.P., G.I.).

Correspondence to: Guido Iaccarino, MD, PhD, FESC, Department of Medicine and Surgery, University of Salerno, Via Salvador Allende, 84081 Baronissi (Salerno), Italy. E-mail giaccarino@unisa.it

Received April 17, 2012; accepted June 21, 2012.

© 2012 The Authors. Published on behalf of the American Heart Association, Inc., by Wiley-Blackwell. This is an Open Access article under the terms of the Creative Commons Attribution Noncommercial License, which permits use, distribution and reproduction in any medium, provided the original work is properly cited and is not used for commercial purposes.

the Ethics Committee of the “Federico II” University. The European Commission Directive 2010/63/EU was followed. We studied male mice with global homozygous deletion of the *CaMK4* gene (*CaMK4*^{-/-}), backcrossed >12 generations onto a C57Bl/6J background. The mice were kindly provided by Anthony Means (Duke University, Durham, NC).⁹ Age-matched wild-type littermates (*CaMK4*^{+/+}) were used as controls. The animals were housed in a 22°C room with a 12-hour light/dark cycle and were allowed food and tap water ad libitum. Two groups of mice (*CAMK4*^{+/+} and *CAMK4*^{-/-}) were subjected to a long-term furosemide treatment (0.35 mg/kg per day) from the age of 3 months until 6 or 18 months. The drug was added directly to the drinking water. The development of the typical target-organ damage (vascular, cardiac, and kidney damage)^{16–18} was evaluated in 18-month-old mice. Longitudinal survival observation on *CAMK4*^{+/+} and *CAMK4*^{-/-} mice was performed over a period of 24 months. Genotypes were determined by polymerase chain reaction amplification of tail DNA. The individual performing all experiments was blinded to the mouse genotype until all data were fully analyzed.

Invasive Arterial BP Measurement

Mice were anesthetized by isoflurane (4%) inhalation and maintained by mask ventilation (isoflurane 1.8%). Direct BP and heart rate measurements were performed with the use of a 1.0F Mikro-Tip catheter (SPR1000, Millar Instruments, Houston, TX), which was advanced through the right external carotid artery and placed in the descending aorta. After implantation, the catheter was connected to a transducer (Gould Instruments Systems, Cleveland, OH) to record BP and heart rate for 15 minutes. The pressure catheter then was advanced through the aortic valve into the left ventricle (LV). Subsequent offline evaluation provided the first derivative of the LV pressure curve (maximum and minimum dP/dt). All data were analyzed with dedicated software (PowerLab-Chart 7.1, ADInstruments, Sydney, Australia).

Echocardiography

Transthoracic echocardiography was performed with a small-animal high-resolution imaging system (VeVo770, VisualSonics, Inc, Toronto, Canada) equipped with a 30-MHz transducer (Real-Time Micro Visualization, RMV-707B). The mice, anesthetized as described previously for BP measurement, were placed in a shallow left lateral decubitus position, with strict thermoregulation (37±1°C) to optimize physiological conditions and reduce hemodynamic variability. Fur was removed from the chest by application of a cosmetic cream (Veet, Reckitt Benckiser, Milan, Italy) to gain a clear image. LV end-diastolic and LV end-systolic diameters were measured at the level of the papillary muscles from the parasternal short-axis

view.^{19,20} Intraventricular septal and LV posterior wall thickness were estimated at end diastole. LV fractional shortening was calculated as follows: $LVFS = [(LVEDD - LVESD) / LVEDD] \times 100$, where LVFS indicates LV fractional shortening; LVEDD, LV end-diastolic diameter; and LVESD, LV end-systolic diameter. LV ejection fraction was calculated automatically by the echocardiography system. All measurements were averaged on 10 consecutive cardiac cycles per experiment and were analyzed by one experienced investigator.

Electrocardiography

Electrocardiography (ECG) was performed under isoflurane (1.5%) anesthesia. Mice were placed on a thermocontrolled plate (37±1°C) and were given 10 minutes to acclimate before ECG recording. Signal-averaged ECG tracings were obtained by subcutaneous placement of 27-gauge steel needle electrodes in each limb, secured with tape. ECG was recorded for 60 minutes with the PowerLab Chart 7.1 system (ADInstruments, Sydney, Australia) and then was analyzed offline.

Angiogenic Response After Peripheral Chronic Ischemia

Peripheral chronic ischemia was induced in 6-month-old mice by means of surgical ligation and excision of the right common femoral artery. We have published a detailed description of the procedure.^{21–23} The angiogenic response was assessed on postoperative days 3, 7, 14, and 21 by laser Doppler (Perimed Instruments, Järfälla, Sweden).²² Furthermore, 3 weeks after surgery, we performed (1) ultrasound Doppler analysis of the posterior tibial artery with a VeVo770 imaging system equipped with a 20- to 60-MHz scanhead (VisualSonics, Inc, Toronto, Canada), (2) dyed-microbead assay on the gastrocnemius muscle, and (3) histological analysis of the anterior tibial muscle.

Myocardial Infarction

Reproducible infarcts of the anterior LV wall were imposed on 6-month-old mice by cryogeny with a 6-mm² cryoprobe. Briefly, after isoflurane (2%) anesthesia, a thoracotomy was performed through the fourth left intercostal space, the pericardium was opened, and the heart was exposed. Cryoinfarction was produced by applying the cryoprobe to the anterior LV free wall, followed by freezing for 10 seconds. The exact position of the probe was set carefully by using the left atrium and pulmonary artery as anatomic landmarks. Rinsing with room-temperature saline was performed to allow nontraumatic detachment of the probe from the LV wall after freezing. Cardiac ultrasound analysis was performed 8 weeks after the lesion was created.

Urinary Protein Excretion

As a marker of renal damage,¹⁶ we assessed urinary protein excretion nephelometry (bicinchoninic acid method; Pierce, Rockford, IL) by placing the mice (n=12 in each group) in metabolic cages (Tecniplast, Buguggiate, Italy) for 24 hours.

Ex Vivo Studies

Vascular Reactivity

Aortic rings (6 to 9 mm) from 6-month-old mice were suspended in isolated tissue baths (Radnoti Glass Technology, Monrovia, CA) filled with 25 mL Krebs-Henseleit solution (in mmol/L: NaCl 118.3, KCl 4.7, CaCl₂ 2.5, MgSO₄ 1.2, KH₂PO₄ 1.2, NaHCO₃ 25, and glucose 5.6) continuously bubbled with a mixture of 5% CO₂ and 95% O₂ (pH 7.38 to 7.42) at 37°C, according to the protocol used in our laboratory.²³ Vasorelaxation was assessed in vessels precontracted with phenylephrine (1 μmol/L) in response to isoproterenol, acetylcholine, or nitroprusside, all from 10 nmol/L to 10 μmol/L, freshly prepared on the day of experiment.²³ Endothelium-independent vasorelaxation also was tested after incubation (10 μmol/L, 15 minutes) with N^G-nitro-L-arginine methyl ester (Sigma-Aldrich, Milan, Italy), a competitive inhibitor of endothelial nitric oxide synthase (eNOS). Concentrations are reported as the final molar value in the organ bath.

Histology

Samples (hearts, kidneys, muscles) were fixed in 10% buffered formalin and processed for paraffin embedding.²⁴ Slides were stained with hematoxylin and eosin for architectural analysis or with Masson's trichrome to assess the presence and extent of interfiber interstitial fibrosis.^{19,24,25} Percent collagen was calculated from high-resolution, color-calibrated digital images of Masson's trichrome-stained sections with the use of dedicated software (NIH ImageJ64), as described.¹⁹ To measure myocyte cross-sectional area (μm²) we used fluorescence-tagged wheat germ agglutinin staining (5.0 μg/mL; with samples incubated in the dark for 10 minutes at 37°C). Images were recorded at 494-nm excitation and 518-nm emission and were evaluated with ImageJ64. Lectin immunohistochemical staining was performed on myocardial and skeletal muscle.^{21,26}

Quantification of Atherosclerotic Lesions

Atherosclerotic lesions in 18-month-old mice were detected by staining with the neutral lipid-targeting lysochrome Oil Red O (Sigma-Aldrich, Milan, Italy). Each aorta was rinsed first in distilled water and then quickly in 60% isopropyl alcohol. Subsequently, vessels were stained for 25 minutes (in a solution of 15 g Oil Red O, 30 mL isopropyl alcohol, and

20 mL distilled water, freshly prepared and filtered) and then were washed. The Oil Red O-stained areas of the inner aortic surfaces were quantified using the free software Fiji. The extent of atherosclerosis was assessed on longitudinally opened aorta and expressed as the percentage of the lipid-accumulating lesion area to the total aortic area analyzed. Acquisition of images and analysis of lesions were performed in a blinded fashion.

In Vitro Assays

Cell Culture

Murine aortic ECs were isolated from 3-month-old *CaMK4*^{-/-} and *CaMK4*^{+/+} animals as previously described.²⁷ Bovine aortic ECs and human embryonic kidney (HEK293) cells were purchased from Lonza (Basel, Switzerland) and American Type Culture Collection (ATCC; Manassas, VA), respectively. Cells were cultured in Dulbecco's modified Eagle medium (Sigma-Aldrich, Milan, Italy) as described.¹⁹ All experiments were performed in triplicate to ensure reproducibility. We used ionomycin (1 μmol/L; Sigma-Aldrich) as activator and KN93 (5 μmol/L; Seikagaku Corporation, Tokyo, Japan) as inhibitor of CaMK.^{5,28}

Immunoprecipitation and Immunoblotting

Immunoblot analysis was performed as previously described and validated.²¹ Blots were probed with mouse monoclonal antibodies against eNOS, phospho-eNOS (peNOS Ser¹¹⁷⁷), CaMKIV (BD Bioscience, Franklin Lakes, NJ), peNOS Ser¹¹⁴, peNOS Ser⁶¹⁵ (Millipore, Billerica, MA), peNOS Thr⁴⁹⁵, pCaMKIV, CaMKII, pCaMKII, and actin (Santa Cruz Biotechnology, Santa Cruz, CA). Images then were digitalized and densitometry was assessed with dedicated software (Image Quant, GE Healthcare, Piscataway, NJ). Data are presented as arbitrary units after normalization for the total corresponding protein or actin as loading control, as indicated.

eNOS Activity Assay

eNOS activity was detected in *CaMK4*^{-/-} and *CaMK4*^{+/+} murine aortic ECs and in bovine aortic ECs by measuring the conversion of L-[³H]arginine to L-[³H]citrulline at 37°C for 30 minutes with the eNOS assay kit (Calbiochem-Nova Biochem, San Diego, CA), according to the manufacturer's instructions. Unlabeled L-arginine was added to L-[³H]arginine (specific activity, 60 Ci/mmol/L) at a ratio of 3:1. Mouse cerebellum extracts, containing elevated amounts of neuronal NOS, were used as positive controls, whereas samples incubated in the presence of N^G-nitro-L-arginine methyl ester (1 mmol/L) were used to determine nonspecific activity.

CaMKIV Activity Assay

The CaMKIV activity assay consisted of 2 reaction steps. Briefly, in the first step, active recombinant full-length CaMKIV (Millipore, Billerica, MA) was incubated at 30°C for 30 minutes with 0.5 mmol/L CaCl₂ and 1 μmol/L CaM in 25 μL of a reaction mixture (25 mmol/L 4-[2-hydroxyethyl]-1-piperazineethanesulfonic acid [HEPES], pH 7.5, 0.5 mmol/L MgCl₂, 1 mmol/L dithiothreitol, 0.5 mg/L BSA, 1 mmol/L sodium orthovanadate, 0.1 mmol/L cold adenosine triphosphate (ATP), and H₂O 0.01% Tween 20). In the second step, a 20-μL aliquot from the first reaction mixture containing active CaMKIV was incubated in 50 μL of a solution containing 0.1 IU of eNOS (Calbiochem-Nova Biochem, San Diego, CA) as substrate and 1 mmol/L EGTA, 0.5 μL [³²P]-γ-ATP (3000 Ci/mmol/L) for 30 minutes at 30°C. The reactions were stopped by the addition of sodium dodecyl sulfate–polyacrylamide gel electrophoresis (SDS-PAGE) sample loading buffer, and the whole reaction mixes were separated on 4% to 12% SDS-PAGE (Life Technologies, Grand Island, NY). Then, the gel was dried and pE NOS was visualized by phosphorImager (GE Healthcare, Piscataway, NJ).

Alternatively, a partially modified protocol was performed without the use of radioactive ATP. In this case, after PAGE, proteins were blotted on nitrocellulose, and eNOS phosphorylation by CaMKIV was also assessed by Western blot by using the previously mentioned antibodies.

Overlay Blot Assay

Twenty nanograms of CaMKIV and 0.1 IU of eNOS-purified proteins were subjected to SDS-PAGE and transferred on nitrocellulose. The membranes were incubated 2 hours at room temperature in 5% blocking solution. At this time, the filters were incubated with CaMKIV or eNOS-purified protein in phosphorylation solution (final concentrations: 20 μmol/L ATP, 1 mmol/L CaCl₂, 20 mmol/L MgCl₂, and 4 mmol/L Tris, pH 7.5). After 1 hour of incubation at room temperature, the blots were cooled rapidly on ice; washed twice with NaCl, Tris, and 0.1% Tween 20; and then fixed with 0.5% formaldehyde for 10 minutes. The filters were washed 3 times with 2% glycine and once with NaCl, Tris, and 0.1% Tween 20. CaMKIV or eNOS-bound proteins were detected by chemiluminescence.²⁹

Human Association Study

Study participants were consecutive hypertensive patients referred to the Hypertension Diagnosis and Care Outpatient Clinic of “Federico II” University of Naples. Age-matched unaffected controls were recruited from a database of normotensive blood donors. The matching design was accounted for in the statistical analyses. All subjects were

white and born within the Campania region in Southern Italy. We had access to a digital archive for each participant.³⁰ Enrollment criteria for hypertensive status were an age of 18 to 80 years and a confirmed diagnosis of essential hypertension. We considered the average systolic and diastolic BP values, according to European guidelines.¹⁶

Analysis of the rs10491334 SNP of *CaMK4* was performed on peripheral blood DNA by restriction fragment length polymorphism.³⁰ Genetic analyses were performed by laboratory personnel blinded to sample identity. Patients' lymphocytes were extracted by means of phicoll purification with HISTOPAQUE-1077 (Sigma-Aldrich) from a 20-mL blood sample, which had been anticoagulated with ethylenediamine-tetraacetic acid.³¹

Data Presentation and Statistical Analysis

Data are presented as mean ± standard error (SE) unless otherwise mentioned. To determine the statistical significance of the results, we used 1-way ANOVA or Kruskal-Wallis test, as appropriate (nonparametric analysis was used when a large number of tests increased the risk of a type α error). Survival curves were compared with the log-rank test.

To assess significant differences between genotype classes in the human studies, we used the Student *t* test for continuous variables and the Fisher exact test for categorical variables. The association between the SNP and hypertension was adjusted for age, sex, heart rate, and body mass index. Statistical significance was set at *P*<0.05. All the analyses were performed with GraphPad Prism version 5.01 (GraphPad Software, San Diego, CA), Systat 13 (Systat software, Inc, Chicago, IL), and Statistical Package for Social Sciences software version 20.0.0 (IBM SPSS Inc, Armonk, NY).

Results

BP, Organ Damage, and Survival

CaMK4^{-/-} mice developed higher systolic and diastolic BP levels than did *CaMK4*^{+/+} littermates, as shown in Table 1. We decided to assess BP-dependent phenotypes, such as target-organ damage, in homozygous mice only. At 6 months, cardiac ultrasound analysis showed that *CaMK4*^{-/-} mice displayed concentric^{25,31,32} LV hypertrophy (LVH) due to increased septum and posterior wall thickness, with no significant changes in internal diameter, as depicted in Table 1. At gross analysis, *CAMK4*^{-/-} hearts were larger both as absolute values (163.1±4.5 versus 136.8±3.1 mg, Figure 1A) and after correction by either body weight (Figure 1B) or tibial length (Figure 1C). Histological analysis showed increased cell size of *CAMK4*^{-/-} cardiomyocytes (Figure 1D and 1E) and augmented interstitial fibrosis

Table 1. Systemic and LV Hemodynamics in *CaMK4*^{+/+} and *CaMK4*^{-/-} Mice

	<i>CaMK4</i> ^{+/+} (n=12)	<i>CaMK4</i> ^{-/-} (n=13)	<i>CaMK4</i> ^{+/+} (n=14)	<i>CaMK4</i> ^{-/-} (n=16)	<i>CaMK4</i> ^{+/+} (n=12)	<i>CaMK4</i> ^{-/-} (n=13)
	3-Month-Old Mice		6-Month-Old Mice		18-Month-Old Mice	
HR, bpm	492±28	486±36	486±18	474±16	460±32	468±28
SBP, mm Hg	111±1.3	113±1.8	110±0.6	123±0.7*	111±1.1	124±1.3*
DBP, mm Hg	81±0.9	82±1.1	81±0.3	90±0.3*	86±0.8	93±0.9*
LVEDD, mm	3.71±0.42	3.73±0.35	3.85±0.32	3.74±0.29	3.89±0.37	4.36±0.3*
LVESD, mm	2.08±0.26	2.15±0.28	2.19±0.27	2.37±0.28	2.22±0.3	3.02±0.46*
IVS, mm	0.72±0.04	0.73±0.05	0.72±0.03	0.88±0.02*	0.82±0.04	0.89±0.03*
LVPW, mm	0.71±0.03	0.72±0.04	0.69±0.02	0.89±0.03*	0.78±0.03	0.92±0.04*
LVFS, %	43.4±4.8	42.6±5.5	42.4±4.5	36.2±6.1*	37.2±5.8	30.2±7.2*
LVEF, %	66.8±8.2	66.3±9.1	64.8±8.6	59.6±7.8	56.4±9.4	50.1±9.8*
+dP/dt, mm Hg/s	6334±602	6211±522	6237±531	5681±498*	6004±582	5014±578*
-dP/dt, mm Hg/s	6420±542	6322±508	6302±504	5702±486*	6080±682	5112±606*

Data are mean±SE. HR indicates heart rate; SBP, systolic BP; DBP, diastolic BP; LVEDD, LV end-diastolic diameter; LVESD, LV end-systolic diameter; IVS, interventricular septum; LVPW, LV posterior wall; LVFS, LV fractional shortening; and LVEF, LV ejection fraction.

**P*<0.05 comparing *CaMK4*^{-/-} to *CaMK4*^{+/+} at each time point; otherwise, *P* not significant.

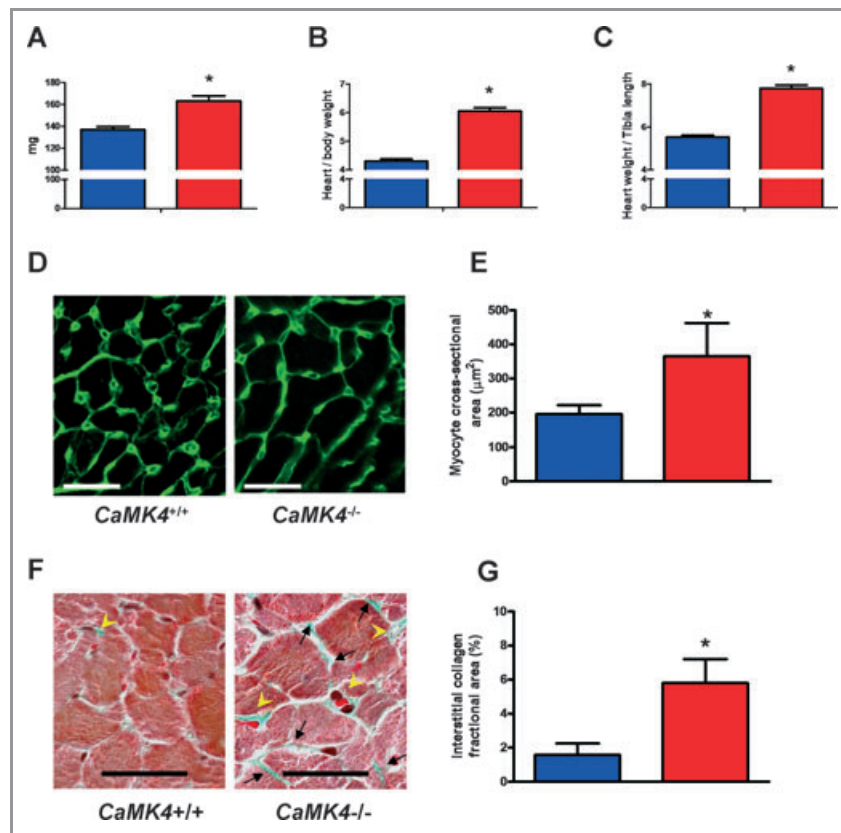


Figure 1. LVH in *CaMK4*^{-/-} mice. *CaMK4*^{-/-} 6-month-old mice present cardiac hypertrophy, as determined by an increase in heart weight (A), normalized by body weight (B) or tibial length (C). Fluorescence-tagged wheat germ agglutinin, which binds to saccharides of cellular membranes, showed increased cardiac myocyte cross-sectional area in *CaMK4*^{-/-} mice (D and E; magnification ×200, scale bar = 15 µm). Masson's trichrome staining (F; magnification ×300, scale bar = 15 µm; interstitial and perivascular collagen deposition indicated by black arrows and yellow arrowheads, respectively) also revealed an increase in fibrosis, quantified as described in Methods (G). Blue bars are *CaMK4*^{+/+} mice; red bars, *CaMK4*^{-/-} mice. **P*<0.05 vs *CaMK4*^{+/+}.

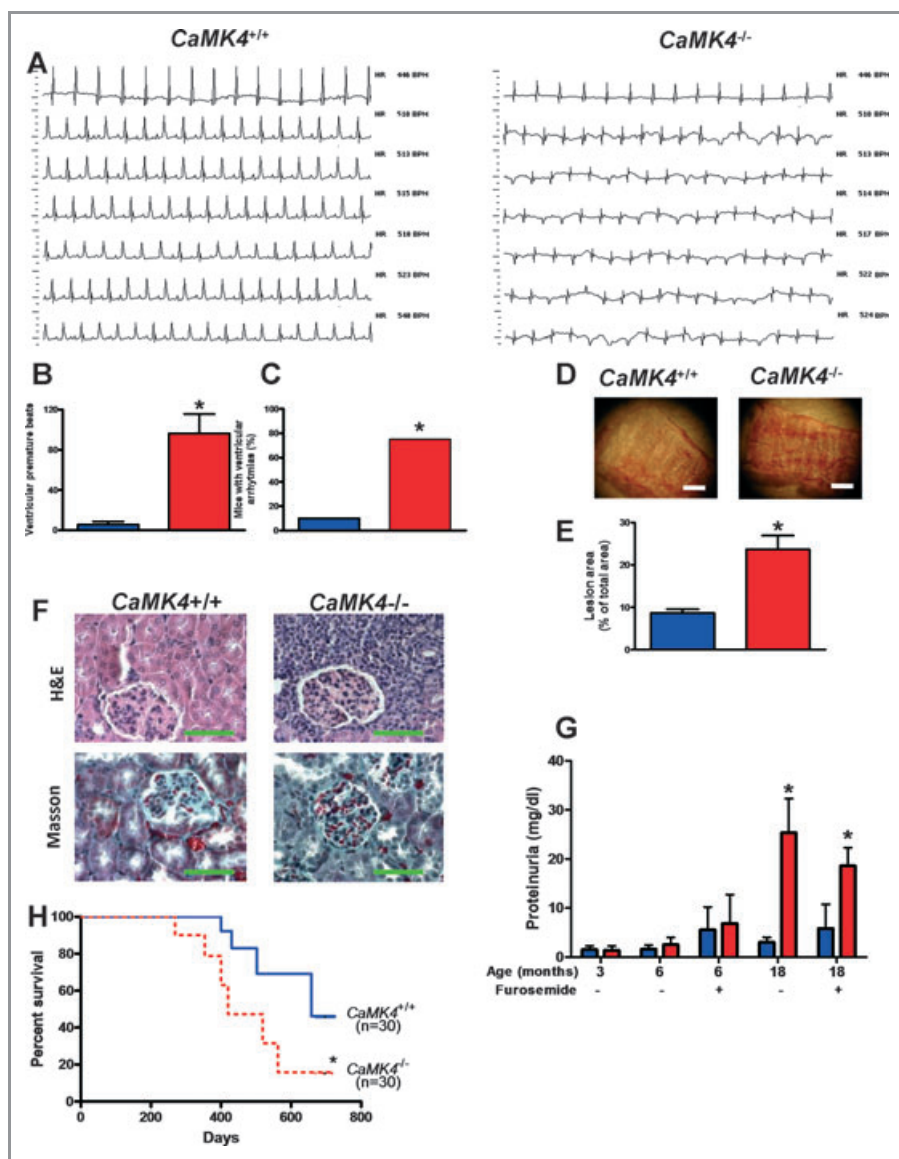


Figure 2. Organ damage in 18-month-old mice. Old $CaMK4^{-/-}$ mice displayed a dilatation of the LV (see also Table 1) and exhibited several spontaneous ventricular arrhythmias (A; representative ECG records at different heart rates). These data are quantified in B and C ($n=10$ per group; $*P<0.05$). Of note, heart rate among mutated animals did not significantly differ (see Table 1). D and E, Lipid deposition in vessels of $CaMK4^{+/+}$ and $CaMK4^{-/-}$ mice ($n=12$ per group). Representative pictures of oil red O–stained ascending aortas (D; white bar = 600 μm); areas of atherosclerotic lesions were quantified using the free software Fiji and are represented as percentage of lesion area to total aortic area (E; $*P<0.05$ vs $CaMK4^{+/+}$). Kidneys (F) from the $CaMK4^{-/-}$ group exhibited increased glomerulosclerosis, inflammatory cell infiltration, and tubulointerstitial fibrosis compared with $CaMK4^{+/+}$ mice ($n=8$ per group; representative pictures of hematoxylin and eosin or Masson’s trichrome staining; magnification $\times 60$; green bar = 100 μm). Moreover, 18-month-old $CaMK4^{-/-}$ mice presented another typical feature of the hypertensive phenotype (G), showing greater proteinuria than $CaMK4^{+/+}$ mice ($n=12$ per group; $*P<0.05$ vs $CaMK4^{+/+}$). In all histograms, blue bars are $CaMK4^{+/+}$ mice; red bars, $CaMK4^{-/-}$ mice. Notably, compared with $CaMK4^{+/+}$ mice, $CaMK4$ -null mice displayed significantly ($*P<0.05$) impaired survival, as well (Kaplan-Meier curves; H). Blue line indicates $CaMK4^{+/+}$ mice; red dotted line, $CaMK4^{-/-}$ mice.

(Figure 1F and 1G), 2 common elements of hypertension-induced LVH.¹⁹ In older mice (18 months old), cardiac damage evolved toward dilatation and dysfunction (Table 1) complicated by arrhythmias, as shown by ECG (Figure 2A through 2C), according to the natural history of untreated hypertension.³³ Indeed, LVH is associated with alterations in

the dispersion of repolarization³⁴ and prolongation of ventricular action potentials.³⁵ These effects result in electrical instability and increase the propensity to develop arrhythmias. When an antihypertensive treatment with furosemide was initiated at 3 months of age, the development of both hypertension and LVH was prevented (Table 2).

Table 2. Effect of Long-Term Diuretic Treatment on Systemic and LV Hemodynamics in *CaMK4^{+/+}* and *CaMK4^{-/-}* Mice

	<i>CaMK4^{+/+}</i> (n=11)	<i>CaMK4^{-/-}</i> (n=16)	<i>CaMK4^{+/+}</i> (n=10)	<i>CaMK4^{-/-}</i> (n=14)
	6-Month-Old Mice Treated (3 Months) With Furosemide		18-Month-Old Mice Treated (15 Months) With Furosemide	
HR, bpm	498±46	492±38	483±52	488±41
SBP, mm Hg	107±6.8	114±1.8	103±6.6	104±1.3
DBP, mm Hg	74±8.5	83±1.1	75±5.9	78±1.2
LVEDD, mm	3.82±0.9	3.83±0.4	3.9±0.8	3.95±0.7
LVESD, mm	2.21±0.8	2.23±0.3	2.26±0.9	2.28±0.5
IVS, mm	0.71±0.08	0.76±0.04	0.78±0.09	0.8±0.05
LVPW, mm	0.69±0.07	0.77±0.05	0.76±0.08	0.79±0.06
LVFS, %	41.6±8.8	39.2±7.3	36.9±8.6	36.5±7.1
LVEF, %	62.8±9.7	62.5±8.4	55.4±8.1	55.1±8.9
+dP/dt, mm Hg/s	6126±684	6088±642	5522±528	5876±627
-dP/dt, mm Hg/s	6188±747	6104±594	5596±639	5892±582

Data are mean±SE. HR indicates heart rate; SBP, systolic BP; DBP, diastolic BP; LVEDD, LV end-diastolic diameter; LVESD, LV end-systolic diameter; IVS, interventricular septum; LVPW, LV posterior wall; LVFS, LV fractional shortening; and LVEF, LV ejection fraction.

Along with increased heart size, *CaMK4^{-/-}* mice over time developed hypertensive vascular damage, as assessed by Oil Red O staining (Figure 2D), which revealed larger atherosclerotic lesions in aortas from 18-month-old *CaMK4^{-/-}* mice versus *CaMK4^{+/+}* mice (Figure 2E). We also found renal damage, another typical feature of the hypertensive phenotype,¹⁶ inasmuch as *CaMK4^{-/-}* mice displayed increased glomerulosclerosis, inflammatory cell infiltration, and tubulointerstitial fibrosis compared with *CaMK4^{+/+}* mice (Figure 2F). The functional correlate to this histological alteration is increased proteinuria in 18-month-old *CaMK4^{-/-}* mice (Figure 2G). Furosemide-treated *CaMK4^{-/-}* mice still presented proteinuria (Figure 2G), although they had normal BP levels.

Eventually, *CaMK4^{-/-}* mice showed significantly reduced lifespan compared with *CaMK4^{+/+}* littermates (Figure 2H).

Assessment of Endothelium-Dependent Phenotypes

Endothelium-dependent vasodilation in ex vivo experiments was assessed on isolated aortic rings. After vasoconstriction obtained through 1 μmol/L phenylephrine (Figure 3A), aortic rings from *CaMK4^{-/-}* mice showed impaired endothelial-dependent vasodilation both to the β-adrenergic agonist isoproterenol and to the muscarinic agonist acetylcholine, which is consistent with our hypothesis of endothelial dysfunction (Figure 3B and 3C), a known hallmark of the hypertensive state.¹³ Moreover, there was no difference in the vascular smooth muscle cell-mediated response to the nitric oxide donor nitroprusside (Figure 3D), and experiments

performed after *N^G*-nitro-L-arginine methyl ester incubation confirmed intact endothelium-independent vasodilation in both *CaMK4^{-/-}* and *CaMK4^{+/+}* vessels (Figure 3E and 3F).

Additionally, we assessed in vivo the angiogenic response to ischemia after femoral artery removal, a phenotype that is largely under the control of the endothelium.^{21,23,36} *CaMK4^{-/-}* mice displayed impaired angiogenesis after 21 days of peripheral ischemia, as assessed by laser Doppler (Figure 4A and 4B), Doppler ultrasound (Figure 4C), dyed microbeads (Figure 4D), and capillary density (Figure 4E and 4F).

Development of Heart Failure After Myocardial Infarction

Increased BP and reduced angiogenesis are expected to precipitate the evolution of the heart failure phenotype after myocardial damage.^{17,37} Indeed, 8 weeks after myocardial cryoinfarction, *CaMK4^{-/-}* mice presented larger LV dilatation and a greater decrease in cardiac function than did *CaMK4^{+/+}* mice, as shown in both Table 3 and Figure 5A. This feature also was accompanied by reduced capillary density in the peri-infarct area (Figure 5B and 5C).

Interaction Between CaMKIV and eNOS

Because endothelium dysfunction can be mimicked by altered production or removal of nitric oxide, we assessed the effect of *CaMK4* knockout on eNOS activation. Indeed, calcium-induced eNOS phosphorylation on Ser¹¹⁷⁷ is impaired in *CaMK4^{-/-}* ECs. (Figures 6A and 7A through 7C). This

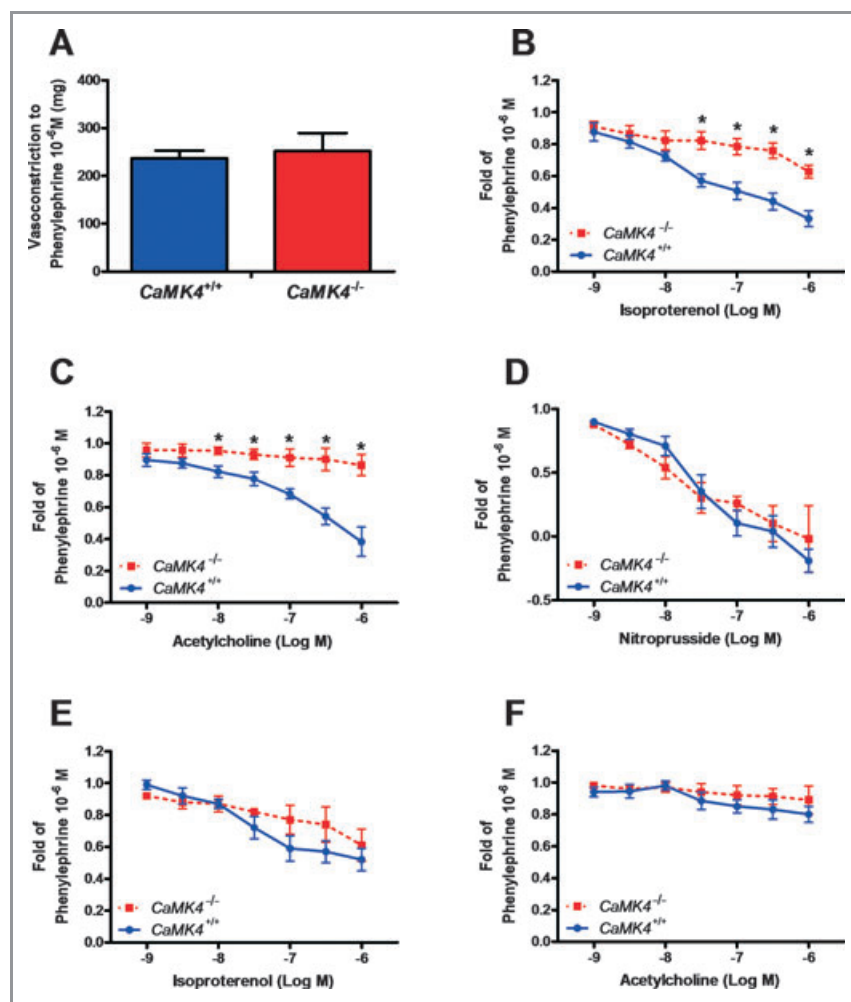


Figure 3. Vascular responses on isolated aortic rings from 6-month-old mice. Vasoconstriction to α_1 -adrenergic agonist phenylephrine was similar in $CaMK4^{+/+}$ and $CaMK4^{-/-}$ mice (A). Endothelium-dependent vasorelaxation induced by the β -adrenergic agonist isoproterenol (B) or by the muscarinic agonist acetylcholine (C) was blunted in $CaMK4^{-/-}$ vessels, whereas endothelium-independent vasodilation to nitroprusside was not different between $CaMK4^{+/+}$ and $CaMK4^{-/-}$ (D). To better explore the role of nitric oxide in endothelial responses, we also evaluated vascular responses in the presence (10 μ mol/L) of the specific eNOS inhibitor N^G -nitro-L-arginine methyl ester (E and F). * P <0.05 vs $CaMK4^{+/+}$.

impairment associates with a reduction in CaMKIV expression and activity in $CaMK4^{-/-}$ EC, whereas activation of CaMKII remains unaffected (Figure 6A). This finding also is endorsed by a reduction in eNOS activity (Figure 8). Interestingly, transgenic restoration of CaMKIV expression in $CaMK4^{-/-}$ ECs also corrects calcium-induced eNOS activation (Figures 6B, 7D, and 7E). CaMKIV and eNOS can coimmunoprecipitate in either naïve or overexpressing cells (Figures 6C and 9). The physical interaction between the 2 proteins can be replicated in an overlay assay with the use of purified CaMKIV and eNOS, which indicates that the interaction is not mediated by a third component (Figure 6D). The result of this physical interaction is the incorporation in eNOS of ³²P (Figure 6E). Also, in vitro, purified CaMKIV can phosphorylate eNOS directly on Ser¹¹⁷⁷ and Ser⁶¹⁵, 2 phosphorylation sites that are regulatory for enzyme activity,

but not on other phosphorylation sites of eNOS, namely Ser¹¹⁴ and Thr⁴⁹⁵ (Figures 6F and 7F through 7I).

Role of rs10491334 T/C Polymorphism of Human *CaMK4* Gene in Hypertensive Patients

The results gained in the $CaMK4^{-/-}$ mouse show a role for this kinase in the setup of hypertension. To confirm the possible relevance of this finding in humans, we studied the frequencies of the rs10491334 T/C SNP.⁶ This polymorphism associates with a reduction in the cellular expression of the kinase.³⁸ We studied 2 populations of normotensive (n=457) and hypertensive subjects (n=730). Clinical characteristics of these individuals are reported in Table 4. We found a higher occurrence of the polymorphism among the hypertensive patients that fell short of statistical significance

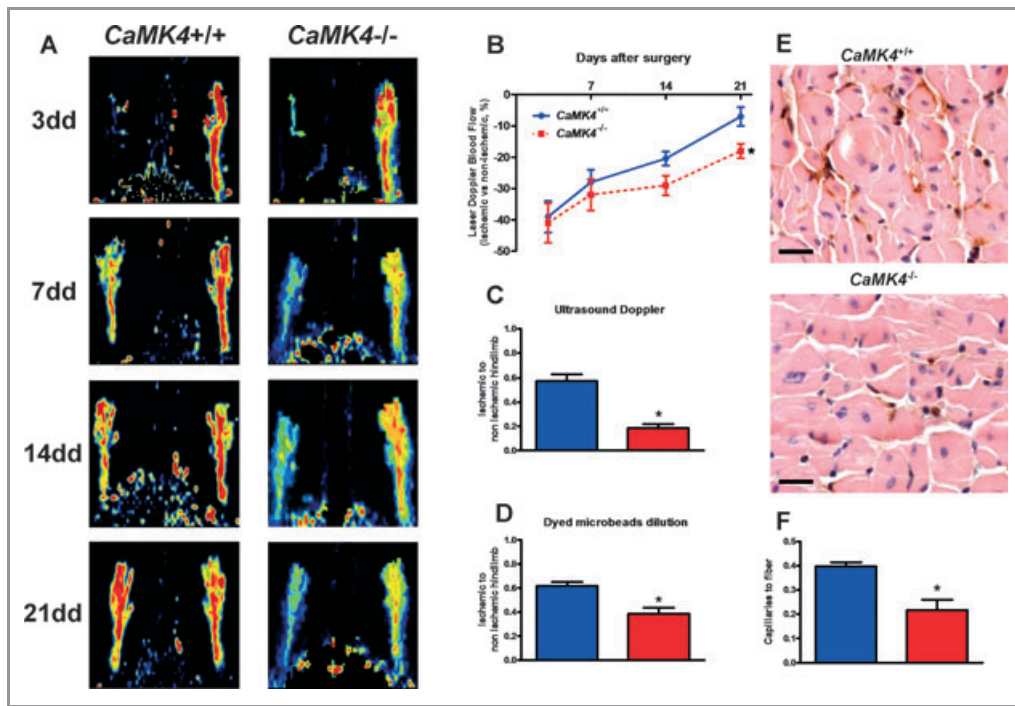


Figure 4. Decreased neoangiogenic responses in *CaMK4*^{-/-} mice during chronic ischemia in vivo (n=6 per group). Determination of laser Doppler blood flow (A and B) on postoperative days 3, 7, 14, and 21 showed a deficit in ischemic hindlimb perfusion, compared with the contralateral hindlimb, that was significantly increased in *CaMK4*^{-/-} vs *CaMK4*^{+/+} mice (*P<0.05, repeated measurements, ANOVA; laser Doppler blood flow data are expressed as percent of ischemic to nonischemic limb). Ultrasound Doppler flowmetry of posterior tibial artery (C), performed 3 weeks after femoral artery removal, confirmed the attenuated blood flow restoration in *CaMK4*^{-/-} mice (*P<0.05 vs *CaMK4*^{+/+}). This result was mirrored by the dyed-bead perfusion analysis (D; *P<0.05 vs *CaMK4*^{+/+}). Lectin staining of capillaries in the ischemic hindlimb (E; magnification ×20, black bar = 100 μm) showed that chronic ischemia produced a greater rarefaction of the capillary density, evaluated as number of capillaries corrected for the number of muscle fibers (F), in *CaMK4*^{-/-} compared with *CaMK4*^{+/+} mice (*P<0.05). In all histograms, blue bars are *CaMK4*^{+/+} mice; red bars, *CaMK4*^{-/-} mice.

Table 3. Systemic and LV Hemodynamics in *CAMK4*^{+/+} and *CAMK4*^{-/-} Mice 8 Weeks After Myocardial Infarction

	<i>CaMK4</i> ^{+/+} (n=12)	<i>CaMK4</i> ^{-/-} (n=14)
HR, bpm	498±20	482±18
SBP, mm Hg	100±0.5	108±0.6*
DBP, mm Hg	74±0.3	82±0.4*
LVEDD, mm	4.16±0.12	4.6±0.11*
LVESD, mm	3.15±0.08	3.71±0.13*
IVS, mm	0.66±0.04	0.85±0.05*
LVPW, mm	0.68±0.03	0.86±0.03*
LVFS, %	24.74±2.9	17.8±2.3*
LVEF, %	49.02±4.8	35.8±3.4*
+dP/dt, mm Hg/s	3784±402	3004±382*
-dP/dt, mm Hg/s	3918±386	3128±394*

Data are mean±SE. Mice were 8 months old (myocardial infarction was induced in 6-month-old animals). HR indicates heart rate; SBP, systolic BP; DBP, diastolic BP; LVEDD, LV end-diastolic diameter; LVESD, LV end-systolic diameter; IVS, interventricular septum; LVPW, LV posterior wall; LVFS, LV fractional shortening; and LVEF, LV ejection fraction. *P<0.05; otherwise, P not significant.

(normotensive patients: 31.32%; hypertensive patients: 41.64%; P=0.0594, Pearson χ^2 analysis). Thus, we dichotomized our hypertensive population according to European Guidelines into categories of severe (Grade 2/3) and not-severe (Grade 1) diastolic hypertension (cutoff: diastolic BP=100 mm Hg)¹⁶ and found a significantly larger frequency of the T variant of the rs10491334 SNP in patients with severe hypertension than in patients with diastolic BP<100 mm Hg (54.42% versus 38.41%; P<0.05, Pearson χ^2 analysis), as shown in Table 5. Intriguingly, hypertensive patients homozygous for the polymorphic T allele showed reduced expression levels of CaMKIV in circulating peripheral blood lymphocytes (Figure 10).

Discussion

In the present study, we provide compelling evidence for a fundamental and previously unrecognized role of CaMKIV in the regulation of vascular function. Indeed, the phenotype of the *CaMK4*^{-/-} mouse indicates that this kinase is extremely important for endothelial function. A paramount finding of this

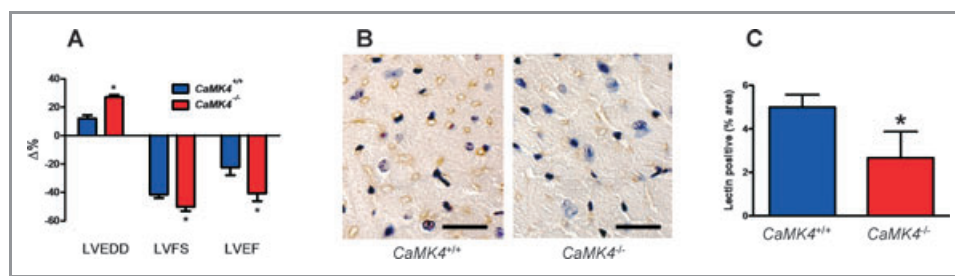


Figure 5. Cardiac evaluation after cryoinjury. Changes in echocardiographic parameters (A) 8 weeks after myocardial infarction. (LVEDD indicates LV end-diastolic diameter; LVFS, LV fractional shortening; and LVEF, LV ejection fraction. n=12 per group. * $P<0.05$ vs $CaMK4^{+/+}$). Immunohistochemical analysis (B; lectin staining, magnification $\times 60$, black bar = 30 μm) of myocardium in mice 8 weeks after infarction. The peri-infarct area demonstrated lower capillary density, as confirmed by quantitative analysis (C); blue bars are $CaMK4^{+/+}$ mice; red bars, $CaMK4^{-/-}$ mice. * $P<0.05$ vs $CaMK4^{+/+}$.

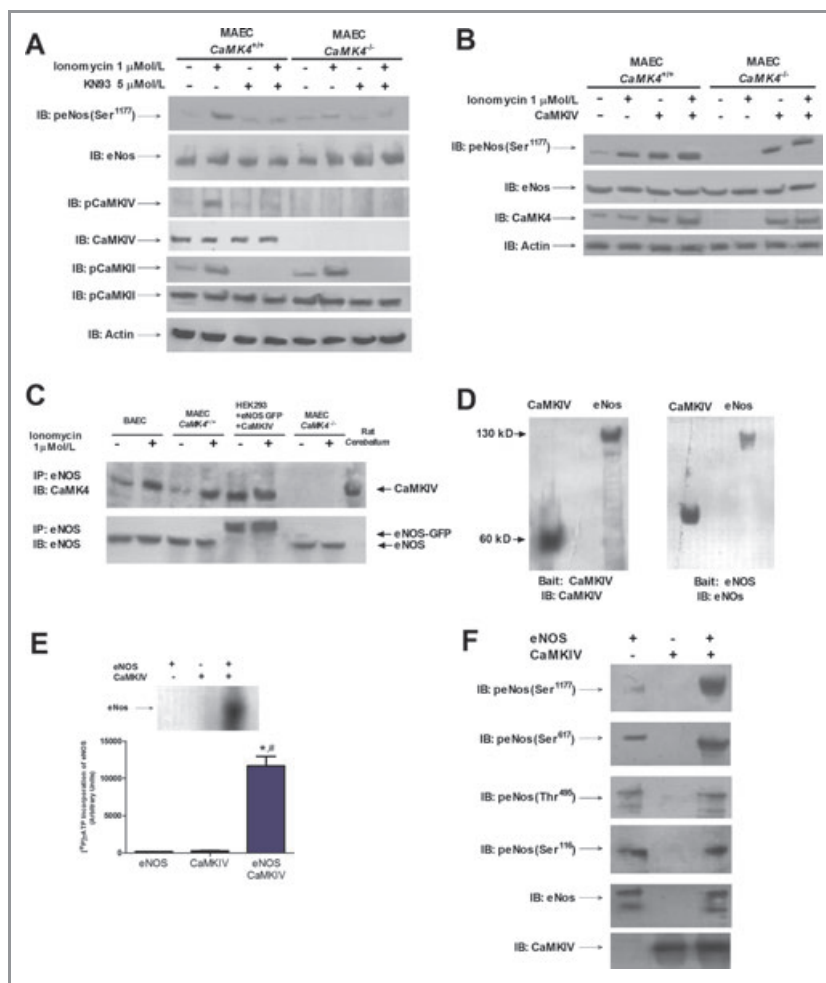


Figure 6. Interaction between CaMKIV and eNOS. eNOS phosphorylation (Ser¹¹⁷⁷) is enhanced by ionomycin, echoing the phosphorylation of CaMKIV, and is prevented by the CaMK inhibitor KN93 (A). Notably, eNOS activation was less evident in $CaMK4^{-/-}$ MAEC, where $CaMK4$ was not expressed (A). Transgenic restoration of CaMKIV expression in $CaMK4^{-/-}$ ECs corrected calcium-induced eNOS activation (B). The interaction between CaMKIV and eNOS was demonstrated by performing immunoprecipitation (IP) experiments in different cellular settings, both in basal conditions and after stimulation with ionomycin (C). Such interaction is shown in BAEC and $CaMK4^{+/+}$ MAEC but not in $CaMK4^{-/-}$ MAEC. In a nonendothelial cell type, HEK293, we confirmed the interaction after reconstituting the system by using a plasmid encoding CaMKIV and a plasmid encoding eNOS linked to GFP (C; rat cerebellum was used as CaMKIV-positive control). The input protein levels are shown in Figure 8. Overlay assay with purified CaMKIV (left blot) or eNOS (right blot) as bait (D). CaMKIV induced eNOS [³²P]-γ-ATP incorporation (E). Purified CaMKIV induced eNOS phosphorylation on Ser¹¹⁷⁷ and Ser⁶¹⁵ but not on Ser¹¹⁴ and Thr⁴⁹⁵ (F). * $P<0.05$ vs eNOS, * $P<0.05$ vs CaMKIV; representative images from triplicate experiments are shown. Densitometric analyses are reported in Figure 7. MAEC indicates murine aortic ECs; BAEC, bovine aortic ECs.

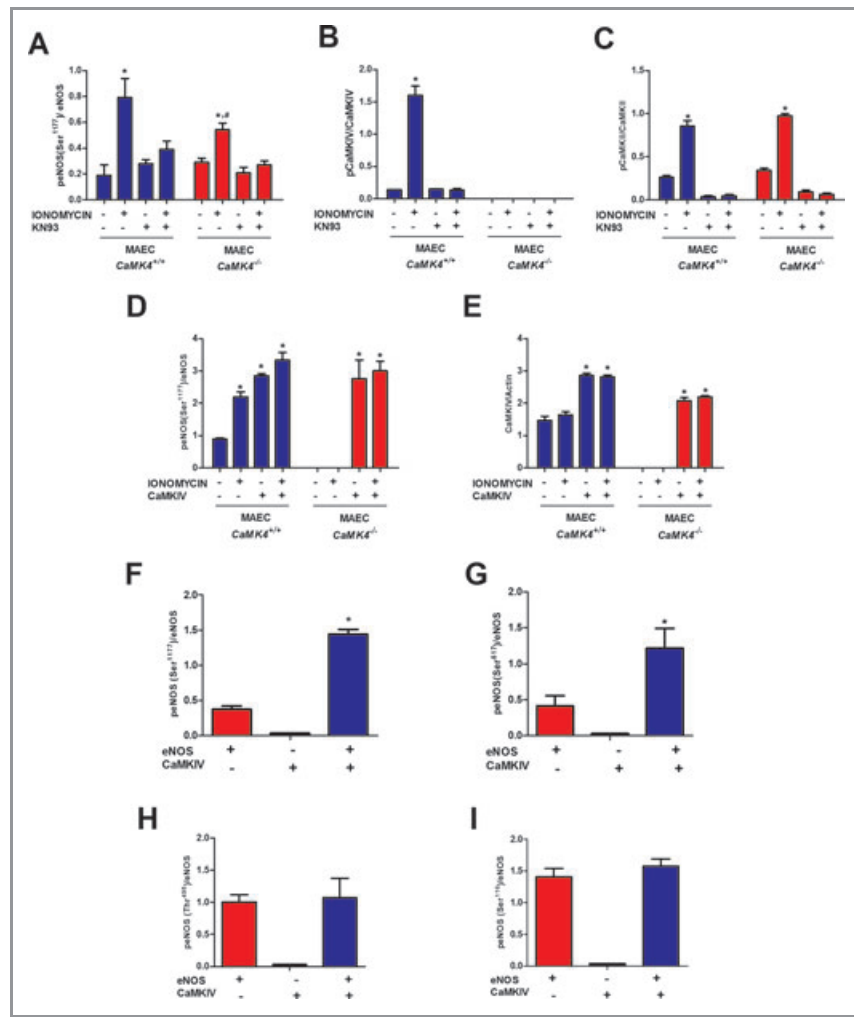


Figure 7. Quantification of blot results presented in Figure 6. Relative protein quantification levels for Figure 6A (A–C) and Figure 6B (D–E). Blue bars are *CaMK4*^{+/+}; red bars, *CaMK4*^{-/-}. **P*<0.05 vs untreated cells; #*P*<0.05 vs MAEC *CaMK4*^{+/+}. MAEC indicates murine aortic ECs. Densitometric analyses for Figure 6F (F–H) showing CaMKIV-mediated eNOS phosphorylation on Ser¹¹⁷⁷ and Ser⁶¹⁵ but not on Ser¹¹⁷⁴ and Thr⁴⁹⁵. Red bars indicate eNOS; black bars, CaMKIV; and blue bars, eNOS and CaMKIV. **P*<0.05 vs eNOS.

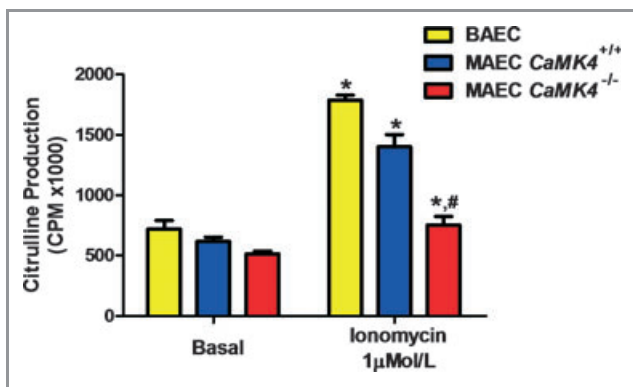


Figure 8. eNOS activity in ECs. eNOS activity, assessed by arginine–citrulline conversion, after stimulation by ionomycin (1 μmol/L) was blunted in *CaMK4*^{-/-} MAEC. **P*<0.05 vs basal; #*P*<0.05 vs *CaMK4*^{+/+}. MAEC indicates murine aortic ECs; CPM, counts per minute.

study is that the loss of *CaMK4* results in the development of hypertension, accompanied by its typical hallmarks: endothelial dysfunction, target-organ damage, and reduced survival rate.^{16,32} Interestingly, furosemide-treated mice did not display LVH, which suggests that LVH is indeed the result of increased BP rather than being genetically determined by *CaMK4* gene removal.¹³ We used a loop diuretic to obtain an effective BP decrease with minimum effect on vascular function.¹⁶ Moreover, other diuretics, such as thiazides, have metabolic implications not present in furosemide treatment¹⁶ that could confuse the cardiovascular phenotype of our *CaMK4*^{-/-} mice further. In our model, endothelial dysfunction could be either primitive to hypertension or, alternatively, secondary to the hypertensive state of *CaMK4*^{-/-} mice. We rule out this second hypothesis on the basis of 2 pieces of evidence: First, diuretic treatment resulted in normalization of

Table 4. Characteristics of the Normotensive and Hypertensive Populations

	Normotensive Subjects (n=457)	Hypertensive Subjects (n=730)
Age, y	52.91±3.4	55.84±2.9
Sex (male/female), n	288/169	452/278
HR, bpm	76.8±9.3	72.8±8.2
SBP, mm Hg	131.67±0.84	147.7±0.72*
DBP, mm Hg	77.06±0.51	96.69±0.48*
Body mass index, kg/m ²	26.03±0.27	27.19±0.21
Smoking (current or former), %	53.6	54.1
Glycemia, mmol/L	4.8±0.72	5.2±0.88
Diabetes, %	4.7	5.9
Total cholesterol, mmol/L	4.35±0.12	4.98±0.18
High-density lipoprotein cholesterol, mmol/L	1.24±0.11	1.21±0.14
Low-density lipoprotein cholesterol, mmol/L	2.96±0.13	3.25±0.19
Triglycerides, mmol/L	1.46±0.09	1.53±0.11
Dyslipidemia, %	37.8	41.2
LV mass index, g/m ²	92.6±4.5	115.34±4.8*
CaMK4 rs10491334 polymorphism (T-allele frequency), %	31.32	41.64

Data are mean±SE; n, or %, as indicated. HR indicates heart rate; SBP, systolic BP; and DBP, diastolic BP.

**P*<0.05; otherwise, *P* not significant.

hemodynamic-dependent LVH but did not correct proteinuria, which is a characteristic of endothelial dysfunction.³⁹ Second, in a hemodynamic-independent setup³⁶ (ie, in isolated ECs), *CaMK4* removal causes endothelial dysfunction as assessed by reduction of eNOS activity, which is corrected only after gene replacement. Endothelial dysfunction is known to induce hypertension, as demonstrated in *eNOS*^{-/-} mice, which show absent endothelial-dependent vasorelaxation and increased BP.¹³

Our study is the first to demonstrate the interaction of CaMKIV and eNOS. Previous reports had suggested the importance of CaMKs in endothelium-dependent relaxation.^{40–42} In addition, 2 independent groups had provided evidence that a nonselective CaMK inhibitor could significantly decrease bradykinin-induced eNOS activity¹² and prevent eNOS phosphorylation²⁸ in rat and porcine aortic ECs, respectively. Our study characterizes the close relationship between CaMKIV and eNOS in the endothelium. Indeed, CaMKIV can phosphorylate eNOS directly in Ser¹¹⁷⁷ and Ser⁶¹⁵, 2 sites that are known to induce eNOS activation. Although we have not investigated all

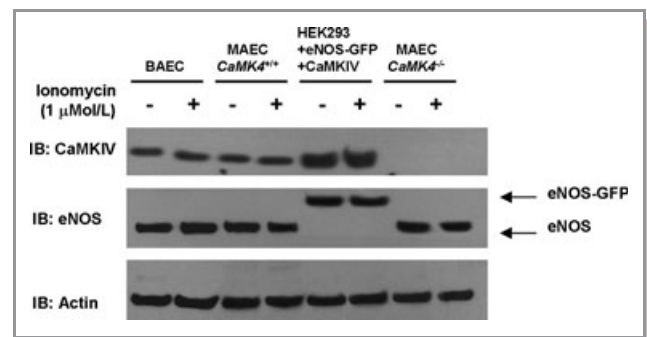


Figure 9. Input Western blots of immunoprecipitation assay represented in Figure 6C. To confirm that equal amounts of proteins were present in the cell lysates used for immunoprecipitation as depicted in Figure 6C, we performed Western blotting on 30 μ g of proteins of corresponding cell lysates with the same antibodies used in the experiment represented in Figure 6C, raised respectively against CaMKIV and eNOS. Furthermore, actin was detected to confirm equal amount of proteins.

Table 5. Characteristics of the Hypertensive Patients, Subdivided Into 2 Populations According to a DBP Cutoff of 100 mm Hg

	Patients With DBP <100 mm Hg (n=583)	Patients With DBP \geq 100 mm Hg (n=147)
Age, y	54.9±3.6	56.2±3.8
Sex, male/female, n	371/212	81/66
HR, bpm	71.6±9.6	72.2±11.3
SBP, mm Hg	142.86±1.58	154.46±1.42*
DBP, mm Hg	91.89±0.74	108.69±0.86*
Body mass index, kg/m ²	26.85±0.63	27.71±1.74
Smoking (current or former), %	55.4	53.3
Glycemia, mmol/L	5.4±0.77	5.1±0.98
Diabetes (%)	5.7	6.1
Total cholesterol, mmol/L	4.77±0.22	5.01±0.28
High-density lipoprotein cholesterol, mmol/L	1.22±0.15	1.17±0.19
Low-density lipoprotein cholesterol, mmol/L	3.32±0.17	3.05±0.23
Triglycerides, mmol/L	1.52±0.13	1.55±0.16
Dyslipidemia, %	43.1	39.8
LV mass index, g/m ²	112.6±4.5	116.86±7.3
CaMK4 rs10491334 polymorphism (T-allele frequency), %	38.41	54.42*

Data are mean±SE; n, or %, as indicated. HR indicates heart rate; SBP, systolic BP; and DBP, diastolic BP.

**P*<0.05; otherwise, *P* not significant.

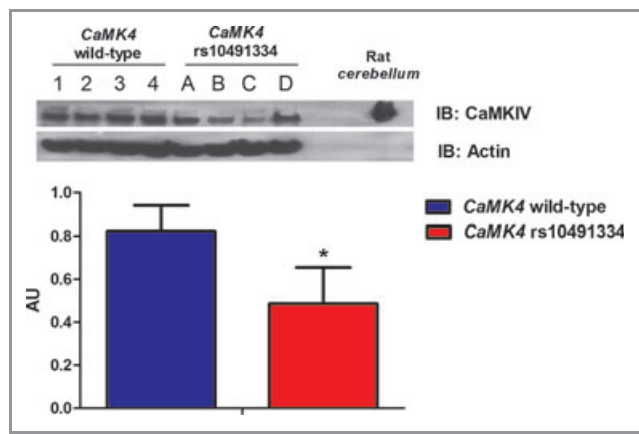


Figure 10. Expression levels of CaMKIV in circulating lymphocytes of hypertensive patients. Western blot analysis of CaMKIV on peripheral blood lymphocytes showed that CaMKIV levels were higher in subjects with the *CaMK4* wild-type genotype (1, 2, 3, and 4 represent samples from 4 different individuals) than in subjects homozygous for the polymorphic *CaMK4* rs10491334 variant (A, B, C, and D represent samples from 4 different individuals). Rat cerebellum was used as CaMKIV-positive control. Data from immunoblots (IB; representative images from 5 experiments are shown) were quantified by densitometric analysis. CaMKIV levels were normalized to actin densitometry. * $P < 0.05$ vs *CaMK4*^{+/+}. AU indicates arbitrary units.

phosphorylation sites of eNOS, these 2 appear to be relevant for the described mechanism.

It is remarkable that CaMKII does not seem to supersede CaMKIV loss. Although CaMKIV and CaMKII often are considered mutually exchangeable, these 2 kinases present differences in tissue distribution and regulation^{43,44} and cannot be considered isoforms.⁵ For the present study, we used mice generated in the Means' laboratory in the 1990s.⁹ The cardiovascular phenotype of this mouse was never before investigated as extensively as we have in the present report. A hint of the higher BP of *CaMK4*^{-/-} mice can be found in the article of Colomer and colleagues,⁴ showing that after constriction of the thoracic aorta, BP gradients were higher in *CaMK4*-null than in wild-type mice. Other reports have failed to describe cardiovascular parameters of these mice. Interestingly, though, *CaMK4*^{-/-} mice present cognitive disorders that are typical of patients in the advanced phases of untreated hypertension,⁴⁵ such as erasure of long-term memory.¹⁰ This phenotype has been ascribed to the loss of *CaMK4* signaling in neurons of *CaMK4*^{-/-} mice but also can be worsened by chronic exposure to increased BP levels.

To find a correlation between our observations in this genetically modified mouse and the human condition, we took advantage of the DNA Bank associated with the Campania Salute database of >5000 hypertensive patients.³⁰ Previously, the Framingham study had identified an association marker for high diastolic BP in the rs10491334 SNP of the human

CaMK4 gene.⁶ Our study confirms this finding: We performed an association analysis with a candidate gene approach and found a significant correlation between the rs10491334 SNP and diastolic BP levels among hypertensive patients. Furthermore, in the present work, we show that this polymorphism associates with a reduction in the cellular expression levels of CaMKIV, similar to that observed in other populations.³⁸ These data are highly suggestive of the intrinsic regulatory nature of CaMKIV in hypertension.

Our study follows the groove of the identification of the physiological implications of CaMKs in the cardiovascular system.¹⁻³ Some authors have investigated the effects of CaMKIV in the heart by overexpressing it in cardiomyocytes, leading to cardiac hypertrophy.⁴⁶ This notion was challenged by a more recent study showing that mice null for *CaMK4* still developed LVH.⁴ Our data reconcile these opposing views by suggesting that dysfunctional CaMKIV, albeit not expressed in the heart, might partake in cardiac organ damage in the context of the hypertensive state.

Conclusion

Our findings establish that CaMKIV plays a relevant role in the regulation of the vascular tone by a mechanism that involves eNOS activation through phosphorylative events. Impairment of CaMK-mediated activation of eNOS, as in *CaMK4* gene deletion, induces hypertension, as demonstrated by the fact that *CAMK4*^{-/-} mice display a hypertensive phenotype that leads to typical organ damage. Extending our observations to the clinical scenario, we show that in hypertensive patients a *CaMK4* polymorphism that causes reduced expression of the protein identifies a subset of patients with higher BP levels. Altogether, our results point to CaMKIV as a novel potential biological target for therapeutic interventions in hypertension.

Acknowledgments

We thank Prof Jean-Luc Balligand, Catholic University of Louvain, Belgium, for providing the plasmid encoding for eNOS-GFP. Author contributions: Dr Santulli conceived the project, performed experiments, analyzed data, and wrote the paper; Drs Cipolletta and Monaco and A.S. Maione performed in vitro experiments; Dr Sorriento, C. Del Giudice, and A. Anastasio performed experiments; Drs Condorelli, Puca, Trimarco, and Illario analyzed data and contributed to discussion; and Dr Iaccarino supervised the project, analyzed data, and wrote the paper.

Sources of Funding

This work was supported by grants from Italian Society of Arterial Hypertension and Italy Health Ministry (PRIN2009 to Dr Iaccarino, PRIN2008 to Dr Trimarco, and PRIN2009 to Dr Illario).

Disclosures

None.

References

- Kushnir A, Shan J, Betzenhauser MJ, Reiken S, Marks AR. Role of CaMKII δ phosphorylation of the cardiac ryanodine receptor in the force frequency relationship and heart failure. *Proc Natl Acad Sci USA*. 2010;107:10274–10279.
- Wagner S, Ruff HM, Weber SL, Bellmann S, Sowa T, Schulte T, Anderson ME, Grandi E, Bers DM, Backs J, Belardinelli L, Maier LS. Reactive oxygen species-activated Ca/calmodulin kinase II δ is required for late I(Na) augmentation leading to cellular Na and Ca overload. *Circ Res*. 2011;108:555–565.
- Zhang T, Brown JH. Role of Ca²⁺/calmodulin-dependent protein kinase II in cardiac hypertrophy and heart failure. *Cardiovasc Res*. 2004;63:476–486.
- Colomer JM, Mao L, Rockman HA, Means AR. Pressure overload selectively up-regulates Ca²⁺/calmodulin-dependent protein kinase II in vivo. *Mol Endocrinol*. 2003;17:183–192.
- Wayman GA, Tokumitsu H, Davare MA, Soderling TR. Analysis of CaM-kinase signaling in cells. *Cell Calcium*. 2011;50:1–8.
- Levy D, Larson MG, Benjamin EJ, Newton-Cheh C, Wang TJ, Hwang SJ, Vasan RS, Mitchell GF. Framingham Heart Study 100K Project: genome-wide associations for blood pressure and arterial stiffness. *BMC Med Genet*. 2007;8(suppl 1):S3.
- Ho N, Liauw JA, Blaeser F, Wei F, Hanissian S, Muglia LM, Wozniak DF, Nardi A, Arvin KL, Holtzman DM, Linden DJ, Zhuo M, Muglia LJ, Chatila TA. Impaired synaptic plasticity and cAMP response element-binding protein activation in Ca²⁺/calmodulin-dependent protein kinase type IV/Gr-deficient mice. *J Neurosci*. 2000;20:6459–6472.
- Miyano O, Kameshita I, Fujisawa H. Purification and characterization of a brain-specific multifunctional calmodulin-dependent protein kinase from rat cerebellum. *J Biol Chem*. 1992;267:1198–1203.
- Ribar TJ, Rodriguez RM, Khiroug L, Wetsel WC, Augustine GJ, Means AR. Cerebellar defects in Ca²⁺/calmodulin kinase IV-deficient mice. *J Neurosci*. 2000;20:RC107.
- Wei F, Qiu CS, Liauw J, Robinson DA, Ho N, Chatila T, Zhuo M. Calcium calmodulin-dependent protein kinase IV is required for fear memory. *Nat Neurosci*. 2002;5:573–579.
- Iaccarino G, Ciccarelli M, Sorriento D, Cipolletta E, Cerullo V, Iovino GL, Paudice A, Elia A, Santulli G, Campanile A, Arcucci O, Pastore L, Salvatore F, Condorelli G, Trimarco B. AKT participates in endothelial dysfunction in hypertension. *Circulation*. 2004;109:2587–2593.
- Schneider JC, El Kebir D, Chereau C, Lanone S, Huang XL, De Buys Roessingh AS, Mercier JC, Dall'Ava-Santucci J, Dinh-Xuan AT. Involvement of Ca²⁺/calmodulin-dependent protein kinase II in endothelial NO production and endothelium-dependent relaxation. *Am J Physiol Heart Circ Physiol*. 2003;284:H2311–H2319.
- Huang PL, Huang Z, Mashimo H, Bloch KD, Moskowitz MA, Bevan JA, Fishman MC. Hypertension in mice lacking the gene for endothelial nitric oxide synthase. *Nature*. 1995;377:239–242.
- Santulli G. Thrombolysis outcomes in acute ischemic stroke patients with prior stroke and diabetes mellitus. *Neurology*. 2012;78:840.
- Position of the American Heart Association on research animal use. *Circulation*. 1985;71:849A–850A.
- Mancia G, De Backer G, Dominiczak A, Cifkova R, Fagard R, Germano G, Grassi G, Heagerty AM, Kjeldsen SE, Laurent S, Narkiewicz K, Ruilope L, Rynkiewicz A, Schmieder RE, Struijker Boudier HA, Zanchetti A, Vahanian A, Camm J, De Caterina R, Dean V, Dickstein K, Filippatos G, Funck-Brentano C, Hellemans I, Kristensen SD, McGregor K, Sechtem U, Silber S, Tendera M, Widimsky P, Zamorano JL, Kjeldsen SE, Erdine S, Narkiewicz K, Kiowski W, Agabiti-Rosei E, Ambrosioni E, Cifkova R, Dominiczak A, Fagard R, Heagerty AM, Laurent S, Lindholm LH, Mancia G, Manolis A, Nilsson PM, Redon J, Schmieder RE, Struijker-Boudier HA, Viigimaa M, Filippatos G, Adamopoulos S, Agabiti-Rosei E, Ambrosioni E, Bertomeu V, Clement D, Erdine S, Farsang C, Gaita D, Kiowski W, Lip G, Mallion JM, Manolis AJ, Nilsson PM, O'Brien E, Ponikowski P, Redon J, Ruschitzka F, Tamargo J, van Zwieten P, Viigimaa M, Waerber B, Williams B, Zamorano JL, The Task Force for the Management of Arterial Hypertension of the European Society of Hypertension, The Task Force for the Management of Arterial Hypertension of the European Society of Cardiology. 2007 Guidelines for the management of arterial hypertension: the Task Force for the Management of Arterial Hypertension of the European Society of Hypertension (ESH) and of the European Society of Cardiology (ESC). *Eur Heart J*. 2007;28:1462–1536.
- Santulli G. Coronary heart disease risk factors and mortality. *JAMA*. 2012;307:1137.
- Donaldson C, Eder S, Baker C, Aronovitz MJ, Weiss AD, Hall-Porter M, Wang F, Ackerman A, Karas RH, Molkentin JD, Patten RD. Estrogen attenuates left ventricular and cardiomyocyte hypertrophy by an estrogen receptor-dependent pathway that increases calcineurin degradation. *Circ Res*. 2009;104:265–275, 211p following 275.
- Sorriento D, Santulli G, Fusco A, Anastasio A, Trimarco B, Iaccarino G. Intracardiac injection of AdGRK5-NT reduces left ventricular hypertrophy by inhibiting NF-kappaB-dependent hypertrophic gene expression. *Hypertension*. 2010;56:696–704.
- Perino A, Ghigo A, Ferrero E, Morello F, Santulli G, Baillie GS, Damilano F, Dunlop AJ, Pawson C, Walser R, Levi R, Altruda F, Silengo L, Langeberg LK, Neubauer G, Heymans S, Lembo G, Wymann MP, Wetzker R, Houslay MD, Iaccarino G, Scott JD, Hirsch E. Integrating cardiac PIP3 and cAMP signaling through a PKA anchoring function of p110gamma. *Mol Cell*. 2011;42:84–95.
- Iaccarino G, Ciccarelli M, Sorriento D, Galasso G, Campanile A, Santulli G, Cipolletta E, Cerullo V, Cimini V, Altobelli GG, Piscione F, Priante O, Pastore L, Chiariello M, Salvatore F, Koch WJ, Trimarco B. Ischemic neoangiogenesis enhanced by beta2-adrenergic receptor overexpression: a novel role for the endothelial adrenergic system. *Circ Res*. 2005;97:1182–1189.
- Ciccarelli M, Santulli G, Campanile A, Galasso G, Cervero P, Altobelli GG, Cimini V, Pastore L, Piscione F, Trimarco B, Iaccarino G. Endothelial alpha1-adrenoceptors regulate neo-angiogenesis. *Br J Pharmacol*. 2008;153:936–946.
- Santulli G, Ciccarelli M, Palumbo G, Campanile A, Galasso G, Ziaco B, Altobelli GG, Cimini V, Piscione F, D'Andrea LD, Pedone C, Trimarco B, Iaccarino G. In vivo properties of the proangiogenic peptide QK. *J Transl Med*. 2009;7:41.
- Santulli G, Lombardi A, Sorriento D, Anastasio A, Del Giudice C, Formisano P, Beguinot F, Trimarco B, Miele C, Iaccarino G. Age-related impairment in insulin release: the essential role of beta2-adrenergic receptor. *Diabetes*. 2012;61:692–701.
- Knoll R, Iaccarino G, Tarone G, Hilfiker-Kleiner D, Bauersachs J, Leite-Moreira AF, Sugden PH, Balligand JL. Towards a re-definition of 'cardiac hypertrophy' through a rational characterization of left ventricular phenotypes: a position paper of the Working Group 'Myocardial Function' of the ESC. *Eur J Heart Fail*. 2011;13:811–819.
- Santulli G, Basilicata MF, De Simone M, Del Giudice C, Anastasio A, Sorriento D, Saviano M, Del Gatto A, Trimarco B, Pedone C, Zaccaro L, Iaccarino G. Evaluation of the anti-angiogenic properties of the new selective alphaVbeta3 integrin antagonist RGDechiHCit. *J Transl Med*. 2011;9:7.
- Lembo G, Iaccarino G, Vecchione C, Barbato E, Morisco C, Monti F, Parrella L, Trimarco B. Insulin enhances endothelial alpha2-adrenergic vasorelaxation by a pertussis toxin mechanism. *Hypertension*. 1997;30:1128–1134.
- Fleming I, Fislthaler B, Dimmeler S, Kemp BE, Busse R. Phosphorylation of Thr (495) regulates Ca(2+)/calmodulin-dependent endothelial nitric oxide synthase activity. *Circ Res*. 2001;88:e68–e75.
- Fusco A, Santulli G, Sorriento D, Cipolletta E, Garbi C, Dorn GW II, Trimarco B, Feliciello A, Iaccarino G. Mitochondrial localization unveils a novel role for GRK2 in organelle biogenesis. *Cell Signal*. 2011;24:468–475.
- Lanni F, Santulli G, Izzo R, Rubattu S, Zanda B, Volpe M, Iaccarino G, Trimarco B. The PI(A1/A2) polymorphism of glycoprotein IIIa and cerebrovascular events in hypertension: increased risk of ischemic stroke in high-risk patients. *J Hypertens*. 2007;25:551–556.
- Santulli G, Campanile A, Spinelli L, Assante di Panzillo E, Ciccarelli M, Trimarco B, Iaccarino G. G protein-coupled receptor kinase 2 in patients with acute myocardial infarction. *Am J Cardiol*. 2011;107:1125–1130.
- Iaccarino G, Keys JR, Rapacciuolo A, Shotwell KF, Lefkowitz RJ, Rockman HA, Koch WJ. Regulation of myocardial betaAR1 expression in catecholamine-induced cardiac hypertrophy in transgenic mice overexpressing alpha1B-adrenergic receptors. *J Am Coll Cardiol*. 2001;38:534–540.
- Nattel S. Effects of heart disease on cardiac ion current density versus current amplitude: important conceptual subtleties in the language of arrhythmogenic ion channel remodeling. *Circ Res*. 2008;102:1298–1300.
- Jin H, Chemaly ER, Lee A, Kho C, Hadri L, Hajjar RJ, Akar FG. Mechanoelectrical remodeling and arrhythmias during progression of hypertrophy. *FASEB J*. 2010;24:451–463.
- Volk T, Nguyen TH, Schultz JH, Faulhaber J, Ehmke H. Regional alterations of repolarizing K⁺ currents among the left ventricular free wall of rats with ascending aortic stenosis. *J Physiol*. 2001;530:443–455.
- Sorriento D, Santulli G, Del Giudice C, Anastasio A, Trimarco B, Iaccarino G. Endothelial cells are able to synthesize and release catecholamines both in vitro and in vivo. *Hypertension*. 2012;60:129–136.

37. Iaccarino G, Lefkowitz RJ, Koch WJ. Myocardial G protein-coupled receptor kinases: implications for heart failure therapy. *Proc Assoc Am Physicians*. 1999;111:399–405.
38. Malovini A, Illario M, Iaccarino G, Villa F, Ferrario A, Roncarati R, Anselmi CV, Novelli V, Cipolletta E, Leggiero E, Orro A, Rusciano MR, Milanesi L, Maione AS, Condorelli G, Bellazzi R, Puca AA. Association study on long-living individuals from southern Italy identifies rs10491334 in the CAMKIV gene that regulates survival proteins. *Rejuvenation Res*. 2011;14:283–291.
39. Ott C, Schneider MP, Delles C, Schlaich MP, Schmieder RE. Reduction in basal nitric oxide activity causes albuminuria. *Diabetes*. 2011;60:572–576.
40. Gadano AC, Sogni P, Yang S, Cailmail S, Moreau R, Nepveux P, Couturier D, Lebrech D. Endothelial calcium-calmodulin dependent nitric oxide synthase in the in vitro vascular hyporeactivity of portal hypertensive rats. *J Hepatol*. 1997;26:678–686.
41. Liu G, Han J, Profirovic J, Strelakova E, Voyno-Yasenetskaya TA. Alpha13 regulates MEF2-dependent gene transcription in endothelial cells: role in angiogenesis. *Angiogenesis*. 2009;12:1–15.
42. You J, Peng W, Lin X, Huang QL, Lin JY. PLC/CAMK IV-NF-kappaB involved in the receptor for advanced glycation end products mediated signaling pathway in human endothelial cells. *Mol Cell Endocrinol*. 2010;320:111–117.
43. Matthews RP, Guthrie CR, Wailes LM, Zhao X, Means AR, McKnight GS. Calcium/calmodulin-dependent protein kinase types II and IV differentially regulate CREB-dependent gene expression. *Mol Cell Biol*. 1994;14:6107–6116.
44. Bok J, Wang Q, Huang J, Green SH. CaMKII and CaMKIV mediate distinct prosurvival signaling pathways in response to depolarization in neurons. *Mol Cell Neurosci*. 2007;36:13–26.
45. Kilander L, Nyman H, Boberg M, Hansson L, Lithell H. Hypertension is related to cognitive impairment: a 20-year follow-up of 999 men. *Hypertension*. 1998;31:780–786.
46. Passier R, Zeng H, Frey N, Naya FJ, Nicol RL, McKinsey TA, Overbeek P, Richardson JA, Grant SR, Olson EN. CaM kinase signaling induces cardiac hypertrophy and activates the MEF2 transcription factor in vivo. *J Clin Invest*. 2000;105:1395–1406.

CORRESPONDENCE

Atrial remodelling in echocardiographic super-responders to cardiac resynchronization therapy

To the Editor In a recent issue of *Heart*, Steffel *et al*¹ showed in an elegant retrospective study that patients with an exceptionally good echocardiographic response to cardiac resynchronisation therapy (CRT) are highly likely to experience a favourable outcome after CRT. We feel that this paper is worthy of comment. The study is well designed and represents an outstanding 'real world' experience. However, we do have several issues. The authors present much echocardiographic data regarding the ventricular function, but there is no information concerning atrial dimensions and function. Given the rising interest about the impact of CRT on atrial function,²⁻³ we believe that such information may be of value to the readers, especially from a population of 'super-responders' with a long-term follow-up. These data about atrial remodelling could be also useful to clarify the role of CRT response in the development of atrial fibrillation.²⁻³ Indeed, in the paper, there is only the baseline percentage of patients with atrial fibrillation without any result of the follow-up. Another moot point²⁻⁴ that the authors can elucidate is the impact of the aetiology of cardiomyopathy (ischaemic vs non-ischaemic) on the response to CRT.

Gaetano Santulli,^{1,2} Cristofaro D'Ascia²

¹New York Presbyterian Hospital / Columbia University Medical Center, New York, NY, USA; ²Division of Cardiology 'Federico II' University, Naples, Italy

Correspondence to Dr Gaetano Santulli, MD Columbia University Medical Center, 1150 St Nicholas Ave, 10032 New York, NY, USA; gs2620@columbia.edu

Competing interests None declared.

Provenance and peer review Not commissioned; internally peer reviewed.

Heart 2012;**98**:517. doi:10.1136/heartjnl-2012-301731

REFERENCES

1. **Steffel J**, Milosevic G, Hürlimann A, *et al*. Characteristics and long-term outcome of echocardiographic super-responders to cardiac resynchronisation therapy: 'real world' experience from a single tertiary care centre. *Heart* 2011;**97**:1668–74.
2. **D'Ascia SL**, D'Ascia C, Marino V, *et al*. Cardiac resynchronisation therapy response predicts occurrence of atrial fibrillation in non-ischaemic dilated cardiomyopathy. *Int J Clin Pract* 2011;**65**:1149–55.
3. **Santulli G**, D'Ascia C, Marino V, *et al*. Atrial Function in Patients Undergoing CRT. *J Am Coll Cardiol Cardiovasc Imaging* 2012;**5**:124–5.
4. **McLeod CJ**, Shen WK, Rea RF, *et al*. Differential outcome of cardiac resynchronization therapy in ischemic cardiomyopathy and idiopathic dilated cardiomyopathy. *Heart Rhythm* 2011;**8**:377–82.

The Authors' reply We are thankful for the interest of Santulli *et al*¹ in our recent manuscript published in *Heart*.² We will gladly respond to their comments.

An increasing body of evidence is implying a beneficial effect of cardiac resynchronisation therapy (CRT) on atrial remodelling and the occurrence of atrial tachyarrhythmias.³⁻⁴ In our study, we indeed looked at the effect of super-responder status on atrial size, but did not include the results in the original paper due to inconsistent findings. While no significant effect of responder status as defined by an increase in ejection fraction (EF) >10% or a decrease in EDVI >30% was observed, we did find an atrial size reduction of borderline significance ($48.7 \pm 7.5 - 45 \pm 8.9$, $p=0.0573$) when super-responders were defined by a decrease in end-systolic volume index (ESVI) >20%. Due to these inconsistencies, we believe that in our cohort we do not have sufficient evidence to postulate an effect of CRT on atrial reverse remodelling. Furthermore, due to the retrospective design of our study, only incomplete data on left atrial volumes, a more robust parameter of atrial size, were available making analysis of changes in left atrial volumes impossible.

Similarly, we did not find an association of Super-Responder Status (according to any of

the definitions) on the occurrence of atrial fibrillation (data not shown). This may be due to the inclusion of a more heterogeneous population in this 'real world' cohort as compared with clinical trials, which may have diluted a potentially beneficial effect. Hence, further research is warranted to address these two issues in real world patients with CRT.

In contrast, and as expected, we did find an impact of underlying coronary artery disease, indicating that super-responders defined by a reduction in ESVI >30% ($p<0.02$) and EDVI reduction >20% ($p=0.09$) were less likely to suffer from coronary artery disease. These results are included in the manuscript (tables 4–6).

David Hürlimann, Jan Steffel

Department of Cardiology, University Hospital Zürich, Zurich, Switzerland

Correspondence to Dr David Hürlimann, Department of Cardiology, University Hospital Zürich, Rämistrasse 100, Zurich 8091, Switzerland; david.huerlimann@usz.ch

Competing interests None.

Provenance and peer review Commissioned; internally peer reviewed.

Heart 2012;**98**:517. doi:10.1136/heartjnl-2011-301450

REFERENCES

1. **Santulli G**, D'Ascia C. Atrial remodelling in echocardiographic super-responders to cardiac resynchronization therapy. *Heart* 2012;**98**:517.
2. **Steffel J**, Milosevic G, Hürlimann A, *et al*. Characteristics and long-term outcome of echocardiographic super-responders to cardiac resynchronisation therapy: 'real world' experience from a single tertiary care centre. *Heart* 2011;**97**:1668–74.
3. **D'Ascia SL**, D'Ascia C, Marino V, *et al*. Cardiac resynchronisation therapy response predicts occurrence of atrial fibrillation in non-ischaemic dilated cardiomyopathy. *Int J Clin Pract* 2011;**65**:1149–55.
4. **Brenyo A**, Link MS, Barsheshet A, *et al*. Cardiac resynchronization therapy reduces left atrial volume and the risk of atrial tachyarrhythmias in madit-crt (multicenter automatic defibrillator implantation trial with cardiac resynchronization therapy). *J Am Coll Cardiol* 2011;**58**:1682–9.



Atrial remodelling in echocardiographic super-responders to cardiac resynchronization therapy

Gaetano Santulli and Cristofaro D'Ascia

Heart 2012 98: 517

doi: 10.1136/heartjnl-2012-301731

Updated information and services can be found at:
<http://heart.bmj.com/content/98/6/517.1.full.html>

These include:

References

This article cites 4 articles, 1 of which can be accessed free at:
<http://heart.bmj.com/content/98/6/517.1.full.html#ref-list-1>

Article cited in:
<http://heart.bmj.com/content/98/6/517.1.full.html#related-urls>

Email alerting service

Receive free email alerts when new articles cite this article. Sign up in the box at the top right corner of the online article.

Notes

To request permissions go to:
<http://group.bmj.com/group/rights-licensing/permissions>

To order reprints go to:
<http://journals.bmj.com/cgi/reprintform>

To subscribe to BMJ go to:
<http://group.bmj.com/subscribe/>

Endothelial Cells Are Able to Synthesize and Release Catecholamines Both In Vitro and In Vivo

Daniela Sorriento, Gaetano Santulli, Carmine Del Giudice, Antonio Anastasio, Bruno Trimarco and Guido Iaccarino

Hypertension. published online June 4, 2012;

Hypertension is published by the American Heart Association, 7272 Greenville Avenue, Dallas, TX 75231

Copyright © 2012 American Heart Association, Inc. All rights reserved.

Print ISSN: 0194-911X. Online ISSN: 1524-4563

The online version of this article, along with updated information and services, is located on the World Wide Web at:

<http://hyper.ahajournals.org/content/early/2012/06/04/HYPERTENSIONAHA.111.189605>

Data Supplement (unedited) at:

<http://hyper.ahajournals.org/content/suppl/2012/06/04/HYPERTENSIONAHA.111.189605.DC1.html>

Permissions: Requests for permissions to reproduce figures, tables, or portions of articles originally published in *Hypertension* can be obtained via RightsLink, a service of the Copyright Clearance Center, not the Editorial Office. Once the online version of the published article for which permission is being requested is located, click Request Permissions in the middle column of the Web page under Services. Further information about this process is available in the [Permissions and Rights Question and Answer](#) document.

Reprints: Information about reprints can be found online at:

<http://www.lww.com/reprints>

Subscriptions: Information about subscribing to *Hypertension* is online at:

<http://hyper.ahajournals.org/subscriptions/>

Endothelial Cells Are Able to Synthesize and Release Catecholamines Both In Vitro and In Vivo

Daniela Sorriento, Gaetano Santulli, Carmine Del Giudice, Antonio Anastasio, Bruno Trimarco, Guido Iaccarino

See Editorial Commentary, pp 12–14

Abstract—Recently it has been demonstrated that catecholamines are produced and used by macrophages and mediate immune response. The aim of this study is to verify whether endothelial cells (ECs), which are of myeloid origin, can produce catecholamines. We demonstrated that genes coding for tyrosine hydroxylase, Dopa decarboxylase, dopamine β hydroxylase (D β H), and phenylethanolamine-*N*-methyl transferase, enzymes involved in the synthesis of catecholamines, are all expressed in basal conditions in bovine aorta ECs, and their expression is enhanced in response to hypoxia. Moreover, hypoxia enhances catecholamine release. To evaluate the signal transduction pathway that regulates catecholamine synthesis in ECs, we overexpressed in bovine aorta ECs either protein kinase A (PKA) or the transcription factor cAMP response element binding, because PKA/cAMP response element binding activation induces tyrosine hydroxylase transcription and activity in response to stress. Both cAMP response element binding and PKA overexpression enhance D β H and phenylethanolamine-*N*-methyl transferase gene expression and catecholamine release, whereas H89, inhibitor of PKA, exerts the opposite effect, evidencing the role of PKA/cAMP response element binding transduction pathway in the regulation of catecholamine release in bovine aorta ECs. We then evaluated by immunohistochemistry the expression of tyrosine hydroxylase, Dopa decarboxylase, D β H, and phenylethanolamine-*N*-methyl transferase in femoral arteries from hindlimbs of C57Bl/6 mice 3 days after removal of the common femoral artery to induce chronic ischemia. Ischemia evokes tyrosine hydroxylase, Dopa decarboxylase, D β H, and phenylethanolamine-*N*-methyl transferase expression in the endothelium. Finally, the pharmacological inhibition of catecholamine release by fusaric acid, an inhibitor of D β H, reduces the ability of ECs to form network-like structures on Matrigel matrix. In conclusion, our study demonstrates for the first time that ECs are able to synthesize and release catecholamines in response to ischemia. (*Hypertension*. 2012;60:129-136.) • **Online Data Supplement**

Key Words: catecholamines ■ ischemia ■ endothelium ■ angiogenesis

Endothelial cells (ECs) cover the interior surface of blood vessels throughout the entire circulatory system, and they are involved in many aspects of vascular biology.^{1–4} Indeed, angiogenesis is a phenomenon intimately associated with EC migration and proliferation during embryonic development.⁵ Similarly, ECs play major roles in immune and inflammatory reactions by regulating lymphocyte and leukocyte migration into tissues by means of direct interaction with ECs.⁶ Moreover, ECs have an important role in the regulation of the vascular tone by releasing vasoactive agents controlling smooth muscle cell proliferation and contractility.

Indeed, ECs are known to release both vasodilators (NO) and vasoconstrictors (thromboxane, platelet-derived

growth factor, and endothelin 1) in response to local and circulating stimuli.^{7–14} To this purpose, the endothelium is regulated in a fine way by a series of receptors that are expressed on its surface, including adrenergic receptors (ARs), such as α_1 and β_2 AR.^{15,16} Circulating catecholamines are thought to be the natural agonist of these receptors, giving the fact that ECs are not reached by sympathetic innervation.¹

The endothelium derives from the embryonic mesenchymal sheet, so it does the population of myeloid lineage-restricted bone marrow progenitors.¹⁷ The common features between the 2 lineages are suggested by the observation that endothelial progenitors are released in the bloodstream from bone

Received December 13, 2011; first decision January 3, 2012; revision accepted May 1, 2012.

From the Dipartimento di Medicina Clinica (D.S., G.S., C.D.G., A.A., B.T.), Scienze Cardiovascolari ed Immunologiche, Università Federico II, Naples, Italy; Università degli Studi di Salerno (G.I.), Salerno, Italy, Istituto Di Ricovero e Cura a Carattere Scientifico Multimedica (G.I.), Milan, Italy.

The online-only Data Supplement is available with this article at <http://hyper.ahajournals.org/lookup/suppl/doi:10.1161/HYPERTENSIONAHA.111.189605/-DC1>.

Correspondence to Guido Iaccarino, Department of Medicine and Surgery, Università di Salerno, Via Salvador Allende, 84081 Baronissi (SA), Italy. E-mail giaccarino@unisa.it

© 2012 American Heart Association, Inc.

Hypertension is available at <http://hyper.ahajournals.org>

DOI: 10.1161/HYPERTENSIONAHA.111.189605

marrow myelocytic progenitors.¹⁸ This finding is consistent with results from several laboratories that have reported circulating cells with myeloid features contributing to human angiogenesis.^{19–22}

Circulating catecholamines, dopamine, norepinephrine (NE), and epinephrine (EPI), regulate vascular tone via α AR activation, leading to vasoconstriction in most systemic arteries and veins. They are synthesized from the amino acid precursor l-tyrosine. Tyrosine hydroxylase (TH) is the first rate-limiting enzyme in catecholamine synthesis that catalyzes the conversion of tyrosine to l-dihydroxyphenylalanine. This latter is converted to dopamine by Dopa decarboxylase (DDC). On turn, dopamine is converted to NE by dopamine β hydroxylase ($D\beta$ H), and NE is converted to EPI by phenylethanolamine-*N*-methyl transferase (PNMT).^{23–26} Once released, catecholamines are quickly inactivated by 2 enzymes that are responsible for their catabolism, catechol-oxymethyltransferase and monoamine oxidase.^{27,28} Monoamine oxidase catalyzes the oxidative deamination of amines, and catechol-oxymethyltransferase methylates the hydroxyl group meta to the side chain of catecholamines.²⁹ Until a few years ago, catecholamines were considered mainly as conventional neurotransmitters and neuroendocrine mediators, synthesized in the adrenal medulla. However, it has been demonstrated recently that they are also produced and used by cells of the immune system.^{30–36} Indeed, catecholamines are actively produced by macrophages and have the capacity to act in an autocrine way on ARs to regulate macrophage production of interleukin 1 β , which has a key role in the inflammatory response.³⁷

Giving the common myeloid origin of ECs and macrophages and the ability of cells of the immune system to produce catecholamines, the aim of this study was to verify whether ECs were also able to autonomously synthesize and release catecholamines for signaling purposes.

Materials and Methods

All of the experiments were performed as described previously.³⁸ Extended details of Methods are described in the online-only Data Supplement.

Results

ECs Produce Catecholamines

To assess the ability of ECs to synthesize catecholamines, we first evaluated the expression of genes coding for the enzymes involved in the synthesis of catecholamines by real-time RT-PCR both in basal conditions and in response to hypoxia. We performed a time course experiment evaluating enzyme gene expression at 1, 3, 6, 16, and 24 hours of hypoxia (Figure 1A). Hypoxia-induced TH, DDC, $D\beta$ H, and PNMT gene expressions respect to basal conditions in a time-dependent manner. At 16 hours of hypoxia, we found the maximum expression of these enzymes, and then cells start to die. Based on such data, we chose to incubate cells in hypoxic conditions for 16 hours, because it is an intermediate time between enzyme maximum expression and cell death. We confirmed this result by Western blot analysis. Figure 1B shows that hypoxia increased protein levels of TH, DDC, $D\beta$ H, and PNMT in whole cell lysates. Total lysate from

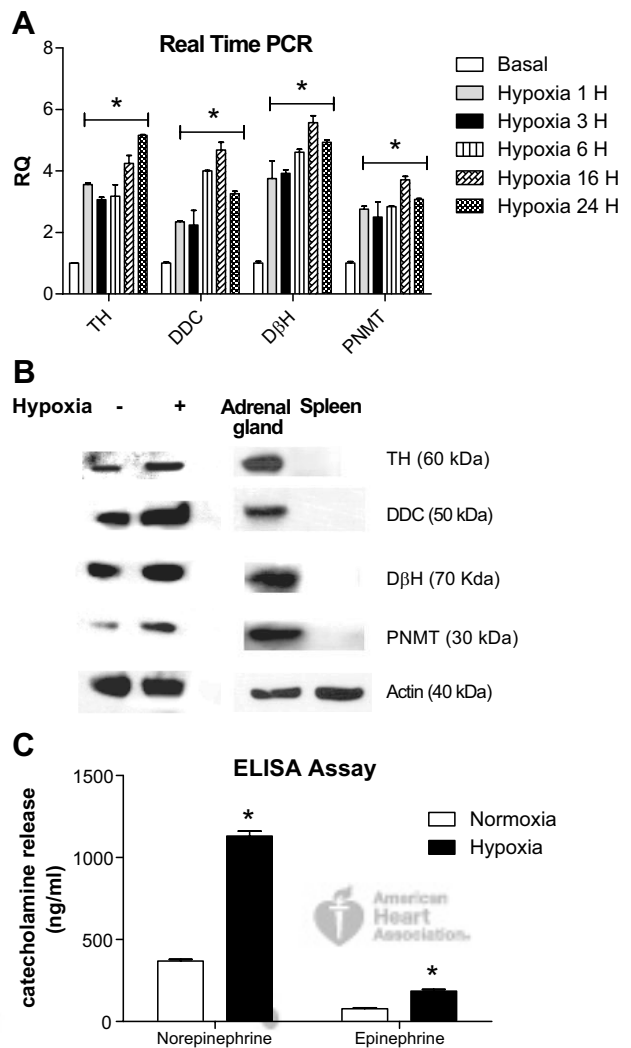


Figure 1. Endothelial cells synthesize catecholamines in response to hypoxia. **A**, RNA from bovine aorta endothelial cells (BAECs) was converted to cDNA and analyzed by real-time PCR to evaluate the expression of tyrosine hydroxylase (TH), Dopa decarboxylase (DDC), dopamine β hydroxylase ($D\beta$ H), and phenylethanolamine-*N*-methyl transferase (PNMT) in response to hypoxia (1, 3, 6, 16, and 24 hours, vertical lines; 16, 24, and 24 hours, dotted). All of the enzymes are expressed in basal conditions and hypoxia enhanced their expression in a time-dependent manner; $*P < 0.05$ vs normoxia. Results are the mean of 5 independent experiments. **B**, TH, DDC, $D\beta$ H, and PNMT levels were evaluated in whole cell lysates by Western blot. Hypoxia increases TH, DDC, $D\beta$ H, and PNMT levels. Lysates from adrenal gland and spleen were used, respectively, as positive and negative controls. Actin was used as loading control. Images are representative of 3 independent experiments. **C**, Catecholamines release was evaluated by ELISA assay in the culture medium of BAECs in basal conditions and after 16 hours of hypoxia. Hypoxia induces both norepinephrine (NE) and epinephrine (EPI) release. $*P < 0.05$ vs normoxia. Results are the mean of 5 independent experiments. \square , normoxia; \blacksquare , hypoxia.

mouse adrenal glands and spleens were used, respectively, as positive and negative controls. We also verified enzyme expression in bovine aorta ECs by immunohistochemistry. TH, DDC, $D\beta$ H, and PNMT were all expressed in basal condition, and their expression was enhanced by hypoxic stimulus (Figure S1, available in the online-only Data Supplement). Immunohistochemistry shows that DDC, $D\beta$ H, and

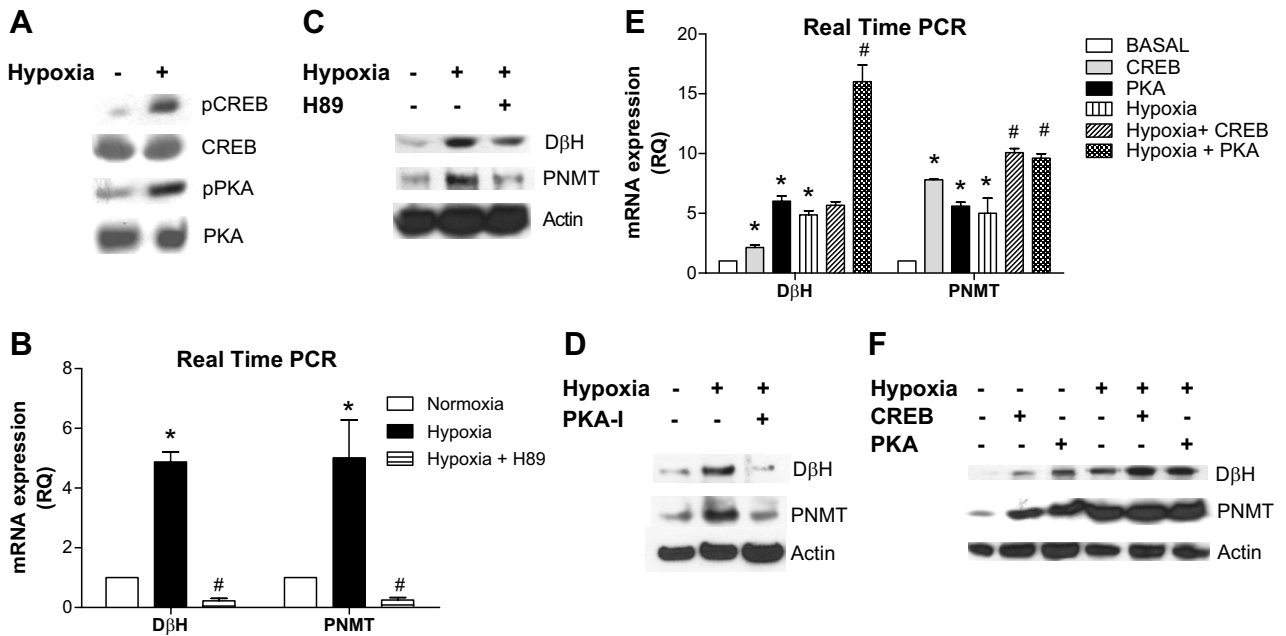


Figure 2. Endothelial cell (EC) regulates catecholamine release by hypoxia-induced protein kinase A (PKA)/cAMP response element binding (CREB) signaling activation. **A**, We evaluated hypoxia-induced CREB and PKA activation by Western blot using an antibody against the phosphorylated form of CREB and PKA. Hypoxia induces both CREB and PKA activation. Images are representative of 3 independent experiments. **B** and **C**, To evaluate the effect of PKA/CREB signaling on catecholamines release in bovine aorta ECs (BAECs), we analyzed by real-time PCR and Western blot the expression of dopamine β hydroxylase (D β H) and phenylethanolamine-N-methyl transferase (PNMT) in response to a selective inhibitor of PKA, H89. H89 inhibits both D β H and PNMT gene expression (**B**) and protein levels (**C**) in response to hypoxia. Actin was used as loading control for western blot analysis; * P <0.05 vs normoxia, # P <0.05 vs hypoxia. Results are the mean of 5 independent experiments. **B**, □, normoxia; ■, hypoxia; horizontal stripe, hypoxia+H89. **D**, To confirm the involvement of PKA in this phenomenon, we inhibited PKA activity by means of a peptidic inhibitor that is more selective and specific respect to H89, peptidic inhibitor of PKA (PKA-I). PKA-I inhibits both D β H and PNMT protein levels in response to hypoxia. Actin was used as loading control. **E** and **F**, To confirm these data, we overexpressed in cells CREB and PKA by transient transfection and analyzed D β H and PNMT levels. Both CREB and PKA overexpression increase D β H and PNMT gene expression (**E**) and protein levels (**F**) both in basal condition and in response to hypoxia. Actin was used as loading control for Western blot analysis; * P <0.05 vs normoxia, # P <0.05 vs hypoxia. Images are representative of 3 independent experiments. **E**, □, basal; ▨, CREB; ■, PKA; vertical lines, hypoxia; ▩, hypoxia+CREB; dots, hypoxia+PKA.

PNMT presented a cytosolic and perinuclear localization, whereas TH was mainly localized in the nucleus. Finally, to confirm the ability of bovine aorta ECs (BAECs) to produce catecholamines, we analyzed NE and EPI release in the culture medium by ELISA assay (Figure 1C). Hypoxia enhanced both NE and EPI release with respect to normoxia.

Hypoxia Regulates Catecholamine Synthesis in EC by Activation of Protein Kinase A/cAMP Response Element Binding Signaling

To assess the signal transduction pathway that regulates catecholamine synthesis in ECs, we evaluated protein kinase A (PKA) signaling, because it is known that PKA/cAMP response element binding (CREB) activation induces TH transcription and activity in response to stress.^{39,40} We first analyzed by Western blot the effect of hypoxia on the activation of CREB and PKA. Figure 2A shows that hypoxia induces the expression of the phosphorylated and activated forms of both CREB and PKA, confirming that, also in BAECs, hypoxia regulates PKA/CREB signaling. Based on such data, we evaluated whether hypoxia-induced PKA/CREB activation regulates catecholamine synthesis in BAECs. In these experiments, we focused on D β H and PNMT expression, being the key enzymes for NE and EPI

synthesis. To assess whether this signaling was involved in the regulation of catecholamine synthesis, we pharmacologically inhibited PKA/CREB signaling using a selective inhibitor of PKA, H89. This latter inhibited hypoxia induced D β H and PNMT gene expression (D β H, $-73.7 \pm 0.03\%$ and PNMT, $-75.2 \pm 0.04\%$ versus hypoxia; Figure 2B) and prevented hypoxia-evoked increase of D β H and PNMT protein levels (Figure 2C). To further confirm these data, we used a peptidic inhibitor of PKA (PKA-I), which is more selective and selective respect to H89. PKA-I reduced both D β H and PNMT protein levels in response to hypoxia (Figure 2D). These data demonstrate that, in BAECs, hypoxia induces PKA/CREB signaling, and the activation of this pathway regulates catecholamine synthesis. To confirm these results, we overexpressed in BAECs both PKA and CREB by means of transient transfection. Both CREB and PKA overexpression enhanced D β H (CREB, $+2.1 \pm 0.09$; PKA, $+6 \pm 2.01$ -fold of basal) and PNMT (CREB, $+9.8 \pm 0.3$; PKA, $+5.6 \pm 1.7$ -fold of basal) gene expression in basal conditions (Figure 2E). PKA overexpression further enhanced the response to hypoxia (D β H $+16 \pm 0.6$ and PNMT $+9.6 \pm 0.2$ versus hypoxia; Figure 2E). Accordingly, Western blot analysis showed that CREB and PKA overexpression increased D β H and PNMT protein levels, and PKA overexpression

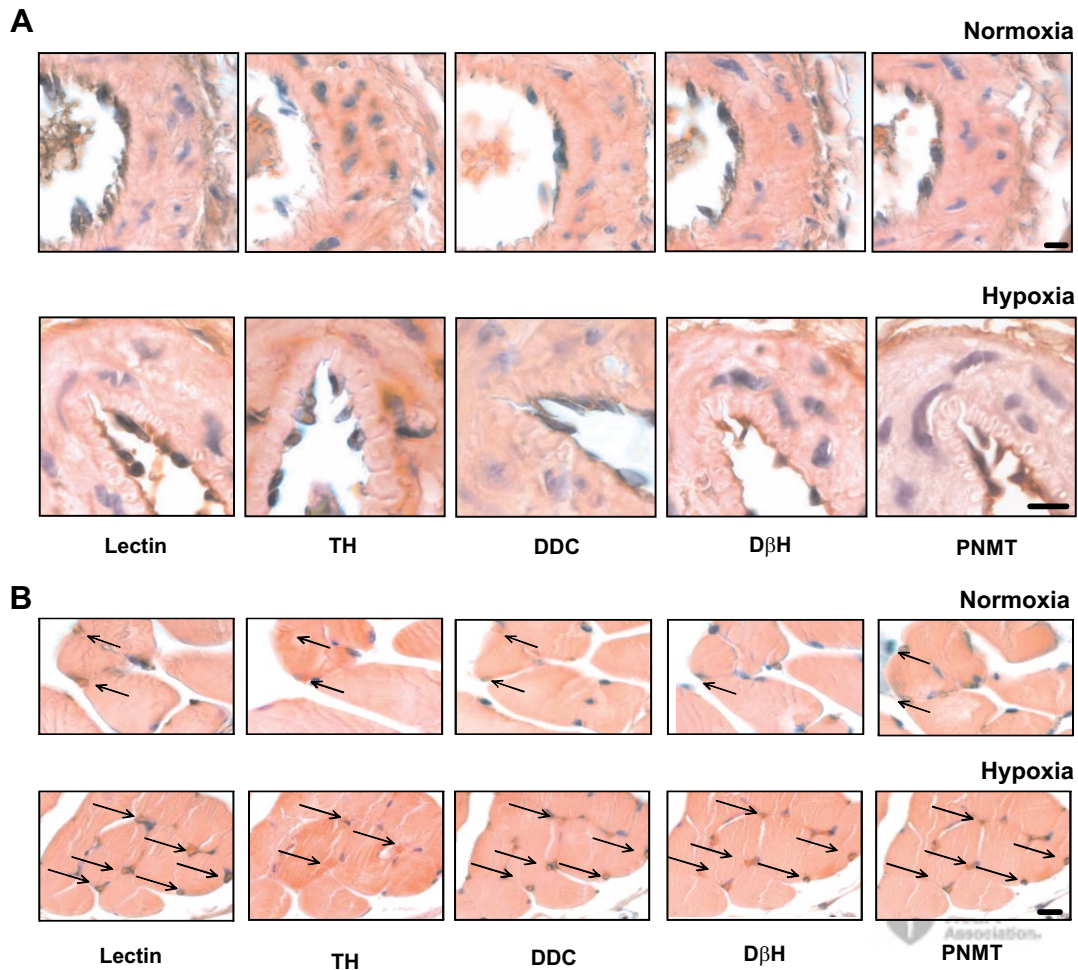


Figure 3. Endothelial cell (EC) produce catecholamines in vivo. Immunohistochemical analysis of tyrosine hydroxylase (TH), Dopa decarboxylase (DDC), dopamine β hydroxylase (D β H), and phenylethanolamine-*N*-methyl transferase (PNMT) expression was performed in superficial femoral arteries from hindlimbs of C57/black mice 3 days after removal of the common femoral artery. Ischemia induces TH, DDC, D β H, and PNMT expression in the endothelium of femoral arteries (A) and in capillaries (B), evidenced in the femoral muscle by lectin staining. The expression of TH in endothelium is just evident at a higher magnification. TH is also expressed in the muscle tissue, and its expression is enhanced in response to ischemia (B). Scale bar is 20 μ m. Images are representative of 3 independent experiments.

further increased the response to hypoxia (Figure 2F). Moreover, PKA/CREB signaling also regulated catecholamine release in the culture medium (Figure S2). Indeed, H89 inhibited hypoxia-induced NE (Figure S2A) and EPI (Figure S2B) release. CREB overexpression caused NE (Figure S2C) and EPI (Figure S2D) release. In these conditions, hypoxia was no longer able to induce further accumulation (Figure S2C and S2D). Also, PKA overexpression increased catecholamine release (Figure S2C and S2D), and in these cells hypoxia was still able to induce a modest increase of catecholamine release. These data indicate that hypoxia-induced activation of the PKA/CREB signaling transduction pathway regulates catecholamine synthesis and release in BAECs.

Endothelium Produces Catecholamines In Vivo

To confirm in vitro data, we evaluated in vivo by immunohistochemistry the expression of TH, DDC, D β H, and PNMT in superficial femoral arteries from hindlimbs of C57Bl/6 mice 3 days after surgery. Ischemia induced DDC, D β H, and

PNMT expression in the endothelium of femoral arteries (Figure 3A) and in capillaries, highlighted in the femoral muscle by lectin staining (Figure 3B). On the contrary, TH was maximally expressed in the cytoplasm of muscle cells, although a higher magnification also revealed an endothelial localization. Negative control with secondary antibody only was shown in Figure S3.

Endothelium-Dependent Catecholamine Release Has a Key Role in Angiogenesis In Vitro

To evaluate the physiopathological role of endothelium-dependent catecholamine release in vitro, we evaluated the ability of BAECs to form network-like structures on Matrigel matrix in the presence or absence of a selective inhibitor of D β H, fusaric acid (FA). Figure S4 shows that hypoxia induced vascular network formation and FA inhibited the response to hypoxia (Figure S4A). To confirm that the effect of FA on angiogenesis is ascribed to its ability to inhibit catecholamine release, we evaluated NE and EPI release in the culture medium by ELISA assay (Figure S4B and S4C).

FA inhibited hypoxia-dependent catecholamine release (NE, $-32 \pm 1.7\%$; EPI, $-37 \pm 2.1\%$ versus hypoxia). These data suggest that ECs autonomously produce catecholamines that have a key role in the regulation of EC proangiogenic responses. To avoid the possibility that FA-dependent inhibition of angiogenesis *in vitro* was attributed to a toxic effect of the drug, we performed a proliferation assay using different dosages of FA. FA turned out to be not toxic for cells at doses from 10 nmol/L to $\leq 500 \mu\text{mol/L}$ (data not shown).

β_2 AR Is Involved in Catecholamine-Induced Angiogenesis in BAECs

We have demonstrated previously that β_2 AR has a key role in angiogenesis both *in vitro* and *in vivo*.^{16,41} In particular, we demonstrated *in vivo* that β_2 AR regulates angiogenesis *in vivo* in response to ischemia, because angiogenesis is impaired in β_2 AR knockout mice and is ameliorated by reinstatement of β_2 AR. Here we tested this effect also on hypoxia-induced angiogenesis in BAECs. To this aim we performed a real-time PCR analysis to evaluate the effect of β_2 AR inhibition by the selective inhibitor ICI 118.551 on vascular endothelial growth factor gene expression. Our data show that β_2 AR blockade is able to reduce vascular endothelial growth factor expression induced by hypoxia (Figure 4A), suggesting a key role for this receptor in catecholamine-induced angiogenesis in response to hypoxia. Furthermore, we evaluated whether catecholamine-induced β_2 AR-dependent angiogenesis could, in turn, be regulated by β_2 AR itself. To this aim, we performed a real-time PCR experiment to evaluate $D\beta\text{H}$ and PNMT gene expression in cells with selective blockade of β_2 AR by ICI 118.551. The blockade of β_2 AR inhibited both $D\beta\text{H}$ (Figure 4B) and PNMT (Figure 4C) gene expression in response to hypoxia. These data suggest that catecholamines from ECs could promote their own synthesis in a paracrine positive feedback manner by means of β_2 AR activation.

Discussion

We report here, for the first time, that ECs are capable of synthesizing catecholamines because they have the complete intracellular machinery for the generation and release of NE and EPI. *In vitro*, ECs expressed all of the enzymes involved in the synthesis of catecholamines in basal conditions, and this expression is enhanced in response to hypoxia. We also identified the molecular mechanism that regulates this phenomenon. Indeed, we demonstrated that hypoxia-induced catecholamine release in the culture medium is regulated by the activation of PKA/CREB signaling, which is already known to regulate most important endothelial functions, such as endothelial NO synthase gene transcriptional activation.⁴² These results are paralleled by data from an *in vivo* model of chronic ischemia, where we demonstrate that TH, DDC, $D\beta\text{H}$, and PNMT are expressed in the endothelium of the femoral artery. TH expression in endothelium, despite the other enzymes, is difficult to detect at low magnification and needs a higher enlargement. This is because of the nuclear localization of TH in BAECs, as demonstrated by immunohistochemical analysis (Figure S1), which is difficult to detect *in vivo* in capillaries. Moreover, the nuclear staining is

masked by hematoxylin counterstain. This nuclear localization of TH is suggested also by other reports, in human epidermal melanocytes⁴³ and in perikarya of rat ventral tegmental area.⁴⁴ Our *in vivo* results also show that TH is localized in the cytoplasm of muscle cells, and it was never described before. However, further experiments are needed to clarify this aspect.

ECs play a critical role in the control of vascular function because they participate in all aspects of vascular homeostasis but also in physiological or pathological processes like vascular wall remodeling, inflammation, or thrombosis. In particular, they have a key role in angiogenesis, in coagulation and fibrinolysis, and in the regulation of vascular tone, as well as in inflammatory reactions and in tumor neoangiogenesis.^{45–50} ECs are capable of synthesizing and releasing a variety of substances that may exert autocrine, paracrine, or endocrine effects. Indeed, they contribute to the regulation of blood pressure and blood flow by releasing vasodilators such as NO and prostacyclin, as well as vasoconstrictors, including endothelin and platelet-activating factor, in response to stimuli.^{14,51,52} Given the evidence that ischemia enhances plasma levels of NE,⁵³ it has been shown recently that catecholamines contribute to arteriogenesis and angiogenesis in pathological conditions such as hindlimb ischemia⁵⁴ and that they contribute to angiogenesis in the wound-healing process.⁵⁵ Based on our and previous data, we hypothesize that the ability of ECs to synthesize and release catecholamines is an autoregulatory physiological mechanism in response to hypoxia to induce neovascularization. Indeed, the inhibition of catecholamine release by FA reduced the proangiogenic phenotype of ECs *in vitro*. This finding puts the ARs on ECs in a different perspective. Indeed, the lack of terminal innervations on ECs has sustained the concept that circulating catecholamines are the natural stimulants to endothelial ARs. Our data allow for the promoting of a new scenario in which ECs produce catecholamines that act in a paracrine way to sustain proangiogenic phenotypes in conditions such as ischemia (Figure 4D). Furthermore, these data are well in agreement with previous reports showing the ability of ECs to produce catecholamine catabolism enzymes, such as monoamine oxidase and catechol-oxyethyltransferase.⁵⁶

We have identified previously the β_2 AR as the adrenergic receptor involved in the regulation of angiogenesis in ECs.^{16,41} Here we demonstrated that β_2 AR is activated by catecholamines released by ECs to induce angiogenesis, and it, in turn, regulates catecholamines release. A future direction of research will address the signaling linking hypoxia and PKA/CREB activation given the potential role of this pathway in the activation of the endothelium. In conclusion, our study demonstrates for the first time the ability of ECs to synthesize and release catecholamines in response to hypoxia (*in vitro*) and ischemia (*in vivo*) and the involvement of this phenomenon in the regulation of angiogenesis.

Perspectives

Our data indicate ECs as a source of catecholamine synthesis and release. This is a further advance in the understanding of endothelial function and physiology that could be useful to

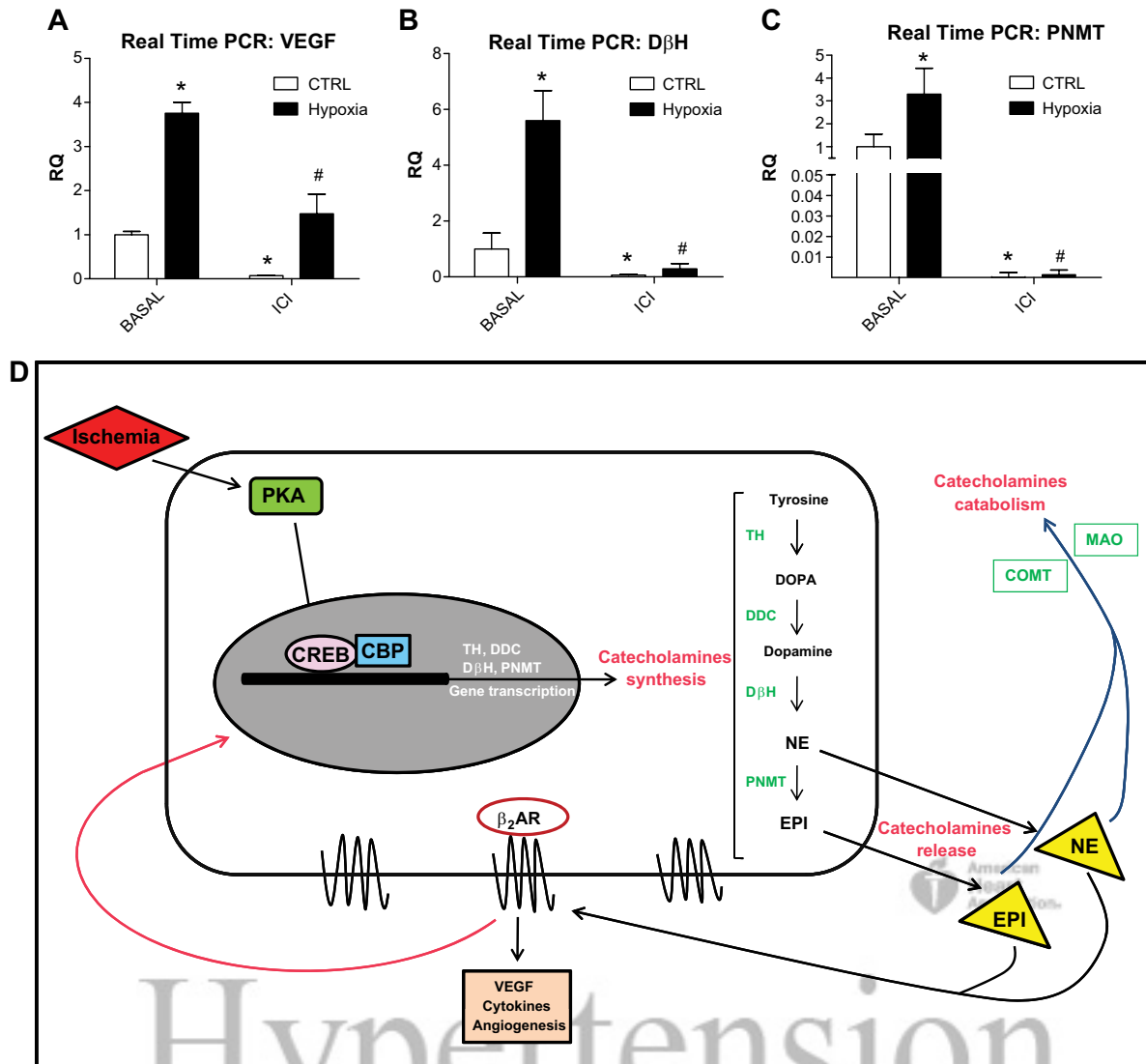


Figure 4. β_2 -adrenergic receptor (AR) is involved in catecholamine-induced angiogenesis in bovine aorta endothelial cells (BAECs). BAECs were treated with ICI 118.551, 100 nmol/L, for 30 minutes and incubated in the hypoxic chamber for 16 hours. **A** through **C**, RNA from BAECs was converted to cDNA and analyzed by real-time PCR to evaluate the expression of vascular endothelial growth factor (VEGF; **A**), dopamine β hydroxylase (D β H; **B**), and phenylethanolamine-*N*-methyl transferase (PNMT; **C**) in response to hypoxia. All of the enzymes are expressed in basal conditions, and hypoxia enhanced their expression. ICI inhibits basal gene expression and reduces the response to hypoxia; * $P < 0.05$ vs normoxia; # $P < 0.05$ vs hypoxia. Results are the mean of 5 independent experiments. □, control (CTRL); ■, hypoxia. **D**, Schematic summary of our results: in endothelial cells, ischemia activates induced protein kinase A (PKA)/cAMP response element binding (CREB) signaling inducing the transcription of genes coding for tyrosine hydroxylase (TH), Dopa decarboxylase (DDC), D β H, and PNMT. All of these enzymes participate in catecholamine synthesis. Norepinephrine (NE) and epinephrine (EPI) are then released and act in a paracrine way on β_2 adrenergic receptors to promote VEGF production and angiogenesis. The enzymes catechol-oxyethyltransferase (COMT) and monoamine oxidase (MAO) regulate catecholamine catabolism.

determine targeted therapies for many diseases, including cancer, cardiovascular disease, and inflammatory conditions.

Acknowledgments

We thank Dr Michele Ciccarelli (Federico II University of Naples, Naples, Italy) for critical reading and Prof Antonio Feliciello (Federico II University of Naples) for providing the peptidic inhibitor of PKA plasmid.

Sources of Funding

This work was funded by a grant from Ministero Istruzione, Università e Ricerca Scientifica (20074MSWYW_003), to G.I.

Disclosures

None.

References

- Aird WC. Phenotypic heterogeneity of the endothelium: I—structure, function, and mechanisms. *Circ Res.* 2007;100:158–173.
- Cook-Mills JM, Deem TL. Active participation of endothelial cells in inflammation. *J Leukoc Biol.* 2005;77:487–495.
- Lamallice L, Le Boeuf F, Huot J. Endothelial cell migration during angiogenesis. *Circ Res.* 2007;100:782–794.
- Vanhoutte PM. Endothelial dysfunction and atherosclerosis. *Eur Heart J.* 1997;18(suppl E)E19–E29.
- Carmeliet P, Jain RK. Molecular mechanisms and clinical applications of angiogenesis. *Nature.* 2011;473:298–307.

6. Sumpio BE, Riley JT, Dardik A. Cells in focus: endothelial cell. *Int J Biochem Cell Biol.* 2002;34:1508–1512.
7. Bowen-Pope DF, Hart CE, Seifert RA. Sera and conditioned media contain different isoforms of platelet-derived growth factor (PDGF) which bind to different classes of PDGF receptor. *J Biol Chem.* 1989; 264:2502–2508.
8. Gellai M, De Wolf R, Fletcher T, Nambi P. Contribution of endogenous endothelin-1 to the maintenance of vascular tone: role of nitric oxide. *Pharmacology.* 1997;55:299–308.
9. Haynes WG, Webb DJ. Endothelin as a regulator of cardiovascular function in health and disease. *J Hypertens.* 1998;16:1081–1098.
10. Iadecola C, Pelligrino DA, Moskowitz MA, Lassen NA. Nitric oxide synthase inhibition and cerebrovascular regulation. *J Cereb Blood Flow Metab.* 1994;14:175–192.
11. Masaki T. Endothelin in vascular biology. *Ann NY Acad Sci.* 1994;714: 101–108.
12. Moncada S, Palmer RM, Higgs EA. Nitric oxide: physiology, pathophysiology, and pharmacology. *Pharmacol Rev.* 1991;43:109–142.
13. Rubanyi GM, Polokoff MA. Endothelins: molecular biology, biochemistry, pharmacology, physiology, and pathophysiology. *Pharmacol Rev.* 1994;46:325–415.
14. Yanagisawa M, Kurihara H, Kimura S, Tomobe Y, Kobayashi M, Mitsui Y, Yazaki Y, Goto K, Masaki T. A novel potent vasoconstrictor peptide produced by vascular endothelial cells. *Nature.* 1988;332:411–415.
15. Ciccarelli M, Santulli G, Campanile A, Galasso G, Cervero P, Altobelli GG, Cimini V, Pastore L, Piscione F, Trimarco B, Iaccarino G. Endothelial α 1-adrenoceptors regulate neo-angiogenesis. *Br J Pharmacol.* 2008;153:936–946.
16. Iaccarino G, Cipolletta E, Fiorillo A, Annechiarico M, Ciccarelli M, Cimini V, Koch WJ, Trimarco B. Beta(2)-adrenergic receptor gene delivery to the endothelium corrects impaired adrenergic vasorelaxation in hypertension. *Circulation.* 2002;106:349–355.
17. Oswald J, Boxberger S, Jorgensen B, Feldmann S, Ehninger G, Bornhauser M, Werner C. Mesenchymal stem cells can be differentiated into endothelial cells in vitro. *Stem Cells.* 2004;22:377–384.
18. Bailey AS, Willenbring H, Jiang S, Anderson DA, Schroeder DA, Wong MH, Grompe M, Fleming WH. Myeloid lineage progenitors give rise to vascular endothelium. *Proc Natl Acad Sci USA.* 2006;103:13156–13161.
19. Elsheikh E, Uzunel M, He Z, Holgersson J, Nowak G, Sumitran-Holgersson S. Only a specific subset of human peripheral-blood monocytes has endothelial-like functional capacity. *Blood.* 2005;106: 2347–2355.
20. Fujiyama S, Amano K, Uehira K, Yoshida M, Nishiwaki Y, Nozawa Y, Jin D, Takai S, Miyazaki M, Egashira K, Imada T, Iwasaka T, Matsubara H. Bone marrow monocyte lineage cells adhere on injured endothelium in a monocyte chemoattractant protein-1-dependent manner and accelerate reendothelialization as endothelial progenitor cells. *Circ Res.* 2003;93: 980–989.
21. Rehman J, Li J, Orschell CM, March KL. Peripheral blood “endothelial progenitor cells” are derived from monocyte/macrophages and secrete angiogenic growth factors. *Circulation.* 2003;107:1164–1169.
22. Zhang R, Yang H, Li M, Yao Q, Chen C. Acceleration of endothelial-like cell differentiation from CD14+ monocytes in vitro. *Exp Hematol.* 2005; 33:1554–1563.
23. Christenson JG, Dairman W, Udenfriend S. Preparation and properties of a homogeneous aromatic l-amino acid decarboxylase from hog kidney. *Arch Biochem Biophys.* 1970;141:356–367.
24. Connett RJ, Kirshner N. Purification and properties of bovine phenylethanolamine n-methyltransferase. *J Biol Chem.* 1970;245:329–334.
25. Craine JE, Daniels GH, Kaufman S. Dopamine- β -hydroxylase: the subunit structure and anion activation of the bovine adrenal enzyme. *J Biol Chem.* 1973;248:7838–7844.
26. Shiman R, Akino M, Kaufman S. Solubilization and partial purification of tyrosine hydroxylase from bovine adrenal medulla. *J Biol Chem.* 1971; 246:1330–1340.
27. Axelrod J, Weinshilboum R. Catecholamines. *N Engl J Med.* 1972;287: 237–242.
28. Kopin IJ. Monoamine oxidase and catecholamine metabolism. *J Neural Transm Suppl.* 1994;41:57–67.
29. Eisenhofer G, Kopin IJ, Goldstein DS. Catecholamine metabolism: a contemporary view with implications for physiology and medicine. *Pharmacol Rev.* 2004;56:331–349.
30. Josefsson E, Bergquist J, Ekman R, Tarkowski A. Catecholamines are synthesized by mouse lymphocytes and regulate function of these cells by induction of apoptosis. *Immunology.* 1996;88:140–146.
31. Bergquist J, Silberring J. Identification of catecholamines in the immune system by electrospray ionization mass spectrometry. *Rapid Commun Mass Spectrom.* 1998;12:683–688.
32. Marino F, Cosentino M, Bombelli R, Ferrari M, Lecchini S, Frigo G. Endogenous catecholamine synthesis, metabolism storage, and uptake in human peripheral blood mononuclear cells. *Exp Hematol.* 1999;27: 489–495.
33. Musso NR, Brenzi S, Setti M, Indiveri F, Lotti G. Catecholamine content and in vitro catecholamine synthesis in peripheral human lymphocytes. *J Clin Endocrinol Metab.* 1996;81:3553–3557.
34. Spengler RN, Chensue SW, Giacherio DA, Blenk N, Kunkel SL. Endogenous norepinephrine regulates tumor necrosis factor- α production from macrophages in vitro. *J Immunol.* 1994;152:3024–3031.
35. Cosentino M, Fietta AM, Ferrari M, Rasini E, Bombelli R, Carcano E, Saporiti F, Meloni F, Marino F, Lecchini S. Human CD4+CD25+ regulatory T cells selectively express tyrosine hydroxylase and contain endogenous catecholamines subserving an autocrine/paracrine inhibitory functional loop. *Blood.* 2007;109:632–642.
36. Bergquist J, Tarkowski A, Ekman R, Ewing A. Discovery of endogenous catecholamines in lymphocytes and evidence for catecholamine regulation of lymphocyte function via an autocrine loop. *Proc Natl Acad Sci USA.* 1994;91:12912–12916.
37. Engler KL, Rudd ML, Ryan JJ, Stewart JK, Fischer-Stenger K. Autocrine actions of macrophage-derived catecholamines on interleukin- β . *J Neuroimmunol.* 2005;160:87–91.
38. Sorriento D, Ciccarelli M, Santulli G, Campanile A, Altobelli GG, Cimini V, Galasso G, Astone D, Piscione F, Pastore L, Trimarco B, Iaccarino G. The G-protein-coupled receptor kinase 5 inhibits NF κ B transcriptional activity by inducing nuclear accumulation of IkappaB α . *Proc Natl Acad Sci USA.* 2008;105:17818–17823.
39. Piech-Dumas KM, Tank AW. CREB mediates the camp-responsiveness of the tyrosine hydroxylase gene: use of an antisense RNA strategy to produce CREB-deficient PC12 cell lines. *Brain Res Mol Brain Res.* 1999;70:219–230.
40. Lim J, Yang C, Hong SJ, Kim KS. Regulation of tyrosine hydroxylase gene transcription by the cAMP-signaling pathway: involvement of multiple transcription factors. *Mol Cell Biochem.* 2000;212:51–60.
41. Ciccarelli M, Sorriento D, Cipolletta E, Santulli G, Fusco A, Zhou RH, Eckhart AD, Poppel K, Koch WJ, Trimarco B, Iaccarino G. Impaired neoangiogenesis in β -adrenoceptor gene-deficient mice: restoration by intravascular human β -adrenoceptor gene transfer and role of NF κ B and CREB transcription factors. *Br J Pharmacol.* 162: 712–721.
42. Min J, Jin YM, Moon JS, Sung MS, Jo SA, Jo I. Hypoxia-induced endothelial NO synthase gene transcriptional activation is mediated through the TAX-responsive element in endothelial cells. *Hypertension.* 2006;47:1189–1196.
43. Gillbro JM, Marles LK, Hibberts NA, Schallreuter KU. Autocrine catecholamine biosynthesis and the β -adrenoceptor signal promote pigmentation in human epidermal melanocytes. *J Invest Dermatol.* 2004;123: 346–353.
44. Bayer VE, Pickel VM. Ultrastructural localization of tyrosine hydroxylase in the rat ventral tegmental area: relationship between immunolabeling density and neuronal associations. *J Neurosci.* 1990;10: 2996–3013.
45. Isermann B, Hendrickson SB, Zogg M, Wing M, Cumiskey M, Kisanuki YY, Yanagisawa M, Weiler H. Endothelium-specific loss of murine thrombomodulin disrupts the protein C anticoagulant pathway and causes juvenile-onset thrombosis. *J Clin Invest.* 2001;108: 537–546.
46. Nathan C. Points of control in inflammation. *Nature.* 2002;420:846–852.
47. Pearson JD. Endothelial cell function and thrombosis. *Baillieres Best Pract Res Clin Haematol.* 1999;12:329–341.
48. Sidelmann JJ, Gram J, Jespersen J, Kluff C. Fibrin clot formation and lysis: basic mechanisms. *Semin Thromb Hemost.* 2000;26:605–618.
49. Yancopoulos GD, Davis S, Gale NW, Rudge JS, Wiegand SJ, Holash J. Vascular-specific growth factors and blood vessel formation. *Nature.* 2000;407:242–248.
50. Folkman J. Endothelial cells and angiogenic growth factors in cancer growth and metastasis: introduction. *Cancer Metastasis Rev.* 1990;9: 171–174.
51. Palmer RM, Ferrige AG, Moncada S. Nitric oxide release accounts for the biological activity of endothelium-derived relaxing factor. *Nature.* 1987; 327:524–526.

52. Barry OP, Pratico D, Lawson JA, Fitzgerald GA. Transcellular activation of platelets and endothelial cells by bioactive lipids in platelet microparticles. *J Clin Invest*. 1997;99:2118–2127.
53. Borovsky V, Herman M, Dunphy G, Caplea A, Ely D. Co2 asphyxia increases plasma norepinephrine in rats via sympathetic nerves. *Am J Physiol*. 1998;274:R19–R22.
54. Chalothorn D, Zhang H, Clayton JA, Thomas SA, Faber JE. Catecholamines augment collateral vessel growth and angiogenesis in hindlimb ischemia. *Am J Physiol Heart Circ Physiol*. 2005;289:H947–H959.
55. Candipan RC, Hsiun PT, Pratt R, Cooke JP. Vascular injury augments adrenergic neurotransmission. *Circulation*. 1994;89:777–784.
56. Baranczyk-Kuzma A, Audus KL, Borchardt RT. Catecholamine-metabolizing enzymes of bovine brain microvessel endothelial cell monolayers. *J Neurochem*. 1986;46:1956–1960.

Novelty and Significance

What Is New?

- ECs respond to stress-releasing catecholamines. These catecholamines stimulate receptors on EC accelerating regenerating processes, such as angiogenesis.

What Is Relevant?

- Endothelial dysfunction seen in hypertension might alter the ability of ECs to release catecholamines in response to stress. This impairment

alters the ability of ECs to adapt to conditions such as ischemia or inflammation.

Summary

We demonstrate that ECs present the enzymes to produce and release NE and EPI, in response to ischemia. These substances, in turn, further sustain the activation of endothelial function, such as angiogenesis.



Hypertension

JOURNAL OF THE AMERICAN HEART ASSOCIATION

ONLINE SUPPLEMENT SECTION

Endothelial cells are able to synthesize and release catecholamines both *in vitro* and *in vivo*

Daniela Sorriento¹, Gaetano Santulli¹, Carmine Del Giudice¹, Antonio Anastasio¹, Bruno Trimarco¹, Guido Iaccarino^{2,3}

Affiliations of Authors: ¹ Dipartimento di Medicina Clinica, Scienze Cardiovascolari ed Immunologiche, Università Federico II, Napoli, Italy; ² Università degli Studi di Salerno, Salerno, Italy, ³ IRCCS Multimedica, Milano, Italy.

Running Title: The endothelium releases catecholamines

Word count of manuscript: 4999

Total number of figures: 4

Address for Correspondence

Guido Iaccarino, MD, PhD, FESC

Department of Medicine and Surgery

Università di Salerno

Via Salvador Allende, 84081 Baronissi (SA), Italy

[Tel:+39089965021](tel:+39089965021), Fax:+39089969642

E-mail: giaccarino@unisa.it

Supplemental Methods

Cell Culture

Bovine aorta EC (BAEC), purchased from Lonza, were cultured in Dulbecco's MEM (DMEM) supplemented with 10% foetal bovine serum (FBS) at 37°C in 95% air and 5% CO₂.

Plasmids

p-CREB and p-PKA were purchased from Stratagene; p-PKA-I was a kind gift of Prof. Antonio Feliciello (Federico II University of Naples). Transient transfection of these plasmids was performed using Lipofectamine 2000 (Invitrogen) in 70% confluent BAEC, accordingly to manufacturer instructions.

Hypoxia

24 hours after transient transfection, culture medium was replaced with hypoxia-medium (116 mM NaCl, 5.4 mM KCl, 0.8 mM MgSO₄, 26.2 mM NaHCO₃, 1 mM NaH₂PO₄, 1.8 mM CaCl₂, 0.01 mM glycine and 0.001 (% w/v) phenol red), previously saturated for 10 min at 1 atm with 95% N₂ and 5% CO₂ mixture. In some plates H89 (10⁻⁶M, Sigma Aldrich), a selective inhibitor of PKA, was added to the culture medium for 30 minutes and then plates were incubated at 37°C in an anaerobic chamber (hypoxia chamber) filled with the same gas mixture for 16 hours.

Western Blot

BAEC were lysed in RIPA/SDS buffer [50 mM Tris-HCl (pH 7.5), 150 mM NaCl, 1% Nonidet P-40, 0, 25% deoxycholate, 9,4 mg/50 ml sodium orthovanadate, 20% SDS]. Protein concentration was determined by using BCA assay kit (Pierce). Total extracts were electrophoresed by SDS/PAGE and transferred to nitrocellulose. Endogenous pCREB, pPKA, TH (Cell signaling), Actin, DDC, DβH and PNMT (Santacruz) were visualized by specific antibodies, anti-rabbit HRP-conjugated secondary antibody (Santa Cruz) and standard chemiluminescence (Pierce).

Immunocytochemistry and Immunohistochemistry

Transfected cells were grown in chamber slides (Nunc, LabTek). Cells were then fixed with -20°C cold methanol and permeabilized with 0.01% Triton X-100 in PBS. Primary antibodies incubation with anti-TH, anti-DDC, anti-DbH and anti-PNMT (Santacruz) at a 1:50 dilution were performed at room temperature for two hours. Specific secondary antibodies (Santacruz) at a 1:100 dilution were incubated at room temperature for 1 hour. The peroxidase was revealed in presence of 0,03% hydrogen peroxide and of an electron donor, 2,5% diaminobenzidine, which becomes visible as a brown precipitate. Cells were then counterstained with hematoxylin, then dehydrated, cleared with histolemon and coverslipped. For immunohistochemistry, femoral muscles and arteries were fixed in formaline, embedded in paraffin and sectioned at 5 μm with a rotary microtome. Sections were dewaxed, rehydrated and immunostaining was performed by the peroxidase anti-peroxidase (PAP) method as described above. Images were taken by using an Eclipse E1000 Fluorescence Microscope (Nikon) and acquired by using Sigma Scan Pro software (Jandel). Images were optimized for contrast in Adobe PhotoShop, but no further manipulations were made.

Real Time RT-PCR

Total RNA was isolated using Trizol reagent (Invitrogen) and cDNA was synthesized by means of Thermo-Script RT-PCR System (Invitrogen), following the manufacturer instruction. After reverse transcription reaction, real-time quantitative polymerase chain reaction (PCR) was performed with the SYBR Green Real Time PCR master mix kit (Applied Biosystems). The reaction was visualized by SYBR Green Analysis (Applied Biosystem) on StepOne instrument (Applied Biosystem).

Primers for gene expression analysis were as follows:

TH: FOR 5'AGCCTGGCCTTCCGCGTGTCCAG3'
 REV 5'CTACGCCTCCCGCATCCAGCGCCC3'
DDC: FOR, 5'CCAGAGACATTTGAGGCCAT3'

DBH: REV 5'TCCAGCCAGAAACGCCTCT3',
 FOR 5'GAACATCAGCTATGCGCAGGA3'
 PNMT: REV 5' AAAAGGCCTCTTGAAGAGCAG3'
 FOR 5'TACCTCCGCAACAACACTACGC3'
 18S: REV 5' CTGTATACGCTCCAGTCGAA3'
 FOR 5'GTAACCCGTTGAACCCATT3'
 VEGF: REV 5'CCATCCAATCGGTAGTAGCG3'
 FOR 5'CAGGCTGTCGTAACGATGAA3'
 REV 5'TTTCCTTGCGCTTTCGTTTTT3'

All values obtained were normalized to the values obtained with the 18S primers (endogenous control) and relative to the reference sample (basal control) using the formula $2^{-\Delta\Delta Ct}$. Obtained results are expressed as relative quantification (RQ).

ELISA assay

The release of catecholamines in the culture medium was analyzed by ELISA assay (Pantec), accordingly to the manufacturer instructions. Cell were transfected and incubated in the hypoxia chamber for 16 hours as described above. In some experiments Fusaric Acid (Sigma, 10 μ M) was added to the culture medium before hypoxic stimulus to inhibit catecholamines release. Culture medium was collected and used for the ELISA assay.

Angiogenesis *in vitro*

Angiogenesis *in vitro* was performed on Matrigel matrix as previously described ¹.

In Vivo Study.

Experiments were carried out, in accordance to Federico II University guidelines and to the [National Institutes of Health \(NIH\) Guide for the Care and Use of Laboratory Animals](#), on 12-week-old C57Bl/6 mice, which had access to food and water *ad libitum*. The model of unilateral hindlimb (HL) ischemia was prepared as described previously ¹. Briefly, anesthesia was performed with an intramuscular injection of a mixture of tiletamine (50 mg/kg) and zolazepam (50 mg/kg); the right common femoral artery was exposed, isolated and permanently closed after the emergence from the inguinal ligament with a non-reabsorbable suture (5-0 silk, Ethicon) whereas the femoral vein was clamped. Afterwards, the common femoral artery was removed and the wound closed in layers. After 3 days, femoral muscles and arteries were extracted from both legs of five animals/group, fixed in formalin and included in paraffin. Paraffin-embedded sections were stained for hematoxylin and eosin. Five micrometer-thick sections were processed for the triple-layered immunohistochemical PAP (peroxidase anti-peroxidase) method as described above. For negative controls, the primary anti-serum was omitted. Lectin staining (1:100, Sigma Aldrich) was used to identify capillaries.

Statistical analysis

All values are presented as mean \pm SEM. Two-way ANOVA was performed to compare the different parameters between the different groups. A P value < 0.05 was considered to be significant. Statistics were computed with GraphPad Prism version 5.01 (GraphPad Software).

Supplemental References

1. Sorriento D, Ciccarelli M, Santulli G, Campanile A, Altobelli GG, Cimini V, Galasso G, Astone D, Piscione F, Pastore L, Trimarco B, Iaccarino G. The g-protein-coupled receptor kinase 5 inhibits nfkappab transcriptional activity by inducing nuclear accumulation of ikappab alpha. *Proc Natl Acad Sci U S A*. 2008;105:17818-17823.

Supplemental Figures

FIGURE S1

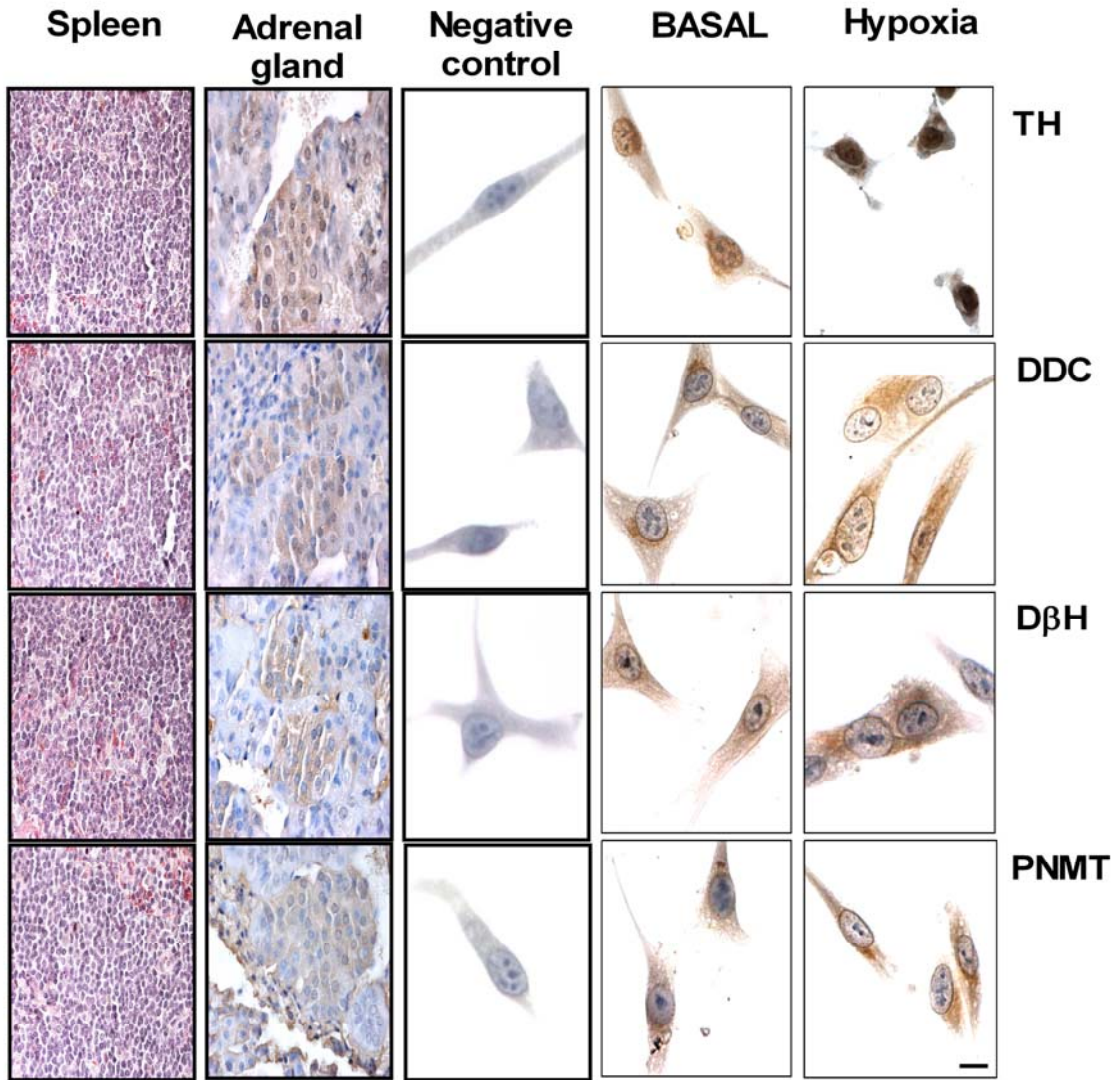


Figure S1. Immunohistochemistry analysis of the expression of TH, DDC, DβH and PNMT in BAEC.

Paraffin embedded sections from adrenal gland and spleen and methanol fixed EC were analyzed by immunohistochemistry using the PAP peroxidase anti-peroxidase system. DDC, DβH and PNMT are localized in the cytosol of EC and their expression is enhanced after 16 hours of hypoxia. TH present a nuclear localization. Scale bar is 20 μm. Adrenal gland was used as positive control and spleen as negative control. A negative control in EC was performed incubating cells with secondary antibody only to avoid false positive. Images are representative of 3 independent experiments.

FIGURE S2

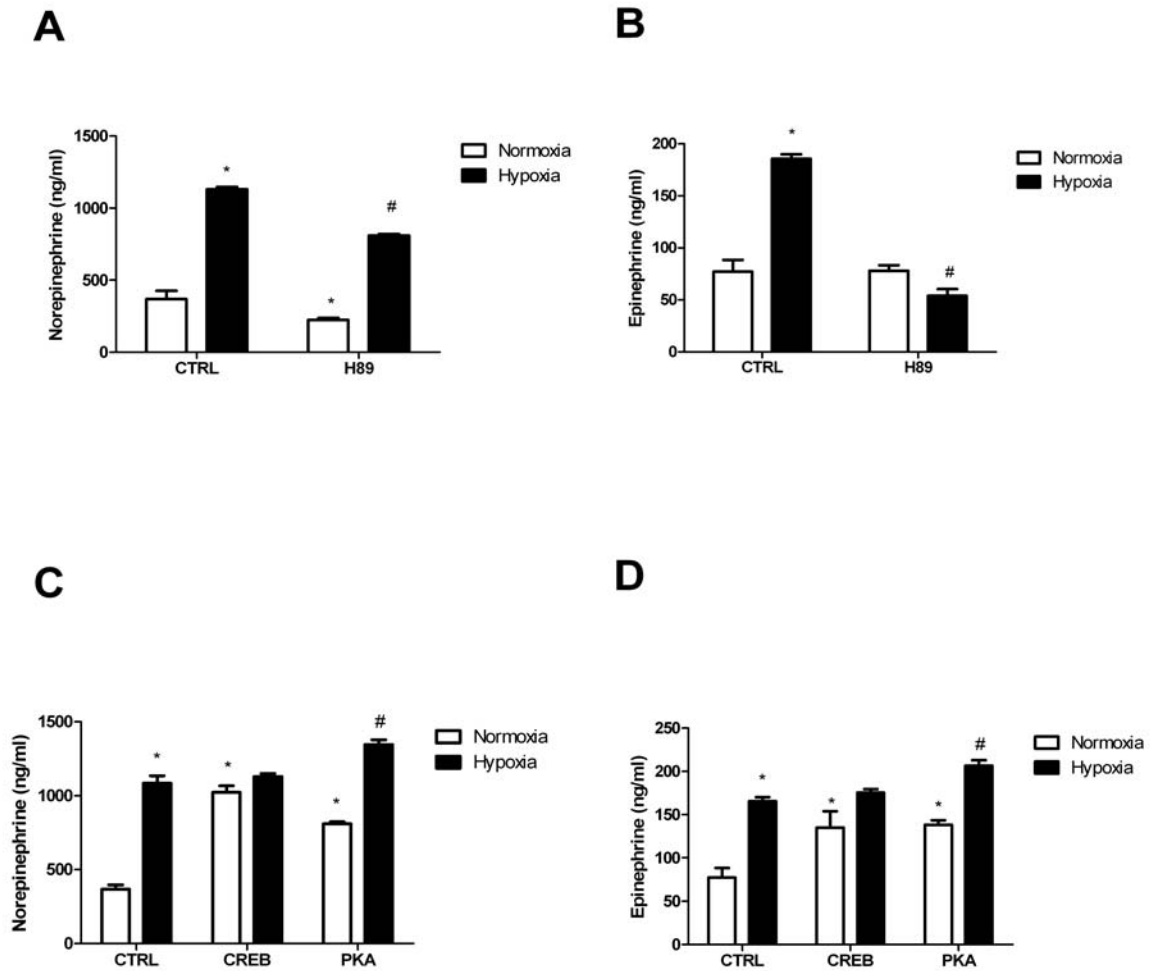


Figure S2: PKA/CREB regulates catecholamines release in the culture medium

BAEC were transfected with p-CREB and p-PKA or treated with H89 and then incubated in the hypoxic chamber for 16 hours. Culture mediums were collected and used for ELISA assay. **A-D)** H89 inhibits catecholamines release induced by hypoxia (A-B). CREB and PKA overexpression increase NE (C) and EPI (D) release respect to basal levels. PKA overexpression further increases the response to hypoxia; * $p < 0.05$ vs normoxia, # $p < 0.05$ vs hypoxia. Results are the mean of 5 independent experiments.

FIGURE S3

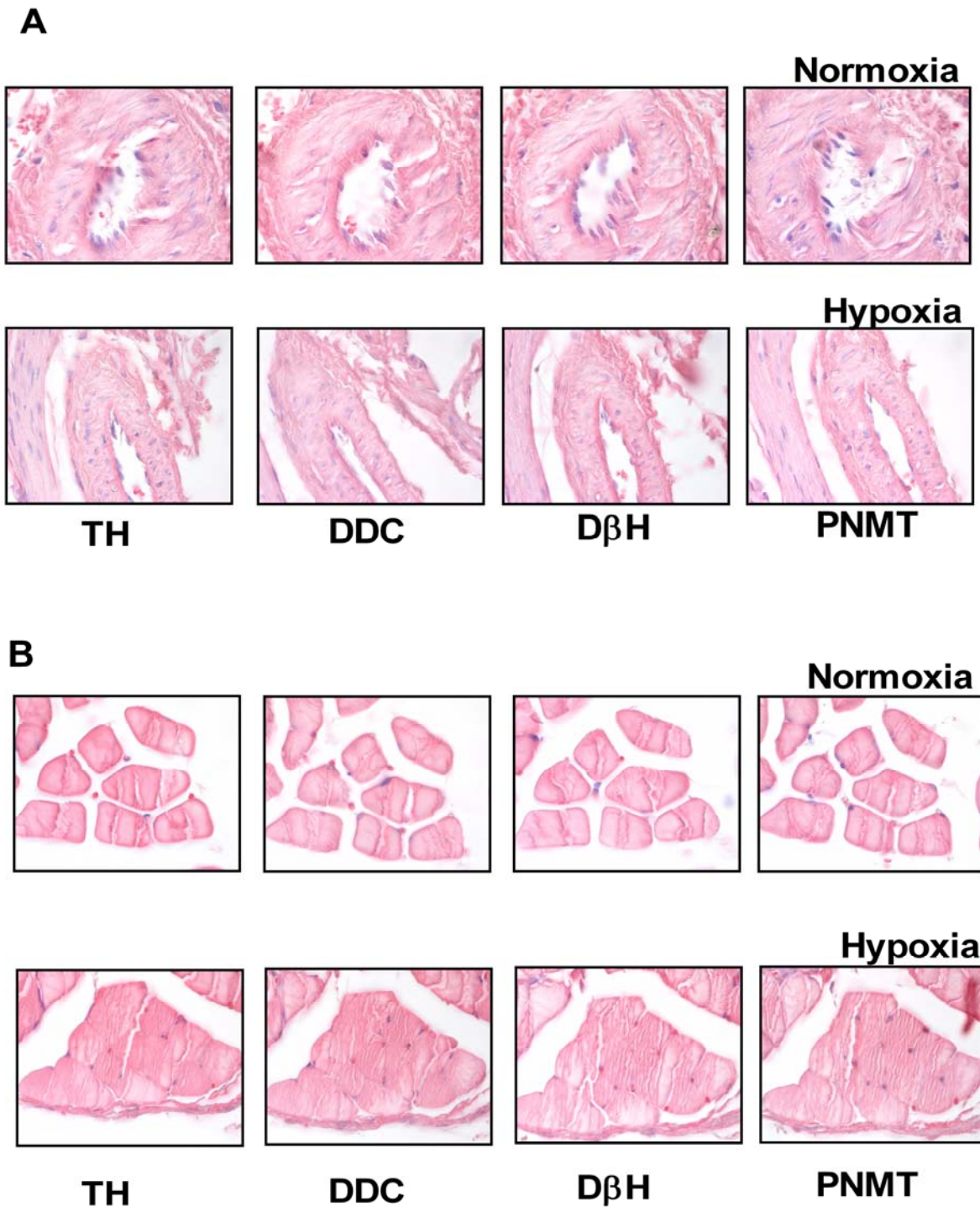
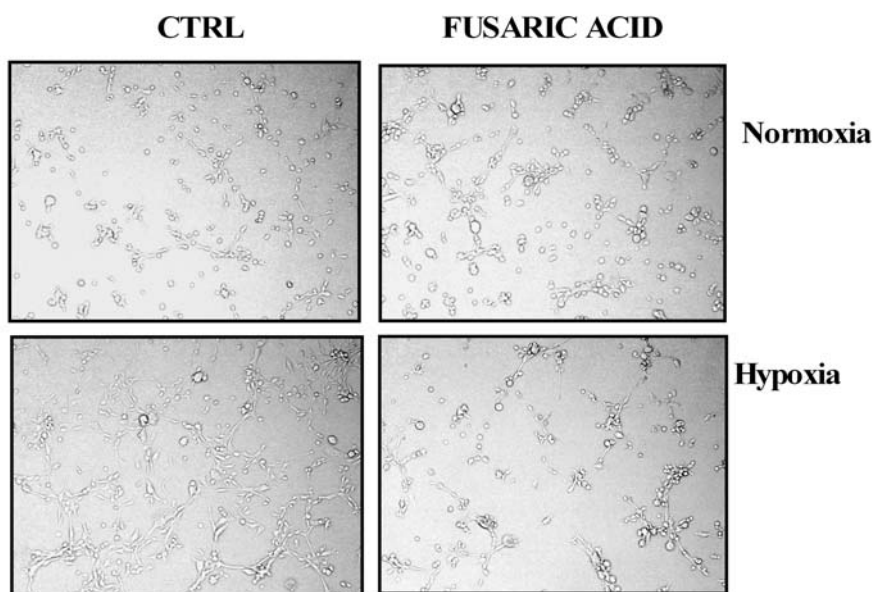


Figure S3: EC produce catecholamines in vivo: negative control

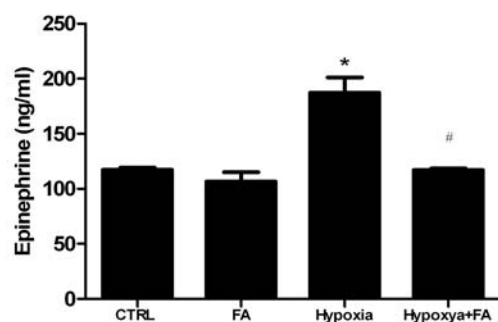
To confirm the specificity of immunohistochemical data about TH, DDC, DβH and PNMT expression in BAEC (Fig. 3) we performed a negative control incubating tissues with secondary antibody only [femoral arteries (A) and in capillaries (B)].

FIGURE S4

A



B



C

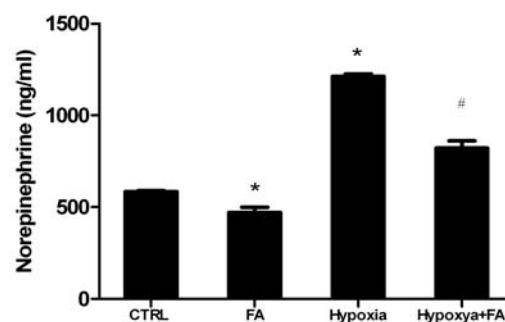


Figure S4: EC dependent catecholamines release has a key role in angiogenesis *in vitro*.

BAEC were treated with fusaric acid (FA, 10 μ M) for 30 min and incubated in the hypoxic chamber for 16 hours. **A**) Cells were plated on matrigel matrix and the formation of network-like structures was analyzed by microscopy. FA inhibits hypoxia induced BAEC organization in tubular structures. Images are representative of 3 independent experiments. **B-C**) Cultured mediums were collected and used for ELISA assay. FA inhibits hypoxia-induced norepinephrine (NE, B) and epinephrine (EPI, C) release. * $p < 0.05$ vs normoxia, # $p < 0.05$ vs hypoxia. Results are the mean of 5 independent experiments.

Regarding the impact of left ventricular size on response to cardiac resynchronization therapy

We read with interest the report by Rickard et al¹ in a recent issue of the journal regarding the impact of left ventricular size on response to cardiac resynchronization therapy (CRT).

In this study, the effect of CRT is clearly analyzed in 668 patients with nondilated and severely dilated cardiomyopathy, 2 underrepresented categories in the medical literature. The authors show a significant improvement of cardiac function after CRT in these subjects.

We have 2 main concerns. First, the role of the different etiology of the cardiomyopathy (ischemic vs nonischemic) on the reverse ventricular remodeling is not well addressed. Given the recent findings about this issue,²⁻⁵ an analysis in a large cohort of subjects¹ could be of keen relevance to the reader.

Second, prior studies have yielded inconsistent results regarding the effect of CRT on the incidence of atrial fibrillation (AF) in patients with heart failure.^{3,6-9} In the study by Rickard et al, the development of AF in the studied groups remains quite unclear. There is a higher incidence of AF in nondilated patients compared with the other groups, but the authors do not present data concerning the relation between CRT and AF. We believe that this information may be remarkable, especially because the authors have a large follow-up subgroup (471 subjects) also with echocardiographic records.

Am Heart J 2012;163:e11.
0002-8703/\$ - see front matter
doi:10.1016/j.ahj.2012.01.001

Gaetano Santulli, MD
New York - Presbyterian Hospital
Columbia University Medical Center
New York, NY
Federico II University
Naples, Italy
E-mail: gs2620@columbia.edu

Salvatore D'Ascia, MD
Cristofaro D'Ascia, MD
Federico II University
Naples, Italy

References

1. Rickard J, Brennan DM, Martin DO, et al. The impact of left ventricular size on response to cardiac resynchronization therapy. *Am Heart J* 2011;162:646-53.
2. McLeod CJ, Shen WK, Rea RF, et al. Differential outcome of cardiac resynchronization therapy in ischemic cardiomyopathy and idiopathic dilated cardiomyopathy. *Heart Rhythm* 2011;8:377-82.
3. D'Ascia SL, D'Ascia C, Marino V, et al. Cardiac resynchronization therapy response predicts occurrence of atrial fibrillation in non-ischaemic dilated cardiomyopathy. *Int J Clin Pract* 2011;65:1149-55.
4. Adelstein EC, Saba S. Scar burden by myocardial perfusion imaging predicts echocardiographic response to cardiac resynchronization therapy in ischemic cardiomyopathy. *Am Heart J* 2007;153:105-12.
5. Iles L, Pfluger H, Lefkovijs L, et al. Myocardial fibrosis predicts appropriate device therapy in patients with implantable cardioverter-defibrillators for primary prevention of sudden cardiac death. *J Am Coll Cardiol* 2011;57:821-8.
6. Fung JW, Yu CM, Chan JY, et al. Effects of cardiac resynchronization therapy on incidence of atrial fibrillation in patients with poor left ventricular systolic function. *Am J Cardiol* 2005;96:728-31.
7. Hoppe UC, Casares JM, Eiskjaer H, et al. Effect of cardiac resynchronization on the incidence of atrial fibrillation in patients with severe heart failure. *Circulation* 2006;114:18-25.
8. Hugel B, Bruns HJ, Unterberg-Buchwald C, et al. Atrial fibrillation burden during the post-implant period after crt using device-based diagnostics. *J Cardiovasc Electrophysiol* 2006;17:813-7.
9. Santulli G, D'Ascia S, Marino V, et al. Atrial function in patients undergoing CRT. *J Am Coll Cardiol Cardiovasc Imaging* 2012;5:124-5.

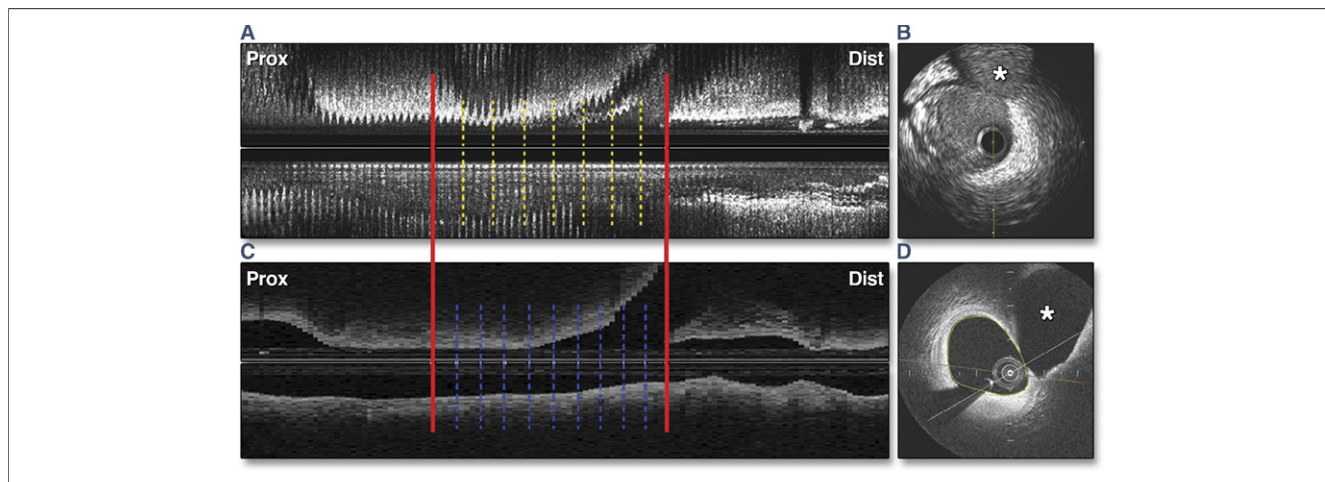


Figure 1. Segmental Analysis of Coronary Lumen Dimensions With IVUS and OCT

Visual representation of methodology used with corresponding horizontal views of intravascular ultrasound (IVUS) (A) and Fourier Domain-optical coherence tomography (FD-OCT) (C) and cross sectional views of IVUS (B) and FD-OCT (D) are shown.

sistent with previous recently reported ex vivo and in vivo findings (1–3), we highlight consistently larger LA measurements obtained with IVUS compared to FD-OCT across all segments, with a further significant reduction in these luminal measurements when measured in smaller-sized coronary segments, and when measured with 3D-QCA. This also supports recent data which has compared Terumo FD-OCT, IVUS, and conventional QCA measurements in stented coronary segments (3). Until further validation studies are conducted, specific lumen-based cut-off values previously validated with IVUS and currently utilised in contemporary interventional practice should not be arbitrarily translated into the FD-OCT and 3D QCA hemispheres. (Fig. 1)

Rishi Puri, MBBS, Adam J. Nelson, MBBS, Gary Y. H. Liew, MBBS, Stephen J. Nicholls, MBBS, PhD, Angelo Carbone, MMedSc, Dennis T. L. Wong, MBBS, James E. Harvey, MD, MSc, Kiyoko Uno, MD, PhD, Barbara Copus, RN, Darryl P. Leong, MBBS, MPH, John F. Beltrame, BMBS, PhD, Stephen G. Worthley, MBBS, PhD, Matthew I. Worthley, MBBS, PhD*

*Cardiovascular Investigational Unit, Royal Adelaide Hospital, Level 6 Theatre Block, North Terrace, Adelaide, South Australia 5000, Australia, E-mail: mattbew.worthley@adelaide.edu.au.

doi:10.1016/j.jcmg.2011.07.012

Please note: Drs. Puri, Leong and Liew are supported by a Postgraduate Medical Research Scholarship from the National Health & Medical Research Council (565579, 519177, and 497809 respectively). Drs. Puri and Leong are jointly funded by the National Heart Foundation of Australia (PC0804045, PC07A3395). Dr. Worthley has a South Australian Early to Mid Career Practitioner Fellowship.

REFERENCES

- Gonzalo N, Serruys PW, Garcia-Garcia HM, et al. Quantitative ex vivo and in vivo comparison of lumen dimensions measured by optical coherence tomography and intravascular ultrasound in human coronary arteries. *Rev Esp Cardiol* 2009;62:615–24.
- Yamaguchi T, Terashima M, Akasaka T, et al. Safety and feasibility of an intravascular optical coherence tomography image wire system in the clinical setting. *Am J Cardiol* 2008;101:562–7.

- Okamura T, Onuma Y, Garcia-Garcia HM, et al. First-in-man evaluation of intravascular optical frequency domain imaging (OFDI) of Terumo: a comparison with intravascular ultrasound and quantitative coronary angiography. *EuroIntervention* 2011;6:1037–45.

Atrial Function in Patients Undergoing CRT

We read with great interest the paper by Carluccio et al. (1) regarding the impact of left ventricular (LV) remodeling on the response to cardiac resynchronization therapy (CRT). In this elegant study, the authors performed a comprehensive assessment of LV function, showing that extensive LV remodeling at baseline is associated with poor improvement after CRT.

We wish to raise an essential issue, which may be of keen interest to the readers.

In recent years, there has been growing interest in the potential impact of CRT on atrial function, but the state of knowledge in this field is still controversial and unsettled (2–4). In the paper by Carluccio et al. (1) several baseline data concerning atrial function are presented (left atrial volume index and mitral regurgitation severity), but unfortunately there is no information related to CRT response. We believe that their excellent echocardiographic data could also be useful to better understand another debated issue (i.e., the effect of CRT on the risk of the development of atrial arrhythmias) that is clearly related to atrial remodeling (4,5).

Gaetano Santulli, MD,* Salvatore D'Ascia, MD, Vittoria Marino, MD, Cristofaro D'Ascia, MD

*Columbia University Medical Center, College of Physicians & Surgeons, St. Nicholas Avenue, New York, New York, 10032. E-mail: gs2620@columbia.edu.

doi:10.1016/j.jcmg.2011.11.002

REFERENCES

1. Carluccio E, Biagioli P, Alunni G et al. Presence of extensive LV remodeling limits the benefits of CRT in patients with intraventricular dyssynchrony. *J Am Coll Cardiol Img* 2011;4:1067-76.
2. Donal E, Tan K, Leclercq C et al. Left atrial reverse remodeling and cardiac resynchronization therapy for chronic heart failure patients in sinus rhythm. *J Am Soc Echocardiogr* 2009;22:1152-8.
3. Yu CM, Fang F, Zhang Q et al. Improvement of atrial function and atrial reverse remodeling after cardiac resynchronization therapy for heart failure. *J Am Coll Cardiol* 2007;50:778-85.
4. D'Ascia SL, D'Ascia C, Marino V et al. Cardiac resynchronisation therapy response predicts occurrence of atrial fibrillation in non-ischaemic dilated cardiomyopathy. *Int J Clin Pract* 2011;65:1149-55.
5. Hoppe UC, Casares JM, Eiskjaer H et al. Effect of cardiac resynchronization on the incidence of atrial fibrillation in patients with severe heart failure. *Circulation* 2006;114:18-25.

REPLY

We would like to thank Dr. Santulli et al. (1) for their interest in our recently published paper. In their letter, they point out an important issue regarding patients undergoing cardiac resynchronization therapy (CRT), namely, the consequences of CRT on left atrial (LA) function and remodeling. Despite extensive evidence of the benefits of CRT on ventricular function, the impact of CRT on atrial function and remodeling has not been thoroughly evaluated. Previous studies demonstrated that in patients in whom left ventricular remodeling occurs, favorable changes in LA volumes and LA function can also be seen (2,3). These changes are expected to translate into reduced incidence of atrial arrhythmias, secondary to positive LA remodeling (2,4). That may be important as occurrence of atrial fibrillation is associated with worse prognosis in heart failure patients (5).

As recently demonstrated through analysis of a large multicenter trial (2), and single-center experience (4), CRT-defibrillator therapy was associated with pronounced reverse remodeling of the LA. This beneficial effect on LA volumes was followed by substantial reduction in the risk of atrial fibrillation. Importantly, patients who

did not report atrial arrhythmias after device implantation showed a significantly lower incidence of heart failure and death (2).

Our study (1) was mainly focused on evaluating the impact of extensive left ventricle remodeling on subsequent response to CRT, in terms of left ventricular ejection fraction improvement and occurrence of cardiac events at follow-up. Hence, the study was not geared to specifically evaluate changes in LA remodeling. However, LA volume index was enlarged at baseline (44 ± 20 ml/m²), and it was significantly reduced at follow-up after CRT (39.6 ± 15 ml/m², $p < 0.01$), as was mitral regurgitation severity (see Carluccio et al. [1]). Whether these beneficial changes on LA remodeling, and their relationship with diastolic left ventricle parameters, are also associated with lower risk of developing atrial arrhythmias remains the object of future studies.

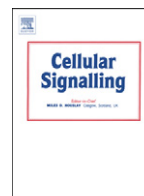
**Erberto Carluccio, MD,* Paolo Biagioli, MD,
Giuseppe Ambrosio, MD, PhD**

*Division of Cardiology, University of Perugia, School of Medicine, Perugia PG 06132, Italy. *E-mail: e.carluccio@alice.it*

doi:10.1016/j.jcmg.2011.11.003

REFERENCES

1. Carluccio E, Biagioli P, Alunni G, et al. Presence of extensive LV remodeling limits the benefits of CRT in patients with intraventricular dyssynchrony. *J Am Coll Cardiol Img* 2011;4:1067-76.
2. Brenyo A, Link MS, Barsheshet A, et al. Cardiac resynchronization therapy reduces left atrial volume and the risk of atrial tachyarrhythmias in MADIT-CRT (Multicenter Automatic Defibrillator Implantation Trial With Cardiac Resynchronization Therapy). *J Am Coll Cardiol* 2011;58:1682-9.
3. Yu CM, Fang F, Zhang Q, et al. Improvement of atrial function and atrial reverse remodeling after cardiac resynchronization therapy for heart failure. *J Am Coll Cardiol* 2007;50:778-85.
4. D'Ascia SL, D'Ascia C, Marino V, et al. Cardiac resynchronisation therapy response predicts occurrence of atrial fibrillation in non-ischaemic dilated cardiomyopathy. *Int J Clin Pract* 2011;65:1149-55.
5. Wang TJ, Larson MG, Levy D, et al. Temporal relations of atrial fibrillation and congestive heart failure and their joint influence on mortality: the Framingham Heart Study. *Circulation* 2003;107:2920-5.



Mitochondrial localization unveils a novel role for GRK2 in organelle biogenesis

Anna Fusco^{a,1}, Gaetano Santulli^{a,2}, Daniela Sorriento^a, Ersilia Cipolletta^a, Corrado Garbi^b, Gerald W. Dorn II^c, Bruno Trimarco^a, Antonio Feliciello^b, Guido Iaccarino^{d,*}

^a Clinical Medicine, Cardiovascular and Immunological Sciences "Federico II" University, Naples, Italy

^b Cellular and Molecular Biology and Pathology "Federico II" University, Naples, Italy

^c Internal Medicine, Washington University in St. Louis, MO63110 USA

^d School of Medicine University of Salerno, Baronissi, (Salerno) 84081, Italy

ARTICLE INFO

Article history:

Received 16 August 2011

Received in revised form 23 September 2011

Accepted 24 September 2011

Available online 1 October 2011

Keywords:

GRK2

Mitochondria

Ischemia/reperfusion

Biogenesis

ATP production

ABSTRACT

Metabolic stimuli such as insulin and insulin like growth factor cause cellular accumulation of G protein coupled receptor kinase 2 (GRK2), which in turn is able to induce insulin resistance. Here we show that in fibroblasts, GRK2 is able to increase ATP cellular content by enhancing mitochondrial biogenesis; also, it antagonizes ATP loss after hypoxia/reperfusion. Interestingly, GRK2 is able to localize in the mitochondrial outer membrane, possibly through one region within the RGS homology domain and one region within the catalytic domain. In vivo, GRK2 removal from the skeletal muscle results in reduced ATP production and impaired tolerance to ischemia. Our data show a novel sub-cellular localization of GRK2 in the mitochondria and an unexpected role in regulating mitochondrial biogenesis and ATP generation.

© 2011 Elsevier Inc. All rights reserved.

1. Introduction

An emerging and intriguing role of the G protein coupled receptor kinase 2 (GRK2) involves its ability to modulate the metabolic state of the cell. Little is known about this feature, opposite to the relevance of the kinase in the regulation of the G protein coupled receptor (GPCR) signaling. Indeed, GRK2 belongs to a family of seven serine/threonine protein kinases, each encoded by a single gene, that specifically phosphorylates the activated form of GPCRs, mediating their desensitization [1,2].

The first suggestion that GRK2 is involved in the cellular metabolism derives from the observation that insulin [3] and insulin like growth factor are both able to induce up regulation of the kinase, which occurs within the time frame of a few minutes. Interestingly, GRK2 accumulation leads to the shut-off of insulin signaling and inhibits glucose extraction [3–5]. Conditions characterized by elevated GRK2 levels such as hypertension or chronic activation of β adrenergic receptor [3], as well as transgenic overexpression of the kinase [6] present resistance to the metabolic effects on the cell induced by insulin. This evidence suggests a novel role of GRK2 in controlling the cellular use of glucose and, more in general, the ability of the cell to master energy production and expenditure.

Mitochondria, of course, play an important role in cell energy production, given their ability to produce ATP in an oxygen dependent manner. The mitochondria functional state varies dramatically depending on the functional and metabolic state of the cell. Post transduction modification of mitochondrial proteins and in particular protein phosphorylation appears to be an important mechanism of mitochondrial function. In the last few years, different reports [7] confirmed that a series of kinases (MAPKs, Akt, PKA and PKC) are present in mitochondria, particularly in the intermembrane space and membranes where they meet mitochondrial constitutive upstream activators.

All of the above considerations prompted us to verify the hypothesis that GRK2 might affect energy cellular production by interfering with mitochondrial function. Pursuing this aim, we demonstrate that GRK2 has capability to localize in the mitochondrial fraction and profoundly affect the biology and the production of energy of these organelles.

2. Materials and methods

2.1. Cell culture

HEK-293 cells were cultured in Dulbecco's minimal essential medium (DMEM) and 25 mM glucose supplemented with 10% fetal bovine serum (FBS) at 37 °C in 95% air and 5% CO₂.

2.2. Primary cultured mouse aorta cells and infection

Primary cultured cells were prepared with little modifications from a previously validated protocol [8] for extraction of cells from

* Corresponding author. Tel.: +39 089965021; fax: +39 089969642.

E-mail address: giaccarino@unisa.it (G. Iaccarino).

¹ Anna Fusco participates in the PhD Program "Model Organisms in Biomedical and Veterinary Research" of the Federico II University.

² Gaetano Santulli participates in the PhD Program "Clinical Pathophysiology and Experimental Medicine".

aortic rings of recombinant mice harboring f-loxed GRK2 alleles (homozygous GRK2^{f/f}) [9,10]. Briefly, vessels were cut in rings and placed on Matrigel (BD Technologies), incubated in Dulbecco's minimal essential medium (DMEM) supplemented with 20% fetal bovine serum (FBS) and incubated at 37 °C in 95% air and 5% CO₂. After 5 to 7 days, aortic rings were removed, and the cells remaining on Matrigel expanded. To obtain GRK2 knock out cells, we incubated GRK2^{f/f} primary cultured cells with an adenovirus encoding for Cre recombinase (AdCre, Vector Biolabs) at MOI of 50 particles per cell for 3 h in a serum free medium. Incubation was repeated after 1 week. GRK2 removal was confirmed by western blot. A similar procedure, using an empty vector (AdEMPTY, Vector Biolabs) was applied to obtain control GRK2^{f/f} cells. Cells were studied between passages 7 and 14.

2.3. GRK2 cloning in pcDNA3.1

Using human GRK2 cDNA (GRK2-WT) in pcDNA3.1 [3] as a template and the primers which contain consensus sequences for the indicated restriction enzymes (Table 1), we amplified the N-Terminal region and catalytic domain, (GRK2 NT-CD, 1–453 amino acids), the catalytic domain and C-Terminal region (GRK2 CD-CT, 191–689 amino acids), the C-Terminal region (GRK2 CT 454–689 amino acids) and the RH domain (GRK2 RH, 54–174 amino acids) (Fig. 3A). These truncated mutants were cloned in pcDNA3.1 (+) Myc/His A by means of T4 DNA ligase (Promega). The right frame and orientation were confirmed by restriction analysis and DNA sequencing by using the above indicated primers (Avant 3100, Applied Biosystem).

2.4. Cell transfections

Cell transfection was performed with lipotransfection reagents (lipofectamine 2000, Invitrogen) using 2 µg of plasmid DNA according to manufacturer's instructions [3,11]. For stable transfected clone selections, after 24 to 48 h cell medium was supplemented with G418 (500 µg/mL) for 2 weeks. The G418-resistant cells were cultured in medium supplemented with G418 to a final concentration of 250 µg/mL and examined for overexpression of GRK2 (GRK2-HEK) by western blotting, using specific antibodies (Santa Cruz Biotechnology).

2.5. Mitochondria extracts preparation and western blot

Cells were washed in ice-cold phosphate buffer (PBS) and disrupted by dounce homogenization in isolation buffer [1B pH 7.4 200 mM sucrose, 1 mM EGTA-Tris and 10 mM Tris-MOPS]. The homogenate was spun at 800 g for 10 min; the supernatant was recovered and further centrifuged for 10 min at 8000 g. The resulting

pellet (mitochondrial fraction) was collected while the supernatant was further spun for 30 min at 100,000 g to obtain the cytosolic fraction, spanned again at 100,000 g to further purify the fraction. The mitochondrial fraction was further purified by centrifuging twice at 8000 g for 10 min. The obtained pellet was purified by centrifugation at 95,000 g for 30 min on a 30% Percoll gradient in IB [12]. The obtained mitochondrial layer was washed free of Percoll and resuspended in IB. Protein concentration was determined by bichinonate assay (Pierce). Cytosol and mitochondria extracts were confirmed by western blot using specific antibodies (Santa Cruz Biotechnology).

Cellular or mitochondria extracts were electrophoresed by SDS/PAGE and transferred to nitrocellulose; GRK2 was visualized by specific antibody (Santa Cruz Biotechnology), anti-mouse HRP-conjugated secondary antibody (Santa Cruz Biotechnology) and standard chemiluminescence (Pierce) on autoradiographic film. Images were then digitalized and densitometric analysis was performed (ImageQuant software).

2.6. Overlay assay

Mitochondrial proteins were electrophoresed by SDS/PAGE and transferred to nitrocellulose. The membrane was incubated with 50 ng of GRK2 purified protein (Invitrogen) in binding buffer [Hepes 0.25 M; MgCl₂ 50 mM; DTT 2.5 mM; Na₃VO₄ 5 mM; H₂O-Tween 0.1%] for 1 h at room temperature. Protein was fixed in 0.5% formaldehyde for 5 min and washed with 2% glycine [13]. GRK2 was visualized by chemiluminescence after incubation with anti-GRK2 antibody (Santa Cruz Biotechnology).

2.7. Kinase assay

Kinase assay was performed by using mitochondrial extracts. Phosphorylation reaction was initiated by adding master mix (Hepes 0.5 M; MgCl₂ 1 M; DTT 1 M; Na₃VO₄ 1 M; H₂O-Tween 0.1%), 50 ng of GRK2 purified protein (Invitrogen) and [³²P]ATP (GE Healthcare) and prolonged for 30 min at 37 °C. Laemmli buffer was added to stop the reaction. Then, 30 µl of the reaction mix were resolved on SDS-PAGE4–12% gradient (Invitrogen), stained with Coomassie blue, destained, vacuum dried, and exposed for autoradiography [14].

2.8. Quantitative analysis of mitochondrial nucleic acids

Cell DNA and total RNA were isolated using commercially available reagents (DNAzol and Trizol, Invitrogen). cDNA was synthesized from RNA by reverse transcriptase (Invitrogen), following the manufacturer's instructions. Real-time quantitative polymerase chain reaction (RT-PCR) was performed on DNA and cDNA as previously described [11] to amplify two mitochondrial (*cytochrome b*, *NADHd*), and one nuclear (*β globin*) genes. The primer sequences used were: [15] *cytochrome b*: For: 5'-CCTAGGCGACCCAGACAATTAT; Rev: 5'-TCAITTCGGGCTTGATGTGG; *NADHd*: For: 5'-CAGCCATTCTCATCCAAACC; Rev: 5'-ATTATGATGC-GACTGT GAGTGC; *β globin*: For: 5'-AGCCTGACCAACATGGTGAAC; Rev: 5'-AGCCACTGAATAGCTGGGACT. All values obtained were normalized to the values obtained with the *β globin* primers. The reaction was visualized by SYBR Green Analysis (Applied Biosystem) on StepOne instrument (Applied Biosystem). The results are expressed as the relative integrated intensity.

2.9. Immunofluorescence

HEK-293 and GRK2-HEK cells were incubated for 30 min with 5 nM mitotracker (Rosamine-based Mitotracker dye-Invitrogen) to identify mitochondria. Then the cells were fixed with –20 °C cold methanol/acetone and permeabilized by incubation in 0.3% Triton X-100 solution for 3 min. Cells were incubated for 1 h at room temperature with mouse anti-GRK2 Ab (Santa Cruz Biotechnology) in PBS containing 1% BSA [14]. After two washings in PBS, the cells were incubated for 1 h at

Table 1
Primer sequences used for amplification of truncated mutants of human GRK2 gene.

Truncated mutants	Primers	Restriction enzymes
GRK2 NT-CD	For: 5'-TAAGCTTGGATGGCGGACCTGGAGGC-3' Rev: 5'-CCCTCTAGAGAAAAGGGGCTCTCTTC-3'	HindIII XbaI
GRK2 CD-CT	For: 5'-TAAGCTTGGATGGAATGACTTCAGCGTGATC-3' Rev: 5'-CCCTCTAGAGAGGCCGTTGGCACTGCCGCG-3'	HindIII XbaI
GRK2 RH	For: 5'-AAAAGATCCTGATGACCTTTGAGAAGATC-3' Rev: 5'-AAAAGATATCTGCAAAACCGTGTGAACCTATC-3'	BamHI EcoRV
GRK2 CT	For: 5'-TAAGCTTGGATGCTCCCTGGACTGGCAGATG-3' Rev: 5'-CCCTCTAGAGAGGCCGTTGGCACTGCCGCG-3'	HindIII XbaI

room temperature with fluorescent-labeled secondary antibody (Invitrogen) in PBS. After washing in PBS, the glass slides were mounted under a coverslip in a 50% glycerol PBS solution. Images were acquired with a Zeiss 510 confocal laser scanning microscope.

2.10. Transmission electron microscopy (TEM) and Immunogold staining

Mitochondrial fractions were washed in PBS and fixed in 4% paraformaldehyde for 4 h at 4 °C. Then samples were incubated with 0.05 M glycine, dehydrated in graded ethanols and 100% acetone and blocked in 5% BSA in PBS for 1 h. Mitochondrial fractions were washed in incubation buffer (IB: 0.8% BSA in PBS and 15 mM Na₂S₂O₃), incubated with anti GRK2 antibody (5 µg/ml) in IB overnight and washed in IB. Subsequently, samples were incubated with secondary antibody (Aurion ultra-small gold reagents) for 1.5 h, washed and incubated with Aurion R-gent SE-EM, according to manufacturer's instructions. Samples were then fixed with 2.5% glutaraldehyde, washed in PBS, fixed in osmium tetroxide, dehydrated in an ethanol series, embedded in epoxy resin, and then examined under a transmission electron microscope (JEM-2000EX), at the Federico II facility for advanced imaging (CISME).

2.11. Cytofluorimetry

Cells were incubated for 30 min with 5 nM mitotracker (Rosamine-based Mitotracker dye-Invitrogen) to identify mitochondria. Then mitotracker stained and unstained control cells were analyzed by flow cytometry (FACSCalibur, BD Biosciences) followed by analysis of mean fluorescence intensity of 10,000 events by Cellquest software (BD Biosciences) [16].

2.12. Assay for oxidative ATP synthesis

Cells were harvested, washed twice in PBS, and counted in a Burker's camera. A replicate for each sample was prepared that had been treated for 1 h with 4 µg/ml rotenone (Sigma). The emission recorded from samples treated with rotenone was defined as baseline luminescence corresponding to a non mitochondrial source of ATP. Assays were performed using the ATP luminescence assay kit (Sigma) according to manufacturer's instructions.

2.13. Cell hypoxia

Cell medium was previously saturated for 10 min at 1 atm with 95% N₂ and 5% CO₂ mixture, containing (mM) concentrations of 116NaCl, 5.4KCl, 0.8MgSO₄, 26.2NaHCO₃, 1NaH₂PO₄, 1.8CaCl₂, 0.01glycine and 0.001 (% w/v) phenol red, and placement in an anaerobic chamber (hypoxia chamber) filled with the same gas mixture and heated to 37 °C. The pH, PO₂ and PCO₂ of the resulting medium were 7.36 ± 0.2, 45.3 ± 1.2 mm Hg, and 35.3 ± 0.8 mm Hg and 7.32 ± 0.9, 32.6 ± 1.1 and 37.9 ± 2.1 mm Hg, before and at the end of hypoxia, respectively [17].

2.14. Mouse skeletal muscle infection

Animal studies were carried out on homozygous GRK2^{ff} mice [9] (n = 23; weight: 26.7 ± 3.1 g) in accordance to Federico II University guidelines. To obtain GRK2 gene removal, mice were anaesthetized by vaporized Isoflurane 3% and intramuscular injection of AdCre (10⁹ pfu/ml) were performed into right quadriceps femoris (200 µl) muscle. GRK2 removal was confirmed by western blot. After 5 days we performed ischemia/reperfusion.

2.15. Mouse surgery

Mice were anaesthetized by isoflurane 4% inhalation and maintained by mask ventilation (isoflurane 2%). A surgical incision was made in the skin overlying the middle portion of the right hind limb and the right

common femoral artery was exposed and isolated, as previously described [18], and a slipknot was placed around the proximal end of the artery with a 5-0 silk suture, maintained for 1 h to induce hind limb ischemia. Groups of 3 mice were sacrificed at the end of 1 h of ischemia, after 15 min or 60 min of reperfusion. These mice were compared to GRK2^{ff} mice subjected to the same procedures (3 for each time point) and to sham-operated GRK2^{ff} (n = 3) and GRK2^{ff;Cre} (n = 3).

2.16. Assay for oxidative ATP synthesis in vivo

At sacrifice, quadriceps femoris muscles were harvested and quickly washed in PBS. Assay was performed using the ATP luminescence assay kit (Sigma) according to manufacturer's instructions. Then, values were normalized according to muscles' weights.

2.17. Statistical analysis

All values are presented as mean ± SEM. Two-way ANOVA was performed to compare the different parameters among the different groups. Bonferroni post hoc testing was performed where applicable. A significance level of p < 0.05 was assumed for all statistical evaluations. Statistics were computed with GraphPad Prism software (San Diego, California).

3. Results

3.1. GRK2 increases oxidative ATP synthesis

To evaluate the relevance of GRK2 in energy production we monitored whether GRK2 modulates mitochondrial ATP synthesis. Fig. 1A shows that human embryonic kidney (HEK-293) fibroblasts stably over expressing a human GRK2 gene (GRK2-HEK) contain higher

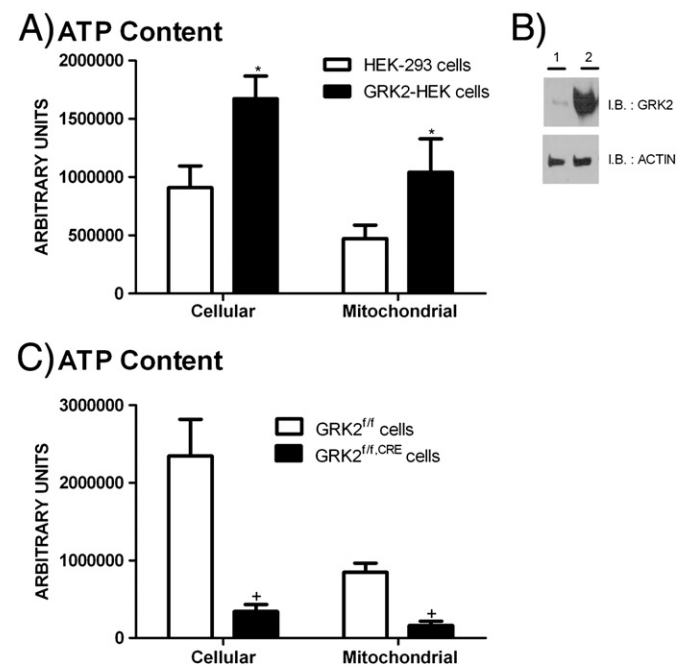


Fig. 1. (A) Cellular and mitochondrial ATP content in HEK-293 and GRK2-HEK cells. (* p < 0.05 vs HEK-293 cells). (B) Infection with AdCRE removes GRK2 gene in GRK2^{ff} cells. Recombinant floxed GRK2 cells were incubated either with adenovirus encoding for Cre recombinase (AdCRE, Vector Biolabs) or an empty virus (AdEMPTY) at MOI of 50 particles for 3 h in a serum free medium. Cells were then maintained in culture and GRK2 removal was confirmed by western blot (1: cells treated with AdCRE; 2: cells treated with AdEMPTY). (C) Cellular and mitochondrial ATP content in GRK2^{ff} and GRK2^{ff;CRE} aortas derived cells. (+ p < 0.05 vs GRK2^{ff} cells).

levels of total and mitochondrial ATP, compared to control cells. We also studied primary cultured cells derived from the aortas of recombinant mice with both copies of the GRK2 gene flanked by two f-lox sites (GRK2^{f/f}). When these cells were infected with AdCre to obtain cellular expression of the bacterial CRE recombinase (GRK2^{f/f,CRE}), GRK2 protein levels became undetectable (Fig. 1B). At the same time, in GRK2^{f/f,Cre} cells (Fig. 1C) there is a significant reduction of total and mitochondrial ATP levels, supporting a positive role of GRK2 in bio-energetic pathway.

3.2. GRK2 is located in mitochondria

To clarify the basis for the possible link between GRK2 and the mitochondria, we evaluated the presence of the kinase in the organelles by co-fractionation experiments on a 30% Percoll gradient. First of all, to verify that the mitochondrial fraction was free from contaminants of other compartments, we observed samples from HEK-293 cells under TEM and confirmed the purity of the mitochondrial fraction (Fig. 2A). On this fraction, immunogold analysis shows that the kinase

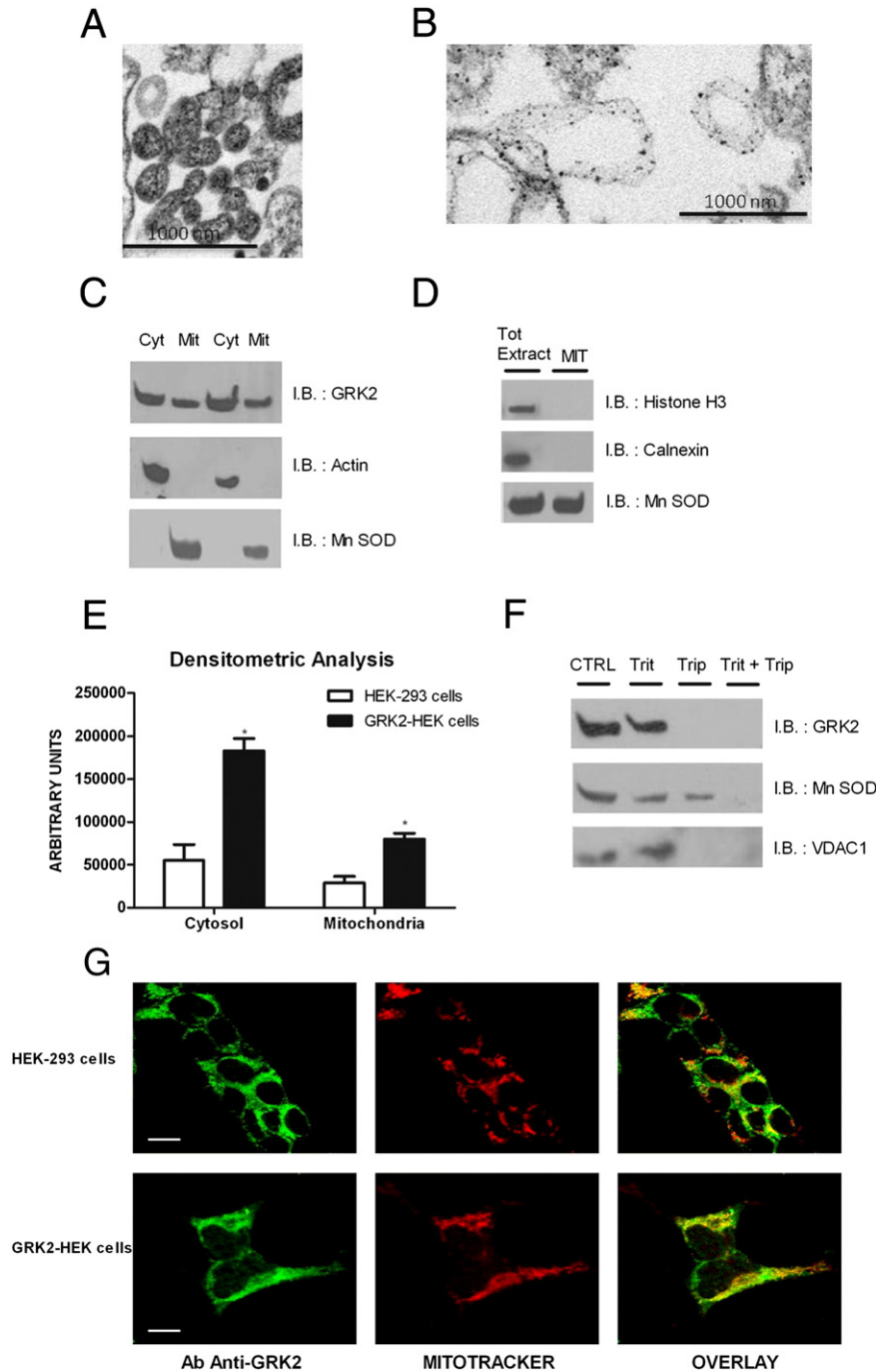


Fig. 2. (A) Mitochondria were obtained by co-fractionation experiments on a 30% Percoll gradient and observed by electron microscopy. (B) GRK2 localization was observed by immunogold on mitochondria extracts using anti-GRK2 antibody. (C) GRK2 levels were analyzed in cytosol (Cyt) and mitochondrial (Mit) extracts by western blot in HEK-293 cells. (D) The absence of Histone H3 and Calnexin in purified mitochondria was confirmed by western blot in HEK-293 cells, using cellular extracts for molecular weight reference. (E) The stable over-expression of GRK2-WT increases GRK2 levels both in cytosol and mitochondria (*p<0.05 vs HEK-293 cells). (F) Mitochondria were incubated with or without trypsin (Trip). To disrupt mitochondrial integrity, triton X-100 (Trit) was added in the digestion buffer. Samples were probed for GRK2, Mn SOD and VDAC1. (G) GRK2 localization was analyzed by immunofluorescence. HEK-293 cells (upper lane) and GRK2-HEK cells (lower lane) were labeled in vivo with mitotracker (red), fixed, and immunostained with anti-GRK2 (green) antibody. Pictures were taken under confocal microscopy. Bars, 10 µm.

is indeed found on the mitochondria, where it targets to the outer membranes (Fig. 2B).

Localization of GRK2 on mitochondria was also confirmed on mitochondria and cytosol fractions isolated from HEK-293 cells by western blot. Fig. 2C shows that endogenous GRK2 partly co-purified with the mitochondria-enriched fraction, as did the Mn-dependent Superoxide Dismutase (Mn SOD), a protein that resides within mitochondrial compartments. We verified that the purified mitochondrial fractions were free from contaminants of the cytosol (actin) (Fig. 2C), nuclei (Histone H3) and sarcoplasmic reticulum (calnexin) (Fig. 2D). The specificity of the antibody for GRK2 is confirmed by the observation that stable overexpression of GRK2 in HEK-293 cells increases the levels of the protein both in cytosol and mitochondria (Fig. 2E).

To confirm the sub-mitochondrial compartment where GRK2 localizes, we subjected the purified mitochondrial fraction to a double treatment with trypsin and triton demonstrating that the kinase targets to outer membrane (Fig. 2F). Confirmation derives from the evidence that the mitochondrial outer membrane protein VDAC1 but not the mitochondrial matrix protein MnSOD localizes in the same sub-mitochondrial fraction as GRK2.

Finally, the ability of GRK2 to co-localize with mitochondria was also demonstrated by confocal microscopy using immunofluorescence (Fig. 2G). In particular, imaging confirms the ubiquitous localization of GRK2 within the cytosol and the membrane compartments, but the nucleus. When the GRK2 and mitochondria signals are merged, it appears clearly that GRK2 can compartmentalize in mitochondria. This feature is further highlighted in presence of GRK2 overexpression (Fig. 2G).

3.3. Two regions within GRK2 sequence show affinity for mitochondria

To map the regions of GRK2 that possess the ability to localize in mitochondria, we generated myc/histidine-tagged, truncated mutants of GRK2 (Fig. 3A). The amino acid sequence 1–453 is able to localize to mitochondria (Fig. 3B). Within this region, we found that the 120 amino acids comprising the RGS homology (GRK2 RH) domain (amino acids 54–174) are able to target mitochondria (Fig. 3C). Also, the region 191–689 which comprises the catalytic and carboxyl termini (CT) domain is able to target the mitochondria. Finally, the CT sequence per se (495–689, Fig. 3E) cannot bind the organelles.

3.4. GRK2 interacts and phosphorylates unidentified mitochondrial proteins

To confirm the ability of GRK2 to localize on mitochondria, we performed an overlay assay with purified GRK2 as bait on HEK-293 and GRK2-HEK cells mitochondria extracts blotted on nitrocellulose. This assay confirms the ability of GRK2 to interact with yet unidentified mitochondrial proteins within the molecular weight range of 30–60 KDa (Fig. 4A).

Using a similar approach, we performed a kinase assay to verify whether GRK2 recognizes substrates among the mitochondrial proteins (Fig. 4B). This experiment confirms that GRK2 phosphorylates mitochondrial proteins within the molecular range of 30–60 KDa.

3.5. GRK2 increases mitochondrial biogenesis

Given the localization of GRK2 on mitochondria, we asked whether GRK2 promotes mitochondrial DNA accumulation. By quantitative

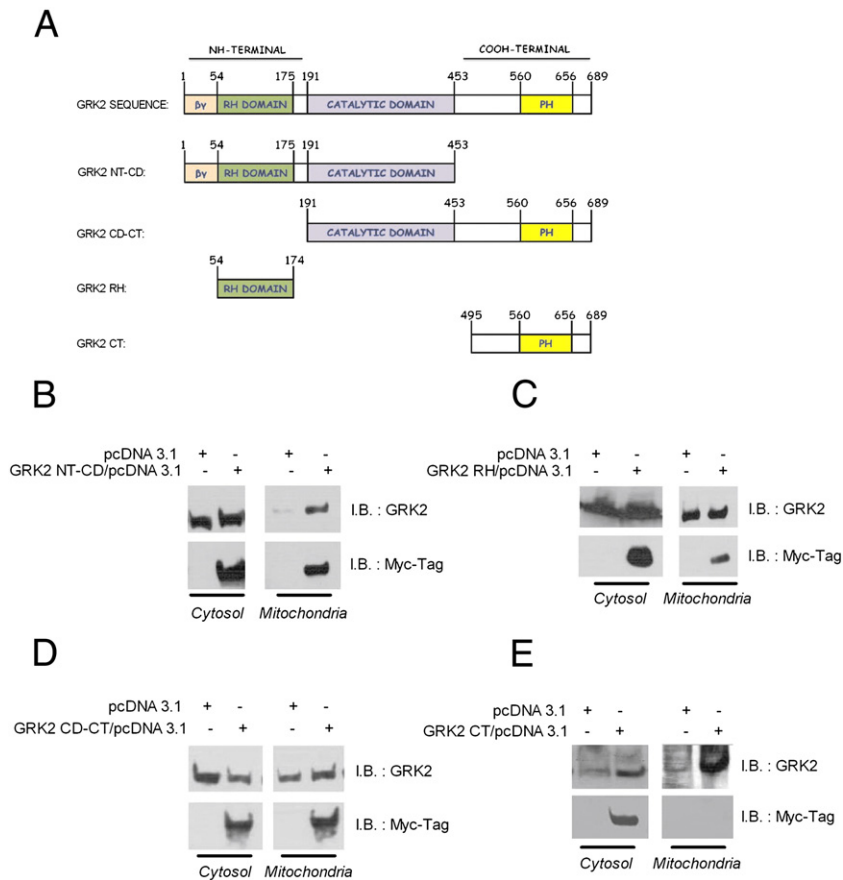


Fig. 3. (A) GRK2 sequence and truncated mutants cloned in pcDNA3.1 (+) Myc/His A. HEK-293 cells were transfected with pcDNA3.1 encoding for GRK2 NT-CD (B), GRK2 RH (C), GRK2 CD-CT (D) and GRK2 CT (E).

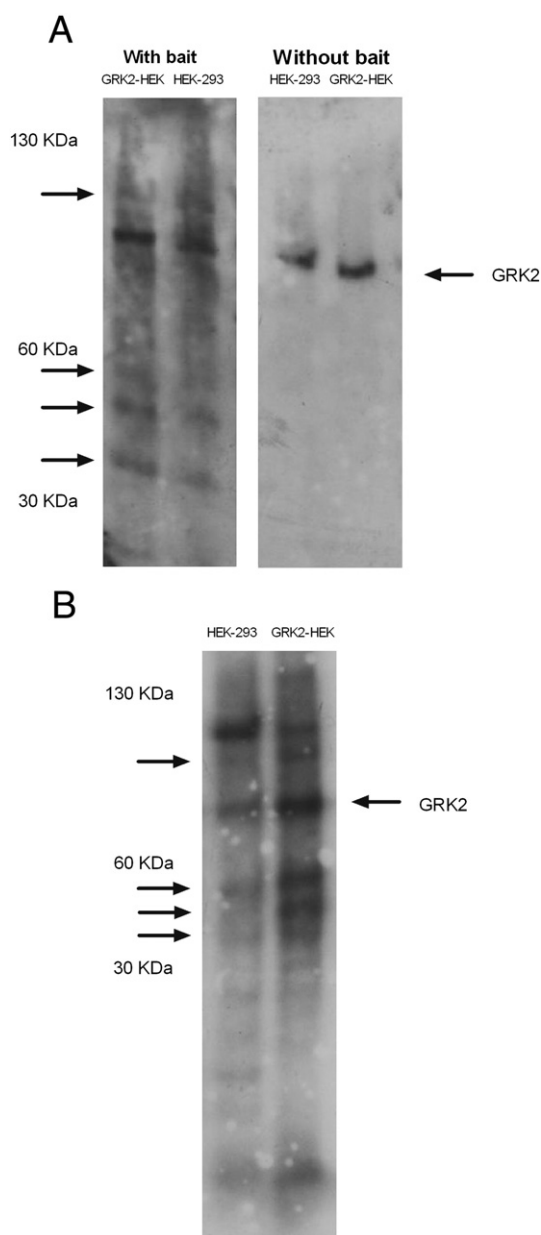


Fig. 4. (A) Overlay assay with (left blot) or without (right blot) purified GRK2 as bait in HEK-293 and GRK2-HEK cells mitochondria blotted on nitrocellulose. (B) Purified GRK2 was incubated with HEK-293 and GRK2-HEK mitochondrial extracts blotted on nitrocellulose in a kinase buffer, in presence of [32 P] γ -ATP. The blot was then extensively washed and exposed to autoradiography.

PCR analysis, we monitored the levels of two mitochondrial genes: NADH de-hydrogenase (NADHd) and cytochrome B (Cyt B), using nuclear β globin gene as internal control. Fig. 5A shows that GRK2 increased the levels of both mitochondrial genes.

To correlate the increased mtDNA with increased expression of mitochondrial proteins, we monitored the expression levels of NADHd and cytochrome B mRNA. Total RNA was extracted from cells and subjected to reverse transcription and quantitative RT-PCR analysis. As shown in Fig. 5B, GRK2 significantly up-regulated the levels of NADHd and cytochrome B mRNAs. Reciprocally, in GRK2^{f/f,CRE} cells, we observed a reduction in the number of copies and the level of expression of the NADHd and cytochrome B as compared to GRK2^{f/f} cells (Figs. 5C and 5D).

To assess the actual change in total mitochondrial mass, we loaded cells with the mitochondrial selective fluorescent dye mitotracker and analyzed the intensity of fluorescent emission by FACS analysis. GRK2 overexpression in HEK-293 induced a rightward shift in the

emission profile of mitotracker, which increased by a 36% (Fig. 5E). Reciprocally, in GRK2^{f/f,Cre} cells, we observed a leftward shift compared to GRK2^{f/f} cells, accounting for a decrease of emission intensity of mitotracker of about 31% (Fig. 5F). These data are compatible with a positive effect of GRK2 on mitochondrial biogenesis.

3.6. GRK2 protects from hypoxia/reperfusion induced ATP loss

Given the ability of GRK2 to promote ATP production through an increase in mitochondria, we verified the effects of the kinase in a mitochondrial threatening condition, the hypoxia/reperfusion. Acute hypoxia (1 h) promotes an increase of total and mitochondrion-associated GRK2 levels, as assessed by western blot analysis. The increase of GRK2 levels in hypoxic conditions was transient, since re-oxygenation for 15 min and 1 h restored the levels of the kinase to normal oxygen conditions (Fig. 6A). In control cells, ATP levels decreased during hypoxia and after oxygen restoration. Over-expression of GRK2 attenuated the loss of ATP production, compared to controls (Fig. 6B). As expected, in GRK2^{f/f,CRE} cells ATP levels were severely reduced under both basal and hypoxia conditions, and the recovery following oxygen restoration was impaired (Fig. 6C).

3.7. Removal of GRK2 gene in GRK2^{f/f,CRE} mice decreases ATP levels

We evaluated the role of GRK2 in the regulation of ATP levels in an in vivo model of muscle ischemia. We used mutant GRK2^{f/f} mice. Intramuscular injection of adenoviral particles (10^9 pfu/ml) encoding for Cre recombinase promoted targeted deletion of GRK2 gene, thus reducing the levels of the kinase by several folds (Fig. 6D). Ischemia causes GRK2 mitochondrial accumulation in mouse hind limb muscle. Ischemia was obtained by ligation of the femoral artery for 1 h, and reperfusion was applied for 15 min. By western blot, ischemia induces an increase of GRK2, which promptly recovers to basal levels after 15 min of reperfusion (Fig. 6E). In control GRK2^{f/f} mice, femoral artery occlusion reduced ATP levels, in quadriceps femoral muscle. Reperfusion of ischemic muscles for 15 min and 1 h partially restored muscular ATP levels. In GRK2^{f/f,CRE} muscles, GRK2 removal parallels a significant reduction of ATP levels. GRK2 deletion also attenuated the recovery of ATP levels following reperfusion of ischemic muscles, compared to GRK2^{f/f} mice (Fig. 6F).

4. Discussion

This report shows for the first time that GRK2 can localize on the mitochondrial outer membrane. Indeed, until now, the paradigm indicates that GRK2 shuttles between the cytosol and the plasma membrane, anchoring to the latter through its pleckstrin homology and G β γ binding domains within the carboxyl terminus [19]. Our data allow us to indicate that also the mitochondria should be included as a cellular compartment on which this molecule can be found. Two regions within the RH and the catalytic domains possess the ability to localize truncated mutants of GRK2 on these organelles. The most compelling finding, though, is that GRK2 modifies the biology of mitochondria. Indeed, the mitochondrial compartment is more than just a reservoir for the kinase. We observed consensual changes in mitochondrial DNA and RNA, as well as mitochondrial mass size, after overexpression or deletion of GRK2, consistent with the ability of the kinase to promote mitochondrial biogenesis. Furthermore, these changes are paralleled by modification of mitochondrial ATP production.

Mitochondria are most important in the settings of the responses to stress, such as the ischemia/reperfusion [20], and under these conditions we report two striking novel and unexpected observations. First, ischemia causes acute cellular and mitochondrial accumulation of GRK2 both in vitro (Fig. 6A) and in vivo (Fig. 6E), an effect reverted by oxygen restoration. This surprising evidence further strengthens the physiological role of GRK2 in the mitochondria. Second, a

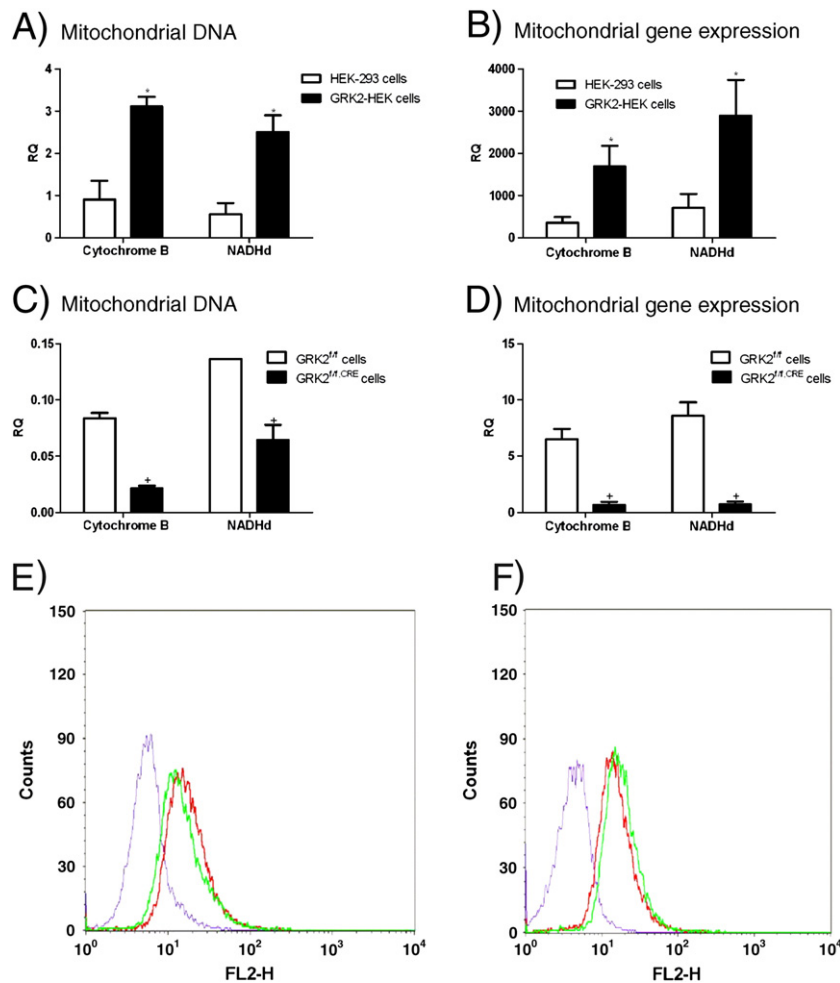


Fig. 5. (A and B) Quantitative RT-PCR analysis in HEK-293 and GRK2-HEK cells of copy numbers and gene expression of the mitochondrial genes Cytochrome B (Cyt B) and NADHd, relative to the nuclear gene β globin. (RQ: relative quantities, * $p < 0.05$ vs HEK-293 cells). (C and D) Same as above, in GRK2^{f/f} and GRK2^{f/f,CRE} cells. (RQ: relative quantities, + $p < 0.05$ vs GRK2^{f/f} cells). (E) Intensity of fluorescent emission in HEK-293 (green) and GRK2-HEK (red) cells and mitotracker unstained control cells (purple) under FACS analysis. (F) Same as above, in GRK2^{f/f} (green) and GRK2^{f/f,CRE} (red) cells and mitotracker unstained control cells (purple).

protective effect of the kinase is revealed, since transgenic overexpression causes mitochondrial accumulation of the kinase and protects ATP production even after hypoxia/reperfusion damage.

Although we do not have evidence regarding the mechanism through which GRK2 localizes in the mitochondria, it is evident that within these organelles, the kinase can bind some protein counterparts, which can also be phosphorylated by the kinase. It is possible to speculate that these unknown substrates favors the accumulation within the mitochondria of GRK2 and in turn get phosphorylated. Indeed, using a catalytic inactive mutant of GRK2 we can observe mitochondrial accumulation, suggesting that the enzymatic activity of the kinase is not needed for the localization (data not shown). The identification of the mitochondrial partner of GRK2 is actively pursued in the lab, and will allow to better understand the mechanisms of biogenesis and mitochondrial protection induced by the kinase.

The favorable activity of GRK2 within the mitochondria turns out to be protective, in particular after ischemia/reperfusion. Previous data in the literature support a protective role of GRK2 for the cell. First, GRK2 gene deletion is detrimental for embryonic cardiac development [21]. Second, in adult life, cardiac selective GRK2 removal alters the cardiac hypertrophy response to chronic β adrenergic receptor stimulation, leading to an eccentric dilatation of the heart similar to that observed in intermediate-advanced phases of heart failure [9]. On the contrary, other data in literature, suggest a detrimental effect of increased GRK2 levels for the cell, and may appear

in contrast to the present observation. In particular, in mice subjected to myocardial infarction, the inducible, cardiac specific removal of GRK2 through gene deletion results in the amelioration of survival, reduced “at risk” ischemic area and improved cardiac performance [22]. This apparent discrepancy could be imputed to differences in timing and model. Indeed, we applied ischemia reperfusion for 1 h in the skeletal muscle. It is possible that in more extensive tissue damage in a more sensitive tissue such as the myocardium, the negative signaling properties of GRK2 prevail on the protective metabolic effects of the kinase.

In conclusion, our data add more support to the building of a new perspective in which GRK2 not only regulates GPCR signaling, but also coordinates a series of metabolic responses to excessive signaling and stress, by starting receptor desensitization [19], reducing glucose extraction [3] and metabolism and activating mitochondrial biogenesis.

Acknowledgments

We are grateful to Dr. Nella Prevete, Dr. Annalisa Carlucci and Sergio Sorbo (CISME) for their technical support. Antonio Feliciello is supported by Associazione Italiana Ricerca sul Cancro (AIRC), Guido Iaccarino by MIUR grant (PRIN 2009EL5WBP) and Anna Fusco is the recipient of the Salvatore Campus fellowship from Società Italiana Ipertensione Arteriosa (SIA). Gerald Dorn is supported by NIH grant R01 HL087871.

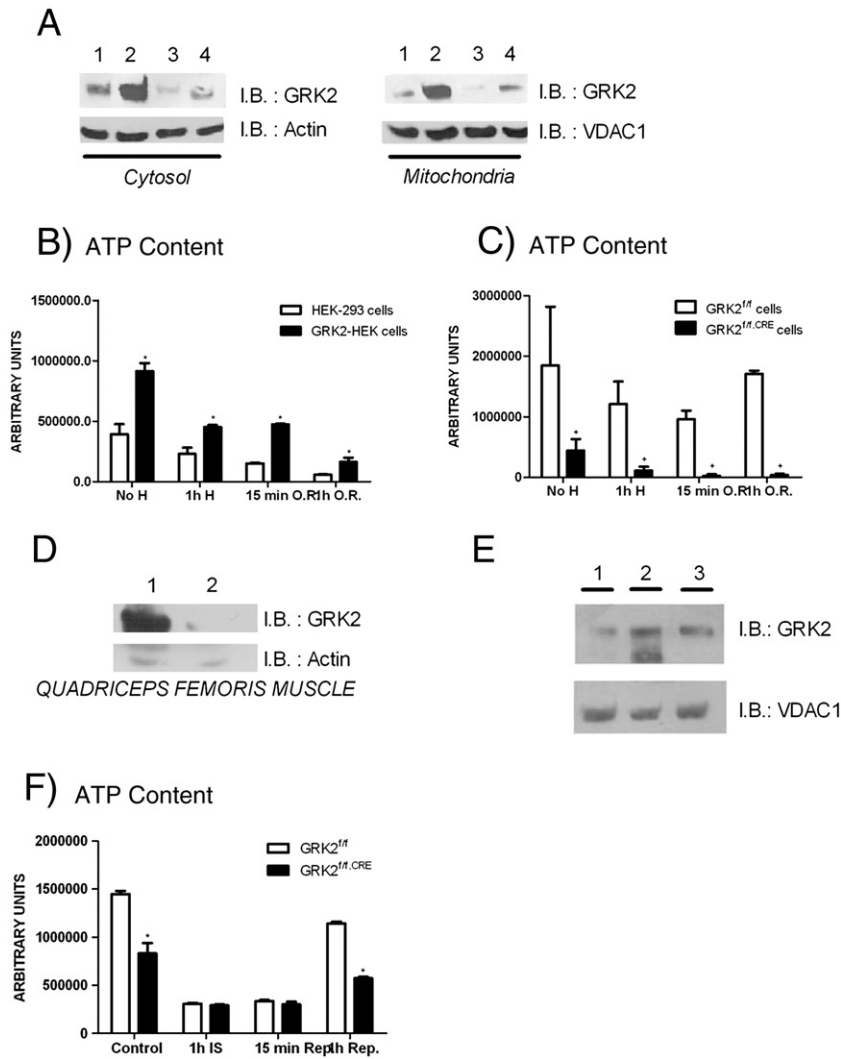


Fig. 6. (A) In cells, GRK2 accumulates during hypoxia and returns to basal levels after oxygen replenishment (1: no hypoxia; 2: 1 h hypoxia; 3: 15 min oxygen replenishment; 4: 1 h oxygen replenishment). (B) Cellular ATP content in HEK-293 and GRK2-HEK cells during hypoxia (H: hypoxia; O.R.: oxygen restoration; * p<0.05 vs HEK-293 cells). (C) Cellular ATP in GRK2^{fl/fl} and GRK2^{fl/fl}.CRE cells during hypoxia (H: hypoxia; O.R.: oxygen restoration; + p<0.05 vs GRK2^{fl/fl} cells). (D) In vivo GRK2 expression, in quadriceps femoris muscle from mice harboring f-loxed GRK2 gene after intramuscular injection of AdCre (10⁹ pfu/ml) (1: AdEMPTY; 2: AdCre). (E) Ischemia induces an increase of GRK2, which promptly recovers to basal levels after 15 min of reperfusion (1: no ischemia; 2: 1 h ischemia; 3: 15 min). (F) ATP content in quadriceps femoris muscle of mice subjected to hind limb ischemia/reperfusion (* p<0.05 vs GRK2^{fl/fl} mice; Control: non ischemic muscle; IS: 1 h ischemia; Rep: reperfusion).

References

[1] J. Inglese, N.J. Freedman, W.J. Koch, R.J. Lefkowitz, *Journal of Biological Chemistry* 268 (32) (1993) 23735–23738.

[2] C. Ribas, P. Penela, C. Murga, A. Salcedo, C. Garcia-Hoz, M. Jurado-Pueyo, I. Aymerich, F. Mayor Jr., *Biochimica et Biophysica Acta* 1768 (4) (2007) 913–922.

[3] E. Cipolletta, A. Campanile, G. Santulli, E. Sanzari, D. Leosco, P. Campiglia, B. Trimarco, G. Iaccarino, *Cardiovascular Research* 84 (3) (2009) 407–415.

[4] M. Ciccarelli, M. Chuprun, J.K. Rengo, G. Gao, E. Wei, Z. Peroutka, R.J. Gold, J.I. Gumpert, A. Chen, M. Otis, N.J. Dorn, G.W. Dorn 2nd, B. Trimarco, G. Iaccarino, W.J. Koch, *Circulation* 123 (18):1953–1962.

[5] I. Usui, T. Imamura, H. Satoh, J. Huang, J.L. Babendure, C.J. Hupfeld, J.M. Olefsky, *EMBO Journal* 23 (14) (2004) 2821–2829.

[6] I. Usui, T. Imamura, J.L. Babendure, H. Satoh, J.C. Lu, C.J. Hupfeld, J.M. Olefsky, *Molecular Endocrinology* 19 (11) (2005) 2760–2768.

[7] V.G. Antico Arciuch, Y. Alippe, M.C. Carreras, J.J. Poderoso, *Advanced Drug Delivery Reviews* 61 (14) (2009) 1234–1249.

[8] M. Ciccarelli, E. Cipolletta, G. Santulli, A. Campanile, K. Pumiglia, P. Cervero, L. Pastore, D. Astone, B. Trimarco, G. Iaccarino, *Cellular Signalling* 19 (9) (2007) 1949–1955.

[9] S.J. Matkovich, A. Diwan, J.L. Klanke, D.J. Hammer, Y. Marreez, A.M. Odley, E.W. Brunskill, W.J. Koch, R.J. Schwartz, G.W. Dorn 2nd, *Circulation Research* 99 (9) (2006) 996–1003.

[10] G. Iaccarino, M. Ciccarelli, D. Sorriento, E. Cipolletta, V. Cerullo, G.L. Iovino, A. Paudice, A. Elia, G. Santulli, A. Campanile, O. Arcucci, L. Pastore, F. Salvatore, G. Condorelli, B. Trimarco, *Circulation* 109 (21) (2004) 2587–2593.

[11] D. Sorriento, A. Campanile, G. Santulli, E. Leggiero, L. Pastore, B. Trimarco, G. Iaccarino, *Molecular Cancer* 8 (2009) 97.

[12] O.M. de Brito, L. Scorrano, *Nature* 456 (7222) (2008) 605–610.

[13] Sorriento D, Santulli G, Fusco A, Anastasio A, Trimarco B, Iaccarino G. *Hypertension*;56(4):696–704.

[14] D. Sorriento, M. Ciccarelli, G. Santulli, A. Campanile, G.G. Altobelli, V. Cimini, G. Galasso, D. Astone, F. Piscione, L. Pastore, B. Trimarco, G. Iaccarino, *Proceedings of the National Academy of Sciences of the United States of America* 105 (46) (2008) 17818–17823.

[15] A. Livigni, A. Scorziello, S. Agnese, A. Adornetto, A. Carlucci, C. Garbi, I. Castaldo, L. Annunziato, E.V. Avvedimento, A. Feliciello, *Molecular Biology of the Cell* 17 (1) (2006) 263–271.

[16] Chowanadisai W, Bauerly KA, Tchapanian E, Wong A, Cortopassi GA, Rucker RB. *J Biol Chem*;285(1):142–152.

[17] M. Ciccarelli, G. Santulli, A. Campanile, G. Galasso, P. Cervero, G.G. Altobelli, V. Cimini, L. Pastore, F. Piscione, B. Trimarco, G. Iaccarino, *British Journal of Pharmacology* 153 (5) (2008) 936–946.

[18] G. Santulli, M. Ciccarelli, G. Palumbo, A. Campanile, G. Galasso, B. Ziaco, G.G. Altobelli, V. Cimini, F. Piscione, L.D. D'Andrea, C. Pedone, B. Trimarco, G. Iaccarino, *Journal of Translational Medicine* 7 (2009) 41.

[19] D.T. Lodowski, J.A. Pitcher, W.D. Capel, R.J. Lefkowitz, J.J. Tesmer, *Science* 300 (5623) (2003) 1256–1262.

[20] A. Carlucci, L. Lignitto, A. Feliciello, *Trends in Cell Biology* 18 (12) (2008) 604–613.

[21] M. Jaber, W.J. Koch, H. Rockman, B. Smith, R.A. Bond, K.K. Sulik, J. Ross Jr., R.J. Lefkowitz, M.G. Caron, B. Giros, *Proceedings of the National Academy of Sciences of the United States of America* 93 (23) (1996) 12974–12979.

[22] P.W. Raake, L.E. Vinge, E. Gao, M. Boucher, G. Rengo, X. Chen, B.R. DeGeorge Jr., S. Matkovich, S.R. Houser, P. Most, A.D. Eckhart, G.W. Dorn 2nd, W.J. Koch, *Circulation Research* 103 (4) (2008) 413–422.



Canadian Journal of Cardiology xx (2011) xxx www.onlinecjc.ca

Letter to the Editor

Development of Atrial Fibrillation in Recipients of Cardiac Resynchronization Therapy: The Role of Atrial Reverse Remodelling

To the Editor:

We congratulate Wilton et al. for their interesting report in a recent issue of the *Canadian Journal of Cardiology*, regarding the role of rate-controlled persistent atrial fibrillation (AF) on the clinical outcome and ventricular remodelling in patients receiving cardiac resynchronization therapy (CRT).¹

In this post hoc analysis there are follow-up data (2.8 ± 1.4 years) for 86 patients (19 with and 67 without persistent AF). Using a composite of objective symptomatic improvement and left ventricular (LV) reverse remodelling, the authors find that subjects with and without AF have a similar likelihood of responding to CRT in the first year of treatment. However, those in the AF group have significantly less improvement in LV end-systolic volume, with a doubled risk of death or cardiac transplantation during long-term follow-up.

We have several comments concerning the relationship between CRT response and the incidence of new-onset AF. Prior reports have yielded controversial results regarding the effect of CRT on the incidence of AF.^{2,3} In the study by Wilton et al., 18% of patients in the non-AF group developed AF during follow-up after CRT, but unfortunately there is no information about the role of CRT response. It would be interesting to know how many patients that developed new-onset AF were “CRT responders” and how many were “nonresponders.” Although LV function was evaluated by multiple gated acquisition we would like to know if there are also data (simple echocardiography could be enough) regarding atrial dimension and function,^{2,3} in order to compare atrial reverse remodelling in CRT responders and nonresponders.³ Moreover, if possible the authors might provide an analysis regarding the role of the etiology of cardiomyopathy (ischemic vs nonischemic) in the development of AF.^{3,4}

Gaetano Santulli, MD
Columbia University Medical Center
New York, New York, USA
Federico II University
Naples, Italy
gs2620@columbia.edu

Salvatore Luca D’ascia, MD
Cristofaro D’ascia, MD
Federico II University
Naples, Italy

Disclosures

The authors have no conflicts of interest to disclose.

References

1. Wilton SB, Kavanagh KM, Aggarwal SG, et al. Association of rate-controlled persistent atrial fibrillation with clinical outcome and ventricular remodelling in recipients of cardiac resynchronization therapy. *Can J Cardiol* 2011;27:787-93.
2. Brenyo A, Link MS, Barsheshet A, et al. Cardiac resynchronization therapy reduces left atrial volume and the risk of atrial tachyarrhythmias in MADIT-CRT (Multicenter Automatic Defibrillator Implantation Trial with Cardiac Resynchronization Therapy). *J Am Coll Cardiol* 2011;58:1682-9.
3. D’Ascia SL, D’Ascia C, Marino V, et al. Cardiac resynchronisation therapy response predicts occurrence of atrial fibrillation in non-ischaemic dilated cardiomyopathy. *Int J Clin Pract* 2011;65:1149-55.
4. McLeod CJ, Shen WK, Rea RF, et al. Differential outcome of cardiac resynchronization therapy in ischemic cardiomyopathy and idiopathic dilated cardiomyopathy. *Heart Rhythm* 2011;8:377-82.

doi:10.1016/j.cjca.2011.11.001

Neurology[®]

Thrombolysis Outcomes in Acute Ischemic Stroke Patients With Prior Stroke and Diabetes Mellitus

Gaetano Santulli

Neurology 2012;78;840

DOI 10.1212/WNL.0b013e31824de51b

This information is current as of May 22, 2012

The online version of this article, along with updated information and services, is located on the World Wide Web at:

<http://www.neurology.org/content/78/11/840.1.full.html>

Neurology® is the official journal of the American Academy of Neurology. Published continuously since 1951, it is now a weekly with 48 issues per year. Copyright © 2012 by AAN Enterprises, Inc. All rights reserved. Print ISSN: 0028-3878. Online ISSN: 1526-632X.



Editors' Note: Dr. Santulli, citing the findings of Dr. Mishra et al. that neither diabetes nor prior stroke affected thrombolysis outcomes, calls for the reevaluation of thrombolysis criteria and the adoption of a clinical score, similar to that used in acute coronary syndrome, to stratify risk. There were 2 WriteClick submissions in reference to the recent article by Dr. Stein et al. comparing high-dose and low-dose vitamin D2 supplementation in relapsing-remitting multiple sclerosis. Dr. Leitner calls attention to the incongruity of epidemiologic trends in MS vs another vitamin D–related illness, rickets, as further reason not to supplement patients with MS without proven vitamin D deficiency at this time. Dr. Grimaldi et al. argue that the study was underpowered and potentially biased. Their own phase II study of high-dose vitamin D3 supplementation is under way.

Megan Alcauskas, MD, and Robert C. Griggs, MD

THROMBOLYSIS OUTCOMES IN ACUTE ISCHEMIC STROKE PATIENTS WITH PRIOR STROKE AND DIABETES MELLITUS

Gaetano Santulli, New York: Mishra et al.¹ examined the influence of diabetes mellitus and prior stroke on the outcomes of patients who received thrombolysis vs nonthrombolysed controls. They found no interaction on outcome between diabetes and prior stroke with thrombolysis treatment.

These results conflict with the European Medicines Evaluation Agency's justification for restricting the use of IV alteplase. As Dr. Demaerschalk mentioned in the accompanying editorial,² recent studies^{1,3,4} have suggested that thrombolysis can be safely used in several groups of patients who do not qualify for treatment due to strict application of exclusion criteria.

In addition, most of the commonly cited thrombolytic exclusion criteria are just consensus-based, not evidence-based.^{2,3} It is time to reevaluate the criteria for thrombolysis, adopting a clinical score to stratify the risk, similar to those used in acute coronary syndrome.⁵ A good risk assessment tool will be able to identify a gradient of mortality risk by using variables that capture the majority of prognostic information to better evaluate the risk/benefit ratio for each patient.

Copyright © 2012 by AAN Enterprises, Inc.

1. Mishra NK, Ahmed N, Davalos A, et al. Thrombolysis outcomes in acute ischemic stroke patients with prior stroke and diabetes mellitus. *Neurology* 2011;77:1866–1872.
2. Demaerschalk BM. Challenging the validity of imposing contraindications to thrombolysis for acute ischemic stroke. *Neurology* 2011;77:1862–1863.
3. Tong D. Are all IV thrombolysis exclusion criteria necessary? Being SMART about evidence-based medicine. *Neurology* 2011;76:1780–1781.
4. Rubiera M, Ribo M, Santamarina E, et al. Is it time to reassess the SITS-MOST criteria for thrombolysis? A comparison of patients with and without SITS-MOST exclusion criteria. *Stroke* 2009;40:2568–2571.
5. Morrow DA, Antman EM, Charlesworth A, et al. TIMI risk score for ST-elevation myocardial infarction: a convenient, bedside, clinical score for risk assessment at presentation: an intravenous nPA for treatment of infarcting myocardium early II trial substudy. *Circulation* 2000;102:2031–2037.

A RANDOMIZED TRIAL OF HIGH-DOSE VITAMIN D2 IN RELAPSING-REMITTING MULTIPLE SCLEROSIS

Helmut H. Leitner, Vienna: Stein et al.¹ compared high- vs low-dose vitamin D2 treatment in MS without benefit in the high-dose treatment group. Sunlight exposure and reduced vitamin D3 levels independently contribute to MS risk. The effect of sunlight exposure is supported by decreased signs of actinic skin damage found in MS patients compared to controls.² It is difficult to determine which of these 2 environmental factors is of primary importance as higher levels of sunlight exposure will enhance vitamin D levels.

The incidence of vitamin D–related rickets disease decreased in the United States and Europe during the last century following the discovery that vitamin D possessed antirachitic properties, whereas the incidence of MS seemed to increase in the same population. In the United States, most of the patients with rickets are African American, whereas the majority of patients with MS are of European ancestry.³ It seems improbable that the same environmental factor should be centrally involved in the etiology of both diseases, which differ clinically and occur in different populations living in the same geographic area.

These findings together with those of Stein et al. do not provide a reason for vitamin D supplementa-



The Ten Commandments of Ethical Publishing

Gaetano Santulli*

Columbia University Medical Center, New York, USA

This article describes the position of the Journal on the major ethical principles of academic publishing. Academic publishing depends, to a great extent, on trust. Editors trust peer reviewers to provide fair assessments, authors trust Editors to select appropriate peer reviewers, and readers put their trust in the peer-review process [1,2]. Publication of ethically uncertain research occurs albeit well-published guidelines set forth in documents such as the Declaration of Helsinki (http://whqlibdoc.who.int/euro/1994-97/EUR_ICP_CEH_212.pdf). Such guidelines exist to aide editorial staff in making decisions regarding ethical acceptability of manuscripts submitted for publication, yet examples of ethically suspect and uncertain publication exist [3,4]. The editor of any medical Journal has to be aware of the ethical and legal framework within which medical research is conducted [5]. With an Open Access Journal, we are committed to the widest possible dissemination of Research outputs observing the highest ethical publication practices [6,7,8].

Authors have a number of duties and responsibilities that are mirrored by those of editors and publishers. Of particular importance are the principles of transparency and integrity. To publish in OMICS Journals, the authors have to be sure that:

1. The corresponding author has the approval of all other listed authors for the submission of the manuscript.
2. All people who have a right to be recognized as authors have been included on the list of authors and everyone listed as an author has made an independent contribution to the manuscript.

The list of authors corresponds to the following criteria: a) substantial contributions to conception and design, or acquisition of data, or analysis and interpretation of data; b) drafting the article or revising it critically for important intellectual content; and c) final approval of the version to be published. All authors must meet these criteria for authorship and conversely, no-one should be omitted from the list if he/she meets these criteria.

3. The work submitted in the manuscript is original and has not been published elsewhere and is not presently under consideration of publication by any other Journal.
4. The material in the manuscript has been acquired according to modern ethical standards and does not contain material plagiarized from anyone else without their written permission. Plagiarism includes both the theft or misappropriation of intellectual property and the substantial unattributed textual copying of another's work. The theft or misappropriation of intellectual property includes the unauthorized use of ideas or unique methods obtained by a privileged communication, such as a grant or manuscript review [4].
5. The material that derives from previously published papers is properly attributed to the prior publication by proper citation.
6. The source of the Research funds has been listed on the paper: the authors should acknowledge all significant funders of the Research pertaining to their article.

7. All relevant conflicts of interest have been declared. Referees are asked to declare their conflicts of interest when returning their report on a paper. If a member of the editorial team feels a conflict of interest in making a decision on a paper, she/he should return the paper to the office and request that it is transferred to an alternative Editor.
8. Concerning studies in humans: the authors must indicate that the study was approved by an institutional review committee and that the subjects gave written informed consent [9]. All studies that involve humans have to adhere to the principles of the Declaration of Helsinki (see the link above).
9. Concerning studies in experimental animals: the authors must indicate that an institutional review committee approved the study. All studies in animals should be conducted in accordance with the National Institutes of Health (NIH) Guide for the Care and Use of Laboratory Animals, or the equivalent. The species, strain, number used, and other relevant characteristics of the animals should be stated. When describing surgical procedures, identify the pre-anesthetic and anesthetic agents used and state the amount or concentration and the route and frequency of administration for each. Generic names of drugs must be given. These details should be included in the Methods section of the article [10].
10. If any of the statements above ceases to be true the authors have a duty to notify the Journal as soon as possible so that the manuscript can be withdrawn. Authors must inform the Journal promptly should their results be later invalidated, and permit inspection or auditing of reports if necessary

References

1. Vlassov V, Groves T (2010) The role of Cochrane Review authors in exposing research and publication misconduct. *Cochrane Database Syst Rev* 8: ED000015.
2. Graf C, Wager E, Bowman A, Fiack S, Scott-Lichter D, et al. (2007) Best Practice Guidelines on Publication Ethics: a publisher's perspective. *Int J Clin Pract Suppl* : 1-26.
3. Coats AJ (2009) Ethical authorship and publishing. *Int J Cardiol* 131: 149-150.
4. Angelski CL, Fernandez CV, Weijer C, Gao J (2012) The publication of ethically uncertain research: attitudes and practices of journal editors. *BMC Med Ethics* 13: 4.
5. Santulli G (2012) Thrombolysis outcomes in acute ischemic stroke patients with prior stroke and diabetes mellitus. *Neurology* 78: 840.
6. Vita J (2012) JAHA: The American Heart Association's Open Access Journal. *Journal of the American Heart Association* 1: 1-2.

*Corresponding author: Gaetano Santulli MD, Columbia University Medical Center, New York, USA, E-mail: gs2620@columbia.edu

Received April 18, 2012; Accepted April 19, 2012; Published April 21, 2012

Citation: Santulli G (2012) The Ten Commandments of Ethical Publishing. *Cell Development Biol* 1:e103. doi:10.4172/cdb.1000e103

Copyright: © 2012 Santulli G. This is an open-access article distributed under the terms of the Creative Commons Attribution License, which permits unrestricted use, distribution, and reproduction in any medium, provided the original author and source are credited.

7. Phelps L, Fox BA, Marincola FM (2012) Supporting the advancement of science: open access publishing and the role of mandates. *J Transl Med* 10: 13.
8. Matarese A, Santulli G (2012) Angiogenesis in Chronic Obstructive Pulmonary Disease: A Translational Appraisal. *Translational Medicine @ UniSa*. 3: 49-56.
9. Santulli G. Coronary heart disease risk factors and mortality. *JAMA* 307: 1137.
10. Santulli G, Lombardi A, Sorriento D, Anastasio A, Del Giudice C, et al. (2012) Age-Related Impairment in Insulin Release: The Essential Role of beta2-Adrenergic Receptor. *Diabetes* 61: 692-701.

Submit your next manuscript and get advantages of OMICS Group submissions

Unique features:

User friendly/feasible website-translation of your paper to 50 world's leading languages
Audio Version of published paper
Digital articles to share and explore

Special features:

200 Open Access Journals
15,000 editorial team
21 days rapid review process
Quality and quick editorial, review and publication processing
Indexing at PubMed (partial), Scopus, DOAJ, EBSCO, Index Copernicus and Google Scholar etc
Sharing Option: Social Networking Enabled
Authors, Reviewers and Editors rewarded with online Scientific Credits
Better discount for your subsequent articles

Submit your manuscript at: <http://omicsgroup.org/editorialtracking/clinical-trials>



RESEARCH PAPER

Impaired neoangiogenesis in β_2 -adrenoceptor gene-deficient mice: restoration by intravascular human β_2 -adrenoceptor gene transfer and role of NF κ B and CREB transcription factors

Correspondence

Guido Iaccarino, Medicina Clinica, Scienze Cardiovascolari ed Immunologiche, Federico II University, Via Pansini 5; Edificio 2, 80131 Naples, Italy. E-mail: guiaccar@unina.it

*These Authors contributed equally to this paper.

Keywords

adrenergic signalling; gene therapy; ischaemic hindlimb; NF κ B activity

Received

7 May 2010

Revised

22 September 2010

Accepted

25 September 2010

Michele Ciccarelli^{1,2*}, Daniela Sorriento^{1*}, Ersilia Cipolletta¹, Gaetano Santulli¹, Anna Fusco¹, Rui-Hai Zhou², Andrea D. Eckhart², Karsten Peppel², Walter J. Koch², Bruno Trimarco¹ and Guido Iaccarino¹

¹Dipartimento di Medicina Clinica, Scienze Cardiovascolari ed Immunologiche, Università Federico II, Napoli, Italy, and ²Center for Translational Medicine, Thomas Jefferson University, Philadelphia, PA, USA

BACKGROUND AND PURPOSE

There is much evidence supporting the role of β_2 -adrenoceptors (β_2 AR) in angiogenesis but the mechanisms underlying their effects have not been elucidated. Hence, we studied post-ischaemic angiogenesis in the hindlimb (HL) of β_2 AR knock-out mice (β_2 AR^{-/-}) *in vivo* and explored possible molecular mechanisms *in vitro*.

EXPERIMENTAL APPROACH

Femoral artery resection (FAR) was performed in wild-type and β_2 AR^{-/-} mice and adaptive responses to chronic HL ischaemia were explored; blood flow was measured by ultrasound and perfusion of dyed beads, bone rarefaction, muscle fibrosis and skin thickness were evaluated by immunofluorescence and morphometric analysis. Intrafemoral delivery of an adenovirus encoding the human β_2 AR (AD β_2 AR) was used to reinstate β_2 ARs in β_2 AR^{-/-} mice. Molecular mechanisms were investigated in mouse-derived aortic endothelial cells (EC) *in vitro*, focusing on NF κ B activation and transcriptional activity.

RESULTS

Angiogenesis was severely impaired in β_2 AR^{-/-} mice subjected to FAR, but was restored by gene therapy with AD β_2 AR. The proangiogenic responses to a variety of stimuli were impaired in β_2 AR^{-/-} EC *in vitro*. Moreover, removal of β_2 ARs impaired the activation of NF κ B, a transcription factor that promotes angiogenesis; neither isoprenaline (stimulates β ARs) nor TNF α induced NF κ B activation in β_2 AR^{-/-} EC. Interestingly, cAMP response element binding protein (CREB), a transcription factor that counter regulates NF κ B, was constitutively increased in β_2 AR^{-/-} ECs. AD β_2 AR administration restored β_2 AR membrane density, reduced CREB activity and reinstated the NF κ B response to isoprenaline and TNF α .

CONCLUSIONS AND IMPLICATIONS

Our results suggest that β_2 ARs control angiogenesis through the tight regulation of nuclear transcriptional activity.

Abbreviations

AD β_2 AR, gene therapy with adenovirus encoding the human β_2 AR; ADU, arbitrary densitometry units; β_2 AR, β_2 adrenoceptor; β_2 AR^{-/-}, β_2 AR knock-out mice; BF, blood flow; CREB, cAMP response element binding protein; EC, endothelial cell; US, ultrasound; VEGF, vascular endothelial growth factor

Introduction

Little is known about the role of the β_2 -adrenoceptor (β_2 AR) in the vasculature. Recently, our group and others have begun to elucidate the mechanisms of β_2 AR control of vascular functions (Lembo *et al.*, 1997; Ferro *et al.*, 1999) and showed that this receptor can activate eNOS in an Akt-dependent manner and induce release of nitric oxide (NO) at the endothelium (Iaccarino *et al.*, 2002; 2004). We have also shown that the adenoviral-mediated endothelial overexpression of the β_2 AR regulates post-ischaemic angiogenesis (Iaccarino *et al.*, 2005), to the extent that β_2 ARs can correct impaired angiogenesis in animal models of cardiovascular disease such as the spontaneously hypertensive rat (Iaccarino *et al.*, 2002; 2005). The mechanisms underlying β_2 AR-regulated angiogenesis have still not been elucidated. One possible explanation is that receptors such as the β_2 AR are able to regulate the transcriptional activity of the cell, in order to promote the release of proangiogenic cytokines such as vascular endothelial growth factor (VEGF). Indeed, β_2 AR overexpression results in VEGF accumulation in the culture medium of endothelial cells. VEGF has a transcriptional regulation that is controlled by the hypoxia responsive transcription factor-1 (HIF-1), and also by NF κ B, which is known to be activated downstream by tumour necrosis factor receptors (TNF-R) superfamily-members and some G protein-coupled, seven transmembrane (7TM) receptors (GPCRs) (Ye, 2001).

The role of NF κ B in angiogenesis is well established, and is linked to its ability to regulate inflammatory cytokine production in many cellular types; these include the endothelium, infiltrating macrophages, vascular smooth muscle cells and pericytes, and skeletal muscle cells. In this context, receptor and transcription factors are major players, allowing the finely tuned response of different cell types. Therefore, NF κ B represents a particularly apt subject for our investigation on the signal transduction mechanisms underlying the proangiogenic effects of β_2 ARs.

The β_2 AR knock-out (β_2 AR $^{-/-}$) mouse model has already proved useful to unveil specific molecular features of the β_2 AR (Chruscinski *et al.*, 1999; Shenoy *et al.*, 2006). We therefore exploited such a model to investigate the adaptive responses to chronic hindlimb (HL) ischaemia in a β_2 AR-negative (β_2 AR $^{-/-}$) situation. Furthermore, using adenoviral-mediated gene transfer, we reconstituted membrane β_2 AR expression in the ischaemic HL. *In vitro*, we explored the possible mechanisms accounting for β_2 AR's beneficial effects on angiogenesis, focusing particularly on NF κ B activation and transcriptional activity.

Methods

Mouse strain and surgical procedures

Previously described β_2 AR $^{-/-}$ and β_2 AR $^{+/+}$ mice (age 14–18 weeks) were used in this study (Chruscinski *et al.*, 1999). Founders were provided by courtesy of Brian Kobilka, Stanford University, CA. Mice were bred in heterozygosity and homozygous β_2 AR $^{-/-}$ or β_2 AR $^{+/+}$ male littermates were used as the study and control population. All procedures were approved by the Thomas Jefferson University Institutional

Animal Care and Use Committee and the Federico II University Ethical Committee for Animal Research. Mice were anaesthetized with a mixture of ketamine (100 mg·kg $^{-1}$) and xylazine (3 mg·kg $^{-1}$) and the right common femoral artery was isolated and removed. In a group of β_2 AR $^{-/-}$ mice ($n = 20$), we placed a silastic catheter into the femoral artery distal to the resection, through which a solution containing 10^{11} tvp of either an adenovirus encoding for LacZ or the human β_2 AR gene was infused into the HL and allowed to remain there for 30 min while the saphenous vein was temporarily occluded (Santulli *et al.*, 2009a). Afterwards, the virus was removed through the catheter, the common femoral artery removed and the wound closed in layers. With this manoeuvre, we ascertained that endothelial cells, vascular smooth muscle cells and skeletal myocytes of the hindlimb express the transgene carried by the viral vector, as found previously (Santulli *et al.*, 2009a). Mice were checked daily for fur loss, skin lesions (blistering), necrosis, self-inflicted amputations of the ischaemic hindlimb. Surgical aftercare and distress surveillance were performed according to institution's guidelines.

Blood flow determination

Blood flow (BF) in the posterior tibial artery of ischaemic and non-ischaemic HL was evaluated by ultrasound (US) (using a VisualSONICS VeVo 770 imaging system with a 710 MHz scanhead) in isoflurane-anaesthetized mice (2% v·v $^{-1}$) immediately after surgery and at days 3, 7, 10 and 14 thereafter. We measured maximal velocity (V_{max}) and maximal diameter of the vessel. After calculation of the vessel area, BF was calculated using the formula: $BF = V_{max}/\text{vessel area}$ (Santulli *et al.*, 2009a). Data are expressed as ischaemic to non-ischaemic ratio. Fourteen days after surgery, mice were anaesthetized as above, and a PE 10 catheter was placed into the abdominal aorta through the left common carotid, as previously described (Iaccarino *et al.*, 2002). Maximal vasodilatation was obtained by administration of nitroglycerin (2 μ g i.a.) followed by injection of 3×10^6 orange-dyed beads (15 μ m diameter, Triton Technologies, San Diego, CA, USA). Animals were then killed by cervical dislocation, samples of the gastrocnemius muscle from the ischaemic and non-ischaemic HL were collected and frozen with liquid nitrogen and stored at -80°C . Next, the samples were homogenized and digested according to manufacturer protocol; the beads were collected and suspended in DMTF. The release of dye was assessed by light absorption at 450 nm (Santulli *et al.*, 2009a). Data are expressed as ischaemic to non-ischaemic muscle ratio.

Immunofluorescence and morphology

At 14 days, we used B mode US for morphological analysis of the ischaemic and contralateral hindlimbs. In particular, we evaluated bone rarefaction, muscle fibrosis and skin thickness, all processes that are associated with HL ischaemia (Santulli *et al.*, 2009b).

The anterior tibial muscle was isolated and harvested for immunostaining as described previously (Zhou *et al.*, 2003). Specimens were fixed in 4% paraformaldehyde and then embedded in paraffin. A series of cross-sections (6 μ m) were obtained. Rat anti-CD31 antibody (1:50, BD Pharmingen, CA) and rabbit anti-von Willebrand (vW) factor (1:50, DAKO,

Carpinteria, CA) were used as primary antibodies for double staining of endothelial cells. As a negative control, normal rat and rabbit IgG were used instead of the primary antibody. The primary antibodies were recognized by Alexa Fluor 594 goat anti-rat (Green) and Alexa Fluor 488 goat anti-rabbit (Blue) secondary antibodies (1:100), respectively (Molecular Probes, Eugene, Oregon). Nuclei were counterstained with VECTASHIELD mounting medium with DAPI (Red) (Vector, Burlingame, CA). Immunofluorescence was visualized under a fluorescence microscope (Olympus IX71, Olympus, Center Valley, CA, USA) and the number of capillaries per 20 fields was measured on each section by two independent operators (M.C., R.H.Z.), blinded to treatment. Another series of tissue sections were stained with haematoxylin/eosin (H&E) for morphological analysis.

β AR radioligand binding

Membrane fractions were obtained from quadriceps muscle homogenates by centrifugation as previously described (Iaccarino *et al.*, 1998). Total receptor density was assessed by β AR radioligand binding studies using the non-selective β AR antagonist [¹²⁵I]-cyanopindolol (¹²⁵I-CYP), as described previously (Iaccarino *et al.*, 2001b). The percentage of β_2 ARs was calculated from the high affinity binding subpopulation using GraphPad Prism.

Adenoviral constructs

We used adenoviral vectors encoding for the human wild-type β_2 AR gene (Ad β_2 AR) and the LacZ (control virus) as previously described (Iaccarino *et al.*, 2002; 2005; Ciccarelli *et al.*, 2007).

Cell culture

Aortic endothelial cells (ECs) from β_2 AR^{-/-} and β_2 AR^{+/+} mice were isolated as previously described (Iaccarino *et al.*, 2002). Vessels were cut into rings, placed on matrigel, incubated in DMEM supplemented with 20% FBS and EC growth supplement (10 mg · 100 mL⁻¹), and incubated at 37°C in 5% CO₂. After 7 days, aortic rings were removed, and the ECs remaining on matrigel were expanded in DMEM containing 10% FBS.

Western blotting

Cells were deprived of serum overnight, exposed to agonists and lysed in RIPA/SDS buffer (50 mmol·L⁻¹ Tris-HCl, pH 7.5, 150 mmol·L⁻¹ NaCl, 1% NP-40, 0.25% deoxycholate, 9.4 mg·50 mL⁻¹ sodium orthovanadate, 20% SDS). Protein concentration was determined using a BSA assay kit (Pierce, ThermoScientific, Rockford, IL, USA). I κ B α was immunoprecipitated from total lysates with anti-I κ B α antibody and protein A/G agarose. Immunocomplexes or total lysates were electrophoresed by SDS/PAGE and transferred to a nitrocellulose filter. Total I κ B α and β_2 AR were visualized by specific antibodies (Santacruz, Santa Cruz, CA, USA), anti-rabbit horseradish peroxidase-conjugated secondary antibody (Santacruz) and standard chemiluminescence (Pierce). Autoradiographies were then digitalized and densitometry quantification performed using dedicated software (ImageQuant, GE HealthCare, Milano, Italy). Data are presented as arbitrary densitometry units (ADU) after

normalization for actin. In other experiments, cells were infected with Ad β_2 AR at a rate of 20:1.

VEGF quantification

Aortic ECs from β_2 AR^{-/-} and β_2 AR^{+/+} mice were deprived of serum overnight and then stimulated with isoprenaline (Iso) for 6 h. Culture medium was collected and VEGF was immunoprecipitated with anti-VEGF antibody (Santacruz) and protein A/G agarose (Santacruz). After being extensively washed, the immunocomplexes were electrophoresed by SDS/PAGE and transferred to nitrocellulose; VEGF was visualized by specific antibody (Santacruz), anti-rabbit HRP-conjugated secondary antibody (Santacruz) and standard chemiluminescence (Pierce). For our analysis, we examined the Western blot band corresponding to VEGF 164 isoform.

Cell transfection and luciferase assay

Transient transfection was performed using Lipofectamine 2000 (Invitrogen, Paisley, UK) according to manufacturer's instruction. Aortic ECs from β_2 AR^{-/-} and β_2 AR^{+/+} mice were transfected with plasmid expression vectors coding cAMP response element binding protein (CREB) and I κ B plasmids (Sorriento *et al.*, 2009; 2010) used for signal transduction studies, or with a κ B-luciferase reporter and β -galactosidase for NF κ B activity. In this latter case, 24 h after transfection, cells were deprived of serum overnight and stimulated with TNF α (20 ng·mL⁻¹), as positive control, and Iso (10⁻⁷ mol·L⁻¹) for 1, 3 and 6 h. Lysates were analysed using the luciferase assay system with reporter lysis buffer from Promega and measured in a β -counter. Relative luciferase activity was normalized against the co-expressed β -galactosidase activity to overcome variations in transfection efficiency between samples. In other experiments, cells were stimulated with Iso (10⁻⁷ mol·L⁻¹) or TNF α (20 ng·mL⁻¹) for 3 h (Santulli *et al.*, 2009b).

Tube formation assay

When plated on matrigel (Becton Dickinson, Bedford, MA, USA), ECs organize themselves into a network-like structure, resembling sinusoids of immature vessels (Ciccarelli *et al.*, 2008). Six-well multidishes were coated with growth factor-reduced matrigel (10 mg·mL⁻¹) according to the manufacturer's instructions. Control and β_2 AR^{-/-} ECs (2 × 10⁵) were incubated at 37°C for 12 h in 1 mL of DMEM medium. Tube formation was defined as a structure exhibiting a length four times its width. Network formation was observed using an inverted phase-contrast microscope (ZEISS). Representative fields were taken, and the average of the total number of complete tubes formed by cells was counted in 15 random fields by two independent investigators (D.S and E.C.).

RT PCR

Total RNA was isolated from ECs deprived of serum overnight or mouse hindlimb muscle using Trizol reagent (Invitrogen) and cDNA was synthesized by means of Thermo-Script RT-PCR System (Invitrogen), following the manufacturer's instruction. After reverse transcription, real-time quantitative polymerase chain reaction (RT-PCR) was performed with the SYBR Green Real Time PCR master mix kit (Applied Biosystems, Carlsbad, CA, USA). The reaction was visualized with

SYBR Green Analysis (Applied Biosystem) software on a StepOne thermocycler (Applied Biosystem). Primers for VEGF-165 and GAPDH gene analysis were as previously described (Sorriento *et al.*, 2009).

Statistical analysis

Data are presented as mean ± SEM. Each experiment was performed from three to five times. *P* values were calculated by Student's *t*-test or two-way ANOVA as appropriate. For distribution statistics, the chi-squared test was performed.

The nomenclature conforms to the British Journal of Pharmacology's 'Guide to Receptors and Channels' (Alexander *et al.*, 2009).

Results

In vivo post-isaemic angiogenesis

Blood perfusion evaluation. As shown in Figure 1A, compared to β₂AR proficient controls, hindlimbs from β₂AR^{-/-} mice present a significantly lower βAR membrane-density. Intra-

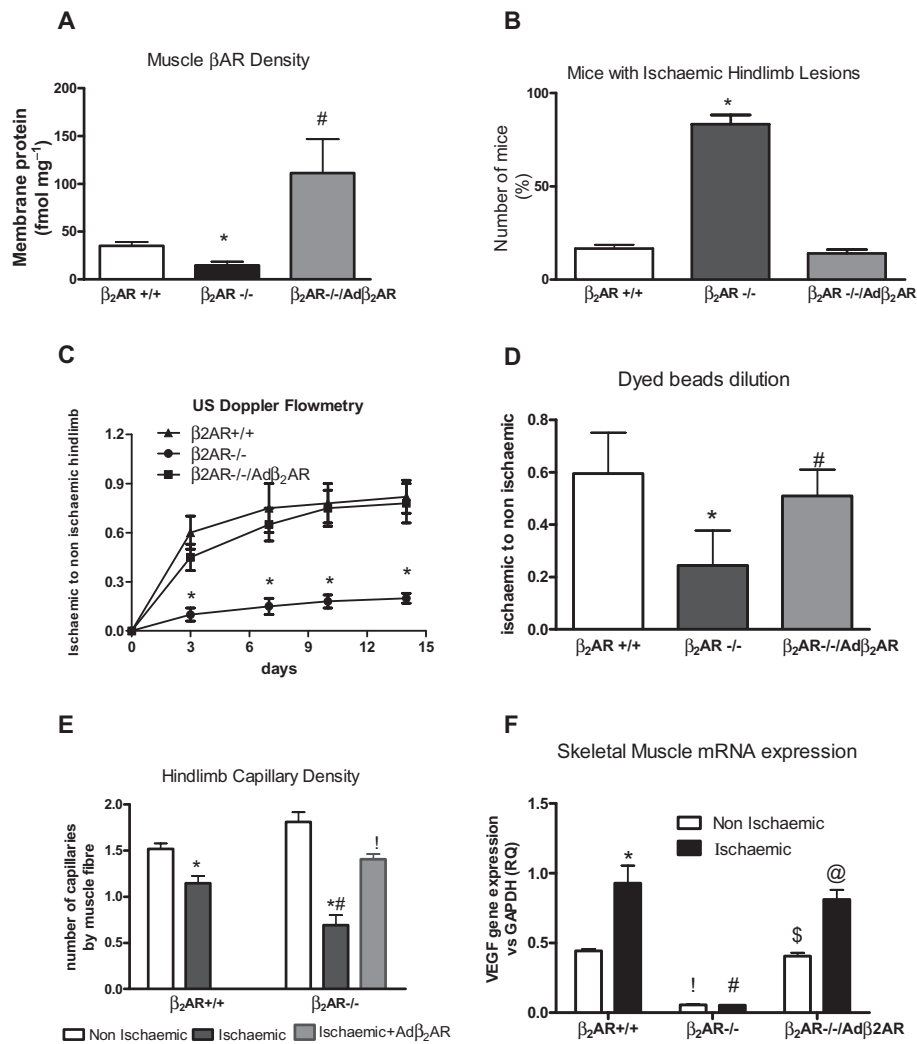


Figure 1

β₂AR knock-out exacerbated the symptoms of ischaemia and impaired perfusion and angiogenesis in ischaemic hindlimbs of mice. (A) Effects of adenoviral-mediated gene transfer on βAR levels (**P* < 0.05 β₂AR^{-/-} vs. β₂AR^{+/+}; # *P* < 0.05, β₂AR^{-/-}/Adβ₂AR vs. β₂AR^{-/-}, *n* = 3 to 5). (B) Ischaemia-induced skin lesions in β₂AR^{-/-} and β₂AR^{+/+} hindlimbs (HLs) (**P* < 0.05 β₂AR^{-/-} vs. β₂AR^{+/+}, χ²test, *n* = 10 per group). (C) HL blood flow over 14 days in β₂AR^{+/+}, β₂AR^{-/-}, and Adβ₂AR-treated β₂AR^{-/-} ischaemic HL, as measured by US Doppler. ADβ₂AR ameliorated blood perfusion in the ischaemic HL (**P* < 0.05 β₂AR^{-/-} vs. β₂AR^{+/+}; # *P* < 0.05, ADβ₂AR vs. β₂AR^{-/-}; *n* = 10 per group). (D) Blood perfusion in the ischaemic HL as evaluated by dyed beads dilution method (**P* < 0.05 β₂AR^{-/-} vs. β₂AR^{+/+}; # *P* < 0.05, β₂AR^{-/-}/Adβ₂AR vs. β₂AR^{-/-}; *n* = 10 per group). (E) HL muscle capillary density. (**P* < 0.05 ischaemic vs. non-ischaemic muscle; # *P* < 0.05 β₂AR^{-/-} vs. β₂AR^{+/+}; ! *P* < 0.05, β₂AR^{-/-}/Adβ₂AR vs. β₂AR^{-/-}; *n* = 5 per each group). (F) VEGF gene expression in ischaemic gastrocnemius muscle 3 days after femoral artery ligation and resection (**P* < 0.05 vs. non-ischaemic, *n* = 3; ! *P* < 0.01 vs. non-ischaemic β₂AR^{+/+}; # *P* < 0.01 vs. ischaemic β₂AR^{+/+}; *n* = 3; \$ *P* < 0.01 vs. non-ischaemic β₂AR^{-/-}; @ *P* < 0.01 vs. ischaemic β₂AR^{-/-} alone; *n* = 3).

vascular delivery of adenovirus leads to the infections mostly of vascular cells, including endothelium and VSMC, and perivascular fibroblasts and skeletal myocytes as shown by LacZ staining (Figure S1A and B). Administration by this route of Ad β_2 AR in β_2 AR $^{-/-}$ mice restores β AR density in the hindlimb (Figure 1A). Gross morphology and functional analysis of mice following chronic ischaemia indicate a higher occurrence of necrosis, autoamputation and limping in β_2 AR $^{-/-}$ mice as compared to β_2 AR $^{+/+}$ controls (Figure 1B). β_2 AR restoration by Ad β_2 AR was also able to prevent this symptom (Figure 1B). US evaluation of hindlimb perfusion (blood flow, BF) immediately after femoral artery removal shows an absence of flow in ischaemic HL in all groups of mice (data not shown). Over two weeks, BF was partially restored in β_2 AR $^{+/+}$ while no improvement was observed in β_2 AR $^{-/-}$ mice (Figure 1C). A similar result was obtained with the dyed beads perfusion analysis (Figure 1D). As assessed by both techniques, the Ad β_2 AR restores blood perfusion through the ischaemic hindlimb (Figure 1C and D). In line with these results, chronic ischaemia appeared to induce a capillary rarefaction that was higher in the β_2 AR $^{-/-}$ compared to the β_2 AR $^{+/+}$ mice, and Ad β_2 AR reversed this effect in the β_2 AR $^{-/-}$ (Figure 1E). β_1 AR mRNA levels were not affected by the β_2 AR removal, nor by Ad β_2 AR gene therapy (Figure S1C). We thus evaluated the production of reactive VEGF in the ischaemic hindlimb. Consistent with the perfusion data, VEGF gene expression was upregulated in the ischaemic hindlimbs of β_2 AR $^{+/+}$ mice, while it was blunted in the

β_2 AR $^{-/-}$ mice both before and after ischaemia (Figure 1F). In the latter, Ad β_2 AR gene therapy restored the VEGF level in basal conditions as well during chronic ischaemia (Figure 1F).

Evaluation of angiogenic phenotypes *in vitro*

Matrigel assay and VEGF production in primary cultures of ECs. In order to study angiogenesis *in vitro*, we tested the ability of mouse EC primary cultures to organize into a network when plated on a matrigel substrate. β_2 AR gene deletion inhibited the ability of ECs to form into vascular tubes compared to wild-type cells (Figure 2A). To verify the relevance of NF κ B to the pro-angiogenic phenotype of EC, we transfected β_2 AR $^{+/+}$ cells with the NF κ B inhibitor I κ B, 48 h before plating cells on matrigel. As expected, I κ B blocked the tubular formation of β_2 AR $^{+/+}$ endothelial cells on matrigel (Figure 2B). We further investigated the pro-angiogenic phenotype of β_2 AR $^{-/-}$ ECs by evaluating VEGF production in basal conditions and after isoprenaline treatment. As shown in Figures 2C and 6 h of stimulation with Iso increased VEGF levels in β_2 AR $^{+/+}$ but not in β_2 AR $^{-/-}$ EC. A similar result was obtained when VEGF mRNA levels were determined by RT-PCR in the same conditions (Figure 2D).

β_2 AR effects on NF κ B signalling. To investigate the ability of β_2 ARs to modulate VEGF production and angiogenesis, we tested the possibility that β_2 AR may regulate the activity of the NF κ B transcription factor. Indeed, in β_2 AR $^{+/+}$ EC, β AR

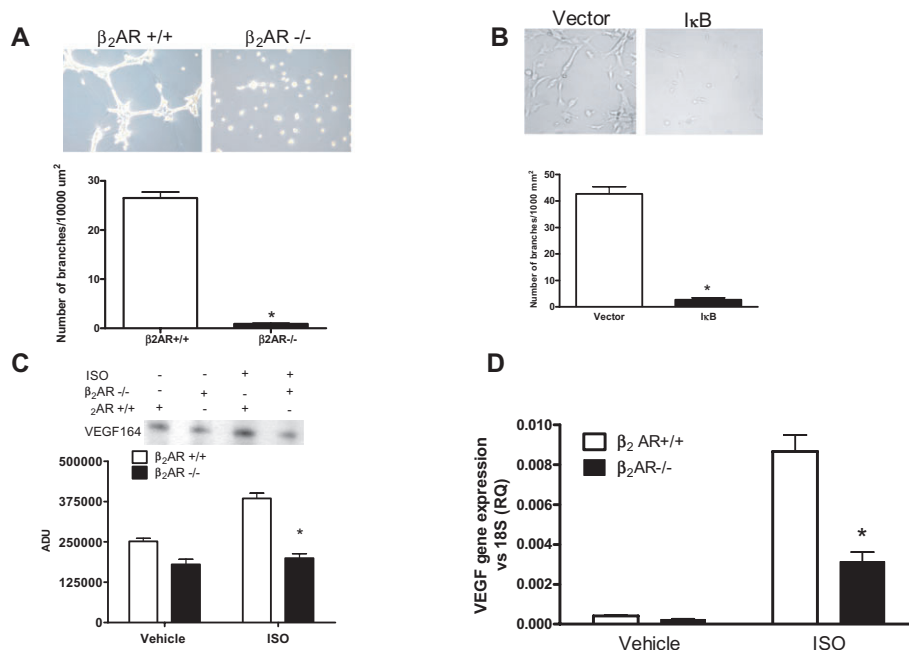


Figure 2

β_2 AR gene deletion inhibits VEGF production and vascular tube formation *in vitro*. (A) Vascular tube formation of endothelial cells (ECs) was assessed on matrigel. β_2 AR $^{-/-}$ and β_2 AR $^{+/+}$ control ECs (2×10^5) were incubated at 37°C for 12 h in 1 mL DMEM. Representative fields were taken, and the average of the total number of complete tubes was counted in 15 random fields by two independent investigators (* $P < 0.05$ vs. β_2 AR $^{+/+}$ EC, 3 experiments). (B) Vascular tube formation of β_2 AR $^{+/+}$ ECs (2×10^5) transfected with an empty Vector or a plasmid encoding for I κ B was assessed on matrigel. Cells were treated as above. (* $P < 0.05$ vs. Vector, 3 experiments). (C) VEGF production in ECs measured by Western blot of extracellular medium. (* $P < 0.05$ vs. β_2 AR $^{+/+}$; $n = 3$ per group). (D) VEGF mRNA in ECs measured by RT-PCR. (* $P < 0.05$ vs. β_2 AR $^{+/+}$; $n = 3$ per group).

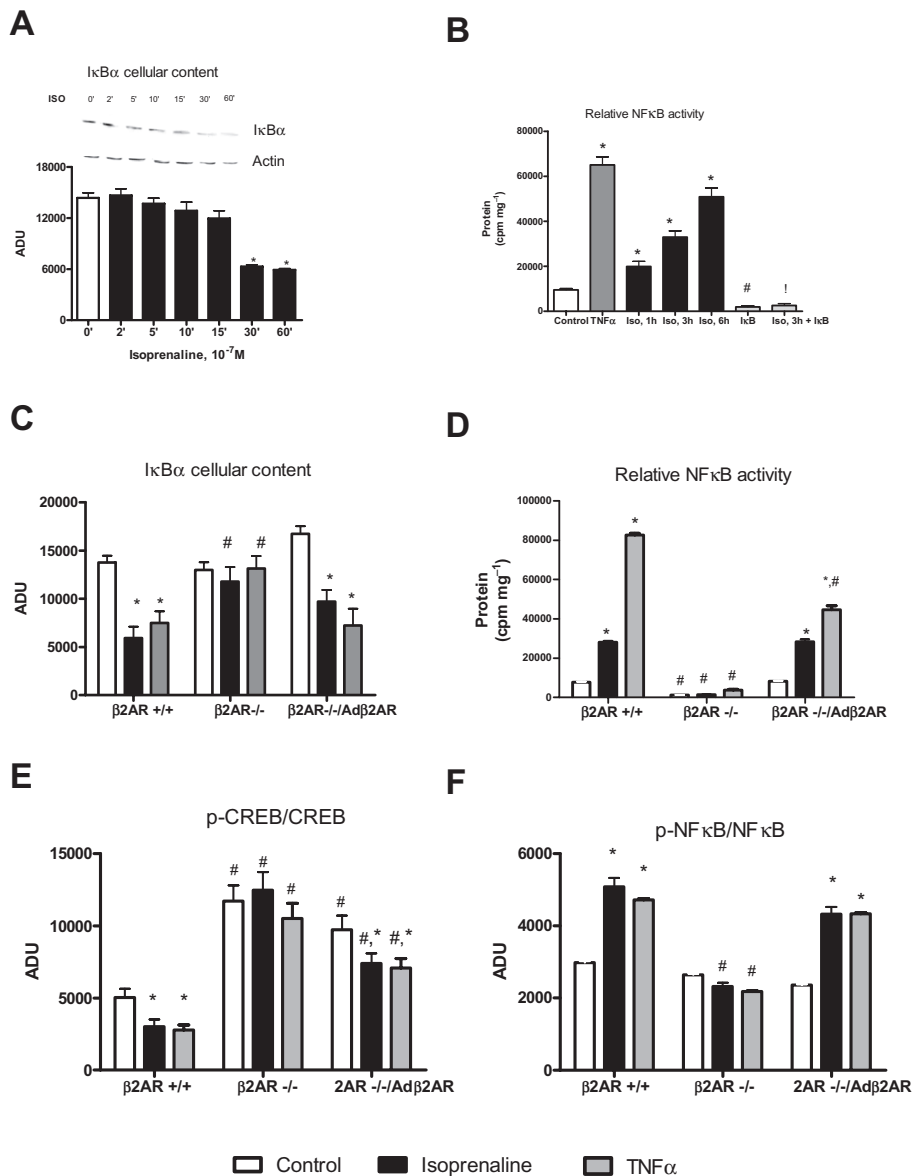


Figure 3

Effects of β₂AR gene deletion on NFκB signalling. (A) IκBα levels visualized by Western blot in β₂AR^{+/+} ECs. Isoprenaline (Iso, 10⁻⁷ M) was kept in the tissue culture medium for the time indicated. Densitometry units (ADU) (results normalized to actin response) are depicted in graphs. (* *P* < 0.05 vs. control, *n* = 3). (B) Effects of TNFα (20 ng·mL⁻¹) for 6 h or Iso (10⁻⁷ M) for 1, 3 and 6 h on NFκB transcriptional activity in β₂AR^{+/+} EC and in β₂AR^{+/+} EC transfected with the IκB plasmid (* *P* < 0.05 vs. control, # *P* < 0.05 vs. control; ! *P* < 0.05 Iso + IκB vs. IκB; *n* = 3 to 5). (C) IκBα levels assessed by Western blot in β₂AR^{-/-} and β₂AR^{+/+} ECs stimulated with Iso (10⁻⁷ M, 1 h) or TNFα (20 ng·mL⁻¹, 1 h) (* *P* < 0.05 vs. control; # *P* < 0.05 vs. β₂AR^{+/+}; *n* = 3 to 5). (D) NFκB activity in EC induced by Iso (10⁻⁷ M) and TNFα (20 ng·mL⁻¹) (* *P* < 0.05 vs. control; # *P* < 0.05 vs. β₂AR^{+/+}; *n* = 3 to 5). (E) ECs were stimulated with Iso (10⁻⁷ M) and TNFα (20 ng·mL⁻¹). CREB phosphorylation was visualized by Western blot, digitalized and corrected for endogenous CREB. (* *P* < 0.05 vs. control; # *P* < 0.05 vs. β₂AR^{+/+}, *n* = 3). (F) EC were stimulated as in (E), and NFκB phosphorylation was visualized by WB, digitalized and corrected for total NFκB. (* *P* < 0.05 vs. control; # *P* < 0.05 vs. β₂AR^{+/+}, *n* = 3).

stimulation with Iso induced a time-dependent degradation of the endogenous NFκB inhibitor, IκBα (Figure 3A). Consistent with this result, the luciferase assays demonstrated a time-dependent increase in NFκB transcriptional activity after Iso stimulation (Figure 3B). As expected, TNFα also increased NFκB transcriptional activity in β₂AR^{+/+} EC, and the overexpression of IκB inhibited the Iso-induced increase in NFκB activity (Figure 3B).

In ECs, β₂AR gene deletion inhibits Iso-induced IκBα downregulation (Figure 3C), confirming that β₂AR may regulate NFκB activation in response to Iso. Surprisingly, β₂AR gene deletion also inhibited TNFα-induced IκBα downregulation (Figure 3C). Accordingly, restoration of β₂ARs by means of Adβ₂AR infection corrected both Iso and TNFα-mediated IκBα degradation to levels comparable to the ones observed in β₂AR^{+/+} EC (Figure 3C), confirming the importance of

β_2 ARs in NF κ B endothelial signalling. In accord with this, in β_2 AR $^{-/-}$ EC, both Iso and TNF α -induced NF κ B-activity were blocked, and Ad β_2 AR restored the responses to both agonists (Figure 3D). These data suggest that β_2 AR knock-out may have a general impact on cytokine transcription.

Recently, CREB, another β_2 AR-controlled transcription factor, has been shown to down-regulate the activity of NF κ B (Ye, 2001). Indeed, CREB binding protein (CBP) and the related cofactor p300 are co-activators able to regulate the activity of transcription factors, and CREB and NF κ B have been shown to compete for limiting amounts of CBP/p300 (Ye, 2001). In fact, the recruitment of these co-activators by CREB reduces their availability for NF κ B. Thus, we evaluated CREB and NF κ B activation by Western blot in β_2 AR $^{-/-}$ ECs stimulated with Iso or TNF α . β_2 AR gene deletion increased CREB phosphorylation both in basal conditions and after

stimulation with Iso or TNF α and the restoration of β_2 ARs by adenovirus-mediated gene transfer decreased p-CREB levels (Figure 3E). Reciprocal results were obtained with NF κ B. Indeed, compared to β_2 AR proficient controls, in β_2 AR $^{-/-}$ ECs, Iso and TNF α failed to induce NF κ B phosphorylation while Ad β_2 AR infection restored the responses to both agonists (Figure 3F).

Identification of signal transduction components. To determine whether CREB upregulation is a common mechanism of inhibition for β_2 AR and TNFR stimulation of NF κ B, we assessed pNF κ B after stimulation with Iso or TNF α in β_2 AR $^{+/+}$ EC transfected with CREB or I κ B. Indeed, both substances resulted in the inhibition of NF κ B activation to both agonists (Figure 4A). Given the ability of the β_2 AR to couple to both Gs and Gi, we tested the possibility that Gi is indeed involved in

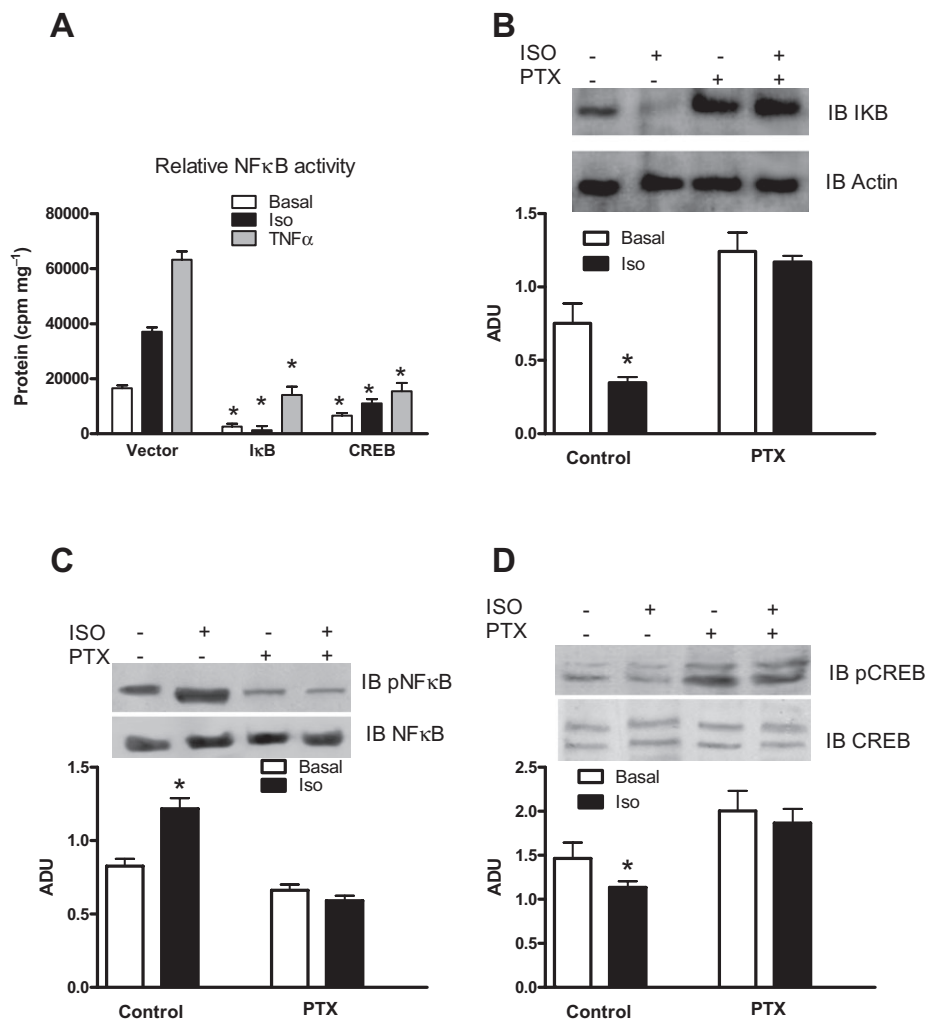


Figure 4

Molecular mechanisms involved in β_2 AR activation of NF κ B. (A) Effects of transgenic expression of I κ B and CREB in β_2 AR $^{+/+}$ EC on NF κ B activation in response to Iso (10^{-7} M, 3 h) and TNF α (20 ng \cdot mL $^{-1}$). * P < 0.05 vs. Vector, n = 3. (B) Evaluation by Western blot of β_2 AR $^{+/+}$ EC of the effects of pertussis toxin (PTX, 10^{-4} M) on Iso-induced I κ B downregulation. * P < 0.05 vs. basal, n = 4; ADU: arbitrary densitometric units. (C) Evaluation by Western blot of β_2 AR $^{+/+}$ EC of the effects of pertussis toxin (PTX, 10^{-4} M) on Iso-induced NF κ B phosphorylation. * P < 0.05 vs. basal, n = 4. (D) Evaluation by Western blot of β_2 AR $^{+/+}$ EC of the effects of pertussis toxin (PTX, 10^{-4} M) on Iso-induced CREB dephosphorylation. * P < 0.05 vs. basal, n = 4.

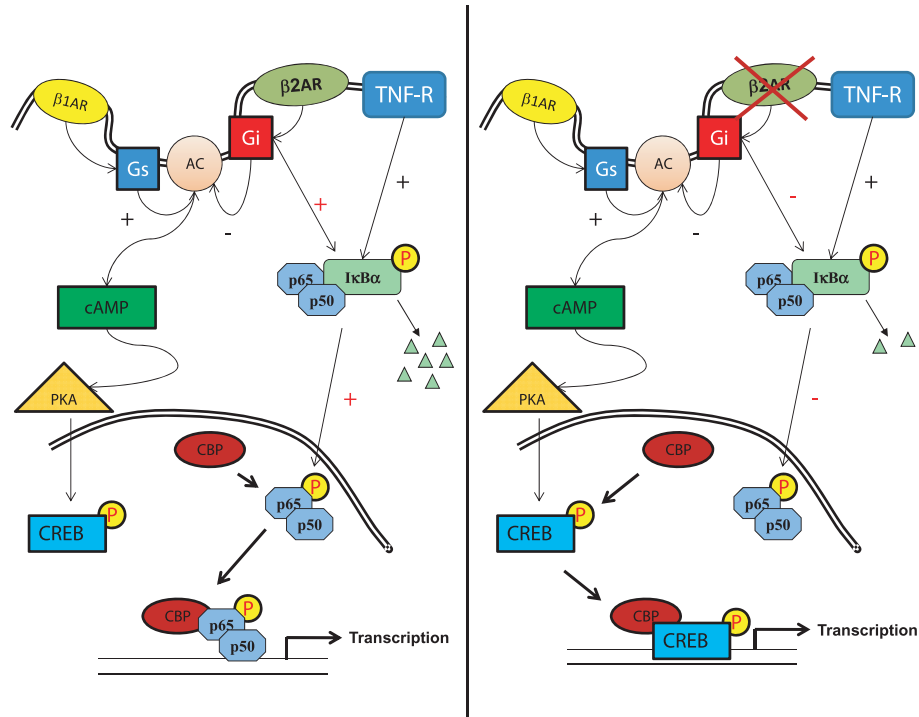


Figure 5

In the wild-type cell (left), the presence of the β₂AR causes a tonic stimulation that fosters the activation of NFκB, which, by translocating to the nucleus upon activation, competes for CBP with CREB. Furthermore, the β₂AR exerts a tonic inhibition on cAMP production, by coupling to Gi. Once the receptor is removed (right), the inhibitory effect on cAMP is released, unbalancing the nuclear transcription towards CREB, which binds more CBP, thus making NFκB binding to the same cofactor unlikely to occur. pP65/p50: NFκB; TNFR: TNFα receptor.

maintaining low levels of CREB within the cell. To test this hypothesis, we treated cells with the Gi inhibitor *Pertussis* toxin for 18 h and then stimulated β₂AR^{+/+} ECs with Iso. Gi inhibition was accompanied by the inhibition of Iso-induced IκB downregulation (Figure 4B) and NFκB phosphorylation (Figure 4C). Furthermore, PTX increased the basal level of pCREB and prevented Iso-induced dephosphorylation of CREB (Figure 4D).

Finally, we have presented these new findings in a cartoon as shown in Figure 5.

Discussion

The results of our study provide compelling evidence that the removal of the β₂AR impairs angiogenesis both *in vitro* and *in vivo*. This finding extends previous knowledge regarding the ability of β₂AR overexpression to enhance angiogenesis *in vivo*, and it further supports the knowledge of the ability of β₂AR to induce VEGF and cytokine production. Indeed, our work adds novel findings concerning the signalling that connects β₂ARs and the nuclear transcriptional activity of NFκB.

Evidence has been obtained suggesting that the adrenergic system is activated within ischaemic regions (Newton *et al.*, 1997) but the physiological relevance of this response is unclear. A teleological explanation would suggest that this activation is needed to better adapt to the ischaemic stress.

Indeed, the regenerative properties of catecholamines have been implicated by the observation that catecholamine-deficient mice undergo inappropriate embryo development (Zhou *et al.*, 1995). During postnatal life, catecholamines participate in cardiac and vascular remodelling and in tissue regeneration in response to various stresses (Iaccarino *et al.*, 2001a; Ciccarelli *et al.*, 2008). Adrenoceptors are the effectors of catecholamines, but their role appears to be redundant, since correct embryo development occurs in all of the AR knock-out models, and in adult life, mice with deletion of AR genes do not present basal phenotypic alterations. Under stress conditions, though, or in the presence of catecholamine challenge, a perturbation in the phenotype of KO mice has been noted (Rohrer *et al.*, 1999). In particular, previous studies in β₂AR^{-/-} mice have shown that β₂ARs are mostly involved in vascular and metabolic mechanisms (Chruscinski *et al.*, 1999; Rohrer *et al.*, 1999). Our study extends this notion and is the first to illustrate the requirement for endogenous β₂ARs in neoangiogenesis following chronic ischaemia, by providing the following evidence: (i) β₂AR^{-/-} mice present impaired tolerance to chronic ischaemia; (ii) this phenotype is rescued by the local restoration of β₂AR membrane-density, induced by adenoviral-mediated gene transfer; (iii) a functional relationship appears to exist between the β₂AR and NFκB, the transcription factor involved in ischaemia-induced cytokine production.

These results accord with our recent observation that overexpression of the β₂AR enhances the adaptive pro-

angiogenic response to ischaemia (Iaccarino *et al.*, 2005). Importantly, the present results add to the hypothesis that other endogenously expressed β AR subtypes cannot undertake this role of β_2 ARs in ischaemic neo-angiogenesis. Intimate differences in the signalling capabilities of this receptor make it unique, and probably this is the reason for our findings. Removal of this receptor alters the intracellular signal transduction pathways to such an extent that the transcriptional status of the cell is modified. Our *in vitro* study revealed that angiogenesis is impaired in β_2 AR $^{-/-}$ EC, probably due to the impaired production of cytokines such as VEGF. The main transcription factors modulating VEGF expression are hypoxia-inducible factor-1 α (HIF-1 α) (Marti *et al.*, 2000) and NF κ B (Kiriakidis *et al.*, 2003). HIF-1 α activates the transcription of target genes in response to hypoxia and is inactive in basal conditions due to ubiquitination and degradation. NF κ B, in contrast, can be activated following stimulation of different receptors. The ability of GPCRs to activate this transcription factor has been established in different cell types, mainly in the immune system. With regard to the β ARs, the evidence showing that β AR agonists are able to induce NF κ B activation is controversial. In monocytes, Farmer and Pugin (2000) showed that a number of β AR agonists had inhibitory effects on LPS-induced TNF α and IL-8 production, and proposed that cAMP through PKA is the mediator of such inhibition (Farmer and Pugin, 2000). In contrast, Chandrasekar *et al.* (2004) showed that in cardiac-derived ECs, Iso induces NF κ B promoter activity in a β_2 AR-dependent manner. These authors concluded that β_2 ARs induce NF κ B activation in a cAMP-independent manner, through the activation of Gi, Pi3K, Akt and IKK with I κ B α degradation. Our results accord with the latter findings, since in β_2 AR $^{+/+}$ EC, Iso induced I κ B α degradation and enhanced NF κ B transcriptional activity in a time-dependent manner. Furthermore, our data indicate that the physical presence of β_2 ARs is needed to activate NF κ B; indeed, β_2 AR gene deletion inhibited NF κ B activity in response to both GPCRs and TNF-Rs. G α s and G α i signalling pathways have opposite effects on NF κ B: Gs-dependent signalling, induces PKA-dependent CREB activation and consequently inhibition of NF κ B activity (Ye, 2001). In contrast, Gi activates NF κ B by inhibiting/removing I κ B. Our hypothesis is that the lack of β_2 ARs that have the ability to couple to Gi tilts the balance towards Gs-dependent signalling, which would lead to PKA-induced CREB activation and CBP/p300 recruitment, making the latter unavailable for NF κ B activation (Figure 5). Indeed, validation of such a hypothesis derives from our studies with the pertussis toxin, showing the relevance of Gi for β_2 AR-induced activation of NF κ B. Irrespective of this result, the observation that regardless of its mechanism of action β_2 AR influenced not only isoprenaline, but also TNF α -dependent activation of NF κ B is strongly suggestive of a pivotal role played by β_2 ARs in the instruction of signals required for the fine-tuning of NF κ B transcriptional activity. We have performed our experiments in the endothelial cells, but it is most likely that the β_2 AR can regulate NF κ B activity also in other cell types. In particular it would be interesting to evaluate the skeletal muscle, which expresses a large number of β_2 ARs and is also an important source of VEGF.

In conclusion, our data indicate that the β_2 AR is important in mediating production of key pro-angiogenic cytok-

ines, such as VEGF. The impairment of the signal transduction of this receptor results in impairment of angiogenesis in response to chronic ischaemia. Our data add a novel piece to the puzzling paradigm of those pathophysiological conditions that are characterized by increased adrenergic neural drive, impaired β adrenoceptor signalling and impaired organ function such as myocardial ischaemia. Under these conditions, the reduction of β_2 ARs signalling is detrimental not only for the cardiac function but also for the development of an adequate compensatory neoangiogenesis, which would worsen the blood supply to the ischaemic heart and accelerate the progression of myocardial dysfunction. The use of therapeutic strategies aimed at improving β AR signalling, may therefore achieve double efficacy, by ameliorating myocardial function and by hastening compensatory angiogenesis.

Acknowledgements

Fundings to GI from Italian Ministry of Research, PRIN 20074MSWYW.

Conflict of interest

The authors declare that they have no competing financial interests.

References

- Alexander SPH, Mathie A, Peters JA (2009). Guide to Receptors and Channels (GRAC), 4th Edition. *Br J Pharmacol* 158 (Suppl. 1): S1–254.
- Chandrasekar B, Marelli-Berg FM, Tone M, Bysani S, Prabhu SD, Murray DR (2004). Beta-adrenergic stimulation induces interleukin-18 expression via beta2-AR, PI3K, Akt, IKK, and NF-kappaB. *Biochem Biophys Res Commun* 319: 304–311.
- Chruscinski AJ, Rohrer DK, Schauble E, Desai KH, Bernstein D, Kobilka BK (1999). Targeted disruption of the beta2 adrenergic receptor gene. *J Biol Chem* 274: 16694–16700.
- Ciccarelli M, Cipolletta E, Santulli G, Campanile A, Pumiglia K, Cervero P *et al.* (2007). Endothelial beta2 adrenergic signaling to AKT: role of Gi and SRC. *Cell Signal* 19: 1949–1955.
- Ciccarelli M, Santulli G, Campanile A, Galasso G, Cervero P, Altobelli GG *et al.* (2008). Endothelial alpha1-adrenoceptors regulate neo-angiogenesis. *Br J Pharmacol* 153: 936–946.
- Farmer P, Pugin J (2000). Beta-adrenergic agonists exert their 'anti-inflammatory' effects in monocytic cells through the IkappaB/NF-kappaB pathway. *Am J Physiol Lung Cell Mol Physiol* 279: L675–L682.
- Ferro A, Queen LR, Priest RM, Xu B, Ritter JM, Poston L *et al.* (1999). Activation of nitric oxide synthase by beta 2-adrenoceptors in human umbilical vein endothelium in vitro. *Br J Pharmacol* 126: 1872–1880.
- Iaccarino G, Tomhave ED, Lefkowitz RJ, Koch WJ (1998). Reciprocal in vivo regulation of myocardial G protein-coupled receptor kinase expression by beta-adrenergic receptor stimulation and blockade. *Circulation* 98: 1783–1789.

- Iaccarino G, Barbato E, Cipoletta E, Fiorillo A, Trimarco B (2001a). Role of the sympathetic nervous system in cardiac remodeling in hypertension. *Clin Exp Hypertens* 23: 35–43.
- Iaccarino G, Barbato E, Cipoletta E, Esposito A, Fiorillo A, Koch WJ *et al.* (2001b). Cardiac betaARK1 upregulation induced by chronic salt deprivation in rats. *Hypertension* 38: 255–260.
- Iaccarino G, Cipoletta E, Fiorillo A, Anneschiarico M, Ciccarelli M, Cimini V *et al.* (2002). Beta(2)-adrenergic receptor gene delivery to the endothelium corrects impaired adrenergic vasorelaxation in hypertension. *Circulation* 106: 349–355.
- Iaccarino G, Ciccarelli M, Sorriento D, Cipoletta E, Cerullo V, Iovino GL *et al.* (2004). AKT participates in endothelial dysfunction in hypertension. *Circulation* 109: 2587–2593.
- Iaccarino G, Ciccarelli M, Sorriento D, Galasso G, Campanile A, Santulli G *et al.* (2005). Ischemic neoangiogenesis enhanced by beta2-adrenergic receptor overexpression: a novel role for the endothelial adrenergic system. *Circ Res* 97: 1182–1189.
- Kiriakidis S, Andreakos E, Monaco C, Foxwell B, Feldmann M, Paleolog E (2003). VEGF expression in human macrophages is NF-kappaB-dependent: studies using adenoviruses expressing the endogenous NF-kappaB inhibitor IkappaBalpha and a kinase-defective form of the IkappaB kinase 2. *J Cell Sci* 116: 665–674.
- Lembo G, Iaccarino G, Vecchione C, Barbato E, Izzo R, Fontana D *et al.* (1997). Insulin modulation of an endothelial nitric oxide component present in the alpha2- and beta-adrenergic responses in human forearm. *J Clin Invest* 100: 2007–2014.
- Marti HJ, Bernaudin M, Bellail A, Schoch H, Euler M, Petit E *et al.* (2000). Hypoxia-induced vascular endothelial growth factor expression precedes neovascularization after cerebral ischemia. *Am J Pathol* 156: 965–976.
- Newton GE, Adelman AG, Lima VC, Seidelin PH, Schampaert E, Parker JD (1997). Cardiac sympathetic activity in response to acute myocardial ischemia. *Am J Physiol* 272: H2079–2084.
- Rohrer DK, Chruscinski A, Schauble EH, Bernstein D, Kobilka BK (1999). Cardiovascular and metabolic alterations in mice lacking both beta1- and beta2-adrenergic receptors. *J Biol Chem* 274: 16701–16708.
- Santulli G, Ciccarelli M, Palumbo G, Campanile A, Galasso G, Ziaco B *et al.* (2009a). In vivo properties of the proangiogenic peptide QK. *J Transl Med* 7: 41.
- Santulli G, Cipoletta E, Campanile A, Maione S, Trimarco V, Marino M *et al.* (2009b). Deletion of the CaMK4 Gene in Mice Determines a Hypertensive Phenotype. *Circulation* 120: S613–S613.
- Shenoy SK, Drake MT, Nelson CD, Houtz DA, Xiao K, Madabushi S *et al.* (2006). beta-arrestin-dependent, G protein-independent ERK1/2 activation by the beta2 adrenergic receptor. *J Biol Chem* 281: 1261–1273.
- Sorriento D, Campanile A, Santulli G, Leggiero E, Pastore L, Trimarco B *et al.* (2009). A new synthetic protein, TAT-RH, inhibits tumor growth through the regulation of NFkappaB activity. *Mol Cancer* 8: 97.
- Sorriento D, Santulli G, Fusco A, Anastasio A, Trimarco B, Iaccarino G (2010). Intracardiac injection of AdGRK5-NT reduces left ventricular hypertrophy by inhibiting NF-[kappa]B-Dependent hypertrophic gene expression. *Hypertension* 56: 696–704.
- Ye RD (2001). Regulation of nuclear factor kappaB activation by G-protein-coupled receptors. *J Leukoc Biol* 70: 839–848.
- Zhou QY, Quaife CJ, Palmiter RD (1995). Targeted disruption of the tyrosine hydroxylase gene reveals that catecholamines are required for mouse fetal development. *Nature* 374: 640–643.
- Zhou RH, Lee TS, Tsou TC, Rannou F, Li YS, Chien S *et al.* (2003). Stent implantation activates Akt in the vessel wall: role of mechanical stretch in vascular smooth muscle cells. *Arterioscler Thromb Vasc Biol* 23: 2015–2020.

Supporting information

Additional Supporting Information may be found in the online version of this article:

Figure S1 Efficient gene delivery via femoral artery catheterization (A-B). Recombinant LacZ Adenovirus was delivered to the ischemic hindlimb via catheterization as described in the Methods section and results in gene transduction of capillaries (A) as well as perivascular muscle fibers (B). Muscle β 1AR mRNA levels measured by RT-PCR (C). Hindlimb muscles processed as described in methods showing unmodified β 1AR mRNA levels among β 2AR +/+, β 2AR -/- and Ad β 2AR treated mice.

Please note: Wiley-Blackwell are not responsible for the content or functionality of any supporting materials supplied by the authors. Any queries (other than missing material) should be directed to the corresponding author for the article.

Cardiac resynchronisation therapy response predicts occurrence of atrial fibrillation in non-ischaemic dilated cardiomyopathy

S. L. D'Ascia,¹ C. D'Ascia,¹ V. Marino,¹ A. Lombardi,² R. Santulli,³ M. Chiariello,^{1,*} G. Santulli^{1,4}

SUMMARY

Aim: The aim of this study was to determine whether or not cardiac resynchronization therapy (CRT) has a favourable effect on the incidence of new-onset atrial fibrillation (AF) in a homogeneous population of patients with non-ischaemic idiopathic-dilated cardiomyopathy and severe heart failure. **Methods:** We designed a single-centre prospective study and enrolled 58 patients AF naïve when received CRT. After 1 year of follow-up our population was subdivided into responders (72.4%) and non-responders (27.6%), so as to compare the incidence of AF after 1, 2 and 3 years of follow-up in these two groups. **Results:** Already after 1 year, there was a significant ($p < 0.05$) difference in new-onset AF in non-responder patients with respect to responders (18.2% vs. 3.3%). These data were confirmed at 2 years (33.3% vs. 12.2%) and 3 years (50.0% vs. 15.0%) follow-up. In particular, 3 years after device implantation non-responders had an increased risk to develop new-onset AF (OR = 5.67). **Conclusions:** This is the first study analysing long-term effects of CRT in a homogeneous population of patients with non-ischaemic dilated cardiomyopathy, indicating the favourable role of this non-pharmacological therapy on the prevention of AF.

Introduction

Cardiac resynchronisation therapy (CRT) has emerged as a highly effective treatment for patients with advanced heart failure (HF) and ventricular conduction delay (1). Several studies have showed the haemodynamic and functional improvement obtained with biventricular pacing, with a subsequent reduction of hospitalisations and a decrease in mortality (2). Nevertheless, despite the positive effects of CRT on haemodynamic, functional status and mortality in HF, approximately 30% of patients do not respond to this therapy, emphasising the need for better selection criteria (1,2). Furthermore, the primary cardiac cause of exacerbation of HF is atrial fibrillation (AF) that is also an independent risk factor for sudden death. HF and AF often coexist; both are responsible for increased mortality, more frequent hospitalisations, reduced exercise capacity and decreased quality-of-life (QoL). Besides, AF and HF are believed to directly predispose to each other (3). In particular, in the setting of advanced HF, 30–40% of patients will develop AF during the course of the disease. So, if CRT influences the

occurrence of AF, this might influence patient selection and possibly programming of the device.

On these grounds, the aims of the present study were: to identify preimplantation characteristics that best can predict which patients will benefit the most from biventricular pacing, in order to make out suitable candidates for CRT (4); to compare the incidence of new-onset AF after 1, 2 and 3 years of follow-up in responder and non-responder patients, so as to assess a possible favourable role of CRT, through means of an atrial reverse remodelling, on the prevention of this arrhythmia.

Methods

Study population

This is a single-centre prospective study that included all the consecutive CRT implants from July 2004 until June 2007 performed at our institution on patients with non-ischaemic idiopathic-dilated cardiomyopathy (coronary angiography failed to reveal stenosis $> 30\%$), following the previously described eligibility criteria for CRT (5). All patients had New York Heart Association (NYHA) functional class III

What's known

Albeit several studies examined the association between cardiac resynchronization therapy and atrial fibrillation in heart failure, results are still unclear and quite conflicting.

What's new

In this study we show that in patients with non-ischaemic dilated cardiomyopathy a positive response to cardiac resynchronization therapy has a favorable role on the prevention of new-onset atrial fibrillation.

¹Division of Cardiology, Department of Clinical Medicine, Cardiovascular and Immunologic Sciences, "Federico II" University, Naples, Italy

²Faculty of Mathematical, Physical and Natural Sciences, University of Salento, Lecce, Italy

³Department of Mathematics, University of Salerno, Fisciano (SA), Italy

⁴College of Physicians and Surgeons, Columbia University Medical Center, New York, NY, USA

Correspondence to:

Dr Gaetano Santulli,
 Division of Cardiology,
 Department of Clinical
 Medicine, Cardiovascular and
 Immunologic Sciences,
 "Federico II" University, Naples,
 Italy
 Tel/Fax: +39 081 746 3075
 Email: gaetano.santulli@unina.it

Disclosures

None.

*Since this paper was submitted this author has died.

or IV symptoms for at least 6 months before enrolment, despite optimal pharmacological treatment (including β blockers, loop diuretics, vasodilators, nitrate, digitalis, angiotensin-converting enzyme inhibitors, angiotensin receptor blockers and spironolactone when tolerated; no antiarrhythmic drugs for VT were administered to the patients), left ventricular ejection fraction (LVEF) $\leq 35\%$ and QRS duration > 120 ms measured on at least three leads on the surface ECG. Exclusion criteria were: recent (previous 3 months) acute coronary syndrome or planned coronary revascularization, previous pacemaker or implantable cardioverter defibrillator (ICD) implantation, requirement of continuous intravenous therapy, a life expectancy of < 1 year due to non-cardiac diseases, history of AF, patients whose major echocardiographic parameters could not be obtained because of poor image quality, systolic blood pressure > 170 or < 80 , heart rate > 140 and kidney failure with serum creatinine levels > 250 $\mu\text{mol/l}$ (5). Detailed clinical and instrumental data (ECG, echocardiogram, QoL evaluation, 6-min walk test, cardiopulmonary exercise test) were collected, with scheduled visits, before implantation and at the 1-, 2- and 3-year follow-up. Patients were also given a diary in which the information of any medical contacts between their follow-up visits was to be recorded. The detection of AF relied on electrocardiography, 24 h Holter examination and strips from continuous telemetric control of implanted devices (every 3 to 6 months, when ICDs were systematically checked) (6). AF was defined as an episode, with or without symptoms, lasting at least 10 min (7,8), similar to a large sub-study of the CARE-HF trial reported by UC. Hoppe et al. (9). Patients were also assessed for HF symptoms (NYHA functional class). QoL was evaluated by the Minnesota Living with HF questionnaire (scores range from 0 to 105, with higher scores reflecting a poorer QoL) (10), while the 6-min walk test was carried out according to Bittner's recommendations (11). The 6-min walk distance and QoL tests were administered by study nurses who had no knowledge of the patients' treatment. Coronary angiography was performed prior to implantation in all patients, also to exclude causes of HF amenable to surgery or intervention. This study protocol was designed in compliance with the Helsinki declaration and approved by the local Ethics Committee. Written informed consent was obtained from each participant.

Non-responders were defined after 12 months of follow-up as patients with at least one of the following characteristics: deteriorating function (HF-related death, need for heart transplantation), increase in LVEF ≤ 4 absolute percentage points (12), worsening

in peak oxygen consumption, in QoL score or in the distance walked in 6 min, as previously described (13,14).

ICD implantation and optimisation

Patients were implanted with a biventricular ICD (Contak Renewal 1 or 2; Guidant Inc., part of Boston Scientific, Natick, MA, USA). All procedures were performed under local anaesthesia. Three transvenous leads were inserted, through the left subclavian vein. The atrial lead was placed in the high right atrium; the right ventricular lead was positioned, in the apex or in the high interventricular septum, as far as possible from the LV lead; LV pacing was obtained after coronary sinus (CS) angiography, advancing a bipolar lead into the lateral or posterolateral cardiac vein. The final lead position was chosen on the basis of visual inspection, assessed by anteroposterior and lateral chest radiography. The atrioventricular interval (electrical delay between atrial and ventricular excitation) was optimised by Doppler echocardiography 1 day after implantation to reach maximal transmitral diastolic filling and maximal biventricular capture and checked every year. Patients in whom transvenous LV lead implantation was acutely unsuccessful ($n = 5$), attributable to several causes [failure to cannulate the CS ($n = 2$), high threshold to chronic pacing ($n = 1$), CS dissection ($n = 1$) and impossibility to obtain a stable lead placement ($n = 1$)] were obviously excluded from the study.

Echocardiographic evaluation

A trans-thoracic, two-dimensional echocardiogram was serially performed in all patients using a Sonos 5500 ultrasound system (Philips, Amsterdam, Netherlands), equipped with a 2.5-MHz transducer. The examination included two-dimensional, M-mode and Doppler data. All recordings were made, as previously described, with the patient in the lateral recumbent position, according to the American Society of Echocardiography recommendations (4). The following parameters were measured using the different axis: LV end-diastolic and end-systolic diameters, LVEF (biplane LV end-systolic and end-diastolic volumes were calculated from apical views according to the modified Simpson's rule), LV end-systolic volume index, left atrial diastolic and systolic areas, amount of mitral regurgitation (calculated as the area of the colour-flow Doppler regurgitant jet divided by the area of the left atrium in systole, both in square centimetres). All echocardiographic studies were performed and analysed by the same study-independent physicians, blinded to the study protocol and to the patients' status. Echocardiographic

measurements were systematically averaged in five consecutive samples (15).

Cardiopulmonary exercise test

Symptom-limited cardiopulmonary exercise testing (Treadmills 'Rammill Series'; Morgan Italia, Bologna, Italy) was performed, conducted on an upright bicycle ergometer with a 10-W/min step protocol, starting with 2 min of unloaded cycling. Measurements of oxygen consumption (VO_2), were taken at rest and during exercise using a moving average of eight breaths. During each stage of exercise, data on heart rate and rhythm and BP were collected. All patients were encouraged to exercise until they felt unable to continue because of dyspnoea and/or fatigue. The ventilatory threshold was measured by the V-slope method (16). The maximum VO_2 was defined as the highest VO_2 value measured (peak VO_2).

Statistical analysis

Unless otherwise specified, data are presented as the mean value \pm SD or absolute numbers with percentages for categorical variables, unless otherwise specified. Data normality was evaluated through the Kolmogorov–Smirnov test. Comparison of quantitative variables was performed using the Student's *t*-test for paired and unpaired data when appropriate, with a Bonferroni correction when multiple comparisons were made (15). Dichotomous or categorical data were assessed with the χ^2 test or Fisher's exact test. The non-normally distributed data within patient groups were compared using the nonparametric Wilcoxon test. Odds ratios were given with the 95% confidence interval (CI). Differences in event rates (AF, death) over time were calculated according to the Kaplan–Meier method and analysed with the use of Cox proportional hazard models.

Table 1 Baseline characteristics of the patients included in the analysis, then (1-year follow-up) sub-divided in responders and non-responders

	All patients	Responders	Non-responders
No.	58	42	16
Age (years)	62.5 \pm 11.1	62.4 \pm 14.2	62.5 \pm 11.9
Male sex: No. (%)	37 (63.8)	27 (64.3)	10 (62.5)
Height (cm)	168.41 \pm 6.9	167.7 \pm 7.38	170.86 \pm 4.9
Weight (kg)	72.37 \pm 13.6	70.3 \pm 13.6	75.65 \pm 14.5
Body mass index	25.41 \pm 3.92	25.07 \pm 3.7	25.8 \pm 4.33
Body surface (m^2)	1.81 \pm 0.18	1.77 \pm 0.192	1.86 \pm 0.18
Heart rate (bpm)	70.89 \pm 5.9	71.5 \pm 5.51	72.23 \pm 7.8
QRS duration from surface ECG (ms)	170.8 \pm 6.1	167.3 \pm 20.6	171.2 \pm 8.5
Systolic blood pressure (mmHg)	122.7 \pm 15.5	122.8 \pm 15.9	125.0 \pm 17.4
Diastolic blood pressure (mmHg)	74.4 \pm 13.4	74.7 \pm 14.6	70.1 \pm 12.8
Diabetes (%)	31.0	28.6	37.5
Hypertension (%)	24.1	23.8	25.0
Smoking (current or former) (%)	19.0	19.0	18.8
Dyslipidemia (%)	41.5	40.0	45.5
NYHA class	3.19 \pm 0.395	3.19 \pm 0.397	3.19 \pm 0.403
NYHA III: No. (%)	47 (81.0)	34 (81.3)	13 (81.0)
NYHA IV: No. (%)	11 (19.0)	8 (19.0)	3 (18.8)
LVEF (%)	27.6 \pm 5.6	27.9 \pm 5.5	26.7 \pm 5.7
LV end-diastolic diameter (mm)	69.8 \pm 6.9	68.1 \pm 7.1	73.2 \pm 9.1*
LV end-systolic diameter (mm)	57 \pm 8.7	56 \pm 9.2	59 \pm 10.7
LV end-systolic volume index (ml/m^2)	121.2 \pm 13.2	118.4 \pm 13.1	121.3 \pm 13.0
LV filling time (s)	0.46 \pm 0.04	0.51 \pm 0.05	0.45 \pm 0.04
Left atrial diastolic area (cm^2)	17.8 \pm 3.7	17.2 \pm 3.8	21.5 \pm 4.2
Left atrial systolic area (cm^2)	26.9 \pm 5.9	26.3 \pm 5.4	29.8 \pm 5.9
Mitral regurgitation area (% of left atrial systolic area)	0.24 \pm 0.02	0.20 \pm 0.02	0.28 \pm 0.02*
QoL score	39.7 \pm 10.8	40.8 \pm 10.01	36.6 \pm 12.5
Distance walked in 6 min (m)	309.7 \pm 5.74	310.2 \pm 5.79	308.4 \pm 5.52
Oxygen uptake at peak exercise ($\text{ml}/\text{kg}/\text{min}$)	12.5 \pm 0.73	12.5 \pm 0.7	12.3 \pm 0.6
Oxygen uptake at anaerobic threshold ($\text{ml}/\text{kg}/\text{min}$)	9.43 \pm 0.9	9.60 \pm 0.9	8.96 \pm 0.7

*= $p < 0.05$ vs. Responders.

Finally, we performed a linear regression analysis to characterise the predictors of AF and a subsequent backward stepwise multivariable analysis, tested for goodness-of-fit, built using only the variables that were associated with new-onset FA in the first regression analysis.

All tests that we performed were two-tailed and a p -value < 0.05 was considered statistically significant. All statistical tests were performed with the SPSS 18.0 statistical package (SPSS Inc., Chicago, IL) and GRAPHPAD PRISM 5.01 (GraphPad software, San Diego, CA) (17).

Results

Population characteristics

We enrolled 58 Caucasian patients who met the inclusion/exclusion criteria. Baseline characteristics of these subjects are depicted in Table 1. The mean age was 62.5 ± 11.1 years; there was a male predominance (63.8%), with a mean LVEF of $27.6 \pm 5.6\%$. Drug therapy for HF did not change significantly over the follow-up period, and all patients had stable biventricular stimulation.

After 1 year, 42 patients (72.4%) were considered responders to CRT according to the previously defined criteria. There were 16 non-responders (27.6%), with 4 HF-related hospitalizations. Two patients died before the 2-year follow-up visit (one responder and one non-responder); four patients died before the 3-year follow-up visit (one responder and three non-responder). No difference in survival was evidenced by Kaplan–Meier analysis (Figure 1A).

Clinical outcomes

Our most interesting finding is that, already after 1 year, there is a significant difference in new-onset AF in non-responder patients (18.2%) vs. responders (3.3%). These data are confirmed at 2 years (33.3% vs. 12.2%) and 3 years (50.0% vs. 15.0%) follow-up. In particular, at 3-year follow-up, non-responders have a markedly increased risk to develop new-onset AF (OR = 5.67, 95% CI = 1.36–23.59, $p = 0.019$). Hence, this disparity in risk persisted throughout the 3-year follow-up period. Furthermore, Kaplan–Meier curves showed a significant difference in developing new-onset AF between the two groups ($p < 0.05$; Figure 1B). Finally, the multivariable analysis confirmed the non-response to CRT as an additive risk factor for new onset AF (OR = 4.32, CI = 2.46–9.63, $p < 0.05$).

As expected, we observed a favourable improvement of clinical status in the group of CRT responders, already evidenced at 1-year follow-up, and supported after 2 and 3 years (Table 2).

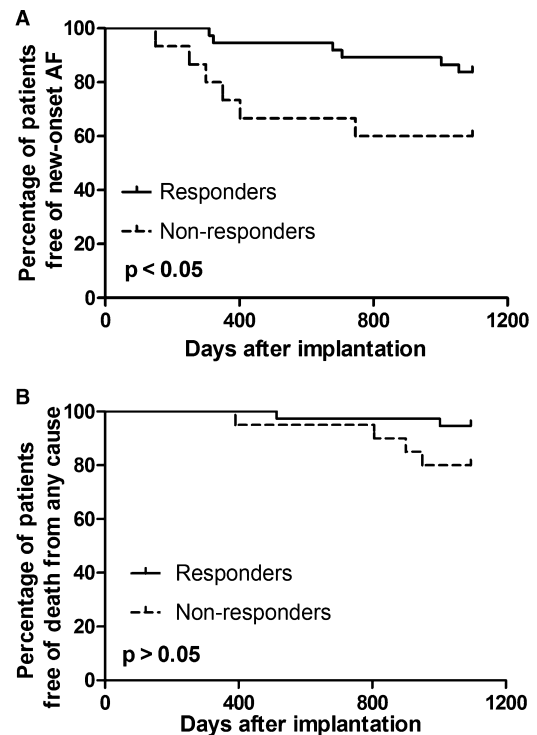


Figure 1 Kaplan–Meier estimate of time to first onset of atrial fibrillation (AF). There is no significant difference in mortality (Panel A), while first onset of AF was significantly earlier in non-responder patients (dotted line) than in responders (continuous line) (Panel B)

Discussion

This is the first study that analyses long-term effects of CRT in a population of patients with idiopathic-dilated cardiomyopathy, with a follow-up of 3 years. The present work confirms the clinical benefit of treating HF patients with CRT and suggests a role of this non-pharmacological therapy in prevention of AF.

The loss of coordination of ventricular contraction contributes to the pathophysiology of HF, reducing the already diminished contractile reserve of the heart. Specifically, dyssynchronous contraction exacerbates inefficient use of energy by the heart (mechano-energetic uncoupling). Indeed, the left lateral wall is activated well after the septum contracts (18). This leads to contraction of the lateral wall during relaxation of the septum resulting in marked mechanical dysfunction. The dyssynchronous failing heart also exhibits deep alterations in protein expression (19,20), such as changes in local calcium handling, as exemplified by a strong decrease of phospholamban in the delayed activated myocardium (21). The purpose of CRT is to restore ventricular relaxation and contraction sequences by simulta-

Table 2 Characteristics of the patients at follow-up visits

	All patients 1 year	Responders 1 year	Non-responders 1 year	Responders 2 years	Non-responders 2 years	Responders 3 years	Non-responders 3 years
No.	58	42	16	41	15	40	12
Age (years)	63.5 ± 11.9	63.5 ± 11.1	63.4 ± 14.2	63.5 ± 10.4	62.9 ± 14.2	64.5 ± 10.4	63.0 ± 14.01
Male sex: No. (%)	37 (63.8)	27 (64.3)	10 (62.5)	26 (63.4)	9 (60.0)	26 (65.0)	8 (66.7)
Height (cm)	168.11 ± 6.9	167.1 ± 7.38	170.86 ± 4.9	167.1 ± 7.41	170.85 ± 4.9	167.1 ± 7.38	170.86 ± 5.0
Weight (kg)	72.39 ± 13.5	70.85 ± 13.01	76.44 ± 14.4	70.4 ± 13.9	76.8 ± 14.62	70.2 ± 14.1	77.95 ± 14.7
Body mass index	25.42 ± 3.9	25.09 ± 3.7	26.2 ± 4.4	25.07 ± 3.8	24.78 ± 7.11	25.0 ± 3.9	25.07 ± 7.32
Body surface (m ²)	1.80 ± 0.183	1.78 ± 0.182	1.87 ± 0.18	1.77 ± 0.196	1.88 ± 0.17	1.77 ± 0.197	1.89 ± 0.18
Heart rate (bpm)	68.41 ± 6.5	67.55 ± 6.19	70.69 ± 7.05	68 ± 6.05	68.3 ± 7.01	67.95 ± 7.05	69 ± 7.5
QRS duration from surface ECG (ms)	168.3 ± 18.1	169.9 ± 17.1	172.9 ± 17.7	169.8 ± 16.8	173.4 ± 17.1	169.7 ± 17.2	173.4 ± 17.0
Systolic blood pressure (mmHg)	123 ± 15.1	122 ± 15.2	124 ± 14.7	125 ± 13.6	122 ± 14.3	126 ± 16.2	118 ± 19.5
Diastolic blood pressure (mmHg)	74.0 ± 13.5	74.7 ± 13.7	71.9 ± 12.9	75 ± 14.1	71.1 ± 10.8	75 ± 11.2	71.4 ± 10.9
NYHA class	2.53 ± 0.82	2.38 ± 0.79	2.94 ± 0.77*	2.32 ± 0.79	3.00 ± 0.84*,†	2.28 ± 0.81	3.0 ± 0.8*,†,‡
NYHA I: No. (%)	2 (4.8)	2 (4.8)	–	3 (7.3)	–	4 (10)	–
NYHA II: No. (%)	33 (59.6)	28 (66.7)	5 (31.3)*	27 (65.9)	5 (33.3)*,†	26 (65)	4 (33.3)*,†,‡
NYHA III: No. (%)	13 (22.4)	6 (14.3)	7 (43.8)*	6 (14.3)	5 (33.3)	5 (12.5)	4 (33.3)†,‡
NYHA IV: No. (%)	10 (17.2)	6 (14.3)	4 (25)*	5 (12.2)	5 (33.3)†	5 (12.5)	4 (33.3)†,‡
LVEF (%)	32.8 ± 6.1	34.3 ± 5.5	28.9 ± 6.0*	33.2 ± 5.2	29.5 ± 5.6*,†	34.1 ± 5.2	29.7 ± 5.8*,†,‡
LV end-systolic volume index (ml/m ²)	121.2 ± 13.8	117.4 ± 12.9	121.1 ± 13.4	117.1 ± 12.2	121.1 ± 13.1	115.4 ± 13.0	121.8 ± 13.1
LV filling time (s)	0.47 ± 0.05	0.52 ± 0.05	0.45 ± 0.03	0.51 ± 0.04	0.45 ± 0.04	0.52 ± 0.03	0.46 ± 0.03
Left atrial diastolic area (cm ²)	17.8 ± 2.5	18.2 ± 2.4	20.5 ± 2.4	18.2 ± 2.4	20.5 ± 2.3	17.6 ± 2.5	23.1 ± 2.4‡
Left atrial systolic area (cm ²)	26.9 ± 2.8	27.3 ± 2.7	28.8 ± 2.7	27.3 ± 2.7	28.8 ± 2.8	27.8 ± 2.8	31.2 ± 3.0
Mitral regurgitation area (% of left atrial systolic area)	0.24 ± 0.02	0.21 ± 0.02	0.27 ± 0.03*	0.21 ± 0.02	0.27 ± 0.02*,†	0.20 ± 0.02	0.28 ± 0.02*,†,‡
QoL score	40 ± 14	34 ± 19	40 ± 16*	33 ± 14	41 ± 15*,†	29.5 ± 15	41.3 ± 21*,†,‡
Distance walked in 6 min (m)	305 ± 10	338 ± 11	304 ± 11*	341 ± 13	302 ± 10*,†	342 ± 11	302 ± 9*,†,‡
Oxygen uptake at peak exercise (ml/kg/min)	12.5 ± 0.73	14.9 ± 0.7	12.5 ± 0.7*	15.2 ± 0.7	12.6 ± 0.7*,†	15.7 ± 0.6	12.6 ± 0.8*,†,‡
Oxygen uptake at anaerobic threshold (ml/kg/min)	9.43 ± 0.9	11.5 ± 0.6	10.0 ± 0.6*	11.7 ± 0.6	10.0 ± 0.4*,†	11.9 ± 0.7	9.9 ± 0.4*,†,‡
New-onset Atrial Fibrillation: No. (%)	–	2 (3.3)	4 (18.2)*	4 (9.7)	5 (33.3)*,†	6 (15.0)	6 (50.0)*,†,‡

* = $p < 0.05$ vs. Responders 1 year; † = $p < 0.05$ vs. Responders 2 years; ‡ = $p < 0.05$ vs. Responders 3 years.

neously pacing both ventricles. Numerous studies have reported positive long-term effects in terms of symptoms, exercise tolerance, QoL and HF prognosis after CRT (22,23) and our work corroborates these findings. A prospective study examining the relation between CRT and AF using as control a HF population that does not receive CRT would be neither ethical nor practical, given the proven efficacy of this therapy in treating HF. So, we decide to compare a homogeneous population of CRT recipients, then subdivided into responders and non-responders. One of the most pressing unresolved questions, however, remained how to identify patients that will not respond to CRT, and how to define whether or not response is really central to the entire issue (4,24), since there is relatively poor correlation between the various measures of CRT response. Thus, as mentioned in methods, we used clear and reproducible

criteria for the definition of non-responder patients, also to avoid any case of misinterpretation.

We recruited only patients with non-ischaemic-dilated cardiomyopathy. Indeed, albeit CRT is an effective alternative therapy in patients with dilated heart disease whether of ischaemic or non-ischaemic origin, the response tends to be slightly lower when the heart disease is ischaemic, maybe because of the presence of necrotic tissue. This is the first study that focalizes on this topic, assuring a homogeneous study population. Indeed, heterogeneity may explain controversial results concerning this issue emerged in literature.

Another chief issue to discuss in analysing the occurrence of AF is how the same AF is detected. We defined AF as an episode, with or without symptoms, lasting 10 min or more, identified by electrocardiography, Holter examination and using the

continuous monitoring capability offered by implanted devices, which were programmed uniformly to capture AF episodes (25–27). During follow-up, device interrogation was scheduled every 3–6 months and all printouts were carefully checked for new-onset AF episodes. Other studies have used a variety of different definitions for AF, also relied on symptoms, which appear clearly inadequate in assessing overall AF burden.

Despite the extensive evidence of the benefits of CRT on ventricular function, data about the effects of CRT on atrial function and on incidence of new-onset AF are conflicting (2,7,28). *Post hoc* analysis of the CARE-HF trial suggested that CRT had no favourable impact on the incidence of AF compared with medical therapy alone, but many of these patients (19%) already had a history of AF (9). A study by the group of JJ. Bax confirmed the clinical importance of new-onset AF after CRT, showing that recipients of CRT who develop new-onset AF have less echocardiographic response to CRT and more cardiac adverse events during follow-up (28). Another recent article described, consistently with our findings, that more than 20% of the overall HF patient population treated with CRT suffered episodes of paroxysmal atrial tachycardia (25).

Anyway, the potential mechanisms to take into account for the effect attributed to CRT in the prevention of AF could be related to an improvement in left ventricular systolic function and a decrease of the degree of mitral regurgitation, with a reduction of structural atrial remodelling of the electrophysiological substrate responsible for the initiation/triggers of atrial arrhythmias (29). Anyway, non-responders have larger atria, larger ventricles and more mitral regurgitation already at baseline. So we cannot exclude these parameters predicting AF independent of supposed non-response to CRT. Indeed, the fact that after 3-year follow-up non-responder patients show an increased left atrial diastolic area than responders is a strong evidence for supporting the hypothesis

that CRT may prevent AF through atrial reverse remodelling (29), probably as a result of a reduction of the overload in the atria (18). What is more, as shown in a previous study by JW. Fung and coll. (30), we also noted a trend of a greater left atrial diastolic area in patients who developed AF. Nevertheless, atrial function is relatively complex, and more quantitative methods are needed to better explore atrial functional improvement. Moreover, because patients with HF who develop AF have a worse outcome (3), it could be interesting to know whether or not the outcome might be improved by CRT.

Our study is limited by the relatively small number of subjects, although they constitute a remarkable patient population, because of selective inclusion and exclusion criteria. The percentage of patients who developed new-onset AF although reach statistical significance when analysed, the absolute number is small. Another limitation is the non-randomised nature of the study. Thus, the results must be interpreted cautiously and further randomised studies, pooling data from multiple centres, are needed to confirm our findings and to assess their clinical impact.

Acknowledgements

We thank the patients and families who have sought clinical evaluation at “Federico II” University Hospital and all of the physicians, technicians and nurses for their tremendous contribution to the data.

Author contributions

GS and CDA and conceived the study; GS, AL and RS performed data analysis, GS and SLDA drafted the manuscript, VM and AL helped to draft the manuscript and collect the data, AL and MC participated in the design and coordination of the study; all authors read and approved the manuscript.

References

- Anand IS, Carson P, Galle E et al. Cardiac resynchronization therapy reduces the risk of hospitalizations in patients with advanced heart failure: results from the Comparison of Medical Therapy, Pacing and Defibrillation in Heart Failure (COMPANION) trial. *Circulation* 2009; **119**: 969–77.
- Cleland JG, Calvert MJ, Verboven Y, Freemantle N. Effects of cardiac resynchronization therapy on long-term quality of life: an analysis from the Cardiac Resynchronisation-Heart Failure (CARE-HF) study. *Am Heart J* 2009; **157**: 457–66.
- Maisel WH, Stevenson LW. Atrial fibrillation in heart failure: epidemiology, pathophysiology, and rationale for therapy. *Am J Cardiol* 2003; **91**: 2D–8D.
- Bax JJ, Gorcsan J 3rd. Echocardiography and non-invasive imaging in cardiac resynchronization therapy: results of the PROSPECT (Predictors of Response to Cardiac Resynchronization Therapy) study in perspective. *J Am Coll Cardiol* 2009; **53**: 1933–43.
- Vardas PE, Auricchio A, Blanc JJ et al. Guidelines for cardiac pacing and cardiac resynchronization therapy: the task force for cardiac pacing and cardiac resynchronization therapy of the European Society of Cardiology. Developed in collaboration with the European Heart Rhythm Association. *Eur Heart J* 2007; **28**: 2256–95.
- D’Ascia SL, Santulli G, Liguori V et al. Advanced algorithms can lead to electrocardiographic misinterpretations. *Int J Cardiol* 2010; **141**: e34–6.
- Fung JW, Yu CM, Chan JY et al. Effects of cardiac resynchronization therapy on incidence of atrial fibrillation in patients with poor left ventricular systolic function. *Am J Cardiol* 2005; **96**: 728–31.
- Santulli G. Coffee and cardiovascular system. *Cardiol Sci* 2006; **4**: 186–8.
- Hoppe UC, Casares JM, Eiskjaer H et al. Effect of cardiac resynchronization on the incidence of atrial

- fibrillation in patients with severe heart failure. *Circulation* 2006; **114**: 18–25.
- 10 Rector TS, Cohn JN. Assessment of patient outcome with the Minnesota Living with Heart Failure questionnaire: reliability and validity during a randomized, double-blind, placebo-controlled trial of pimobendan. Pimobendan Multicenter Research Group. *Am Heart J* 1992; **124**: 1017–25.
 - 11 Bittner V. Six-minute walk test in patients with cardiac dysfunction. *Cardiologia* 1997; **42**: 897–902.
 - 12 Mangiacavalli M, Gasparini M, Faletta F et al. Clinical predictors of marked improvement in left ventricular performance after cardiac resynchronization therapy in patients with chronic heart failure. *Am Heart J* 2006; **151**: 477 e1–e6.
 - 13 St John Sutton MG, Plappert T, Abraham WT et al. Effect of cardiac resynchronization therapy on left ventricular size and function in chronic heart failure. *Circulation* 2003; **107**: 1985–90.
 - 14 Lawo T, Borggrefe M, Butter C et al. Electrical signals applied during the absolute refractory period: an investigational treatment for advanced heart failure in patients with normal QRS duration. *J Am Coll Cardiol* 2005; **46**: 2229–36.
 - 15 Santulli G, Campanile A, Spinelli L et al. G Protein-coupled receptor kinase 2 in patients with acute myocardial infarction. *Am J Cardiol* 2011; **107**: 1125–30.
 - 16 Beaver WL, Wasserman K, Whipp BJ. A new method for detecting anaerobic threshold by gas exchange. *J Appl Physiol* 1986; **60**: 2020–7.
 - 17 Santulli G, Basilicata MF, De Simone M et al. Evaluation of the anti-angiogenic properties of the new selective alphaVbeta3 integrin antagonist RGDechiHCit. *J Transl Med* 2011; **9**: 7.
 - 18 Sade LE, Demir O, Atar I et al. Effect of mechanical dyssynchrony and cardiac resynchronization therapy on left ventricular rotational mechanics. *Am J Cardiol* 2008; **101**: 1163–9.
 - 19 Santulli G, Illario M, Cipolletta E et al. Deletion of the CaMK4 gene in mice determines a hypertensive phenotype. *Cardiovasc Res* 2010; **87**: 89.
 - 20 Vanderheyden M, Bartunek J. Cardiac resynchronization therapy in dyssynchronous heart failure: zooming in on cellular and molecular mechanisms. *Circulation* 2009; **119**: 1192–4.
 - 21 Spragg DD, Leclercq C, Loghmani M et al. Regional alterations in protein expression in the dyssynchronous failing heart. *Circulation* 2003; **108**: 929–32.
 - 22 Gasparini M, Regoli F, Ceriotti C et al. Remission of left ventricular systolic dysfunction and of heart failure symptoms after cardiac resynchronization therapy: temporal pattern and clinical predictors. *Am Heart J* 2008; **155**: 507–14.
 - 23 Jansen AH, van Dantzig J, Bracke F et al. Improvement in diastolic function and left ventricular filling pressure induced by cardiac resynchronization therapy. *Am Heart J* 2007; **153**: 843–9.
 - 24 Yu CM, Wing-Hong Fung J, Zhang Q, Sanderson JE. Understanding nonresponders of cardiac resynchronization therapy—current and future perspectives. *J Cardiovasc Electrophysiol* 2005; **16**: 1117–24.
 - 25 Leclercq C, Padeletti L, Cihak R et al. Incidence of paroxysmal atrial tachycardias in patients treated with cardiac resynchronization therapy and continuously monitored by device diagnostics. *Europace* 2010; **12**: 71–7.
 - 26 Bottoni N, Donato P, Quartieri F et al. Outcome after cavo-tricuspid isthmus ablation in patients with recurrent atrial fibrillation and drug-related typical atrial flutter. *Am J Cardiol* 2004; **94**: 504–8.
 - 27 Fuster V, Ryden LE, Asinger RW et al. ACC/AHA/ESC Guidelines for the Management of Patients with Atrial Fibrillation: Executive Summary A Report of the American College of Cardiology/American Heart Association Task Force on Practice Guidelines and the European Society of Cardiology Committee for Practice Guidelines and Policy Conferences (Committee to Develop Guidelines for the Management of Patients with Atrial Fibrillation) Developed in Collaboration with the North American Society of Pacing and Electrophysiology. *Circulation* 2001; **104**: 2118–50.
 - 28 Borleffs CJ, Ypenburg C, van Bommel RJ et al. Clinical importance of new-onset atrial fibrillation after cardiac resynchronization therapy. *Heart Rhythm* 2009; **6**: 305–10.
 - 29 Wijffels MC, Kirchhof CJ, Dorland R et al. Electrical remodeling due to atrial fibrillation in chronically instrumented conscious goats: roles of neurohumoral changes, ischemia, atrial stretch, and high rate of electrical activation. *Circulation* 1997; **96**: 3710–20.
 - 30 Fung JW, Yip GW, Zhang Q et al. Improvement of left atrial function is associated with lower incidence of atrial fibrillation and mortality after cardiac resynchronization therapy. *Heart Rhythm* 2008; **5**: 780–6.

Paper received March 2011, accepted May 2011

G Protein-Coupled Receptor Kinase 2 in Patients With Acute Myocardial Infarction

Gaetano Santulli, MD^{a,b,†}, Alfonso Campanile, MD^{c,†}, Letizia Spinelli, MD^{b,c}, Emiliano Assante di Panzillo, MD^{b,c}, Michele Ciccarelli, MD, PhD^a, Bruno Trimarco, MD^{a,b}, and Guido Iaccarino, MD, PhD^{a,b,*}

Lymphocyte G protein-coupled receptor kinase 2 (GRK2) levels are increased in patients with chronic heart failure, and in this condition, they correlate with cardiac function. The aim of this study was to assess the prognostic role of GRK2 during acute cardiac dysfunction in humans. A study was designed to investigate the role of GRK2 levels in patients with acute coronary syndromes. Lymphocyte GRK2 levels were examined at admission and after 24 and 48 hours in 42 patients with acute coronary syndromes, 32 with ST-segment elevation myocardial infarction and 10 with unstable angina as a control group. Echocardiographic parameters of systolic and diastolic function and left ventricular remodeling were evaluated at admission and after 2 years. GRK2 levels increased during ST-segment elevation myocardial infarction and were associated with worse systolic and diastolic function. This association held at 2-year follow-up, when GRK2 was correlated with the ejection fraction and end-systolic volume, indicating a prognostic value for GRK2 levels during acute ST-segment elevation myocardial infarction. In conclusion, lymphocyte GRK2 levels increase during acute myocardial infarction and are associated with worse cardiac function. Taken together, these data indicate that GRK2 could be predictive of ventricular remodeling after myocardial infarction and could facilitate the tailoring of appropriate therapy for high-risk patients. © 2011 Elsevier Inc. All rights reserved. (*Am J Cardiol* 2011;107:1125–1130)

In recent years, the overall prevalence of heart failure (HF) has increased.¹ Ischemic heart disease represents a leading cause of HF, and a plethora of studies have assessed the clinical evolution of ST-segment elevation myocardial infarction (STEMI) toward HF.^{2–6} Given the complexity of HF, interest has intensified in developing biologic markers to provide prognostic information about the disease.⁷ Indeed, several multivariate prognostic models have been developed to allow risk stratification.^{6,8} Because biomarkers may reflect various pathophysiologic processes,⁷ the use of a multimarker approach has been suggested to better identify patients who are at high risk,⁹ paving the way for more accurate treatment.^{3–5} A candidate biomarker in cardiovascular scenario is the G protein-coupled receptor kinase 2 (GRK2).¹⁰ This protein is involved in the desensitization and downregulation of G protein-coupled receptors, such as the β -adrenergic receptor, and is the most important G protein-coupled receptor kinase expressed in the heart. Increased cardiac GRK2 levels have been described in chronic HF and are associated with elevated sympathetic nervous system activity.^{11–13} We previously showed that increased

cardiac GRK2 levels are associated with the impairment of cardiac function and that cardiac protein levels can be monitored using peripheral lymphocytes, thus circumventing the problem of tissue sampling.¹⁴ Nevertheless, the role of GRK2 as a marker for HF progression after acute myocardial infarction (MI) remains to be clarified. Thus, we designed a study to investigate GRK2 levels during the early phases of MI to define its relevance as a biomarker in the evolution toward HF.

Methods

We enrolled 32 patients consecutively admitted to the Coronary Care Unit of “Federico II” University with a diagnosis of acute (<24-hour) STEMI, defined by typical chest pain and persistent ST-segment elevation on electrocardiography.^{15,16} MI was confirmed by increased serum creatine kinase and assessed by cardiac ultrasound using the wall motion score index. We also recruited 10 age-matched patients with unstable angina pectoris as a control group.³ Angiography was performed in all patients according to standard indications.¹⁵ GRK2 levels were evaluated at admission and after 24 hours. All patients provided written informed consent. The study was approved by the ethics committee of “Federico II” University. We used a database reporting characteristics of each patient, including clinical, biochemical, and echocardiographic data and anthropomorphic parameters including age, gender, height, weight, body mass index, and body surface area (BSA). Patients were then reexamined at 2-year follow-up. Outcome variables

Divisions of ^aInternal Medicine and ^bCardiac Intensive Care Unit and ^cGeriatrics, Department of Clinical Medicine and Cardiovascular and Immunologic Sciences, “Federico II” University, Naples, Italy. Manuscript received October 20, 2010; revised manuscript received and accepted December 15, 2010.

*Corresponding author: Tel: 39-081-746-2220; fax: 39-081-746-2256. E-mail address: guiaccar@unina.it (G. Iaccarino).

[†]Drs. Santulli and Campanile contributed equally to this study.

Table 1
Baseline clinical characteristics of patients at admission

Variable	Patients With UAP (n = 10)	Patients With STEMI (n = 32)	High GRK2 (n = 15)	Low GRK2 (n = 17)	β -Blocker Therapy (n = 24)	No β -Blocker Therapy (n = 8)
Men/women	7/3	30/2	13/2	17/0	22/2	8/0
Age (years)	60.9 \pm 3.1	59.9 \pm 1.9	57.7 \pm 3.3	61.8 \pm 2.3	58.4 \pm 2.7	63.9 \pm 3.2
Weight (kg)	75.7 \pm 4.6	76.3 \pm 1.7	75.1 \pm 2.8	77.4 \pm 2.2	77.1 \pm 1.7	73.9 \pm 4.9
Height (cm)	164.6 \pm 1.6	162.3 \pm 5.3	166.8 \pm 1.4	158.3 \pm 9.9	160.8 \pm 7	166.9 \pm 2.2
Body mass index (kg/m ²)	23.4 \pm 3.3	27.17 \pm 0.59	27.1 \pm 0.9	27.3 \pm 0.7	27.4 \pm 0.6	26.5 \pm 1.6
BSA (m ²)	1.8 \pm 0.1	1.85 \pm 0.1	1.8 \pm 0.3	1.86 \pm 0.4	1.8 \pm 0.03	1.8 \pm 0.1
Systolic blood pressure (mm Hg)	133.1 \pm 6.0	119.8 \pm 3.9	123.7 \pm 4.8	116.5 \pm 5.9	119.4 \pm 4	121.2 \pm 8.3
Diastolic blood pressure (mm Hg)	76.9 \pm 4.0	72.9 \pm 2.3	75 \pm 2.8	71.2 \pm 3.6	73.3 \pm 2.7	71.9 \pm 4.8
Heart rate (beats/min)	70.5 \pm 3.8	72.6 \pm 2.1	73.60 \pm 2.8	71.65 \pm 3.1	75.2 \pm 2.2	64.6 \pm 3.9*

* $p < 0.05$.

UAP = unstable angina pectoris.

Table 2
Echocardiographic parameters of patients with ST-segment elevation myocardial infarction

Variable	Patients With STEMI (n = 32)	High GRK2 (n = 15)	Low GRK2 (n = 17)	β -Blocker Therapy (n = 24)	No β -Blocker Therapy (n = 8)
Systolic parameters					
Ejection fraction (%)	43.2 \pm 1.4	43.9 \pm 1.7	41.2 \pm 2	41.4 \pm 2.7	45.1 \pm 1.9
Shortening fraction (%)	27.7 \pm 1.1	29.1 \pm 1.9	26.5 \pm 1.2	26.8 \pm 2.1	31.1 \pm 2.2
Stroke volume (ml)	40.1 \pm 1.7	36.5 \pm 1.2	43.3 \pm 2.9*	40.9 \pm 2.2	37.6 \pm 2.3
Cardiac output (L/min)	3.0 \pm 0.1	2.8 \pm 0.1	3.17 \pm 0.1*	3.1 \pm 0.2	2.6 \pm 0.2
Cardiac index (L/min/m ²)	1.6 \pm 0.1	1.5 \pm 0.1	1.71 \pm 0.1	1.7 \pm 0.1	1.4 \pm 0.1
Wall motion score index	1.9 \pm 0.1	1.9 \pm 0.1	1.91 \pm 0.1	2.0 \pm 0.1	1.8 \pm 0.1
Diastolic parameters					
E (cm/s)	66.6 \pm 3.4	68.7 \pm 4.45	64.8 \pm 5.1	64.62 \pm 3.8	72.6 \pm 7.5
A (cm/s)	68.1 \pm 2.8	69.7 \pm 4.13	66.6 \pm 4.0	64.8 \pm 2.9	77.9 \pm 6.3*
E/A ratio	1.0 \pm 0.1	1.0 \pm 0.1	1.0 \pm 0.1	1.1 \pm 0.2	1.0 \pm 0.1
Deceleration time (ms)	163.9 \pm 9.7	143.5 \pm 10.4	183 \pm 15.1*	168.2 \pm 11.7	149.1 \pm 17
Isovolumic relaxation time (ms)	92.2 \pm 2.8	91.7 \pm 2.3	92.8 \pm 5.9	90.3 \pm 3.9	98.2 \pm 5.5
PVs (cm/s)	47.5 \pm 1.9	51.7 \pm 2.2	44.3 \pm 2.9	46.6 \pm 2.3	50.4 \pm 4.1
PVd (cm/s)	40.5 \pm 2.4	38.4 \pm 3.1	42.1 \pm 3.7	39.9 \pm 3.1	42.6 \pm 3.8
PVs/PVd ratio	1.3 \pm 0.1	1.4 \pm 0.1	1.2 \pm 0.1	1.3 \pm 0.1	1.3 \pm 0.2
E' (cm/s)	5.7 \pm 0.5	6.2 \pm 0.8	5.3 \pm 1.3	5.44 \pm 0.6	6.6 \pm 1.05
E/E' ratio	13.9 \pm 1.1	13.6 \pm 2.01	14.2 \pm 1.3	13.96 \pm 1.1	13.7 \pm 3.3

* $p < 0.05$.

PVd = diastolic pulmonary venous flow; PVs = systolic pulmonary venous flow.

analyzed during this examination were echocardiographic (systolic and diastolic function, MI size, and ventricular remodeling) and clinical (compliance with therapy, rehospitalization).

Patients' lymphocytes were extracted from 20-ml blood samples, as previously described, by means of Ficoll purification using Histopaque-1077 (Sigma Aldrich, St. Louis, Missouri) at admission and after 24 and 48 hours.^{14,17} Samples thus obtained were frozen and stored at -80°C .

We performed immunodetection of lymphocyte levels of GRK2 and actin using detergent-solubilized cell extracts or cytosol fractions obtained by centrifugation, using polyclonal anti-GRK2 and antiactin antibodies (Santa Cruz Biotechnology, Santa Cruz, California), as previously described.^{11,14} The proteins were visualized using standard enhanced chemiluminescence (ECL Kit; Amersham Biosciences, Piscataway, New Jersey).^{17,18} Quantization was done by scanning the autoradiographic film and using dedicated

software (ImageQuant; Molecular Dynamics, Piscataway, New Jersey). GRK2 levels indicate GRK2 expression corrected by actin expression and by lymphocyte levels for each patient (in corrected densitometry units). All laboratory work was performed in blinded fashion with respect to the identity of the samples.¹⁷⁻¹⁹

Cardiac ultrasound evaluation was performed using Vivid 7 (GE Healthcare, Milwaukee, Wisconsin) by the same operator (L.S.) in the enrollment phase and at 2-year follow-up. Systolic functional parameters including the ejection fraction, shortening fraction, cardiac output, stroke volume, and cardiac index were analyzed. We also evaluated diastolic functional parameters including E-wave velocity (E), A-wave velocity (A), the E/A ratio, deceleration time, systolic and diastolic pulmonary venous flow, isovolumetric relaxation time, mitral annular motion velocity (E') with Doppler tissue imaging, and the E/E' ratio. Infarct size was assessed using the wall motion score index. Left ven-

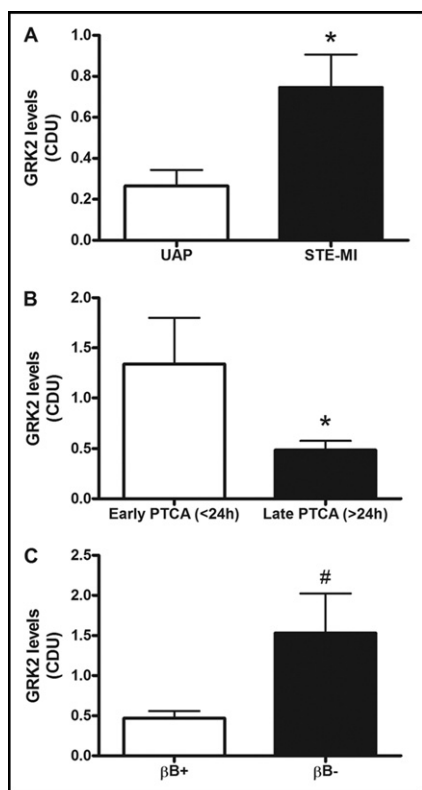


Figure 1. Determinants of GRK2 levels at admission. (A) Western blot analysis of GRK2 on lymphocytes showed that peripheral GRK2 levels were higher in patients with STEMI than in controls with unstable angina pectoris (UAP). (B) Of interest, in patients with STEMI, treatment affected GRK2 levels, as higher GRK2 levels were observed in patients receiving primary percutaneous transluminal coronary angioplasty (PTCA) compared with those receiving late elective PTCA. (C) Furthermore, patients receiving β blockers (β Bs) had lower levels of GRK2 than patients not receiving β Bs. CDU = corrected densitometry units. * $p < 0.05$ (independent-samples Student's t test); # $p < 0.01$ (independent-samples Student's t test).

tricular remodeling was assessed by measuring end-systolic volume (ESV) and its long-term variation corrected by BSA ($\Delta\%$ -ESV/BSA).^{8,20}

Statistical analysis was performed using SPSS version 18.0 (SPSS, Inc., Chicago, Illinois) and GraphPad Prism version 5.01 (GraphPad Software, San Diego, California). Data are expressed as mean \pm SE. We performed chi-square tests to compare categorical variables and independent-samples Student's t tests for continuous variables. All analyses were performed using a 2-sided model. A p value < 0.05 was considered significant. Some continuous variables were transformed into categorical variables using the median values as cutoffs. In particular, we divided our population according to GRK2 level at admission into 2 groups using a cut-off value of 0.47 corrected densitometry units: elevated GRK2 and low GRK2. Moreover, we studied the effects of β -blocker therapy and revascularization on GRK2 levels. Indeed, we subdivided our STEMI population into patients treated with β blockers and those who did not receive β blockers because of contraindications. Similarly, to investigate whether time of revascularization could affect GRK2 levels, we subdivided our population into patients treated

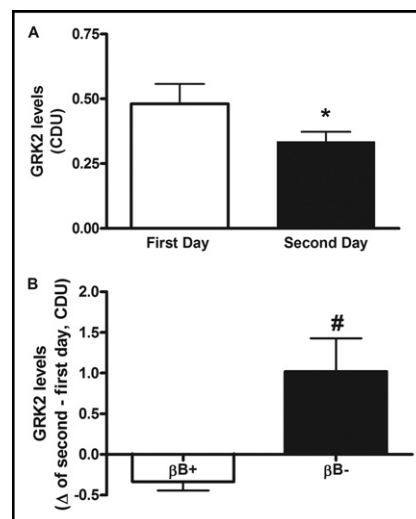


Figure 2. Determinants of GRK2 levels on the second day. (A) In patients with STEMI, GRK2 levels were reduced on the second day of observation. (B) This reduction was particularly observed in patients receiving β blockers (β Bs), whereas those not receiving β Bs did not have reduced GRK2 levels. CDU = corrected densitometry units. * $p < 0.05$ (independent-samples Student's t test); # $p < 0.01$ (independent-samples Student's t test).

with early percutaneous transluminal coronary angioplasty, defined as angioplasty performed on the infarct-related vessel during the first 24 hours of an acute MI,¹⁵ and late percutaneous transluminal coronary angioplasty (patients who received medical therapy and were referred later [> 24 hours] to coronary intervention).³ We also performed independent-samples Student's t tests, Pearson's correlations, and linear regressions between GRK2 levels at admission and echocardiographic variables considered at 2-year follow-up. In this case, we considered as continuous variables not only the absolute value of ultrasound parameters but also their variations from admission values. Finally, we performed a linear regression analysis to characterize the most significant variables at admission associated with $\Delta\%$ -ESV/BSA and a back-step multiple regression analysis to define the best predictive model of $\Delta\%$ -ESV/BSA.²⁰

Results

Clinical characteristics of patients are listed in Table 1. As expected, patients with STEMI presented with impaired cardiac function, as indicated by the ultrasound parameters listed in Table 2. GRK2 levels at admission were higher in patients with STEMI than in those with unstable angina pectoris (Figure 1). Two pivotal determinants of GRK2 levels were treatment and time. In particular, early revascularization and β -blocker therapy clearly affected GRK2 levels. Indeed, GRK2 levels were higher in patients treated with early percutaneous transluminal coronary angioplasty than in those who received late percutaneous transluminal coronary angioplasty (Figure 1). This finding could be related to the reperfusion injury, consistent with previous reports.^{13,21} Also, patients treated with β blockers had lower GRK2 levels compared with those who did not receive β blockers (Figure 1).

Time also affected GRK2 levels. In particular, during the second day of observation, GRK2 levels decreased (Figure 2),

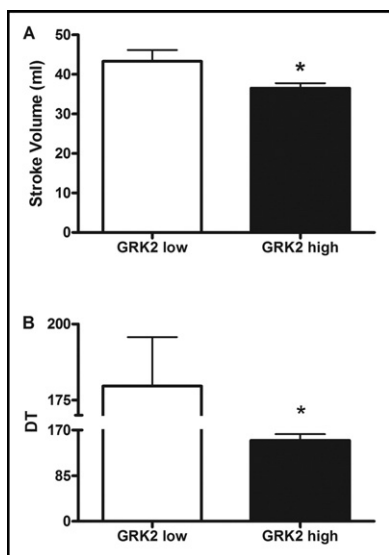


Figure 3. GRK2 levels and cardiac function. (A) Patients with high GRK2 levels had worse systolic function as assessed by stroke volume compared to those with low GRK2 levels (independent-samples Student's *t* test). (B) GRK2 levels were also associated with worse diastolic function, assessed by deceleration time (DT) (independent-samples Student's *t* test).

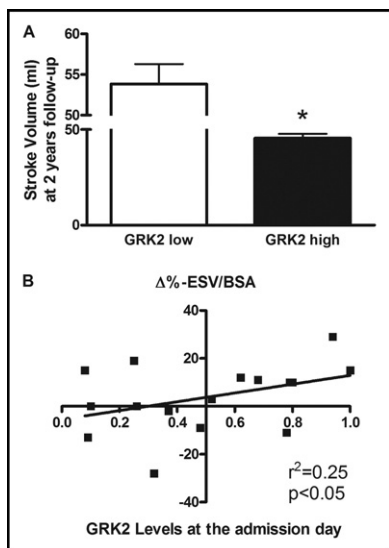


Figure 4. GRK2 levels and outcomes. (A) After 2 years, patients with higher GRK2 levels at admission had worse systolic function, with lower stroke volumes, than those with low GRK2 levels (independent-samples Student's *t* test). (B) Also, cardiac remodeling, assessed by the change in ESV after 2 years of follow-up ($\Delta\%$ -ESV/BSA) was correlated with GRK2 level at admission ($r^2 = 0.25$, $p < 0.05$).

and this trend was more evident in patients who received β blockers (Figure 2). Furthermore, when we considered the β -blocker group ($n = 24$ [75%]), some patients had reductions of GRK2 levels (responders, 62.5% [$n = 15$]), whereas others did not have reduced GRK2 levels after treatment (nonresponders, 37.5% [$n = 9$]) during the 2 days of observation. Of interest, nonresponders had worse wall motion score indexes (2.27 ± 0.23 vs 1.81 ± 0.1) than responders.

Table 3

Admission variables associated with long-term variation of end-systolic volume corrected by body surface area

Independent Variable at Admission	r^2	p Value
Shortening fraction	0.1636	0.045
Stroke volume	0.1885	0.030
Wall motion score index	0.2283	0.016
E/E' ratio	0.1611	0.047
Creatine kinase	0.4837	0.000
GRK2 level	0.2547	0.012

We found a relation between GRK2 levels at admission and stroke volume, a parameter of systolic function. Patients with high GRK2 levels had worse cardiac function, with lower stroke volumes, than those with low GRK2 levels (Figure 3). Furthermore, we found a relation between peripheral GRK2 levels and diastolic functional parameters such as deceleration time and the E/E' ratio. Indeed, at admission, patients with high GRK2 levels had lower deceleration times than those with low GRK2 levels (Figure 3).

Twenty-six patients (81.25%) completed 2-year follow-up. We found a relation between GRK2 levels on the first day of analysis and stroke volume. Indeed, after 2 years, patients with high GRK2 levels had worse cardiac function, with lower stroke volumes, than those with low GRK2 levels (Figure 4). Furthermore, we observed a correlation and a linear regression between admission GRK2 level and $\Delta\%$ -ESV/BSA (Figure 4). The most important admission variables associated with $\Delta\%$ -ESV/BSA were shortening fraction, stroke volume, wall motion score index, E/E' ratio, creatine kinase, and GRK2 level (Table 3). Multiple regression analysis conducted using a backward stepwise method including variables showing significant associations on univariate analysis ($p < 0.05$) revealed that admission GRK2 level ($p = 0.011$) was the best predictor of $\Delta\%$ -ESV/BSA.

Discussion

The present investigation sheds light on the role of GRK2 in acute MI. The first compelling evidence is that GRK2 increases quickly after STEMI. This increase had already been shown in experimental models of myocardial ischemia in the rat.¹² The deleterious effect of this kinase on β -adrenergic receptor signaling has been also explored in mice, showing that GRK2 gene deletion could prevent the development of post-MI HF and restore heart function.¹³

Another major finding of our work concerns the determinants affecting the increase in GRK2, in particular angioplasty and β -blocker therapy. To the best of our knowledge, this is the first study reporting that early reperfusion causes an increase in GRK2 level. Furthermore, the observation that β blockers are able to reduce GRK2 levels is somewhat consistent with previous reports,^{10,22,23} but we extend it to 2 essential novelties. First, GRK2 level at admission was associated with worse cardiac function acutely and after 2 years. Indeed, we found that patients with high GRK2 levels had worse systolic and diastolic function acutely and after 2 years. At 2-year follow-up, we found that patients with high GRK2 levels had lower stroke volumes and also increases in $\Delta\%$ -ESV/BSA (Figure 4)

compared to those with low GRK2 levels. These results can be justified by the negative inotropic implications of elevated GRK2 levels.^{10–14} Second, in our STEMI population, not all patients showed reduced GRK2 levels in response to β -blocker therapy, and interestingly, nonresponders had worse cardiac performance, suggesting the importance of early therapy with β blockers in patients with acute coronary syndromes.

Altogether, our results indicate that GRK2 is strictly associated with cardiac remodeling. Indeed, the implications of neurohormonal mechanisms in the progression of left ventricular remodeling have been extensively studied.^{5,24–26} It is well known that this process starts rapidly after MI, usually within the first few hours, sustained by activation of the sympathetic activity adrenergic response that, at least initially, provides support for the failing myocardium.^{5,24} Continuous activation of neurohormonal systems and adrenergic response, leading to excessive vasoconstriction and volume expansion, becomes deleterious to the heart, with progressive deterioration of cardiac function.²⁷ Classic measures to assess left ventricular remodeling include heart size, shape, and mass; ejection fraction; shortening fraction; and ESV. A recent study demonstrated that ESV is the strongest indicator of HF hospitalization in patients with coronary heart disease, being statistically superior to other echocardiographic measures of ventricular enlargement and systolic function such as the ejection fraction and shortening fraction.⁸ The close statistical relation between GRK2 and ESV supports the prognostic role of peripheral GRK2 levels. Therapeutic agents, such as β blockers, are superior to other classes of drugs to induce reverse remodeling, with a stronger correlation between dose and effect.^{28,29} It is therefore remarkable to note that β -blocker therapy can reduce GRK2 levels and that this phenomenon is associated with better cardiac function.²² Thus, GRK2 levels in the early stages of STEMI could provide valuable information about ventricular remodeling and progression toward HF.^{1,30} They may also constitute a valid tool to assess and monitor the efficacy of β blockers in patients with acute coronary syndromes, detecting those patients in need of more intensive treatment to improve their outcomes.^{28,30}

The most important limitation of this study was the small sample size, which prevented us from performing a statistical analysis on the basis of a hard end point (death or revascularization). A larger study would also have allowed stratification of the outcome according to β -blocker therapy. Moreover, we have no data on GRK2 levels at 2-year follow-up, and we did not perform a crossover analysis between patients treated with β blockers and those not treated. Further studies with larger populations are needed to validate our analysis. This task must be addressed through the development of a rapid bench test to quantify GRK2 levels in humans. Peripheral GRK levels could be used as a biomarker for monitoring prognosis and effectiveness of treatment in patients with STEMI. Indeed, biomarkers linked to mechanisms involved in the development of HF, such as GRK2, seem best suited for serving as early biologic markers to select therapy or assess progression. Further studies ongoing in our laboratory are actively pursuing this issue. Randomized trials are needed to address

this translational gap before the use of novel biomarkers becomes common practice to facilitate tailored treatment after an acute coronary event.

- Ramani GV, Uber PA, Mehra MR. Chronic heart failure: contemporary diagnosis and management. *Mayo Clin Proc* 2010;85:180–195.
- Yeh RW, Sidney S, Chandra M, Sorel M, Selby JV, Go AS. Population trends in the incidence and outcomes of acute myocardial infarction. *N Engl J Med* 2010;362:2155–2165.
- Acharjee S, Qin J, Murphy SA, McCabe C, Cannon CP. Distribution of traditional and novel risk factors and their relation to subsequent cardiovascular events in patients with acute coronary syndromes (from the PROVE IT-TIMI 22 trial). *Am J Cardiol* 2010;105:619–623.
- McCann CJ, Glover BM, Menown IB, Moore MJ, McEneny J, Owens CG, Smith B, Sharpe PC, Young IS, Adgey JA. Prognostic value of a multimarker approach for patients presenting to hospital with acute chest pain. *Am J Cardiol* 2009;103:22–28.
- Fertin M, Hennache B, Hamon M, Ennezat PV, Biaisque F, Elkohen M, Nugue O, Tricot O, Lamblin N, Pinet F, Bauters C. Usefulness of serial assessment of B-type natriuretic peptide, troponin I, and C-reactive protein to predict left ventricular remodeling after acute myocardial infarction (from the REVE-2 study). *Am J Cardiol* 2010;106:1410–1416.
- Wang TJ, Gona P, Larson MG, Tofler GH, Levy D, Newton-Cheh C, Jacques PF, Rifai N, Selhub J, Robins SJ, Benjamin EJ, D'Agostino RB, Vasan RS. Multiple biomarkers for the prediction of first major cardiovascular events and death. *N Engl J Med* 2006;355:2631–2639.
- Chen WC, Tran KD, Maisel AS. Biomarkers in heart failure. *Heart* 2010;96:314–320.
- McManus DD, Shah SJ, Fabi MR, Rosen A, Whooley MA, Schiller NB. Prognostic value of left ventricular end-systolic volume index as a predictor of heart failure hospitalization in stable coronary artery disease: data from the Heart and Soul Study. *J Am Soc Echocardiogr* 2009;22:190–197.
- Sabatine MS, Morrow DA, de Lemos JA, Gibson CM, Murphy SA, Rifai N, McCabe C, Antman EM, Cannon CP, Braunwald E. Multi-marker approach to risk stratification in non-ST elevation acute coronary syndromes: simultaneous assessment of troponin I, C-reactive protein, and B-type natriuretic peptide. *Circulation* 2002;105:1760–1763.
- Iaccarino G, Tomhave ED, Lefkowitz RJ, Koch WJ. Reciprocal in vivo regulation of myocardial G protein-coupled receptor kinase expression by beta-adrenergic receptor stimulation and blockade. *Circulation* 1998;98:1783–1789.
- Hata JA, Williams ML, Schroder JN, Lima B, Keys JR, Blaxall BC, Petrofski JA, Jakoi A, Milano CA, Koch WJ. Lymphocyte levels of GRK2 (betaARK1) mirror changes in the LVAD-supported failing human heart: lower GRK2 associated with improved beta-adrenergic signaling after mechanical unloading. *J Card Fail* 2006;12:360–368.
- Ungerer M, Kessebohm K, Kronsbein K, Lohse MJ, Richardt G. Activation of beta-adrenergic receptor kinase during myocardial ischemia. *Circ Res* 1996;79:455–460.
- Raake PW, Vinge LE, Gao E, Boucher M, Rengo G, Chen X, De-George BR Jr, Matkovich S, Houser SR, Most P, Eckhart AD, Dorn GW II, Koch WJ. G protein-coupled receptor kinase 2 ablation in cardiac myocytes before or after myocardial infarction prevents heart failure. *Circ Res* 2008;103:413–422.
- Iaccarino G, Barbato E, Cipolletta E, De Amicis V, Margulies KB, Leosco D, Trimarco B, Koch WJ. Elevated myocardial and lymphocyte GRK2 expression and activity in human heart failure. *Eur Heart J* 2005;26:1752–1758.
- Mangiapapa F, Muller O, Ntalianis A, Trana C, Heyndrickx GR, Bartunek J, Vanderheyden M, Wijns W, De Bruyne B, Barbato E. Comparison of 600 versus 300-mg Clopidogrel loading dose in patients with ST-segment elevation myocardial infarction undergoing primary coronary angioplasty. *Am J Cardiol* 2010;106:1208–1211.
- Galasso G, Santulli G, Piscione F, De Rosa R, Trimarco V, Piccolo R, Cassese S, Iaccarino G, Trimarco B, Chiariello M. The GPIIIa P1A2 polymorphism is associated with an increased risk of cardiovascular adverse events. *BMC Cardiovasc Disord* 2010;10:41.
- Izzo R, Cipolletta E, Ciccarelli M, Campanile A, Santulli G, Palumbo G, Vasta A, Formisano S, Trimarco B, Iaccarino G. Enhanced GRK2

- expression and desensitization of betaAR vasodilatation in hypertensive patients. *Clin Transl Sci* 2008;1:215–220.
18. Lasorella A, Stegmüller J, Guardavaccaro D, Liu G, Carro MS, Rothschild G, de la Torre-Ubieta L, Pagano M, Bonni A, Iavarone A. Degradation of Id2 by the anaphase-promoting complex couples cell cycle exit and axonal growth. *Nature* 2006;442:471–474.
 19. Santulli G, Ciccarelli M, Palumbo G, Campanile A, Galasso G, Ziaco B, Altobelli GG, Cimini V, Piscione F, D'Andrea LD, Pedone C, Trimarco B, Iaccarino G. In vivo properties of the proangiogenic peptide QK. *J Transl Med* 2009;7:41.
 20. Lanni F, Santulli G, Izzo R, Rubattu S, Zanda B, Volpe M, Iaccarino G, Trimarco B. The Pl(A1/A2) polymorphism of glycoprotein IIIa and cerebrovascular events in hypertension: increased risk of ischemic stroke in high-risk patients. *J Hypertens* 2007;25:551–556.
 21. Brinks H, Boucher M, Gao E, Chuprun JK, Pesant S, Raake PW, Huang ZM, Wang X, Qiu G, Gumpert A, Harris DM, Eckhart AD, Most P, Koch WJ. Level of G protein-coupled receptor kinase-2 determines myocardial ischemia/reperfusion injury via pro- and anti-apoptotic mechanisms. *Circ Res* 2010;107:1140–1149.
 22. Leineweber K, Rohe P, Beilfuss A, Wolf C, Sporkmann H, Bruck H, Jakob HG, Heusch G, Philipp T, Brodde OE. G-protein-coupled receptor kinase activity in human heart failure: effects of beta-adrenergic blockade. *Cardiovasc Res* 2005;66:512–519.
 23. Santulli G, Lombardi A, Sorriento D, Anastasio A, Iovino S, Del Giudice C, Miele C, Formisano P, Iaccarino G. Beta 2 adrenergic knock-out mice develop insulin resistance. *Eur Heart J* 2010;31:936.
 24. Lympopoulos A, Rengo G, Gao E, Ebert SN, Dorn GW II, Koch WJ. Reduction of sympathetic activity via adrenal-targeted GRK2 gene deletion attenuates heart failure progression and improves cardiac function after myocardial infarction. *J Biol Chem* 2010;285:16378–16386.
 25. Sorriento D, Santulli G, Fusco A, Anastasio A, Trimarco B, Iaccarino G. Intracardiac injection of AdGRK5-NT reduces left ventricular hypertrophy by inhibiting NF-kappaB-dependent hypertrophic gene expression. *Hypertension* 2010;56:696–704.
 26. Santulli G, Illario M, Cipolletta E, Sorriento D, Del Giudice C, Anastasio A, Trimarco B, Iaccarino G. Deletion of the CaMK4 gene in mice determines a hypertensive phenotype. *Cardiovasc Res* 2010;87:89.
 27. Rengo G, Leosco D, Zincarelli C, Marchese M, Corbi G, Liccardo D, Filippelli A, Ferrara N, Lisanti MP, Koch WJ, Lympopoulos A. Adrenal GRK2 lowering is an underlying mechanism for the beneficial sympathetic effects of exercise training in heart failure. *Am J Physiol Heart Circ Physiol* 2010;298:H2032–H2038.
 28. Frigerio M, Roubina E. Drugs for left ventricular remodeling in heart failure. *Am J Cardiol* 2005;96(suppl):10L–18L.
 29. Udelson JE. Ventricular remodeling in heart failure and the effect of beta-blockade. *Am J Cardiol* 2004;93(suppl):43B–48B.
 30. Abraham WT, Greenberg BH, Yancy CW. Pharmacologic therapies across the continuum of left ventricular dysfunction. *Am J Cardiol* 2008;102(suppl):21G–28G.



RESEARCH

Open Access

Evaluation of the anti-angiogenic properties of the new selective $\alpha_v\beta_3$ integrin antagonist RGDechiHCit

Gaetano Santulli¹, Maria Felicia Basilicata¹, Mariarosaria De Simone², Carmine Del Giudice¹, Antonio Anastasio¹, Daniela Sorriento¹, Michele Saviano³, Annarita Del Gatto⁴, Bruno Trimarco¹, Carlo Pedone², Laura Zaccaro⁴, Guido Iaccarino^{1*}

Abstract

Background: Integrins are heterodimeric receptors that play a critical role in cell-cell and cell-matrix adhesion processes. Among them, $\alpha_v\beta_3$ integrin, that recognizes the aminoacidic RGD triad, is reported to be involved in angiogenesis, tissue repair and tumor growth. We have recently synthesized a new and selective ligand of $\alpha_v\beta_3$ receptor, referred to as RGDechiHCit, that contains a cyclic RGD motif and two echistatin moieties.

Methods: The aim of this study is to evaluate *in vitro* and *in vivo* the effects of RGDechiHCit. Therefore, we assessed its properties in cellular (endothelial cells [EC], and vascular smooth muscle cells [VSMC]) and animal models (Wistar Kyoto rats and c57Bl/6 mice) of angiogenesis.

Results: In EC, but not VSMC, RGDechiHCit inhibits intracellular mitogenic signaling and cell proliferation. Furthermore, RGDechiHCit blocks the ability of EC to form tubes on Matrigel. *In vivo*, wound healing is delayed in presence of RGDechiHCit. Similarly, Matrigel plugs demonstrate an antiangiogenic effect of RGDechiHCit.

Conclusions: Our data indicate the importance of RGDechiHCit in the selective inhibition of endothelial $\alpha_v\beta_3$ integrin *in vitro* and *in vivo*. Such inhibition opens new fields of investigation on the mechanisms of angiogenesis, offering clinical implications for treatment of pathophysiological conditions such as cancer, proliferative retinopathy and inflammatory disease.

Introduction

Angiogenesis is a complex multistep phenomenon consisting of the sprouting and the growth of new capillary blood vessels starting from the pre-existing ones. It requires the cooperation of several cell types such as endothelial cells (ECs), vascular smooth muscle cells (VSMCs), macrophages, which should be activated, proliferate and migrate to invade the extracellular matrix and cause vascular remodeling [1,2]. The angiogenic process is finely tuned by a precise balance of growth and inhibitory factors and in mammals it is normally dormant except for some physiological conditions, such as wound healing and ovulation. When this balance is

altered, excessive or defective angiogenesis occur and the process becomes pathological. Excessive angiogenesis gives also rise to different dysfunctions, including cancer, eye diseases, rheumatoid arthritis, atherosclerosis, diabetic nephropathy, inflammatory bowel disease, psoriasis, endometriosis, vasculitis, and vascular malformations [3]. Therefore the discovery of angiogenesis inhibitors would contribute to the development of therapeutic treatments for these diseases.

The integrins are cell adhesion receptors that mediate cell-cell and cell-matrix interactions and coordinate signaling allowing a close regulation of physiological phenomena including cellular migration, proliferation and differentiation. In particular, the α_v integrins, combined with distinct β subunits, participate in the angiogenic process. An extensively studied member of this receptor class is integrin $\alpha_v\beta_3$, that is strongly overexpressed in

* Correspondence: guiaccar@unina.it

¹Department of Clinical Medicine, Cardiovascular & Immunologic Sciences, "Federico II" University of Naples, Italy

Full list of author information is available at the end of the article

activated EC, melanoma, glioblastoma and prostate cancers and in granulation tissue, whereas is not detectable in quiescent blood vessels or in the dermis and epithelium of normal skin [4-6]. This integrin participates in the activation of vascular endothelial growth factor receptor-2 (VEGFR-2), providing a survival signal to the proliferating vascular cells during new vessel growth [7,8] and also seems to be essential in the step of vacuolation and lumen formation [9]. It has been also reported that $\alpha_v\beta_3$ is under the tight control of VEGF: this integrin is not expressed in quiescent vessels [10], but VEGF induces $\alpha_v\beta_3$ expression *in vitro* and, interestingly, the VEGF and $\alpha_v\beta_3$ integrin expression are highly correlated *in vivo* [11,12]. Therefore, $\alpha_v\beta_3$ should be considered a tumor and activated endothelium marker.

$\alpha_v\beta_3$ is able of recognizing many proteins of the extracellular matrix, bearing an exposed Arg-Gly-Asp (RGD) tripeptide [5,13,14]. Even if different integrins recognize different proteins containing the RGD triad, many studies have demonstrated that the aminoacids flanking the RGD sequence of high-affinity ligands appear to be critical in modulating their specificity of interaction with integrin complexes [15,16].

Several molecules including peptides containing RGD motif [11] have been recently developed as inhibitors of $\alpha_v\beta_3$ integrin, in experiments concerning tumor angiogenesis, showing a reduction of functional vessel density associated with retardation of tumor growth and metastasis formation [6,17]. So far, the pentapeptide c(RGDf[NMe]V), also known as cilengitide (*EMD 121974*), is the most active $\alpha_v\beta_3/\alpha_v\beta_5$ antagonist reported in literature [18,19] and is in phase III clinical trials as antiangiogenic drug for glioblastoma therapy [15]. The development of more selective antiangiogenic molecule would help to minimize the side-effects and increase the therapeutic effectiveness.

We have recently designed and synthesized a novel and selective peptide antagonist, referred to as RGDechiHCit, to visualize $\alpha_v\beta_3$ receptor on tumour cells [20]. It is a chimeric peptide containing a cyclic RGD motif and two echistatin C-terminal moieties covalently linked by spacer sequence. Cell adhesion assays have shown that RGDechiHCit selectively binds $\alpha_v\beta_3$ integrin and does not cross-react with $\alpha_v\beta_5$ and $\alpha_{IIb}\beta_3$ integrins [20]. Furthermore, PET and SPECT imaging studies have confirmed that the peptide localizes on $\alpha_v\beta_3$ expressing tumor cells in xenograft animal model [21]. Since $\alpha_v\beta_3$ is also a marker of activated endothelium, the main purpose of this study was to evaluate *in vitro* and *in vivo* effects of RGDechiHCit on neovascularization. Thus, we first assessed the *in vitro* peptide properties on bovine

aortic ECs, and then *in vivo*, in Wistar Kyoto (WKY) rats and c57BL/6 mice, the ability of this cyclic peptide to inhibit angiogenesis.

Methods

Peptides

RGDechiHCit was prepared for the *in vitro* and *in vivo* studies as previously described [20]. To test the biological effects of RGDechiHCit, we synthesized the cyclic pentapeptide c(RGDf[NMe]V), also known as cilengitide or *EMD 121974* [14,19]. We also investigated RGDechiHCit and c(RGDf[NMe]V) peptides degradation in serum. Both peptides were incubated and the resulting solutions were analyzed by liquid chromatography/mass spectrometry (LC/MS) at different times. 20 μ L of human serum (Lonza, Basel, Switzerland) were added to 8 μ L of a 1 mg/ml solution of either RGDechiHCit or c(RGDf[NMe]V) at 37°C. After 1, 2, 4 and 24h, samples were centrifuged for 1min at 10000g. Solutions were analyzed by LCQ Deca XP Max LC/MS system equipped with a diode-array detector combined with an electrospray ion source and ion trap mass analyzer (ThermoFinnigan, San Jose, CA, USA), using a Phenomenex C₁₈ column (250 \times 2 mm; 5 μ m; 300 Å) and a linear gradient of H₂O (0.1%TFA)/CH₃CN (0.1%TFA) from 10 to 80% of CH₃CN (0.1%TFA) in 30 min at flow rate of 200 μ L/min.

In vitro studies

In vitro studies were performed on cell cultures of ECs or VSMCs, cultured in Dulbecco's modified Eagle's medium (DMEM; Sigma-Aldrich, Milan, Italy) as previously described and validated [22,23]. Cell culture plates were filled with 10 μ g/cm² of human fibronectin (hFN, Millipore[®], Bedford, MA, USA) as described [24]. All experiments were performed in triplicate with cells between passages 5 and 9.

Cell proliferation assay

Cell cultures were prepared as previously described [25]. Briefly, cells were seeded at density of 100000 per well in six-well plates, serum starved, pre-incubated at 37°C for 30' with c(RGDf[NMe]V) or RGDechiHCit (10⁻⁶ M). Proliferation was induced using hFN (100 μ g/ml). Cell number was measured at 3, 6 and 20 h after stimulation as previously described [26,27].

DNA synthesis

DNA synthesis was assessed as previously described [27]. Briefly, cells were serum-starved for 24 h and then incubated in DMEM with [³H]thymidine and 5% FBS. After 3, 6 and 20 h, cells were fixed with trichloroacetic acid (0.05%) and dissolved in 1M NaOH. Scintillation

liquid was added and [³H]thymidine incorporation was assessed as previously described [27].

VEGF quantification

VEGF production was measured as previously described [26]. Briefly, ECs were seeded at a density of 600000 per well in six well plates, serum starved overnight, seeded with c(RGDf[NMe]V) or RGDechiHCit (10^{-6} M) and then stimulated with hFN for 6 hours. Cultured medium was collected and VEGF production was revealed by western blot.

Endothelial Matrigel assay

The formation of network-like structures by ECs on an extracellular matrix (ECM)-like 3D gel consisting of Matrigel[®] (BD Biosciences, Bedford, MA, USA), was performed as previously described and validated [27,28]. The six-well multidishes were coated with growth factor-reduced Matrigel in according to the manufacturer's instructions. ECs (5×10^4) were seeded with c(RGDf[NMe]V) or RGDechiHCit (10^{-6} M), in the absence (negative control) or presence (100 µg/ml) of hFN [24]. Cells were incubated at 37°C for 24h in 1 ml of DMEM. After incubation, ECs underwent differentiation into capillary-like tube structures. Tubule formation was defined as a structure exhibiting a length four times its width [27]. Network formation was observed using an inverted phase-contrast microscope (Zeiss). Representative fields were taken, and the average of the total number of complete tubes formed by cells was counted in 15 random fields by two independent investigators.

Western blot

Immunoblot analyses were performed as previously described and validated [23,28]. Mouse monoclonal antibodies to extracellular signal regulated kinase (ERK2) and phospho-ERK, anti-rabbit VEGF and actin were from Santa Cruz Biotechnology (Santa Cruz, CA, USA). Levels of VEGF were determined using an antibody raised against VEGF-165 (Santa Cruz Biotechnology) [26]. Experiments were performed in triplicate to ensure reproducibility. Data are presented as arbitrary densitometry units (ADU) after normalization for the total corresponding protein or actin as internal control [24].

In vivo studies

Wound healing assay was performed on 14-week-old (weight 293 ± 21 g) normotensive WKY male rats (Charles River Laboratories, Calco (LC), Italy; n = 18), and Matrigel plugs experiments were carried out on 16-week-old (weight 33 ± 4 g) c57BL/6 mice (Charles River Laboratories, Milan, Italy; n = 13). All animal procedures were performed in accordance with the *Guide for*

the Care and Use of Laboratory Animals published by the National Institutes of Health in the United States (NIH Publication No. 85- 23, revised 1996) and approved by the Ethics Committee for the Use of Animals in Research of "Federico II" University [23].

Wound Healing

The rats (n = 18) were anesthetized using vaporized isoflurane (4%, Abbott) and maintained by mask ventilation (isoflurane 1.8%) [29]. The dorsum was shaved by applying a depilatory creme (Veet, Reckitt-Benckiser, Milano, Italy) and disinfected with povidone iodine scrub. A 20 mm diameter open wound was excised through the entire thickness of the skin, including the *panniculus carnosus* layer, as described and validated [1,28]. Pluronic gel (30%) containing (10^{-6} M) c(RGDf[NMe]V) (n = 6), RGDechiHCit (n = 7), or saline (n = 5) was placed daily directly onto open wounds, then covered with a sterile dressing. Two operators blinded to the identity of the sample examined and measured wound areas every day, for 8 days. Direct measurements of wound region were determined by digital planimetry (pixel area), and subsequent analysis was performed using a computer-assisted image analyzer (ImageJ software, version 1.41, National Institutes of Health, Bethesda, MD, USA). Wound healing was quantified as a percentage of the original injury size. Eight days after wounding, rats were euthanized. Wounds did not show sign of infection. The lesion and adjacent normal skin were excised, fixed by immersion in phosphate buffered saline (PBS, 0.01 M, pH 7.2-7.4)/formalin and then embedded in paraffin to be processed for immunohistology, as described [1].

Matrigel Plugs

Mice (n = 13), anesthetized as described above, were subcutaneously injected midway on the dorsal side, using sterile conditions, with 0.2 ml of Matrigel[®] basement matrix, pre-mixed with 10^{-6} M VEGF and 10^{-5} M c(RGDf[NMe]V) (n = 4), 10^{-6} M VEGF and 10^{-5} M RGDechiHCit (n = 5), or 10^{-6} M VEGF alone (n = 4). After seven days, mice were euthanized and the implanted plugs were harvested from underneath the skin, fixed in 10% neutral-buffered formalin solution and then embedded in paraffin. Invading ECs were identified and quantified by analysis of lectin immunostained sections, as described [1,2].

Histology

All tissues were cut in 5 µm sections and slides were counterstained with a standard mixture of hematoxylin and eosin. For Masson's trichrome staining of collagen fibers, useful to assess the scar tissue formation, slides were stained with Weigert Hematoxylin (Sigma-Aldrich,

St. Louis, MO, USA) for 10 minutes, rinsed in PBS (Invitrogen) and then stained with Biebrich scarlet-acid fuchsin (Sigma-Aldrich) for 5 minutes. Slides were rinsed in PBS and stained with phosphomolybdic/phosphotungstic acid solution (Sigma-Aldrich) for 5 minutes then stained with light green (Sigma-Aldrich) for 5 minutes [30]. ECs were identified by lectin immunohistochemical staining (Sigma-Aldrich) [2] and quantitative analysis was performed using digitized representative high resolution photographic images, with a dedicated software (Image Pro Plus; Media Cybernetics, Bethesda, MD, USA) as previously described [28].

Data presentation and statistical analysis

All data are presented as the mean value \pm SEM. Statistical differences were determined by one-way or two-way ANOVA and Bonferroni post hoc testing was performed where applicable. A p value less than 0.05 was considered to be significant. All the statistical analysis and the evaluation of data were performed using GraphPad Prism version 5.01 (GraphPad Software, San Diego, CA, USA).

Results

Peptides

RGDechiHCit and c(RGDf[NMe]V) peptides stabilities were evaluated in serum. The degradation of the peptides were followed by LC/MS. The reversed-phase high performance liquid chromatography (RP-HPLC) of RGDechiHCit before the serum incubation showed a single peak at $t_r = 11.82$ min corresponding to the complete sequence (theoretical MW = 2100.1 g mol⁻¹) as indicated by the $[M+H]^+$, $[M+2H]^{2+}$ and $[M+3H]^{3+}$ molecular ion adducts in the MS spectrum (Figure 1A). After 1h, chromatography showed two peaks, ascribable to RGDechiHCit and to a fragment of the complete sequence (theoretical MW = 1929.1 g mol⁻¹), respectively, as confirmed by MS spectrum. Finally, after 24h a further peak at $t_r = 10.93$ min corresponding to another RGDechiHCit degradation product (theoretical MW = 1775.8 g mol⁻¹) appeared, as indicated by the molecular ion adducts in the MS spectrum, although the peaks attributed to the RGDechiHCit and to the first fragment were still present (Figure 1B).

In contrast with RGDechiHCit, c(RGDf[NMe]V) showed high stability in serum. The RP-HPLC profile of the peptide before the incubation showed a single peak at $t_r = 16.64$ min, ascribable to the complete sequence by the MS spectrum (Figure 1C). After 24h of incubation chromatogram and mass profiles failed to identify any degradation product (Figure 1D).

Since RGDechiHCit showed a low stability, we replenished antagonists every six hours in experiments involving chronic exposure.

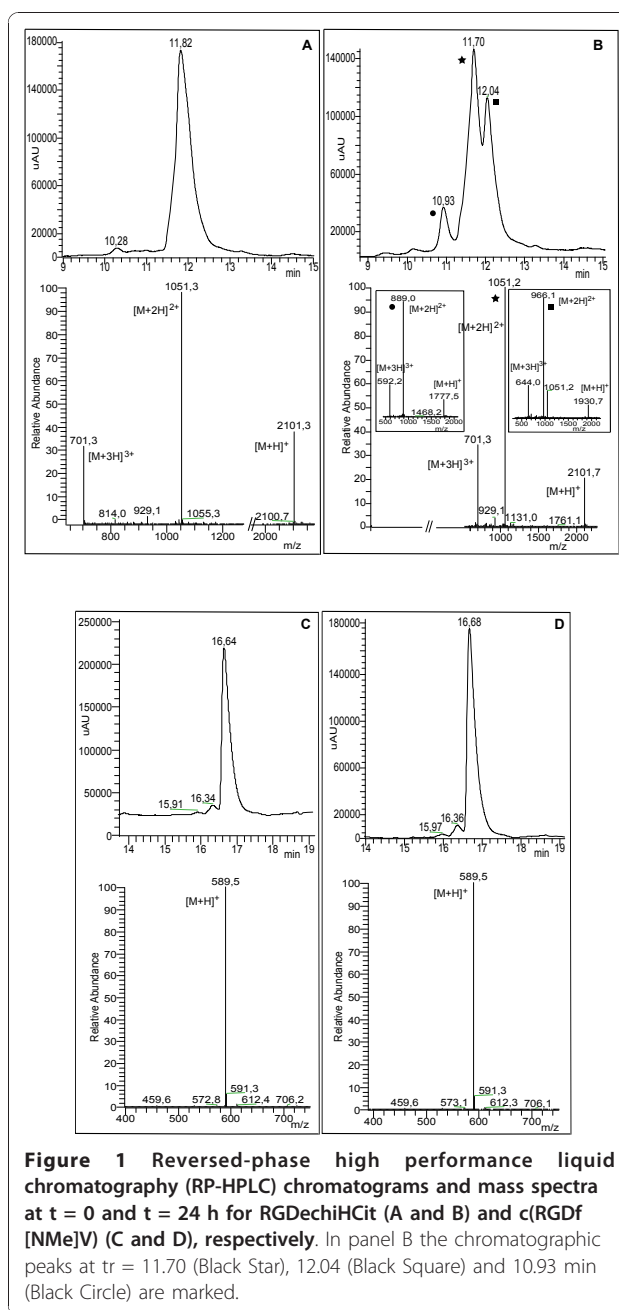


Figure 1 Reversed-phase high performance liquid chromatography (RP-HPLC) chromatograms and mass spectra at $t = 0$ and $t = 24$ h for RGDechiHCit (A and B) and c(RGDf[NMe]V) (C and D), respectively. In panel B the chromatographic peaks at $t_r = 11.70$ (Black Star), 12.04 (Black Square) and 10.93 min (Black Circle) are marked.

In vitro experiments

Cell proliferation and DNA synthesis

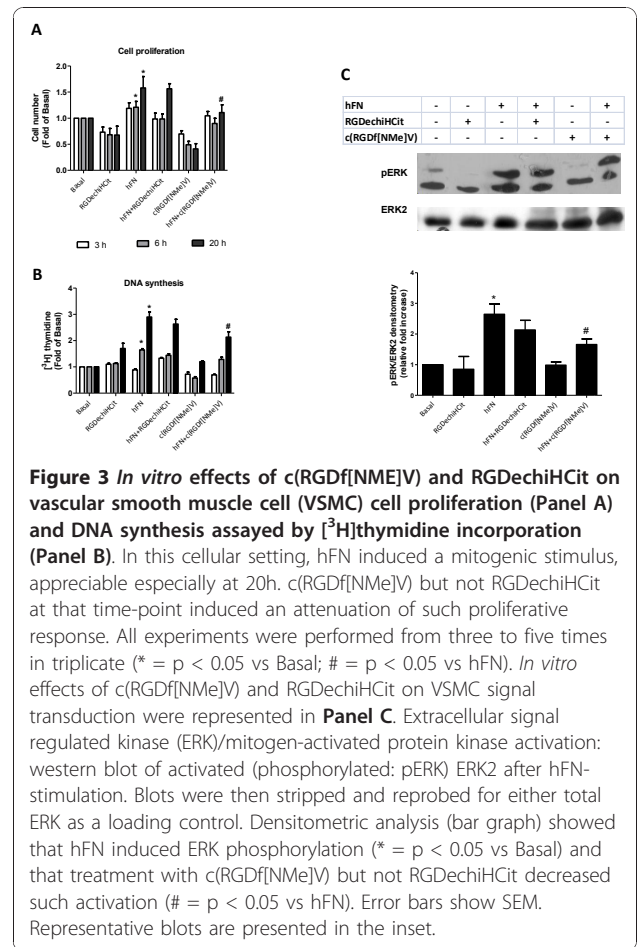
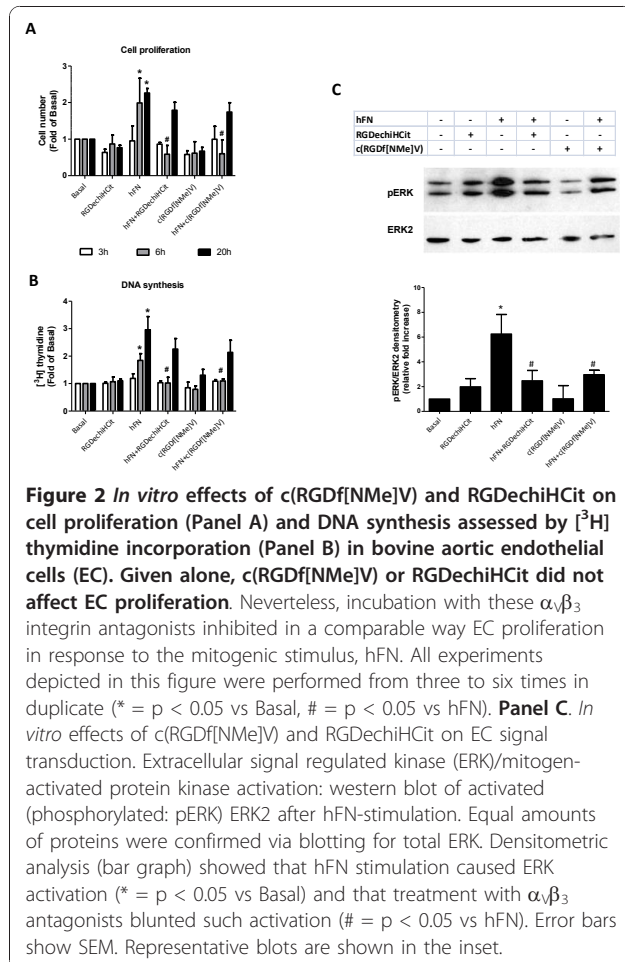
Because angiogenesis is intimately associated to EC proliferation, we explored the effects of RGDechiHCit and c(RGDf[NMe]V) on hFN-stimulated EC. In this cellular setting, after 6 hours, both $\alpha_v\beta_3$ integrin antagonists inhibited in a comparable way the ability of hFN to induce proliferation (hFN: $+1.98 \pm 0.6$; hFN+RGDechiHCit: $+0.58 \pm 0.24$; hFN+c(RGDf[NMe]V): $+0.6 \pm 0.38$ fold over basal; $p < 0.05$, ANOVA) as depicted in Figure

2A. After 20 hours such inhibitory effect was less marked (Figure 2A). In VSMC there was only a trend of an anti-proliferative effect for these peptides, due to the less evident action of hFN in this specific cellular setting (hFN: $+1.21 \pm 0.1$; hFN+RGDechiHCit: $+0.93 \pm 0.07$; hFN+c(RGDf[NMe]V): $+0.9 \pm 0.09$ fold over basal; NS; Figure 3A).

The effects of RGDechiHCit and c(RGDf[NMe]V) on EC and VSMC proliferation were also measured by assessing the incorporation of [³H]Thymidine in response to hFN. This assay confirmed the anti-proliferative action of both these peptides, which is more evident after 6 hours and in ECs (hFN: $+1.84 \pm 0.24$; hFN+RGDechiHCit: $+1.02 \pm 0.2$; hFN+c(RGDf[NMe]V): $+1.09 \pm 0.07$ fold over basal; $p < 0.05$, ANOVA; Figure 2B). On the contrary, the effect of RGDechiHCit on VSMC did not reach statistical significance in comparison to the c(RGDf[NMe]V) used as control (Figure 3B).

Effects on cellular signal transduction

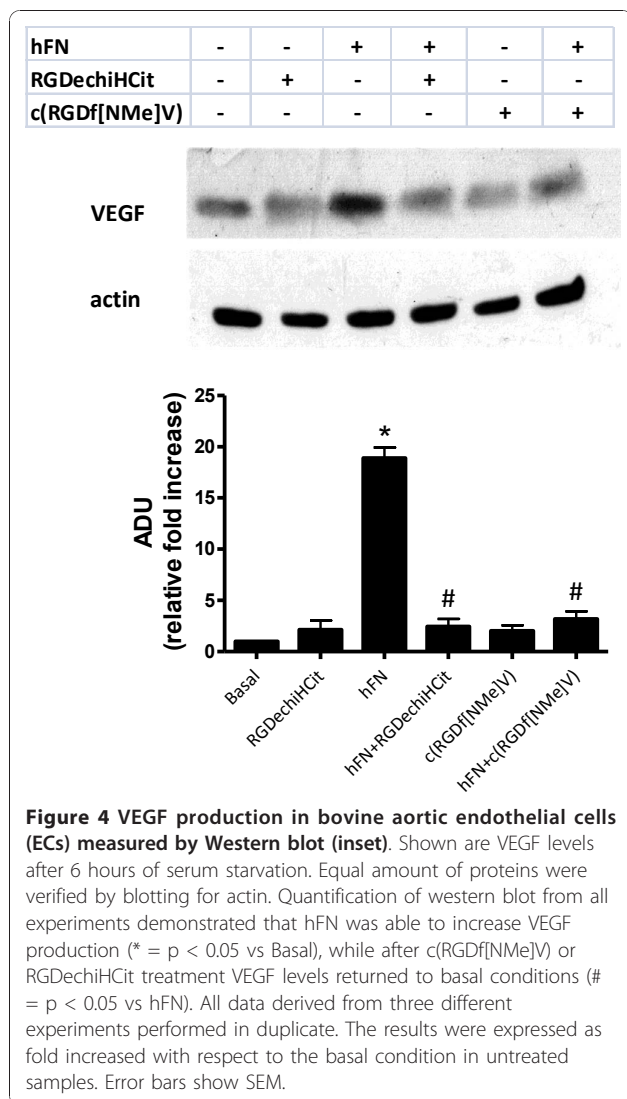
Since hFN-mediated activation of ERK2 is linked to angiogenesis [16,24,31], we analyzed the ability of



RGDechiHCit and c(RGDf[NMe]V) to inhibit hFN-induced phosphorylation of ERK2 in EC and VSMC. In accordance with the results on cell proliferation and [³H]Thymidine incorporation, in EC both RGDechiHCit and c(RGDf[NMe]V) significantly inhibited the hFN-induced phosphorylation of mitogen-activated protein ERK2 (Figure 2C). Also, in VSMC, there was no significant inhibition of ERK2 phosphorylation by the RGDechiHCit compound c(RGDf[NMe]V) (Figure 3C).

Evaluation of VEGF expression

Angiogenesis is largely dependent on ERK2 activation, which in turn promotes cellular proliferation and expression of VEGF. This cytokine promotes infiltration of inflammatory cells, proliferation of ECs and VSMCs and sustains the proangiogenic phenotype [12]. The early release (6 hours) of the cytokine is therefore an important readout when studying angiogenesis *in vitro*. On these grounds, we assessed the expression levels of this pivotal proangiogenic factor in EC after 6 hours of stimulation with hFN. hFN induces VEGF release and such response was blunted by incubation with either integrin antagonist, as depicted in Figure 4

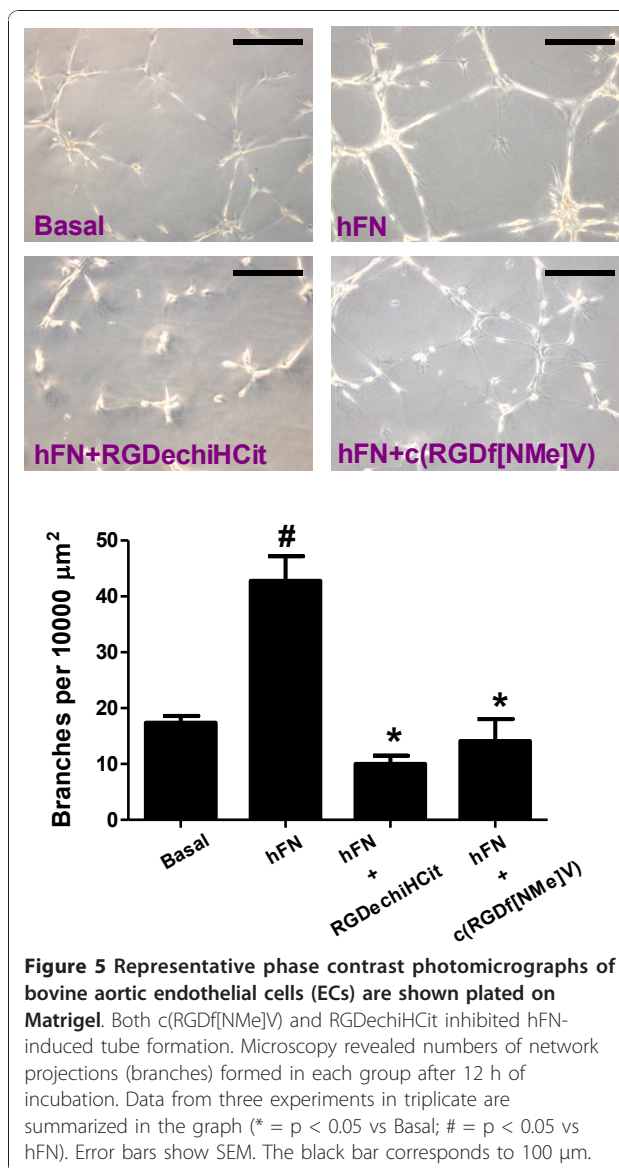


(hFN: $+18.9 \pm 1.02$; hFN+RGDechiHCit: $+2.44 \pm 0.76$; hFN+c(RGDf[NMe]V): $+3.19 \pm 0.73$ fold over basal, ADU; $p < 0.05$, ANOVA).

Endothelial Matrigel assay

The formation of capillary-like tube structures in the ECM by ECs is a pivotal step in angiogenesis and is also involved in cell migration and invasion [26]. To evaluate any potential antiangiogenic activity of our novel integrin antagonist, *in vitro* angiogenesis assays were conducted by evaluating hFN-induced angiogenesis of ECs on Matrigel.

As shown in Figure 5, when ECs were plated on wells coated with Matrigel without the addition of hFN, they showed formation of only a few spontaneous tube structures (17.4 ± 1.2 branches per $10000 \mu\text{m}^2$). On the other hand, when the cells were plated on Matrigel with the addition of hFN, cells formed a characteristic



capillary-like network (42.8 ± 4.4 branches per $10000 \mu\text{m}^2$; $p < 0.05$ vs Basal, ANOVA). In the presence of RGDechiHCit or c(RGDf[NMe]V), the extent of tube formation hFN-induced was significantly reduced (10.03 ± 1.44 ; 14.11 ± 3.9 , respectively; $p < 0.05$ vs hFN alone, ANOVA; Figure 5).

In vivo experiments

Wound healing

The examination of full-thickness wounds in the back skin showed that both RGDechiHCit and c(RGDf[NMe]V) slowed down healing (Figure 6). At a macroscopic observation, the delay in the wound healing in treated rats was evident, with raised margins, more extensive wound debris and scab, that persisted for at least 7 days after surgery. Moreover, histological

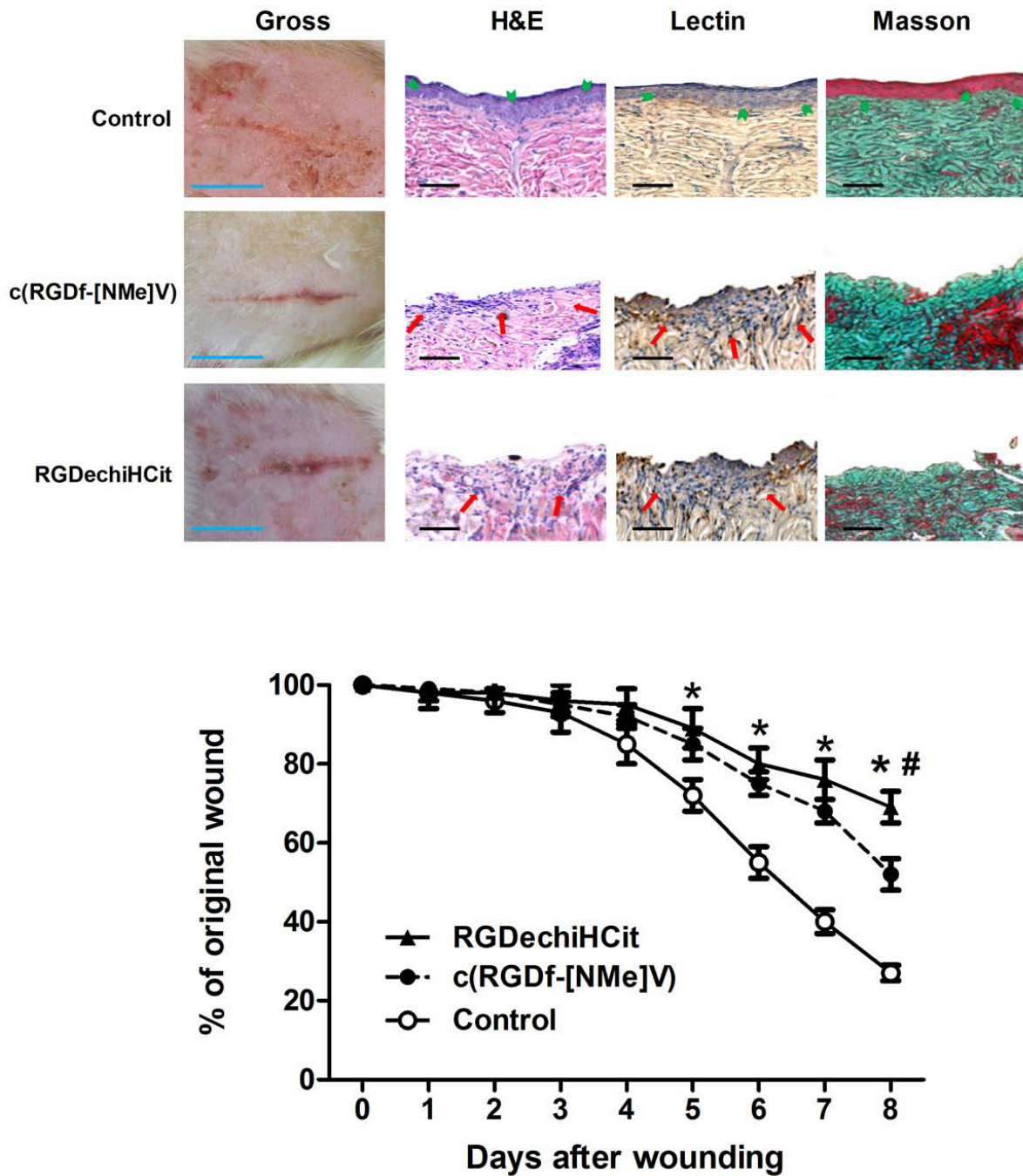
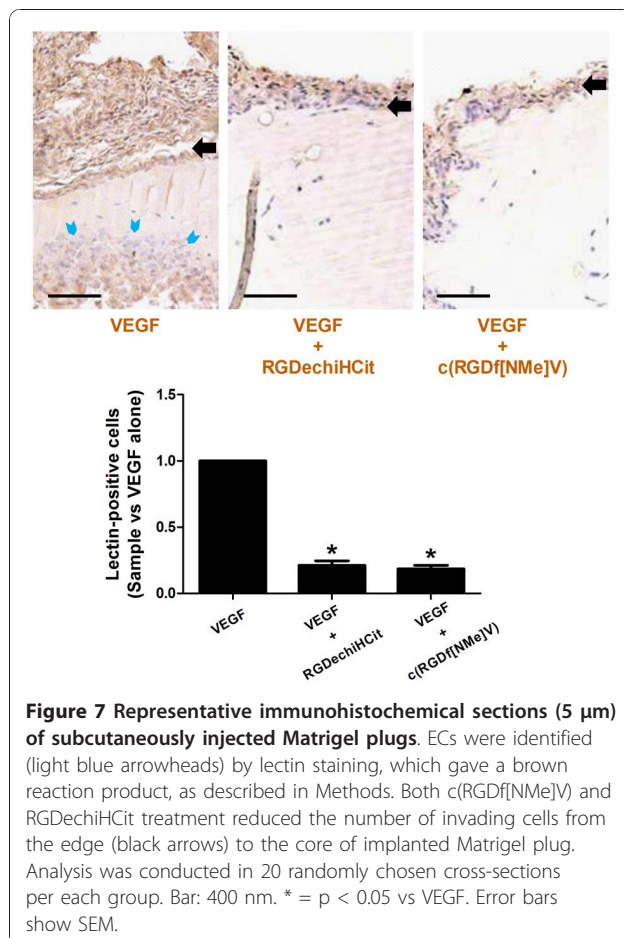


Figure 6 Both c(RGDf[NMe]V) and RGDechiHCit slowed down the closure of full thickness punch biopsy wounds. Three to five rats were analyzed at each time point. Gross appearance (representative digital photographs, light blue bar: 1 cm) after 5 days of the wound treated with pluronic gel containing c(RGDF-[NMe]V), RGDechiHCit (10^{-6} M) or saline. Diagram of the kinetics of wound closure; * = $p < 0.05$ vs Control; # = $p < 0.05$ vs c(RGDF-[NMe]V, ANOVA). Error bars show SEM. Representative sections (5 μ m) of wounds excised 8 days after surgery (see Methods): Hematoxylin & Eosin, Lectin immunohistochemistry, Masson's trichrome; black bar: 100 μ m. Histological analysis revealed a retarded repair pattern in treated rats, which is consistent with inhibition of angiogenesis in the granulation tissue. In particular, in control animals, epidermal cell growth achieved complete re-epithelialization (green arrowheads) and there was a well defined fibrous core of scar tissue. Both in c(RGDF[NMe]V) and RGDechiHCit treated rats there was a chronic inflammatory infiltrate (red arrows) and lectin staining showed (in brown) the presence of vessels in the granulation tissue.

analysis showed that while control rats presented a dermal scar tissue consisting of a well defined and organized fibrous core with minimal chronic inflammatory cells, skin wounds exposed to RGDechiHCit or c(RGDf[NMe]V) exhibited a retarded repair pattern. Indeed, there was an intense inflammatory infiltrate, extended from the wound margin into the region of the *panniculus carnosus* muscle and hypodermis. Moreover, the basal epidermis was disorganized and epidermal cell growth failed to achieve re-epithelialization, as shown in Figure 6.

Matrigel plugs

After injection, Matrigel implants containing the angiogenic stimulant VEGF (10^{-5} M) formed a plug into which ECs can migrate. Matrigel pellets evidenced a significant lower EC infiltration, identified through means of immunohistochemical lectin staining, in c(RGDf[NMe]V) and RGDechiHCit treated plugs respect to VEGF alone (VEGF+RGDechiHCit: 0.211 ± 0.034 ; VEGF+c(RGDf[NMe]V): 0.185 ± 0.027 fold over VEGF alone; $p < 0.05$, ANOVA), as depicted in Figure 7.



Discussion

In the present study, we evaluated the anti-angiogenic properties of RGDechiHCit peptide *in vitro* on EC and VSMC cells and *in vivo* on animal models of rats and mice. The data here reported recapitulate the well-known antiangiogenic properties of c(RGDf[NMe]V), that was used as control. We previously described the design and synthesis of RGDechiHCit, a novel and selective ligand for $\alpha_v\beta_3$ integrin, containing a cyclic RGD motif and two echistatin C-terminal moieties [20]. *In vitro* studies showed that this molecule is able to selectively bind $\alpha_v\beta_3$ integrin and not to cross-react with other type of integrins. Furthermore, PET and SPECT imaging studies have confirmed that the peptide localizes on $\alpha_v\beta_3$ expressing tumor cells in xenograft animal model [21]. Given the presence in the molecule of the RGD sequence it was obvious to speculate that RGDechiHCit acted as an antagonist. Our report is the first evidence that our peptide acts as antagonist for $\alpha_v\beta_3$ integrin. Its ability to inhibit hFN-induced cell proliferation is comparable to that of c(RGDf[NMe]V), although the half-life is quite reduced.

A major evidence that is brought up by our results is the peculiar selectivity of RGDechiHCit towards EC, as compared to c(RGDf[NMe]V). Indeed, RGDechiHCit fails to inhibit VSMC proliferation *in vitro*, opposite to c(RGDf[NMe]V). We believe that this feature is due to the selectivity of such a novel compound toward $\alpha_v\beta_3$. Indeed, VSMCs express $\alpha_v\beta_3$ only during embryogenesis [31], but express other integrins which may be blocked by c(RGDf[NMe]V). On the contrary, $\alpha_v\beta_3$ is expressed by ECs [8], thus conferring RGDechiHCit selectivity toward this cell type. This issue is relevant cause the effect *in vivo* is similar between the two antagonists on wound healing and Matrigel plugs invasion. Indeed, our data suggest that inhibition of the endothelial integrin system is sufficient to inhibit angiogenesis. It is possible to speculate that the higher specificity of RGDechiHCit for the endothelium would result in a lower occurrence of side effects than the use of less selective inhibitors. This is only an indirect evidence, that needs further investigation in more specific experimental setups. Indeed, of the wide spectrum of integrins that are expressed on the surface of ECs, $\alpha_v\beta_3$ receptor has been identified as having an especially interesting expression pattern among vascular cells during angiogenesis, vascular remodeling, tumor progression and metastasis [6,32,33]. What is more, two pathways of angiogenesis have been recently identified based on the related but distinct integrins $\alpha_v\beta_3$ and $\alpha_v\beta_5$ [4]. In particular, $\alpha_v\beta_3$ integrin activates VEGF receptors and inhibition of β_3 subunit has been shown to reduce phosphorylation of VEGF receptors [7], thereby limiting the biological

effects of VEGF [1]. Further, Mahabeleshwar and coworkers have shown the intimate interaction occurring between $\alpha_v\beta_3$ integrin and the VEGFR-2 in primary human EC [12]. The relevance of this molecule to angiogenesis and its potential as a therapeutic target has, therefore, been well established [34,35] and in this report we show that its activity is highly critical for both hFN or VEGF-stimulated ECs proliferation.

Our results concerning RGDechiHCit in angiogenic processes are of immediate translational importance, because deregulation of angiogenesis is involved in several clinical conditions including cancer, ischemic, and inflammatory diseases (atherosclerosis, rheumatoid arthritis, or age-related macular degeneration) [34-36]. Therefore, the research for drugs able to modulate angiogenesis constitutes a crucial investigation field. Since RGDechiHCit is rapidly removed in serum it is possible to increase its effect by engineering the molecule to elongate its lifespan. In the present paper we circumvented this issue by increasing the times of application of the drug both *in vitro* and *in vivo*, or by reducing the times of observation. This issue can be solved by the use of a more stable aromatic pharmacophore that recapitulates the binding properties of RGDechiHCit. Clearly, further investigations are also needed to fully understand the basic cell biological mechanisms underlying growth factor receptors and integrin function during angiogenesis. The knowledge of molecular basis of this complex mechanism remains a challenge of fascinating interest, with clinical implications for treatment of a large number of pathophysiological conditions including but not limited to solid tumors [17,37], diabetic retinopathy [38,39] and inflammatory disease [36].

Conclusions

The present study indicates the importance of RGDechiHCit in the selective inhibition of endothelial $\alpha_v\beta_3$ integrin. Such inhibition opens new fields of investigation on the mechanisms of angiogenesis, offering clinical implications for the treatment of several conditions such as proliferative retinopathy, inflammatory disease and cancer.

Author details

¹Department of Clinical Medicine, Cardiovascular & Immunologic Sciences, "Federico II" University of Naples, Italy. ²Department of Biological Sciences, "Federico II" University of Naples, Italy. ³Institute of Crystallography (Consiglio Nazionale delle Ricerche, CNR), Bari, Italy. ⁴Institute of Biostructures and Bioimaging (Consiglio Nazionale delle Ricerche, CNR), Naples, Italy.

Authors' contributions

GS and GI designed research; GS, MFB, MDS, CDG, AA, and DS carried out the experiments; GS and GI performed the statistical analysis; GS, GI and LZ drafted the manuscript; GS, MS, ADG, BT, CP and GI supervised the project; GS and MFB equally contributed to this work. All authors read and approved the final manuscript.

Competing interests

We have no financial or personal relationships with other people or organizations that would bias our work. No benefits in any form have been received or will be received from a commercial party related directly or indirectly to the subject of our article.

Received: 28 June 2010 Accepted: 13 January 2011

Published: 13 January 2011

References

1. Santulli G, Ciccarelli M, Palumbo G, Campanile A, Galasso G, Ziaco B, Altobelli GG, Cimini V, Piscione F, D'Andrea LD, et al: **In vivo properties of the proangiogenic peptide QK.** *J Transl Med* 2009, **7**:41.
2. Bonauer A, Carmona G, Iwasaki M, Mione M, Koyanagi M, Fischer A, Burchfield J, Fox H, Doebele C, Ohtani K, et al: **MicroRNA-92a controls angiogenesis and functional recovery of ischemic tissues in mice.** *Science* 2009, **324**:1710-1713.
3. Desgrosellier JS, Cheresch DA: **Integrins in cancer: biological implications and therapeutic opportunities.** *Nat Rev Cancer* 2010, **10**:9-22.
4. Hood JD, Frausto R, Kiosses WB, Schwartz MA, Cheresch DA: **Differential alphav integrin-mediated Ras-ERK signaling during two pathways of angiogenesis.** *J Cell Biol* 2003, **162**:933-943.
5. Takahashi S, Moser M, Montanez E, Nakano T, Seo M, Backert S, Inoue I, Awata T, Katayama S, Komoda T, Fassler R: **The fibronectin RGD motif is required for multiple angiogenic events during early embryonic development.** *Arterioscler Thromb Vasc Biol* 2010, **30**:e1.
6. Castel S, Pagan R, Garcia R, Casaroli-Marano RP, Reina M, Mitjans F, Piulats J, Vilario S: **Alpha v integrin antagonists induce the disassembly of focal contacts in melanoma cells.** *Eur J Cell Biol* 2000, **79**:502-512.
7. Soldi R, Mitola S, Strasly M, Defilippi P, Tarone G, Buscino F: **Role of alphavbeta3 integrin in the activation of vascular endothelial growth factor receptor-2.** *Embo J* 1999, **18**:882-892.
8. Lu H, Murtagh J, Schwartz EL: **The microtubule binding drug laulimalide inhibits vascular endothelial growth factor-induced human endothelial cell migration and is synergistic when combined with docetaxel (taxotere).** *Mol Pharmacol* 2006, **69**:1207-1215.
9. Bayless KJ, Salazar R, Davis GE: **RGD-dependent vacuolation and lumen formation observed during endothelial cell morphogenesis in three-dimensional fibrin matrices involves the alpha(v)beta(3) and alpha(5) beta(1) integrins.** *Am J Pathol* 2000, **156**:1673-1683.
10. Brooks PC, Stromblad S, Sanders LC, von Schalscha TL, Aimes RT, Stetler-Stevenson WG, Quigley JP, Cheresch DA: **Localization of matrix metalloproteinase MMP-2 to the surface of invasive cells by interaction with integrin alpha v beta 3.** *Cell* 1996, **85**:683-693.
11. Abumiya T, Lucero J, Heo JH, Tagaya M, Koziol JA, Copeland BR, del Zoppo GJ: **Activated microvessels express vascular endothelial growth factor and integrin alpha(v)beta3 during focal cerebral ischemia.** *J Cereb Blood Flow Metab* 1999, **19**:1038-1050.
12. Mahabeleshwar GH, Feng W, Reddy K, Plow EF, Byzova TV: **Mechanisms of integrin-vascular endothelial growth factor receptor cross-activation in angiogenesis.** *Circ Res* 2007, **101**:570-580.
13. Xiong JP, Stehle T, Zhang R, Joachimiak A, Frech M, Goodman SL, Arnaout MA: **Crystal structure of the extracellular segment of integrin alpha Vbeta3 in complex with an Arg-Gly-Asp ligand.** *Science* 2002, **296**:151-155.
14. Aumailley M, Gurrath M, Muller G, Calvete J, Timpl R, Kessler H: **Arg-Gly-Asp constrained within cyclic pentapeptides. Strong and selective inhibitors of cell adhesion to vitronectin and laminin fragment P1.** *FEBS Lett* 1991, **291**:50-54.
15. Schottelius M, Laufer B, Kessler H, Wester HJ: **Ligands for mapping alphavbeta3-integrin expression in vivo.** *Acc Chem Res* 2009, **42**:969-980.
16. Eliceiri BP, Klemke R, Stromblad S, Cheresch DA: **Integrin alphavbeta3 requirement for sustained mitogen-activated protein kinase activity during angiogenesis.** *J Cell Biol* 1998, **140**:1255-1263.
17. Bai J, Zhang J, Wu J, Shen L, Zeng J, Ding J, Wu Y, Gong Z, Li A, Xu S, et al: **JWA regulates melanoma metastasis by integrin alpha(V)beta(3) signaling.** *Oncogene* 2010, **29**:1227-1237.
18. Eskens FA, Dumez H, Hoekstra R, Perschl A, Brindley C, Bottcher S, Wynendaele W, Drevs J, Verweij J, van Oosterom AT: **Phase I and pharmacokinetic study of continuous twice weekly intravenous administration of Cilengitide (EMD 121974), a novel inhibitor of the**

- integrins alphavbeta3 and alphavbeta5 in patients with advanced solid tumours. *Eur J Cancer* 2003, **39**:917-926.
19. Dechantsreiter MA, Planker E, Matha B, Lohof E, Holzemann G, Jonczyk A, Goodman SL, Kessler H: **N-Methylated cyclic RGD peptides as highly active and selective alpha(V)beta(3) integrin antagonists.** *J Med Chem* 1999, **42**:3033-3040.
 20. Del Gatto A, Zaccaro L, Grieco P, Novellino E, Zannetti A, Del Vecchio S, Iommelli F, Salvatore M, Pedone C, Saviano M: **Novel and selective alpha (v)beta3 receptor peptide antagonist: design, synthesis, and biological behavior.** *J Med Chem* 2006, **49**:3416-3420.
 21. Zannetti A, Del Vecchio S, Iommelli F, Del Gatto A, De Luca S, Zaccaro L, Papaccioli A, Sommella J, Panico M, Speranza A, et al: **Imaging of alphavbeta3 expression by a bifunctional chimeric RGD peptide not cross-reacting with alphavbeta5.** *Clin Cancer Res* 2009, **15**:5224-5233.
 22. Ciccarelli M, Cipolletta E, Santulli G, Campanile A, Pumiglia K, Cervero P, Pastore L, Astone D, Trimarco B, Iaccarino G: **Endothelial beta2 adrenergic signaling to AKT: role of Gi and SRC.** *Cell Signal* 2007, **19**:1949-1955.
 23. Iaccarino G, Ciccarelli M, Sorriento D, Cipolletta E, Cerullo V, Iovino GL, Paudice A, Elia A, Santulli G, Campanile A, et al: **AKT participates in endothelial dysfunction in hypertension.** *Circulation* 2004, **109**:2587-2593.
 24. Illario M, Cavallo AL, Monaco S, Di Vito E, Mueller F, Marzano LA, Troncone G, Fenzi G, Rossi G, Vitale M: **Fibronectin-induced proliferation in thyroid cells is mediated by alphavbeta3 integrin through Ras/Raf-1/MEK/ERK and calcium/CaMKII signals.** *J Clin Endocrinol Metab* 2005, **90**:2865-2873.
 25. Iaccarino G, Smithwick LA, Lefkowitz RJ, Koch WJ: **Targeting Gbeta gamma signaling in arterial vascular smooth muscle proliferation: a novel strategy to limit restenosis.** *Proc Natl Acad Sci USA* 1999, **96**:3945-3950.
 26. Iaccarino G, Ciccarelli M, Sorriento D, Galasso G, Campanile A, Santulli G, Cipolletta E, Cerullo V, Cimini V, Altobelli GG, et al: **Ischemic neoangiogenesis enhanced by beta2-adrenergic receptor overexpression: a novel role for the endothelial adrenergic system.** *Circ Res* 2005, **97**:1182-1189.
 27. Ciccarelli M, Santulli G, Campanile A, Galasso G, Cervero P, Altobelli GG, Cimini V, Pastore L, Piscione F, Trimarco B, Iaccarino G: **Endothelial alpha1-adrenoceptors regulate neo-angiogenesis.** *Br J Pharmacol* 2008, **153**:936-946.
 28. Sorriento D, Ciccarelli M, Santulli G, Campanile A, Altobelli GG, Cimini V, Galasso G, Astone D, Piscione F, Pastore L, et al: **The G-protein-coupled receptor kinase 5 inhibits NFkappaB transcriptional activity by inducing nuclear accumulation of IkappaB alpha.** *Proc Natl Acad Sci USA* 2008, **105**:17818-17823.
 29. Sorriento D, Santulli G, Fusco A, Anastasio A, Trimarco B, Iaccarino G: **Intracardiac Injection of AdGRK5-NT Reduces Left Ventricular Hypertrophy by Inhibiting NF-(kappa)B-Dependent Hypertrophic Gene Expression.** *Hypertension* 2010, **56**:696-704.
 30. Santulli G, Illario M, Palumbo G, Sorriento D, Cipolletta E, Trimarco V, Del Giudice C, Ciccarelli M, Trimarco B, Iaccarino G: **CaMK4 participates in the settings of the hypertensive phenotype: a human genome wide analysis supported by animal model.** *Eur Heart J* 2009, **30**(Suppl.1):161.
 31. Astrof S, Hynes RO: **Fibronectins in vascular morphogenesis.** *Angiogenesis* 2009, **12**:165-175.
 32. Zaccaro L, Del Gatto A, Pedone C, Saviano M: **Peptides for tumour therapy and diagnosis: current status and future directions.** *Curr Med Chem* 2009, **16**:780-795.
 33. Verbisck NV, Costa ET, Costa FF, Cavalher FP, Costa MD, Muras A, Paixao VA, Moura R, Granato MF, Ierardi DF, et al: **ADAM23 negatively modulates alpha(v)beta(3) integrin activation during metastasis.** *Cancer Res* 2009, **69**:5546-5552.
 34. Laitinen I, Saraste A, Weidl E, Poethko T, Weber AW, Nekolla SG, Leppanen P, Yla-Herttuala S, Holzlwimmer G, Walch A, et al: **Evaluation of alphavbeta3 integrin-targeted positron emission tomography tracer 18F-galacto-RGD for imaging of vascular inflammation in atherosclerotic mice.** *Circ Cardiovasc Imaging* 2009, **2**:331-338.
 35. Furundzija V, Fritzsche J, Kaufmann J, Meyborg H, Fleck E, Kappert K, Stawowy P: **IGF-1 increases macrophage motility via PKC/p38-dependent alphavbeta3-integrin inside-out signaling.** *Biochem Biophys Res Commun* 2010, **394**:786-791.
 36. Vanderslice P, Woodside DG: **Integrin antagonists as therapeutics for inflammatory diseases.** *Expert Opin Investig Drugs* 2006, **15**:1235-1255.
 37. Tani N, Higashiyama S, Kawaguchi N, Madarame J, Ota I, Ito Y, Ohoka Y, Shiosaka S, Takada Y, Matsuura N: **Expression level of integrin alpha 5 on tumour cells affects the rate of metastasis to the kidney.** *Br J Cancer* 2003, **88**:327-333.
 38. Crawford TN, Alfaro DV, Kerrison JB, Jablon EP: **Diabetic retinopathy and angiogenesis.** *Curr Diabetes Rev* 2009, **5**:8-13.
 39. Santulli RJ, Kinney WA, Ghosh S, Decorte BL, Liu L, Tuman RW, Zhou Z, Huebert N, Bursell SE, Clermont AC, et al: **Studies with an orally bioavailable alpha V integrin antagonist in animal models of ocular vasculopathy: retinal neovascularization in mice and retinal vascular permeability in diabetic rats.** *J Pharmacol Exp Ther* 2008, **324**:894-901.

doi:10.1186/1479-5876-9-7

Cite this article as: Santulli et al.: Evaluation of the anti-angiogenic properties of the new selective $\alpha_v\beta_3$ integrin antagonist RGDchiHCit. *Journal of Translational Medicine* 2011 **9**:7.

Submit your next manuscript to BioMed Central and take full advantage of:

- Convenient online submission
- Thorough peer review
- No space constraints or color figure charges
- Immediate publication on acceptance
- Inclusion in PubMed, CAS, Scopus and Google Scholar
- Research which is freely available for redistribution

Submit your manuscript at
www.biomedcentral.com/submit



Integrating Cardiac PIP₃ and cAMP Signaling through a PKA Anchoring Function of p110 γ

Alessia Perino,¹ Alessandra Ghigo,^{1,12} Enrico Ferrero,^{1,12} Fulvio Morello,^{1,12} Gaetano Santulli,^{2,13} George S. Baillie,³ Federico Damilano,¹ Allan J. Dunlop,³ Catherine Pawson,⁴ Romy Walser,⁵ Renzo Levi,⁶ Fiorella Altruda,¹ Lorenzo Silengo,¹ Lorene K. Langeberg,⁴ Gitte Neubauer,⁷ Stephane Heymans,⁸ Giuseppe Lembo,⁹ Matthias P. Wymann,⁵ Reinhard Wetzker,¹⁰ Miles D. Houslay,³ Guido Iaccarino,¹¹ John D. Scott,^{4,*} and Emilio Hirsch^{1,*}

¹Department of Genetics, Biology and Biochemistry, Molecular Biotechnology Center, University of Torino, Torino 10126, Italy

²Division of Internal Medicine, Department of Clinical Medicine and Cardiovascular Sciences, Federico II University of Napoli, Napoli 80131, Italy

³Division of Biochemistry and Molecular Biology, Wolfson Building FBL5, University of Glasgow, Glasgow G12 8QQ, Scotland

⁴Department of Pharmacology, Howard Hughes Medical Institute, University of Washington, School of Medicine, Seattle, WA 98195, USA

⁵Department of Biomedicine, Institute of Biochemistry and Genetics, University of Basel, Basel 4058, Switzerland

⁶Department of Animal and Human Biology, University of Torino, Torino 10123, Italy

⁷Cellzome AG, Heidelberg 69117, Germany

⁸Department of Cardiology, Cardiovascular Research Institute Maastricht, Maastricht University, Maastricht 6211, The Netherlands

⁹Department of Molecular Medicine, "Sapienza" University of Rome, c/o IRCCS Neuromed, Pozzilli (IS) 86077, Italy

¹⁰Department of Molecular Cell Biology, Jena University Hospital, Friedrich Schiller University, Jena 07745, Germany

¹¹Faculty of Medicine and Surgery, University of Salerno, Baronissi (SA) 84081, Italy

¹²These authors contributed equally to this work

¹³Present address: College of Physicians and Surgeons, Columbia University Medical Center, New York, NY 10032, USA

*Correspondence: scottjd@u.washington.edu (J.D.S.), emilio.hirsch@unito.it (E.H.)

DOI 10.1016/j.molcel.2011.01.030

SUMMARY

Adrenergic stimulation of the heart engages cAMP and phosphoinositide second messenger signaling cascades. Cardiac phosphoinositide 3-kinase p110 γ participates in these processes by sustaining β -adrenergic receptor internalization through its catalytic function and by controlling phosphodiesterase 3B (PDE3B) activity via an unknown kinase-independent mechanism. We have discovered that p110 γ anchors protein kinase A (PKA) through a site in its N-terminal region. Anchored PKA activates PDE3B to enhance cAMP degradation and phosphorylates p110 γ to inhibit PIP₃ production. This provides local feedback control of PIP₃ and cAMP signaling events. In congestive heart failure, p110 γ is upregulated and escapes PKA-mediated inhibition, contributing to a reduction in β -adrenergic receptor density. Pharmacological inhibition of p110 γ normalizes β -adrenergic receptor density and improves contractility in failing hearts.

INTRODUCTION

In cardiomyocytes, stimulation of G protein-coupled β -adrenergic receptors (β -ARs) by catecholamines engages tandem signaling pathways that utilize the second messengers cyclic AMP (cAMP) and phosphatidylinositol(3,4,5)-trisphosphate (PtdIns(3,4,5)P₃ or PIP₃) (Rockman et al., 2002). cAMP is generated upon engagement of β -AR/G_s-triggered stimulation of ad-

enylyl cyclase, thus leading to the activation of protein kinase A (PKA), which in turn controls myocardial contractility (Xiang and Kobilka, 2003). Instead, PtdIns(3,4,5)P₃ is produced from PtdIns(4,5)P₂ by the main G protein-coupled phosphoinositide 3-kinases (PI3Ks), PI3K β and γ (Guillemet-Guibert et al., 2008; Hirsch et al., 2000).

Signals processed through myocardial cAMP/PKA and PI3K γ /PtdIns(3,4,5)P₃ pathways are tightly coupled, thus generating intracellular sites for crosstalk between the cAMP and PtdIns(3,4,5)P₃ responsive enzymes. For instance, PI3K γ cooperates with β -ARK1 to dampen cAMP signaling by promoting desensitization and downregulation of β -ARs (Naga Prasad et al., 2001). Additionally, PtdIns(3,4,5)P₃ is needed for AP-2 adaptor recruitment at the plasma membrane and for the consequent organization of clathrin-coated pits (Naga Prasad et al., 2002). This mechanism contributes to the pathological decrease in myocardial β -AR density and function during the natural history of heart failure (Bristow et al., 1982; Nienaber et al., 2003; Perrino et al., 2007). PI3K γ also attenuates the cAMP/PKA pathway by working as an activator of the phosphodiesterases PDE3B and PDE4, which hydrolyze cAMP to 5'-AMP (Conti and Beavo, 2007; Kerfant et al., 2007; Patrucco et al., 2004). Although little is known about the regulation of PDE3B by PI3K γ , previous reports have demonstrated that this is operated within a macromolecular complex including both the catalytic (p110 γ) and the adaptor (p84/87) subunits of PI3K γ (Patrucco et al., 2004; Voigt et al., 2006). Importantly, the functional interaction between p110 γ and PDE3B does not involve the kinase activity of p110 γ , which instead acts as a scaffold for PDE3B (Hirsch et al., 2009). As a result, mice lacking p110 γ exhibit decreased myocardial PDE3B activity and elevated cAMP, while PDE3B function and cAMP levels are normal in mice expressing a kinase-inactive p110 γ . In p110 γ null mice subjected to cardiac pressure overload

and not in mice expressing a kinase-dead p110 γ , cAMP rises uncontrolled, thus leading to cardiomyopathy and heart failure (Crackower et al., 2002; Patrucco et al., 2004).

Therefore, p110 γ might constitute a molecular hub connecting the cAMP and PtdIns(3,4,5) P_3 signaling axes in cardiomyocytes. However, the molecular mechanisms operating this interplay remain unclear. We show herein that crosstalk between myocardial cAMP and PtdIns(3,4,5) P_3 signaling pathways is mediated by the formation of a previously unidentified multiprotein complex that couples p110 γ to PDE3B activation. Within this complex, p110 γ acts as an A-kinase anchoring protein (AKAP) tethering the phosphodiesterase near its activator, PKA. Functional studies further confirm that anchoring of PKA to p110 γ inhibits its lipid kinase activity in a phosphorylation-dependent manner. Coupling of cAMP and PtdIns(3,4,5) P_3 signaling mediated by the anchoring function of p110 γ is perturbed in mouse models of congestive heart failure, leading to β -AR downregulation. Inhibition of p110 γ can restore compromised β -AR density and improve contractility, highlighting the potential for therapeutic interventions.

RESULTS

p110 γ Activates PDE3B in a PKA-Dependent Manner

To elucidate the mechanisms linking PDE3B activity to p110 γ , these proteins were overexpressed in HEK293T cells. p110 γ and PDE3B could be coimmunoprecipitated in this cell type as in mouse cardiomyocytes (Figures 1A, lane 3, and 1B, lane 1). The cotransfection of p110 γ wild-type or p110 γ kinase-dead with PDE3B resulted in a higher phosphodiesterase activity than in cells expressing PDE3B alone (Figures 1C, column 3, and S1A). This confirmed that p110 γ activates PDE3B in a kinase-independent manner. One interpretation was that p110 γ may associate with an activator of PDE3B, and PKA appeared as a likely candidate (Degerman et al., 1998). Indeed, recombinant PKA phosphorylated PDE3B in vitro (Figure S1B). Furthermore, cAMP/PKA-mediated phosphorylation of PDE3B was enhanced in the presence of p110 γ (Figure S1C). Treatment with PKA inhibitors H89 or PKI blunted the increase in PDE3B-mediated cAMP hydrolysis (Figures 1C, column 4, and 1D, column 2). Taken together, our results imply that PKA residing in the p110 γ -PDE3B complex enhances the activity of PDE3B. Further support for this model was provided by evidence that p110 γ copurified with PKA activity (Figure 1E, column 1). Additional experiments demonstrated the copurification of p110 γ and PDE3B with the regulatory (R11 α) and catalytic (C) subunits of PKA (Figure 1F, lane 1). In contrast, other class I PI3Ks expressed in the heart, p110 α and p110 β , did not associate with PKA and PDE3B (Figures S1D and S1E). Interestingly, p110 γ was found to associate with the PKA regulatory subunit R11 α but not with the R1 α isoform (Figure S1F). In this complex, we could also detect the p110 γ regulatory subunit p84/87, but not p101 (Figure 1G, lane 1).

Further characterization of the p110 γ -PKA complex was conducted in the mouse heart. Coimmunoprecipitation confirmed the interaction of p110 γ with PKA in the myocardium (Figures S2A and S2B). Immunofluorescence staining further illustrated that p110 γ , R11 α , and PDE3B signals overlapped in mouse adult cardiomyocytes (Figures 1H, S2C, and S2D). More stringent

biochemical analyses showed that, in myocardial lysates, R11 α coimmunoprecipitates with PDE3B, the catalytic subunit of PKA, as well as the p110 γ and p84/87 subunits of PI3K γ (Figure 1I, lane 1). Additional control experiments established that the p101 subunit of PI3K γ was not present in this signaling complex. These results establish p110 γ as the key element in a PI3K γ /PDE3B/PKA ternary complex controlling PDE3B activity through PKA.

p110 γ Acts as an A-Kinase Anchoring Protein

A critical role for p110 γ as a scaffold protein in the complex suggests that p110 γ could act as an AKAP. AKAPs directly bind the regulatory subunits of PKA to orchestrate the compartmentalization of cAMP/PKA signaling through association with target effectors, substrates, and signal terminators (Carr et al., 1991; Scott and Pawson, 2009). Accordingly, recombinant R11 α subunits of PKA copurified with recombinant p110 γ in an in vitro pull-down experiment (Figure 2A, lane 1). Further support for this interaction was provided by surface plasmon resonance measurements, which calculated a dissociation constant (K_D) of $1.86 \pm 0.01 \mu\text{M}$ for the interaction of p110 γ with R11 α (Figure 2B). R11 overlay experiments detected a binding band of 116 kDa in p110 γ immunoprecipitates (Figure 2C, lane 1, upper panel). This R11-binding band was absent in control blots pretreated with the PKA anchoring inhibitor peptide, AKAP-*IS* (Figure 2C, lane 1, lower panel). Immunoblot analysis of PKA R11 α immunoprecipitates established that treatment with AKAP-*IS* could disrupt the R11 α -p110 γ interaction (Figures 2D, lane 2, and 2E, column 2). Control experiments indicated that other AKAPs expressed in cardiomyocytes, including AKAP18 α , AKAP79, and AKAP-Lbc, do not coimmunoprecipitate with p110 γ (Figures S3A–S3C). Mapping studies have revealed that residues 1–45 of R11 α form a docking and dimerization domain that serves as a binding surface for AKAPs (Gold et al., 2006; Hausken et al., 1994). R11 α fragments lacking this region (PKA R11 α Δ 1–45) did not bind p110 γ , as assessed by coprecipitation (Figure 2F, lane 2), indicating that the N terminus of PKA R11 α is essential for the interaction with p110 γ . Collectively, these results show that p110 γ is a bona fide AKAP.

Mapping of the p110 γ -PKA R11 α Interaction

Mapping studies in HEK293T cells using a series of p110 γ deletion fragments (Figure S4A) revealed that R11 α interacts with an amino-terminal portion of p110 γ spanning residues 114–280 (Figure 3A, lane 2). Further investigation with a solid-phase peptide array located the R11 α binding determinants between residues 126 and 150 of p110 γ (Figure S4B). These results were independently confirmed when a peptide encompassing these residues of p110 γ selectively disrupted the R11 α -p110 γ interaction in a dose-dependent manner (Figures 3B, lanes 2 and 3, and 3C, columns 2 and 3). Importantly, loss of PKA anchoring led to a concomitant decrease in p110 γ -associated PDE3B activity (Figure S4C).

More definitive analysis of the p110 γ 126–150 peptide revealed that N-terminal residues are required for the binding to PKA R11 α (Figure S4D). In addition, spot array analysis of C-terminal truncations indicated that the exposure of charged or hydrophobic residues flanking this region blunted the binding

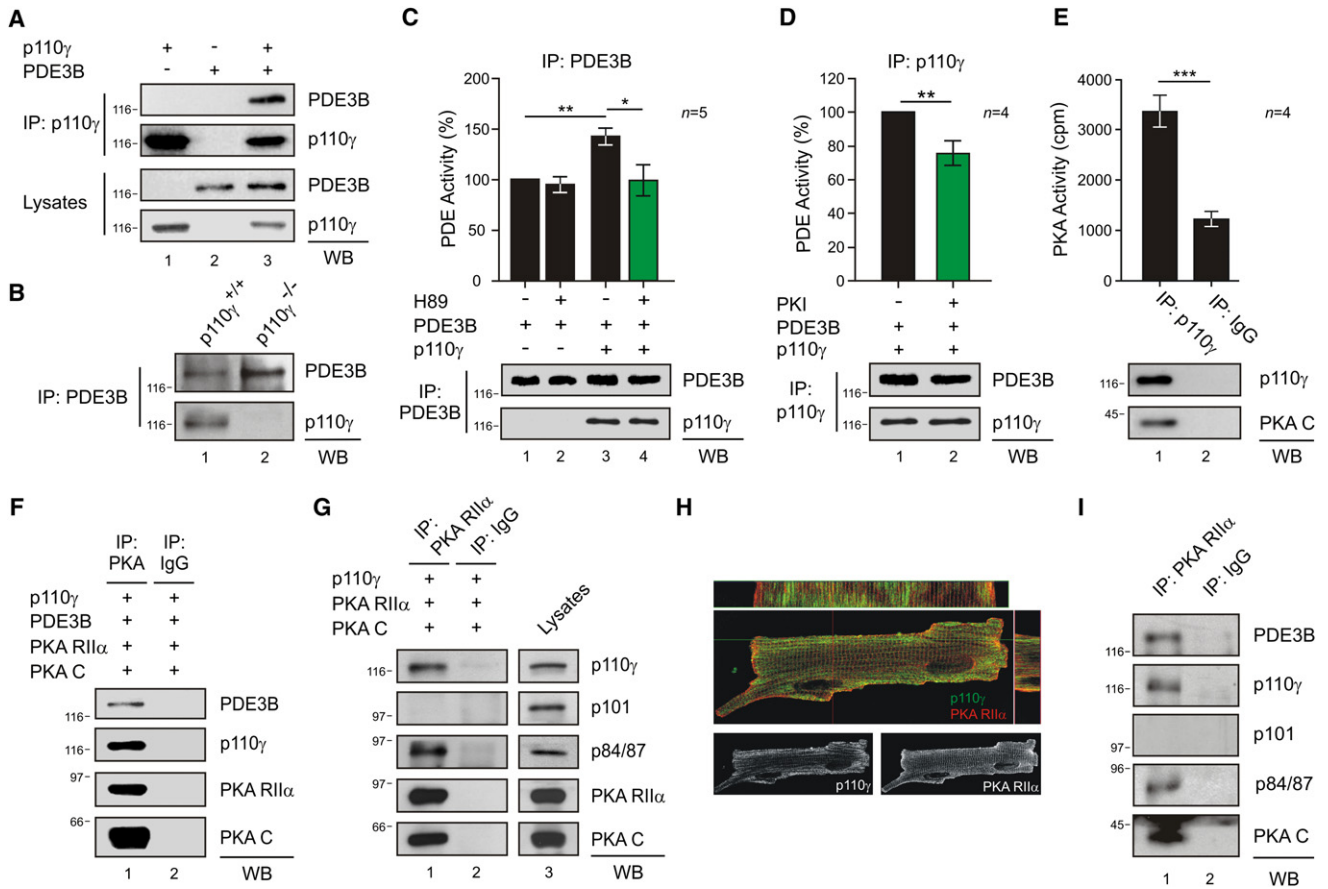


Figure 1. p110 γ Activates PDE3B through PKA within a PI3K γ -PKA-PDE3B Complex
 (A) Coimmunoprecipitation of PDE3B with p110 γ in HEK293T cells transfected with p110 γ and PDE3B-Flag.
 (B) Coimmunoprecipitation of p110 γ with PDE3B in wild-type (p110 $\gamma^{+/+}$) but not in p110 γ knockout (p110 $\gamma^{-/-}$) mouse neonatal cardiomyocytes.
 (C) Phosphodiesterase activity in PDE3B immunoprecipitates upon transfection of HEK293T cells with PDE3B-Flag (PDE3B) or with PDE3B-Flag and p110 γ . Cells were treated with PKA inhibitor H89 (5 μ M, 10 min) or vehicle as indicated. PDE activity (%) was calculated relative to the activity of single PDE3B transfectants.
 (D) Phosphodiesterase activity (%) of double p110 γ , PDE3B-Flag transfectants treated with PKA inhibitor Myr-PKI (5 μ M, 10 min) or vehicle.
 (E) PKA activity (cpm) in a p110 γ immunoprecipitate from transfected HEK293T cells.
 (F) Coimmunoprecipitation of transfected p110 γ , PDE3B-Flag, PKA RII α -ECFP (PKA RII α), and PKA CAT-YFP (PKA C) from HEK293T extracts.
 (G) Coimmunoprecipitation of p110 γ and p84/p87, but not p101, with PKA RII α from HEK293T transfected cells.
 (H) Colocalization (yellow spots) of p110 γ (green) and PKA RII α (red) by immunofluorescence in mouse adult cardiomyocytes. Longitudinal and transverse sections are shown in the upper and right panels, respectively. Single p110 γ and PKA RII α localizations are presented in the lower panels.
 (I) PDE3B, p110 γ , p84/p87, and PKA CAT (PKA C), but not p101, coimmunoprecipitate with PKA RII α in myocardial tissue extracts of wild-type mice. A representative immunoprecipitation is presented in (A)–(G) and (I). For all bar graphs, values represent mean \pm SEM of a minimum of four independent experiments. * p < 0.05, ** p < 0.01, *** p < 0.001. See also Figures S1 and S2.

to RII α (Figure S4E). Alanine scanning of this region suggested that while single point mutations did not disrupt the binding (data not shown), the substitution of basic residues 126 (K) and 130 (R) with A abolished the interaction with RII α (Figure 3D). Cell-based analyses confirmed that a p110 γ K126A,R130A mutant exhibited a reduced ability to copurify with the PKA holoenzyme (Figure 3E, lane 3). Moreover, this PKA-anchoring defective p110 γ mutant failed to increase PDE3B activity (Figures 3F, column 3 and S4F). Thus, association of PKA with p110 γ allows PKA to modulate PDE3B activity, thereby suppressing local accumulation of cAMP.

PKA Phosphorylates p110 γ and Inhibits p110 γ Lipid Kinase Activity

We further reasoned that anchored PKA might phosphorylate p110 γ to modulate its catalytic activity. Indeed, recombinant PKA mediated the incorporation of ³²P into p110 γ , and this effect was blocked in the presence of the specific PKA inhibitor peptide PKI (Figures 4A and S5A). Studies in cultured cells indicated that the forskolin-evoked accumulation of intracellular cAMP induced the phosphorylation of p110 γ by PKA (Figure 4B, lane 2). Conversely, PKA failed to phosphorylate the p110 γ K126A,R130A mutant that does not bind PKA RII α (Figures 4C,

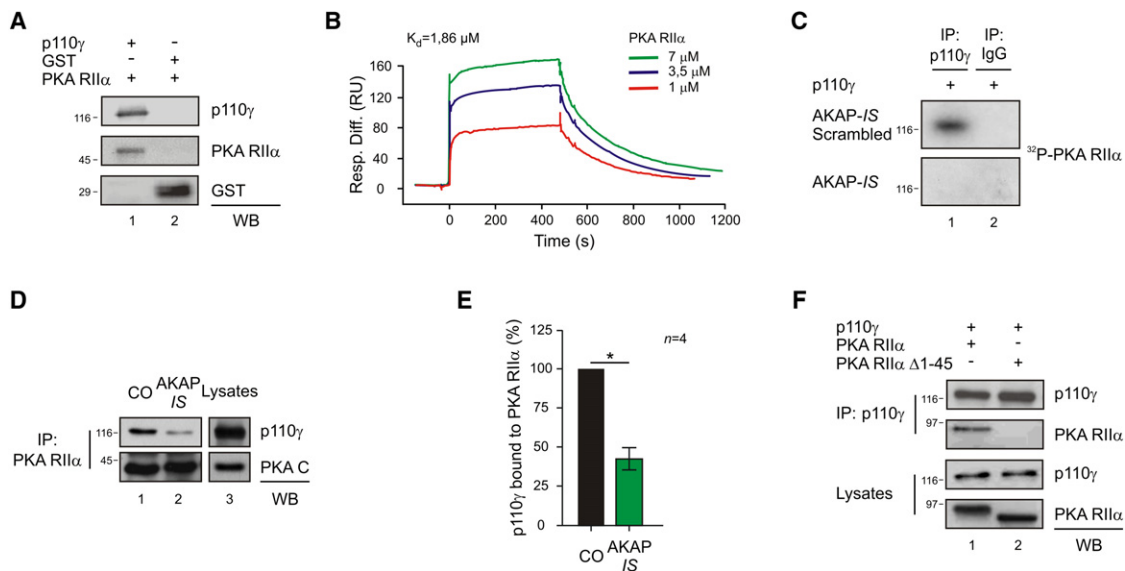


Figure 2. p110 γ Is a Bona Fide AKAP

(A) In vitro copurification of p110 γ -GST and PKA RII α -6His in a GST pull-down assay.

(B) Direct interaction of p110 γ and PKA RII α in a surface plasmon resonance assay. p110 γ was immobilized on the chip, and PKA RII α was injected at three different concentrations.

(C) Binding of ^{32}P -labeled PKA RII α to immunoprecipitated p110 γ in the presence of AKAP-IS scrambled peptide but not in the presence of AKAP-IS peptide.

(D) Competition of the p110 γ -PKA RII α coimmunoprecipitation with AKAP-IS peptide.

(E) Quantitative densitometry of the competition experiment represented in (D). Values represent mean \pm SEM of four independent experiments. *p < 0.05.

(F) Loss of the coimmunoprecipitation of PKA RII α with p110 γ by truncation of the 1–45 amino acids of RII α -ECFP (PKA RII α Δ 1–45). A representative assay is presented in all figures. See also Figure S3.

lane 4 and 4D, column 4). We then proceeded to identify the PKA phosphorylation site on p110 γ using sequential bioinformatic, biochemical, and functional approaches. Bioinformatic screening of the p110 γ sequence identified a number of putative PKA phosphorylation sites (Table S1). However, only two of them (S400 and T1024) (1) appeared conserved among different species and (2) contained an R side chain at the -3 position, which is optimal for PKA substrate recognition (Figure S5B). Peptides containing these residues were not covered in a phosphoproteomic analysis, but peptide arrays of p110 γ phosphorylated by PKA showed a signal in two overlapping peptides containing T1024 but not in sequences containing S400 (Figure S5C). Most relevantly, only the T1024D and the T1024A mutations, but not S400A, resulted in a significant decrease in the phosphorylation of p110 γ by PKA (Figures 4E, lane 4, 4F, column 2, and S5D), indicating that T1024 represents the main phosphorylation site of p110 γ by PKA. It is worthy to note that the T1024 is conserved in p110 γ orthologs and is not present in the other class I PI3Ks (Figure S5E).

Lipid kinase assays showed that the incubation of PKA with recombinant p110 γ reduced the kinase activity of p110 γ on both PtdIns and PtdIns(4,5) P_2 (Figures 4G, lane 2, and S6A). Yet treatment with the PKI peptide abolished this effect (Figure S6B), thus demonstrating that PKA negatively regulates the lipid kinase activity of p110 γ . Similarly, cell-based studies demonstrated that forskolin-dependent activation of PKA resulted in a decrease in p110 γ lipid kinase activity, which was blocked by PKI (Figure 4H, lanes 3 and 4). Forskolin treatment also significantly

reduced, by 28.9%, PtdIns(3,4,5) P_3 production in cells stimulated with PGE₂, a G protein-coupled receptor agonist activating p110 γ (Figure 4I, column 3). Collectively, these observations establish that PKA inhibits p110 γ through direct phosphorylation. Of note, the phosphomimetic T1024D mutant showed reduced lipid kinase activity compared to wild-type p110 γ (Figure 4J, lane 2), indicating that the phosphorylation of p110 γ by PKA on T1024 represents a crucial mechanism controlling p110 γ lipid kinase activity.

p110 γ Is Inhibited by PKA in Cardiomyocytes

Next, the functional interaction between p110 γ and PKA was explored in vivo. Wild-type mouse hearts stimulated with β -AR agonist isoproterenol, which triggers the PKA axis, showed a rapid inhibition of the lipid kinase activity of p110 γ (Figure 5A). Although this is apparently in contrast with the notion that β -AR activation triggers the PI3K/Akt pathway (Jo et al., 2002; Leblais et al., 2004), isoproterenol induced PtdIns(3,4,5) P_3 rise and Akt phosphorylation in p110 γ kinase-dead mice (Figures 5B, columns 3 and 4, and 5C, columns 4–6). Adrenergic-evoked response was instead lost in p110 β kinase-dead mice (Figures 5B, columns 5 and 6, and 5C, columns 7–9), supporting the view that only p110 γ activity is repressed upon β -AR activation. The inhibition of p110 γ was further confirmed in ex vivo Langendorff perfused hearts, where isoproterenol blunted p110 γ activity by 77.3% \pm 12%, while coprefusion with the PKA inhibitor H89 left p110 γ activity unchanged compared to control hearts (Figure 5D, lanes 2 and 3). Moreover, in isolated adult

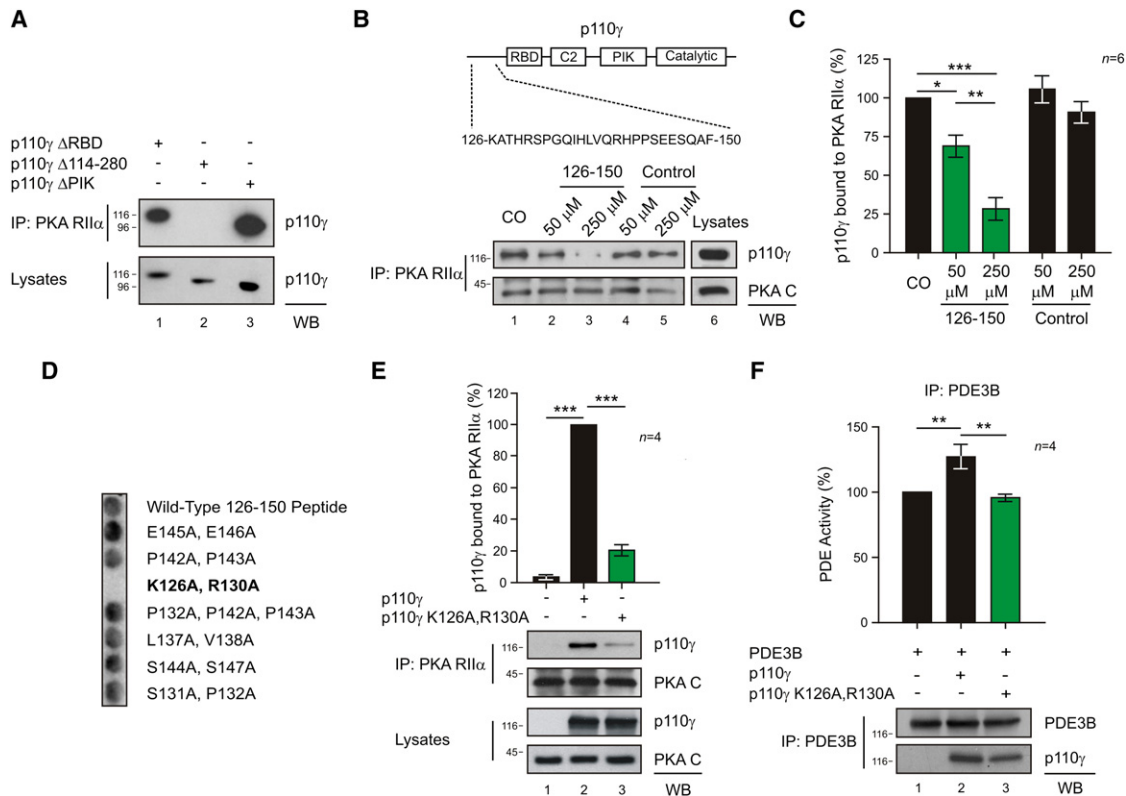


Figure 3. Mapping of the p110 γ -PKA RII α Interaction

(A) Loss of the coimmunoprecipitation of p110 γ -Myc with PKA RII α by deletion of amino acids 114–280 (p110 γ Δ 114–280) but not by deletion of the Ras-binding domain (p110 γ Δ RBD) or the PIK domain (p110 γ Δ PIK) of p110 γ -Myc.
 (B) Sequence of the 126–150 peptide is represented on a scheme of p110 γ . In dose-dependent competition experiments, the 126–150 peptide, but not a scrambled control peptide, antagonized the p110 γ -RII α protein-protein interaction.
 (C) Quantitative densitometry of the competition experiment represented in (B).
 (D) Binding of PKA RII α to a set of alanine mutant 126–150 p110 γ peptides in a solid-phase peptide array.
 (E) Mutation of K¹²⁶ and R¹³⁰ of p110 γ to A (p110 γ K126A,R130A) blunts coimmunoprecipitation of p110 γ with PKA RII α in transfected HEK293T cells. Values were obtained by quantitative densitometry and normalized over control.
 (F) Phosphodiesterase activity (%) of PDE3B immunoprecipitates upon transfection of HEK293T cells with PDE3B-Flag alone or with PDE3B-Flag and either wild-type or mutant p110 γ (p110 γ K126A,R130A). A representative immunoprecipitation is provided for (A), (B), (E), and (F). For all bar graphs, values represent mean \pm SEM of a minimum of four independent experiments. * p < 0.05, ** p < 0.01, *** p < 0.001. See also Figure S4.

rat cardiomyocytes, isoproterenol reduced the lipid kinase activity of p110 γ by 53.3% \pm 7% (Figure 5E, lane 2). Inhibition of PKA with PKI restored p110 γ activity (Figure 5E, lane 3). We then investigated the *in vivo* regulation of p110 γ activity by PKA in a mouse model of cardiac pressure overload characterized by endogenous adrenergic stimulation of the myocardium as well as compensatory hypertrophy (Figure 5F, insets). After 1 week of transverse aortic constriction (TAC), the p110 γ lipid kinase activity was markedly reduced, by 50% \pm 7%, when compared to sham-operated mice (Figure 5F, lane 2). Taken together, these findings show that signaling by the β -AR/cAMP/PKA pathway inhibits cardiac p110 γ .

Regulation of p110 γ Kinase Activity by PKA Impacts on β -Adrenergic Density

The kinase activity of p110 γ is known to reduce myocardial β -AR density (Nienaber et al., 2003; Perrino et al., 2007). We thus hypothesized that the regulation of p110 γ by PKA could

contribute to this process by mediating a feedback loop controlling β -AR cell surface expression. Therefore, β -AR density was measured in wild-type, p110 β kinase-dead (p110 β ^{KD/KD}), p110 γ knockout (p110 γ ^{-/-}), and p110 γ kinase-dead (p110 γ ^{KD/KD}) hearts. The loss of p110 γ but not of p110 β activity was associated with a significant increase in β -AR density (p110 γ ^{-/-} + 36.4% and p110 γ ^{KD/KD} + 25.8% versus wild-type controls) (Figure 6A, columns 3 and 4). Similarly, treatment of wild-type mice with a selective p110 γ inhibitor (AS605240) determined a significant 28.1% upregulation of cardiac β -AR density, while AS605240 did not modify β -AR density in p110 γ ^{KD/KD} hearts, indicating that this compound is specific for p110 γ (Figure S7A).

A reduction of cell surface β -ARs is a key trait of heart failure (Bristow et al., 1982, 1990; Denniss et al., 1989; Engelhardt et al., 1996). This prompted us to investigate whether abnormal regulation of p110 γ activity might be involved in this pathological condition. We thus examined β -AR surface expression and

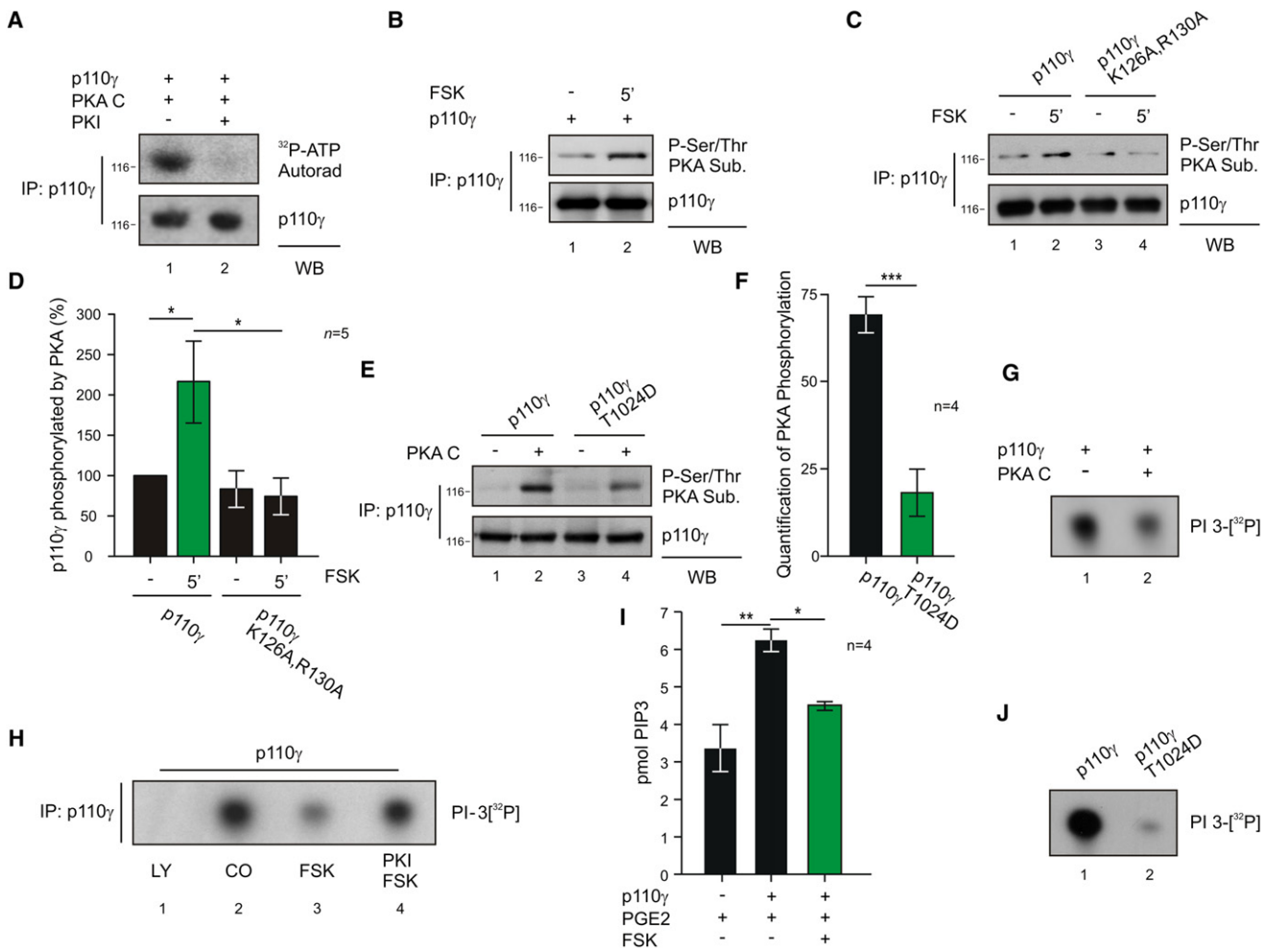


Figure 4. PKA Phosphorylates and Inhibits p110 γ

(A) Phosphorylation of p110 γ immunoprecipitated from transfected HEK293T cells in the presence of recombinant PKA C, ³²P-ATP, and PKA inhibitor PKI (1 μ M) or vehicle.

(B) PKA-mediated phosphorylation of p110 γ immunoprecipitated from HEK293T cells upon stimulation with forskolin (FSK 20 μ M, 5 min).

(C) PKA-mediated phosphorylation of p110 γ or p110 γ K126A,R130A immunoprecipitated from HEK293T cells upon stimulation with forskolin (FSK 20 μ M, 5 min).

(D) Quantitative densitometry of the experiment represented in (C).

(E) PKA-mediated phosphorylation of p110 γ or p110 γ T1024D mutant immunoprecipitated from HEK293T cells and incubated or not with active PKA (30 min).

(F) Quantitative densitometry of PKA phosphorylation (background subtracted) of the experiment represented in (E).

(G) Lipid kinase activity of recombinant p110 γ -GST incubated *in vitro* with or without recombinant PKA C (30 min).

(H) Lipid kinase activity of p110 γ immunoprecipitated from transfected HEK293T cells treated with vehicle, pan-p110 inhibitor LY-294002 (LY, 20 μ M, 15 min), forskolin (FSK, 20 μ M, 5 min) or FSK plus PKA inhibitor Myr-PKI (1 μ M).

(I) Measurement of cellular PtdIns(3,4,5)P₃ (pmol PIP₃) levels in transfected HEK293T treated with the GPCR agonist PGE2 (100 nM, 10 min) alone or in combination with FSK (50 μ M, 3 min).

(J) Lipid kinase activity of p110 γ wild-type or p110 γ T1024D mutant immunoprecipitated from transfected HEK293T cells. In lipid kinase assays (G, H, J), the ability of p110 γ to phosphorylate phosphoinositide was detected by autoradiography following incubation with ³²P-ATP substrate. A representative assay is presented in all figures. For all bar graphs, values represent mean \pm SEM of a minimum of four independent experiments. *p < 0.05, **p < 0.01, ***p < 0.001. See also Figures S5 and S6.

p110 γ lipid kinase activity in hearts isolated from mice after 20 weeks of TAC, a time sufficient to develop a hypokinetic dilative cardiomyopathy (left ventricle fractional shortening <30%). At this stage, wild-type animals presented a 58.4% reduction in β -AR density compared to sham controls (Figure 6B, column 2). In contrast, β -AR membrane density remained normal when p110 γ ^{KD/KD} mice were subjected to 20 weeks of aortic banding

(Figure 6B, column 4). This indicated that p110 γ stimulates β -AR downregulation in the myocardium. Since PtdIns(3,4,5)P₃ is critical in this process (Naga Prasad et al., 2001), PtdIns(3,4,5)P₃ levels were measured after 20 week TAC. In p110 γ ^{KD/KD} hearts, PtdIns(3,4,5)P₃ was 39% lower than in wild-types (Figure 6C, column 3). This paralleled a 37.5% \pm 6% increase in p110 γ activity in 20 week TAC-treated wild-type mice compared to

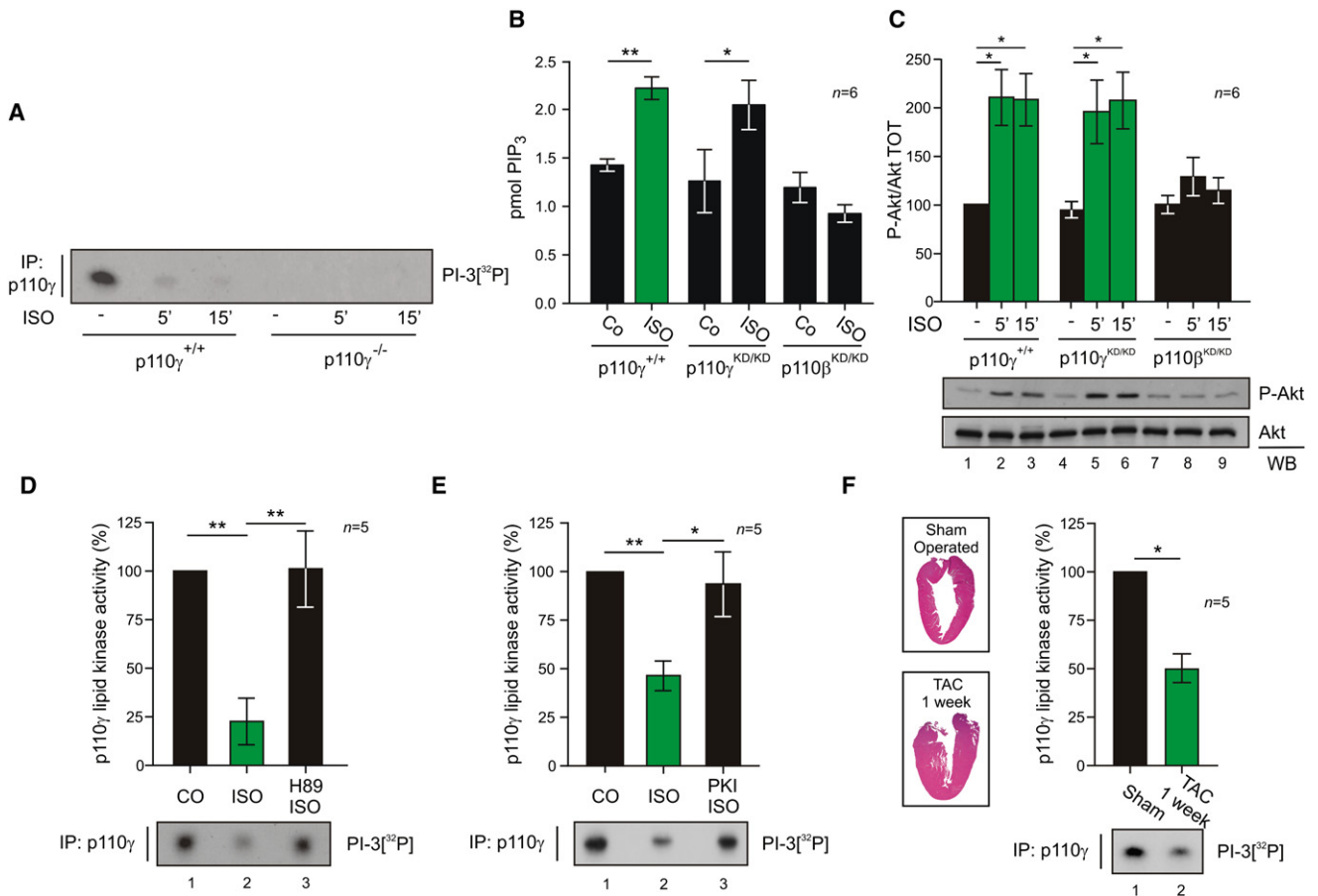


Figure 5. PKA Inhibits the Lipid Kinase Activity of p110 γ in the Myocardium

(A) Lipid kinase activity of p110 γ immunoprecipitated from myocardial tissue lysates following treatment of wild-type (p110 $\gamma^{+/+}$) or p110 γ knockout mice (p110 $\gamma^{-/-}$) with β -AR agonist isoproterenol (ISO, 1.25 mg/kg i.p. for 5 or 15 min) or vehicle.

(B) Measurement of myocardial PtdIns(3,4,5)P₃ (pmol PIP₃) levels in wild-type (p110 $\gamma^{+/+}$), p110 γ kinase-dead (p110 $\gamma^{KD/KD}$), and p110 β kinase-dead (p110 $\beta^{KD/KD}$) mice treated with isoproterenol (ISO, 1.25 mg/kg i.p. for 5 min) or vehicle.

(C) Phospho-Akt (P-Akt) and total Akt (Akt) levels in myocardial tissue lysates following treatment of wild-type (p110 $\gamma^{+/+}$), p110 γ kinase-dead (p110 $\gamma^{KD/KD}$), and p110 β kinase-dead (p110 $\beta^{KD/KD}$) mice with β -AR agonist isoproterenol (ISO, 1.25 mg/kg i.p. for 5 or 15 min) or vehicle.

(D) Lipid kinase activity of p110 γ immunoprecipitated from myocardial tissue lysates following ex vivo cardiac Langendorff perfusion (5 min) with vehicle, isoproterenol (ISO 10 μ M), or ISO plus PKA inhibitor H89 (10 μ M).

(E) Lipid kinase activity of p110 γ immunoprecipitated from rat adult cardiomyocytes treated with isoproterenol (ISO, 1 μ M, 3 min), ISO plus PKA inhibitor Myr-PKI (1 μ M, 5 min), or vehicle.

(F) Lipid kinase activity of p110 γ immunoprecipitated from myocardial tissue lysates of mice subjected to transverse aortic constriction for 1 week (TAC 1 week) or to sham operation. Insets are representative hematoxylin and eosin stainings of left ventricular sections from sham-operated and 1 week TAC mice. A representative assay is presented in all figures. For all bar graphs, values, obtained by quantitative densitometry and normalized over control, represent mean \pm SEM of a minimum of five mice per group. * $p < 0.05$, ** $p < 0.01$.

sham (Figure 6D, lane 2). These data suggested that, during heart failure, p110 γ -dependent PtdIns(3,4,5)P₃ might become independent from PKA-mediated restraint. Consistently, after 20 weeks of TAC, p110 γ levels rose significantly while PKA RII α and PKA C expression remained unaltered (Figure 6E and 6F). Furthermore, proportionally less PKA copurified with p110 γ isolated from these hearts (Figure 6E, column 2). Ratio of densitometry of p110 γ and the coimmunoprecipitated PKA C from the same blots showed that exposure to prolonged pressure overload evoked a 56.4% \pm 9% decrease in the detection of PKA catalytic subunit anchored to p110 γ (Figure 6E, column 2).

This was further supported by the finding that, during heart failure, expression of PI3K γ adaptor subunits is altered. While p84/87 remained constant, p101, the adaptor excluded from the PKA-containing complex, followed p110 γ upregulation at both mRNA and protein level (Figures 6F, S7B, and 6G). As a consequence of this modulation, the association of p110 γ with p84/87 did not change (Figures 6H, lane 2, and S7C). In contrast, p110 γ association with p101 significantly increased in failing hearts (Figure 6I, lane 2), resulting in an unphysiological balance between p110 γ and its adaptors. Thus, the functional consequence of this pathological reorganization of PI3K γ

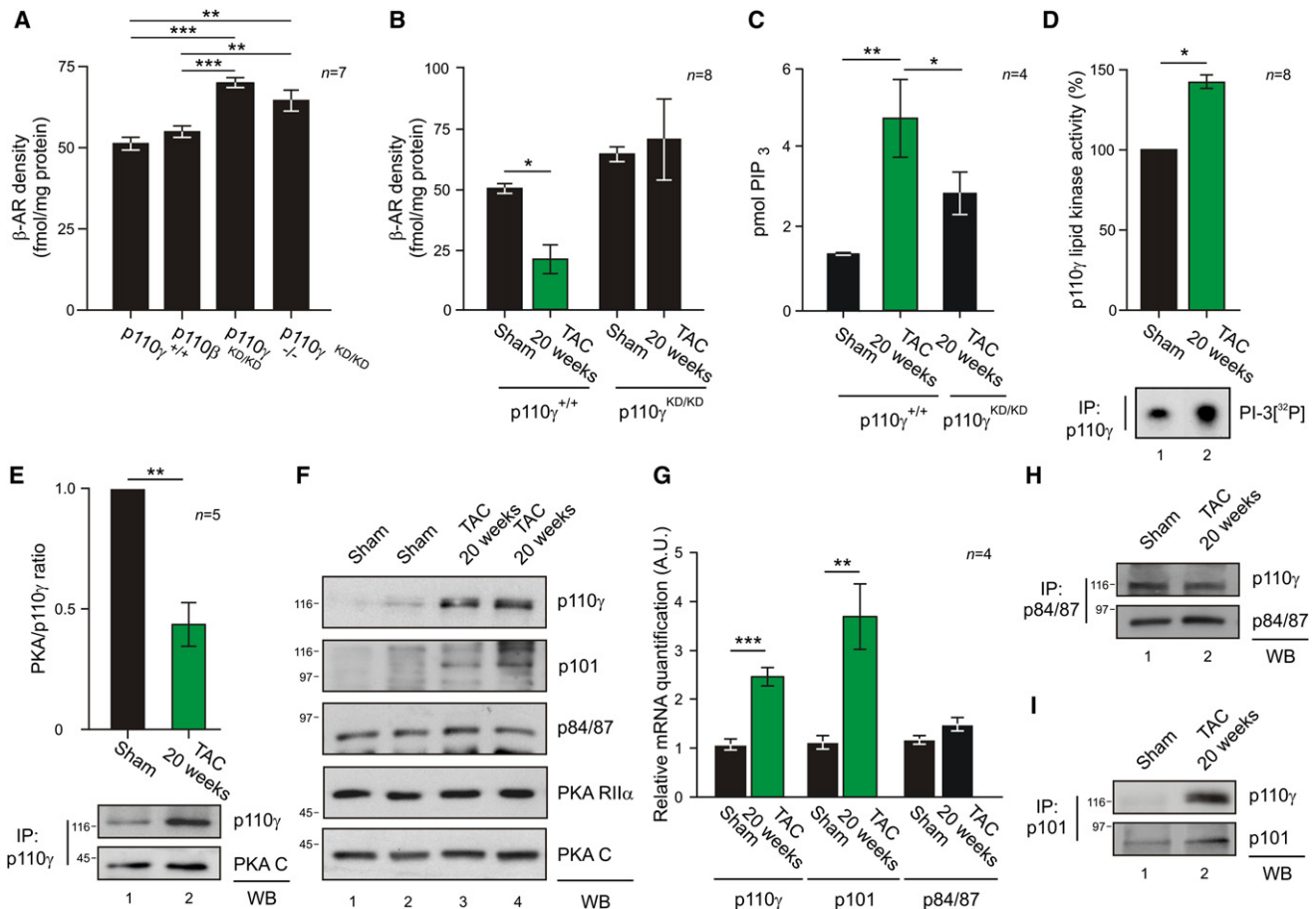


Figure 6. Modulation of p110 γ Lipid Kinase Activity by PKA Affects β -AR Density

(A) Myocardial β -AR density in wild-type (p110 $\gamma^{+/+}$), p110 β kinase-dead (p110 $\beta^{KD/KD}$), p110 γ knockout (p110 $\gamma^{-/-}$), and p110 γ kinase-dead (p110 $\gamma^{KD/KD}$) mice. (B) Myocardial β -AR density of p110 $\gamma^{+/+}$ and p110 $\gamma^{KD/KD}$ mice subjected to sham operation or to aortic constriction for 20 weeks (TAC 20 weeks). (C) Myocardial PtdIns(3,4,5)P₃ (pmol PIP₃) levels in hearts obtained from sham-operated mice or from 20 week TAC-treated wild-type or p110 $\gamma^{KD/KD}$ mice. (D) Lipid kinase activity of p110 γ immunoprecipitated from myocardial tissue lysates of sham-operated or 20 week TAC-treated mice. Values were obtained by quantitative densitometry and normalized over control. (E) Coimmunoprecipitation of p110 γ and PKA C from myocardial lysates from mice subjected to pressure overload for 20 weeks or to sham operation. After quantitative densitometry, p110 γ -bound PKA was expressed as the ratio of coimmunoprecipitated PKA C over immunoprecipitated p110 γ . (F) Total levels of the indicated proteins in myocardial tissue lysates from sham-operated mice or from mice subjected to pressure overload for 20 weeks. (G) mRNA levels of p110 γ , p101, and p84/p87 in hearts from sham-operated mice or mice subjected to 20 weeks of TAC. (H) Coimmunoprecipitation of p110 γ with p84/87 from myocardial lysates of mice subjected to pressure overload for 20 weeks or to sham operation. (I) Coimmunoprecipitation of p110 γ with p101 from myocardial lysates of mice subjected to pressure overload for 20 weeks or to sham operation. In β -AR density measurements (A and B), receptor density is expressed as the B_{max} after saturation binding using [¹²⁵I]-labeled cyanopindolol ligand (fmol/mg protein). A representative assay is presented in (D)–(I). For all bar graphs, values represent mean \pm SEM of a minimum of four independent experiments or six mice per group. *p < 0.05, **p < 0.01, ***p < 0.001. See also Figure S7.

subunits is to override cAMP responsive suppression of p110 γ lipid kinase activity.

Inhibition of p110 γ Kinase Activity Improves Cardiac Function in Heart Failure

Patients with severe aortic stenosis, similar to mice subjected to TAC, showed an increase in p110 γ protein expression (Figure 7A, right panel, and Table S2). This is in line with a previous study conducted on patients with end-stage heart failure (Perrino et al., 2007). We thus hypothesized that the development of heart failure involves the aberrant activation of p110 γ . We tested this

model by treating aortic banded mice with failing hearts (fractional shortening <30%) for 1 week with the selective p110 γ inhibitor AS605240. Indeed, AS605240 restored a significant proportion of myocardial β -ARs on the plasma membrane (37.2%) when compared to vehicle-treated controls (Figure 7B, column 3). Accordingly, echocardiographic measurements detected a significant increase (27.7%) in left ventricular fractional shortening after treatment with AS605240 (Figures 7C, column 2, and S7D and Table S3). The p110 γ inhibitor restored fractional shortening to that of p110 $\gamma^{KD/KD}$ mice subjected to 20 weeks of aortic banding (Figure 7C, column 3). These findings

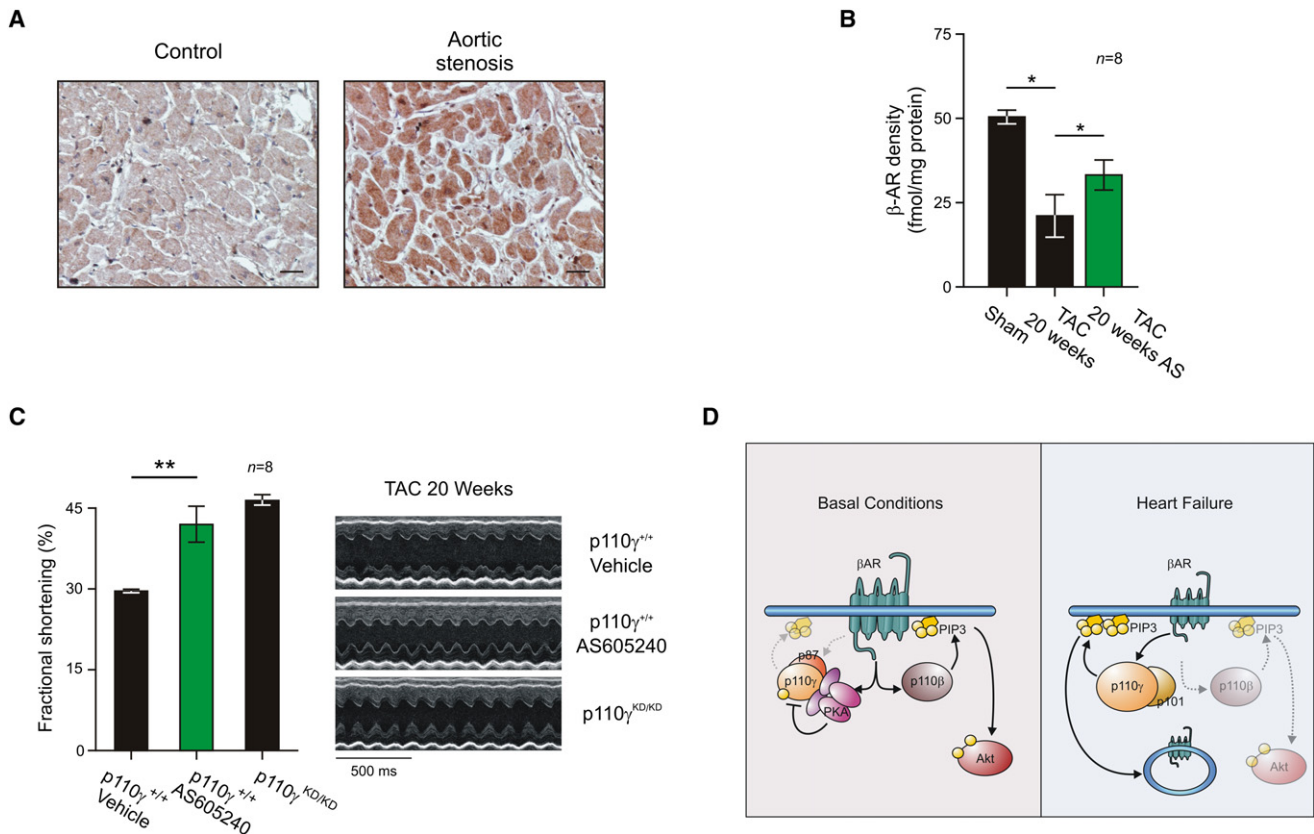


Figure 7. p110 γ Inhibition Restores β -AR Density and Cardiac Function in Heart Failure

(A) Immunohistochemistry for p110 γ in human hearts from healthy control patients or patients with aortic stenosis. Bar graph is 25 μ m. Representative images are presented.

(B) Myocardial β -AR density of wild-type mice with heart failure (obtained by 20 weeks of pressure overload) treated with selective p110 γ inhibitor AS605240 (AS 10 mg/kg i.p. q.d. for 1 week) or vehicle.

(C) Left ventricular fractional shortening of wild-type mice with heart failure treated with AS605240 (10 mg/kg i.p. q.d. for 1 week) or vehicle or of p110 $\gamma^{KD/KD}$ mice subjected to aortic constriction for 20 weeks. Representative M-mode echocardiographic snapshots are presented (right). For all bar graphs, values represent mean \pm SEM of eight mice per group. * $p < 0.05$, ** $p < 0.01$.

(D) Schematic representation of the diverse function of p110 γ and p110 β in cardiac physiology and pathology. See also Figure S7.

indicate that the pharmacological inhibition of p110 γ counteracts the reduction in β -AR density in failing hearts, thus preserving physiological adrenergic signaling and protecting the myocardium from the deterioration of the systolic function in heart failure.

DISCUSSION

Our results establish that myocardial p110 γ physically and functionally interacts with PKA. We provide evidence that p110 γ orchestrates a physiological crosstalk between cAMP and PtdIns(3,4,5) P_3 pathways, modulating PDE3B activity and β -AR internalization. In heart failure, this functional coupling operated by p110 γ is perturbed, leading to impaired contractility.

While we previously reported that the loss of p110 γ results in a defective activity of PDE3B (Patrucco et al., 2004), the molecular mechanism of p110 γ -dependent regulation of PDE3B has remained elusive. We now establish that p110 γ directly binds PKA, a recognized activator of PDE3B, and that the phosphory-

lation of PDE3B by PKA is favored when both the kinase and the phosphodiesterase are tethered to p110 γ . Whereas the association of p110 γ with PKA is direct, the interaction with PDE3B is mediated by the p84/87 PI3K γ regulatory subunit (Voigt et al., 2006). This supports the selective involvement of p84/87, and not of p101, in constraining the assembly of this ternary complex.

A broader implication of our results is that multiprotein assemblies involving p84/87/p110 γ , PDE3B, and PKA coordinate the spatial and temporal modulation of cAMP signaling in the myocardium, acting in a manner similar to other AKAPs such as mA-KAP, AKAP350, and gravin (Dodge et al., 2001; Taskén et al., 2001; Willoughby et al., 2006). These signaling complexes tether PKA in proximity to PDEs to locally modulate cAMP signaling, thereby optimizing signal termination. In respect to what has been shown for other AKAPs, an important finding of the present study is that we provide evidence of the colocalization of PKA and PDE3B in a macromolecular complex. By interacting with PKA and PDE3B, the p84/87/p110 γ heterodimer appears involved in a crucial negative feedback controlling the

cAMP pathway. In p110 γ -deficient animals, loss of this feedback leads to cAMP accumulation in resting conditions (Crackower et al., 2002) and to cAMP-mediated cardiac damage under stress (Patrucco et al., 2004).

While p110 γ appears to behave like an AKAP in that it directly binds the RII α subunit, its PKA-anchoring site appears to be atypical. Classical AKAPs bind to PKA RII α through a conserved amphipathic helix (Carr et al., 1991), and their association can be disrupted by synthetic peptides designed to reproduce this helical structure (Alto et al., 2003; Gold et al., 2006). As expected, the p110 γ /PKA RII α interaction could also be disrupted by AKAP-IS, a consensus RII-anchoring disruptor peptide (Alto et al., 2003). However, the p110 γ sequence defined by the peptide array is not predicted to form a helical domain, and the interaction with RII α appears to rely on two positively charged residues. Nonetheless, these findings are in line with the notion that the family of AKAPs, which currently includes 45 genes and their splice variants, exhibits substantial heterogeneity in sequence, yet always featuring the ability to tether PKA at subcellular locations.

The PKA associated with p110 γ not only influences the catalytic activity of PDE3B, but also modulates the lipid kinase activity of p110 γ itself. Indeed, the proximity of PKA and p110 γ within the same macromolecular complex allows active PKA to phosphorylate both PDE3B and p110 γ . The phosphorylation of p110 γ by PKA on T1024 results in a negative modulation of p110 γ kinase activity. T1024 resides in an α helix situated in close proximity to the ATP-binding pocket, and therefore the functional effects of this phosphorylation on the kinase activity of p110 γ may derive from a conformational change disturbing the catalytic pocket. This mechanism is supported by our findings with the phosphomimetic T1024D mutant, which resulted in decreased lipid kinase activity. T1024 of p110 γ is highly conserved among species and is not represented in the other class I PI3K isoforms, which are, however, inhibited by their autophosphorylation within the catalytic domain (Czupalla et al., 2003).

Modulation of p110 γ by PKA has relevant functional implications *in vivo* in the myocardium. While the β -AR/cAMP pathway that activates PKA also triggers the PI3K pathway (Jo et al., 2002; Leblais et al., 2004), our results indicate that in physiological conditions, p110 γ activity is negligible, owing to its low expression levels and to the inhibitory phosphorylation by PKA. Instead, other G protein-coupled p110 isoforms, such as p110 β (Ciraolo et al., 2008; Guillermet-Guibert et al., 2008; Jia et al., 2008), appear to be the main PI3K catalytic subunits responsible for the production of PtdIns(3,4,5) P_3 and the consequent activation of Akt upon β -AR stimulation. Our findings are in line with the view that, in physiological conditions, p110 γ activity undergoes a delicate negative regulation in response to cAMP production and PKA activation. This inhibitory effect can be linked to the well-established view that, while class IA exerts beneficial effects on the myocardium (Oudit and Penninger, 2009), p110 γ function is associated with detrimental responses to cardiac stress (Crackower et al., 2002; Rockman et al., 2002). In heart failure, p110 γ is upregulated, and due to defective PKA-mediated inhibition, its activity is significantly enhanced. Of note, PtdIns(3,4,5) P_3 measurement in TAC-treated hearts

showed that only in p110 γ ^{KD/KD} and not in p110 β ^{KD/KD} hearts (data not shown) is PtdIns(3,4,5) P_3 lower than in wild-type controls, thus confirming a prominent role of the p110 γ isoform in heart failure (Figure 7D).

The negative influence exerted by p110 γ catalytic activity on the development of heart failure appears to be related to its impact on β -AR pathway, a key regulator of heart contractility (Rockman et al., 2002). Indeed, p110 γ promotes the desensitization and downregulation of β -ARs through its interaction with β -ARK1 (Naga Prasad et al., 2001) and through the recruitment of PH domain-containing proteins such as AP-2 (Naga Prasad et al., 2002), required for the assembly of β -AR downregulation machinery. Consistent with these observations, genetic ablation of p110 γ , expression of a catalytically inactive p110 γ , or administration of a selective p110 γ inhibitor to wild-type mice slightly but significantly increased cardiac β -AR density. A trend toward elevated β -AR surface expression has been already reported in a previous study conducted on p110 γ -deficient mice (Nienaber et al., 2003). In our hands, while basal myocardial β -AR expression was only marginally affected by the inactivation of p110 γ , the effect of p110 γ on β -AR downregulation appeared prominent during adrenergic stress and pressure overload-induced heart failure. Consistently, in failing hearts, p110 γ catalytic activity appeared significantly enhanced and occurred in a context where expression of p110 γ and its adaptor p101 was dramatically upregulated. This effect limited the organization of complexes with p84/87 and PKA, thus reducing PKA-mediated inactivation of p110 γ . In agreement, blockade of p110 γ activity either genetically or pharmacologically led to a renormalization of β -AR density in heart failure, improving compromised cardiac contractility.

In summary, our results establish that myocardial p110 γ connects the PtdIns(3,4,5) P_3 and cAMP signaling pathways. We show that anchored PKA is the key regulator of enzymes in this macromolecular complex and that PKA locally controls PDE3B activity, reducing cAMP levels. This finding provides an explanation for the longstanding conundrum of how the p110 γ kinase-independent function can promote cAMP degradation (Patrucco et al., 2004). On the other hand, PKA inhibits p110 γ activity to maintain myocardial β -ARs on the cell surface. In heart failure, uncoupling of p110 γ from its negative regulator PKA results in β -AR downregulation. Pharmacological inhibition of p110 γ restores the physiological condition, with beneficial effects on β -AR density and, ultimately, on cardiac contractility, thus establishing p110 γ targeting as a potential treatment for heart failure.

EXPERIMENTAL PROCEDURES

Mice

p110 γ knockout (Hirsch et al., 2000), p110 γ kinase-dead (Patrucco et al., 2004), and p110 β kinase-dead mice (Ciraolo et al., 2008) are all in a C57BL/6J background. C57BL/6J wild-type mice were used as controls.

Hearts and Cell Lysis, Protein Immunoprecipitation, and Western Blotting

Hearts, adult rat cardiomyocytes, and HEK293T cells were homogenized in 1% Triton X-100 buffer with protease and phosphatase inhibitors. Lysates were cleared by centrifugation at 13,000 rpm for 15 min at 4°C. Supernatants

were analyzed for immunoblotting or for immunoprecipitation with the indicated antibodies.

Lipid Kinase Assay

Immunoprecipitated p110 γ was incubated in lipid kinase buffer containing phosphatidylinositol, phosphatidylserine, ATP, and 5 μ Ci of 32 P-ATP for 10 min at 30°C at 1200 rpm. The reaction was stopped by addition of HCl, and lipids were extracted using chloroform/methanol. The organic phase was spotted on thin-layer chromatography plates and resolved with chloroform/methanol/ammonium hydroxide/water. Dried plates were exposed for autoradiography.

Transverse Aortic Constriction and AS605240 Treatment

In vivo pressure overload was imposed on the left ventricle by surgical banding of the transverse aorta, as previously described (Patrucco et al., 2004). Sham-operated animals underwent the same surgical procedure without TAC. 2D guided M-mode echocardiography was performed in anesthetized mice to assess cardiac function. Fractional shortening (FS) lower than 30% was used as a threshold to discriminate between compensated and decompensated hearts. Mice displaying a 25%–30% FS were injected i.p. daily for 1 week with either 10 mg/kg AS605240 or vehicle.

β -AR Density Measurement

Mouse hearts were homogenized in 250 mM sucrose, 5 mM EDTA, 5 mM Tris-HCl (pH 7.5), 2 μ M leupeptin, 100 μ M benzamidine, and 100 μ M PMSF and centrifuged at 800 *g* for 15 min at 4°C. Supernatants were filtered and centrifuged at 25,000 *g* for 30 min at 4°C. The pelleted membranes were washed in acidified ice-cold binding buffer before being resuspended in binding buffer. Total β -AR density was determined by incubation of membrane proteins with a saturating concentration of 125 I-labeled cyanopindolol. Nonspecific binding was determined as previously described (Ciccarelli et al., 2008). Reactions were conducted at 37°C for 1 hr and terminated by vacuum filtration. After ice-cold washing, bound radioactivity was assessed on a gamma counter. All assays were performed in triplicate, and receptor density (femtomoles) was normalized to milligrams of membrane protein.

Data and Statistical Analyses

Prism software (GraphPad) was used for statistical analysis. All data were expressed as mean \pm SEM. P values were calculated by using Student's *t* test and one-way ANOVA test, followed by Bonferroni's post hoc analysis when appropriate. *p* < 0.05 was considered significant (*), *p* < 0.01 was considered very significant (**), and *p* < 0.001 was considered extremely significant (***). See Supplemental Experimental Procedures for details and for remaining procedures.

SUPPLEMENTAL INFORMATION

Supplemental Information includes Supplemental Experimental Procedures, Supplemental References, seven figures, and three tables and can be found with this article online at doi:10.1016/j.molcel.2011.01.030.

ACKNOWLEDGMENTS

We would like to thank M. Zaccolo (University of Glasgow), J. Beavo (University of Washington), J. Hamm (University of Torino), and all the members of E.H.'s lab. This work was supported by grants from Fondation Leducq (06CDV02 to E.H., J.D.S., G.S.B., and M.D.H.), the European Union Sixth Framework Program EuGeneHeart (E.H.), Telethon (E.H.), Regione Piemonte (E.H.), University of Torino (E.H.), AIRC (E.H.), NIH (grant HL08836 to J.D.S.), and Medical Research Council UK (G0600675 to G.S.B. and M.D.H.).

Received: September 14, 2010

Revised: December 20, 2010

Accepted: January 24, 2011

Published: April 7, 2011

REFERENCES

- Alto, N.M., Soderling, S.H., Hoshi, N., Langeberg, L.K., Fayos, R., Jennings, P.A., and Scott, J.D. (2003). Bioinformatic design of A-kinase anchoring protein-in silico: a potent and selective peptide antagonist of type II protein kinase A anchoring. *Proc. Natl. Acad. Sci. USA* 100, 4445–4450.
- Bristow, M.R., Ginsburg, R., Minobe, W., Cubicciotti, R.S., Sageman, W.S., Lurie, K., Billingham, M.E., Harrison, D.C., and Stinson, E.B. (1982). Decreased catecholamine sensitivity and beta-adrenergic-receptor density in failing human hearts. *N. Engl. J. Med.* 307, 205–211.
- Bristow, M.R., Hershberger, R.E., Port, J.D., Gilbert, E.M., Sandoval, A., Rasmussen, R., Cates, A.E., and Feldman, A.M. (1990). Beta-adrenergic pathways in nonfailing and failing human ventricular myocardium. *Circulation* 82 (2, Suppl), I12–I25.
- Carr, D.W., Stofko-Hahn, R.E., Fraser, I.D., Bishop, S.M., Acott, T.S., Brennan, R.G., and Scott, J.D. (1991). Interaction of the regulatory subunit (RII) of cAMP-dependent protein kinase with RII-anchoring proteins occurs through an amphipathic helix binding motif. *J. Biol. Chem.* 266, 14188–14192.
- Ciccarelli, M., Santulli, G., Campanile, A., Galasso, G., Cervèro, P., Altobelli, G.G., Cimini, V., Pastore, L., Piscione, F., Trimarco, B., and Iaccarino, G. (2008). Endothelial alpha1-adrenoceptors regulate neo-angiogenesis. *Br. J. Pharmacol.* 153, 936–946.
- Ciraolo, E., Iezzi, M., Marone, R., Marengo, S., Curcio, C., Costa, C., Azzolino, O., Gonella, C., Rubinetto, C., Wu, H., et al. (2008). Phosphoinositide 3-kinase p110beta activity: key role in metabolism and mammary gland cancer but not development. *Sci. Signal.* 1, ra3.
- Conti, M., and Beavo, J. (2007). Biochemistry and physiology of cyclic nucleotide phosphodiesterases: essential components in cyclic nucleotide signaling. *Annu. Rev. Biochem.* 76, 481–511.
- Crackower, M.A., Oudit, G.Y., Koziarzki, I., Sarao, R., Sun, H., Sasaki, T., Hirsch, E., Suzuki, A., Shioi, T., Irie-Sasaki, J., et al. (2002). Regulation of myocardial contractility and cell size by distinct PI3K-PTEN signaling pathways. *Cell* 110, 737–749.
- Czupalla, C., Culo, M., Müller, E.C., Brock, C., Reusch, H.P., Spicher, K., Krause, E., and Nürnberg, B. (2003). Identification and characterization of the autophosphorylation sites of phosphoinositide 3-kinase isoforms beta and gamma. *J. Biol. Chem.* 278, 11536–11545.
- Degerman, E., Landström, T.R., Wijkander, J., Holst, L.S., Ahmad, F., Belfrage, P., and Manganiello, V. (1998). Phosphorylation and activation of hormone-sensitive adipocyte phosphodiesterase type 3B. *Methods* 14, 43–53.
- Denniss, A.R., Marsh, J.D., Quigg, R.J., Gordon, J.B., and Colucci, W.S. (1989). Beta-adrenergic receptor number and adenylate cyclase function in denervated transplanted and cardiomyopathic human hearts. *Circulation* 79, 1028–1034.
- Dodge, K.L., Khouangsathiene, S., Kapiloff, M.S., Mouton, R., Hill, E.V., Houslay, M.D., Langeberg, L.K., and Scott, J.D. (2001). mAKAP assembles a protein kinase A/PDE4 phosphodiesterase cAMP signaling module. *EMBO J.* 20, 1921–1930.
- Engelhardt, S., Böhm, M., Erdmann, E., and Lohse, M.J. (1996). Analysis of beta-adrenergic receptor mRNA levels in human ventricular biopsy specimens by quantitative polymerase chain reactions: progressive reduction of beta 1-adrenergic receptor mRNA in heart failure. *J. Am. Coll. Cardiol.* 27, 146–154.
- Gold, M.G., Lygren, B., Dokurno, P., Hoshi, N., McConnachie, G., Taskén, K., Carlson, C.R., Scott, J.D., and Barford, D. (2006). Molecular basis of AKAP specificity for PKA regulatory subunits. *Mol. Cell* 24, 383–395.
- Guillemet-Guibert, J., Bjorklof, K., Salpekar, A., Gonella, C., Ramadani, F., Bilancio, A., Meek, S., Smith, A.J., Okkenhaug, K., and Vanhaesebroeck, B. (2008). The p110beta isoform of phosphoinositide 3-kinase signals downstream of G protein-coupled receptors and is functionally redundant with p110gamma. *Proc. Natl. Acad. Sci. USA* 105, 8292–8297.
- Hausken, Z.E., Coghlan, V.M., Hastings, C.A., Reimann, E.M., and Scott, J.D. (1994). Type II regulatory subunit (RII) of the cAMP-dependent protein kinase

- interaction with A-kinase anchor proteins requires isoleucines 3 and 5. *J. Biol. Chem.* 269, 24245–24251.
- Hirsch, E., Katanaev, V.L., Garlanda, C., Azzolino, O., Pirola, L., Silengo, L., Sozzani, S., Mantovani, A., Altruda, F., and Wymann, M.P. (2000). Central role for G protein-coupled phosphoinositide 3-kinase gamma in inflammation. *Science* 287, 1049–1053.
- Hirsch, E., Braccini, L., Ciraolo, E., Morello, F., and Perino, A. (2009). Twice upon a time: PI3K's secret double life exposed. *Trends Biochem. Sci.* 34, 244–248.
- Jia, S., Liu, Z., Zhang, S., Liu, P., Zhang, L., Lee, S.H., Zhang, J., Signoretti, S., Loda, M., Roberts, T.M., and Zhao, J.J. (2008). Essential roles of PI(3)K-p110beta in cell growth, metabolism and tumorigenesis. *Nature* 454, 776–779.
- Jo, S.H., Leblais, V., Wang, P.H., Crow, M.T., and Xiao, R.P. (2002). Phosphatidylinositol 3-kinase functionally compartmentalizes the concurrent G(s) signaling during beta2-adrenergic stimulation. *Circ. Res.* 91, 46–53.
- Kerfant, B.G., Zhao, D., Lorenzen-Schmidt, I., Wilson, L.S., Cai, S., Chen, S.R., Maurice, D.H., and Backx, P.H. (2007). PI3Kgamma is required for PDE4, not PDE3, activity in subcellular microdomains containing the sarcoplasmic reticular calcium ATPase in cardiomyocytes. *Circ. Res.* 101, 400–408.
- Leblais, V., Jo, S.H., Chakir, K., Maltsev, V., Zheng, M., Crow, M.T., Wang, W., Lakatta, E.G., and Xiao, R.P. (2004). Phosphatidylinositol 3-kinase offsets cAMP-mediated positive inotropic effect via inhibiting Ca²⁺ influx in cardiomyocytes. *Circ. Res.* 95, 1183–1190.
- Naga Prasad, S.V., Barak, L.S., Rapacciuolo, A., Caron, M.G., and Rockman, H.A. (2001). Agonist-dependent recruitment of phosphoinositide 3-kinase to the membrane by beta-adrenergic receptor kinase 1. A role in receptor sequestration. *J. Biol. Chem.* 276, 18953–18959.
- Naga Prasad, S.V., Laporte, S.A., Chamberlain, D., Caron, M.G., Barak, L., and Rockman, H.A. (2002). Phosphoinositide 3-kinase regulates beta2-adrenergic receptor endocytosis by AP-2 recruitment to the receptor/beta-arrestin complex. *J. Cell Biol.* 158, 563–575.
- Nienaber, J.J., Tachibana, H., Naga Prasad, S.V., Esposito, G., Wu, D., Mao, L., and Rockman, H.A. (2003). Inhibition of receptor-localized PI3K preserves cardiac beta-adrenergic receptor function and ameliorates pressure overload heart failure. *J. Clin. Invest.* 112, 1067–1079.
- Oudit, G.Y., and Penninger, J.M. (2009). Cardiac regulation by phosphoinositide 3-kinases and PTEN. *Cardiovasc. Res.* 82, 250–260.
- Patrucco, E., Notte, A., Barberis, L., Selvetella, G., Maffei, A., Brancaccio, M., Marengo, S., Russo, G., Azzolino, O., Rybalkin, S.D., et al. (2004). PI3Kgamma modulates the cardiac response to chronic pressure overload by distinct kinase-dependent and -independent effects. *Cell* 118, 375–387.
- Perrino, C., Schroder, J.N., Lima, B., Villamizar, N., Nienaber, J.J., Milano, C.A., and Naga Prasad, S.V. (2007). Dynamic regulation of phosphoinositide 3-kinase-gamma activity and beta-adrenergic receptor trafficking in end-stage human heart failure. *Circulation* 116, 2571–2579.
- Rockman, H.A., Koch, W.J., and Lefkowitz, R.J. (2002). Seven-transmembrane-spanning receptors and heart function. *Nature* 415, 206–212.
- Scott, J.D., and Pawson, T. (2009). Cell signaling in space and time: where proteins come together and when they're apart. *Science* 326, 1220–1224.
- Taskén, K.A., Collas, P., Kemmner, W.A., Witczak, O., Conti, M., and Taskén, K. (2001). Phosphodiesterase 4D and protein kinase a type II constitute a signaling unit in the centrosomal area. *J. Biol. Chem.* 276, 21999–22002.
- Voigt, P., Dorner, M.B., and Schaefer, M. (2006). Characterization of p87PIKAP, a novel regulatory subunit of phosphoinositide 3-kinase gamma that is highly expressed in heart and interacts with PDE3B. *J. Biol. Chem.* 281, 9977–9986.
- Willoughby, D., Wong, W., Schaack, J., Scott, J.D., and Cooper, D.M. (2006). An anchored PKA and PDE4 complex regulates subplasmalemmal cAMP dynamics. *EMBO J.* 25, 2051–2061.
- Xiang, Y., and Kobilka, B.K. (2003). Myocyte adrenoceptor signaling pathways. *Science* 300, 1530–1532.

RESEARCH ARTICLE

Open Access

The GPIIIA PIA2 polymorphism is associated with an increased risk of cardiovascular adverse events

Gennaro Galasso, Gaetano Santulli, Federico Piscione*, Roberta De Rosa, Valentina Trimarco, Raffaele Piccolo, Salvatore Cassese, Guido Iaccarino, Bruno Trimarco, Massimo Chiariello

Abstract

Background: The clinical impact of PIA2 polymorphism has been investigated in several diseases, but the definition of its specific role on thrombotic cardiovascular complications has been challenging. We aimed to explore the effect of PIA2 polymorphism on outcome in patients with atherosclerosis.

Methods: We studied 400 consecutive patients with coronary artery disease (CAD) undergoing percutaneous coronary intervention. A replication study was conducted in 74 hypertensive patients with cerebrovascular events while a group of 100 healthy subjects was included as control population. PIA genotype was determined by PCR-RFLP on genomic DNA from peripheral blood cells. Major adverse cardiac events (MACE), were considered as end points, and recorded at a mean follow up of 24 ± 4.3 months.

Results: The frequencies of PIA2 polymorphism was similar between groups and genotype distribution was in Hardy-Weinberg equilibrium. In patients with CAD, the presence of PIA2 allele was associated with higher incidence of cardiac death (13.1% vs. 1.5%, $p = 0.0001$), myocardial infarction (10.7% vs. 2.6%, $p = 0.004$) and needs of new revascularization (34.8% vs. 17.7%, $p = 0.010$). Accordingly, the Kaplan-Meier analysis for event free survival in patients harboring the PIA2 allele showed worse long-term outcome for these patients ($p = 0.015$). Cox regression analysis identified the presence of PIA2 as an independent predictor of cardiac death (OR: 9.594, 95% CI: 2.6 to 35.3, $p = 0.002$) and overall MACE (OR: 1.829, 95% CI: 1.054 to 3.176, $p = 0.032$). In the replication study, the PIA2 polymorphism increased the risk of stroke (OR: 4.1, 95% CI: 1.63-12.4, $p = 0.02$) over TIA and was identified as an independent risk factor for stroke (B: -1.39; Wald: 7.15; $p = 0.001$).

Conclusions: Our study demonstrates that in patients with severe atherosclerosis the presence of PIA2 allele is associated with thrombotic cardiovascular complications.

Background

Atherosclerosis manifesting as myocardial infarction, angina pectoris, cerebral ischemia and peripheral artery disease is a multifactorial disease with the environment and genetics contributing to its pathogenesis. During the last decade several genes involved in the atherosclerotic process and their polymorphisms have been suspected to increase the thrombotic predisposition and to influence the risk for acute coronary syndromes. Among these genes, polymorphisms of those involved in platelet function have been extensively studied. Indeed, platelets play a pivotal role in atherothrombosis [1] and

their function is strongly related to the interactions of the glycoprotein IIb/IIIa receptor (GP IIb/IIIa) and the von Willebrand factor, as well as fibrinogen, leading to platelets aggregation [2-4]. GP IIIa is a high polymorphic protein with platelet antigen 1 (PIA1) and 2 (PIA2) as the most common allelic isoforms [5]. In the PIA2 allele, cytosine is substituted for thymidine in exon 2, which is phenotypically translated in the substitution of proline for leucine at position 33 of the mature GP IIIa [6]. A previous in vitro study demonstrates that the PIA2 variant enhances the binding of the GPIIb/IIIa receptor to fibrinogen and therefore increases the platelet aggregation induced by agonists [7]. The clinical impact of PIA2 polymorphism has been investigated in several diseases, in which thrombus formation is a key pathogenetic factor, but the definition of the specific

* Correspondence: piscione@unina.it
Department of Clinical Medicine, Cardiovascular and Immunologic Sciences,
Federico II University School of Medicine, Naples, Italy

role of such polymorphisms on thrombotic coronary and cerebrovascular complications has been challenging. Weiss et al. [8] observed a strong association between the PLA2 polymorphism of the GP IIIa gene and acute coronary thrombosis, and this association was strongest in patients who had had coronary events before the age of 60 years, suggesting this polymorphism as an inherited risk factor for coronary thrombosis. These findings were further expanded on peripheral artery disease by Mikkelsen [9] who reported an association between PLA2 variant and the progression of atherosclerosis in the abdominal aorta. Similarly, in the Copenhagen City Heart Study, a prospective study with 9,149 subjects, there was a three-fold and four-fold risk of ischemic cardiovascular disease and MI in men <40 years homozygous for PLA2 polymorphism [10]. On the other hand, several studies failed to confirm this association; indeed a meta-analysis of 23 of such negative studies, showed the lack of association between the PLA2 allele and the risk of myocardial infarction and this negative result persisted even after subgroup analyses [11]. Therefore, up to date, available data are hugely uncertain and still debated. Several issues common to epidemiologic risk factor studies can be accountable for the difficulty encountered in reproducing the results of genetic association studies. Among these limitations there is inaccurate phenotyping [12]. In particular, atherosclerotic disease may present with different clinical manifestations. It is therefore pivotal to accurately select the clinical phenotype that can be affected by the genetic variability. To address this issue, and therefore gain more insight on the role of PLA2 polymorphism on atherothrombotic disease, we performed a prospective study in a cohort of patients selected for angiography documented severe coronary artery disease (CAD), which needed percutaneous coronary intervention (PCI). Moreover, to assess the role of this polymorphism on cerebrovascular disease, a replication study was performed in an independent population of hypertensive subjects, screened for large vessel atherosclerotic disease, and previous ischemic cerebrovascular events, namely stroke or transient ischemic attack (TIA). Finally, a group of 100 healthy subjects was included as control population of our study.

Methods

Patients

To assess the role of PLA2 polymorphism on cardiovascular disease we analyzed the incidence of this gene variant in a total of 574 unrelated individuals. A first group was constituted by 400 consecutive patients (mean age 60.5 ± 10 , 83% male) undergoing elective or urgent PCI for CAD documented by a positive stress test or by Tl single photon emission computed tomography. To

perform a replication analysis we selected an independent population of patients with cerebrovascular disease. Therefore, a population of 74 unrelated patients (mean age 61.58 ± 2 , 63% male) with cerebrovascular events was examined, recruited from those admitted to the Hypertension Diagnosis and Care Outpatient Clinic of "Federico II" University of Naples and participating in the 'Campania Salute Project' [13]. Finally, to identify normal distribution of the PLA genotype, we enrolled a control population of 100 gender- and age-matched healthy unrelated individuals (60 ± 10 years, 83% male), recruited from blood donors of our blood bank. Controls were free from heart disease, medication use, and cardiovascular risk factors, except for smoking habits. To help to diminish the likelihood of bias and reduce population stratification case and controls individuals were drawn from the same geographic region (Campania, Southern Italy) and matched for age, sex and race. All clinical data and biochemical features of enrolled patients were stored in a computerized database. A written informed consent was obtained from all patients according to the Ethics Committee of the "Federico II" University of Naples School of Medicine. The Ethic Committee regulations of our Institution approved the study protocol.

Percutaneous coronary intervention

PCI was performed according to the American Heart Association/American College of Cardiology guidelines [14]. Antegrade perfusion was graded by Thrombolysis In Myocardial Infarction (TIMI) criteria [15]. Angiographic lesion morphology was classified according to American Heart Association/American College of Cardiology classification [16]. Stenoses >50% were considered significant. Bare-metal stents (BMS) were used in the 80% of patients, while drug-eluting stent (DES) in the remaining 20%. Glycoprotein IIb/IIIa inhibitors were used in 30% of patients. After the procedures, all patients were on dual antiplatelet therapy with aspirin and clopidogrel for at least 30 days after BMS implantation and for 12 months after DES. Other cardioactive drugs for long-term medical treatment were left to the discretion of the attending cardiologists.

Outcome evaluation

In the evaluation of long-term clinical outcome, major adverse cardiac events (MACE) were considered as end points, including cardiac death, acute myocardial infarction (AMI), and needs of any new myocardial revascularization (considering re-PCI or coronary artery by-pass graft). All deaths were considered as cardiac, unless it was unequivocally proven non-cardiac. AMI was defined as recurrent chest pain with ST-segment or T-wave changes and recurrent elevation of cardiac enzyme

levels. The follow-up was based on a direct systematic review of all patients' clinical files for a mean study period of 24 ± 4.3 months, contacting relatives or a patient's physician when necessary. Follow-up was completed in all patients and data stored in a computerized database. A second population was identified among the hypertensive cohort of patients afferent to the 'Campania Salute Project' [13]. We selected 74 patients affected by cerebrovascular events, either TIA or stroke. In particular, the diagnosis of TIA or stroke was confirmed by neurological evaluation according to current standards for care [17]. This included patient personal and family history, physical examination, computed tomography or magnetic resonance imaging, and laboratory testing. The diagnosis of stroke was based on WHO criteria, confirmed by TC or MR, when needed. The cause of stroke was identified in large-vessel disease, according to the clinical features and results of the diagnostic workup, based on TOAST pathophysiological classification [18]. TIA was defined as an episode of focal neurological symptoms with abrupt onset and rapid resolution lasting <24 hours that is due to altered circulation to a localized portion of the brain [19].

GpIIa genotyping

Using a commercially available kit (Midiprep DNA, Qiagen, Valencia, California), genomic deoxyribonucleic acid (DNA) was isolated from 2 ml of the peripheral blood samples. PIA2 polymorphism was studied using combined polymerase chain reaction (PCR) and restriction fragment length polymorphism technique (RFLP) on PCR amplified products using PCR conditions and primers on a Thermocycler (MJ Research, St. Bruno, Canada) and DNA polymerase (TAQ, Qiagen) as previously reported [20,21].

Statistical Analysis

Continuous variables are presented as mean \pm SD and categorical variables as absolute number and percentage value. Differences between groups were assessed using univariate analysis of variance for continuous variables, with a Bonferroni post-hoc test for evaluation of multiple comparisons. Categorical variables were analyzed by chi-square test, and odds ratio (OR) with 95% confidence intervals (CIs) or by the Fisher exact test when the expected values in any of the cells of the test, given the frequencies and the overall sample size, was below 10; p value <0.05 was considered significant. Difference in event-free survival between groups were evaluated by the Kaplan-Meier method, comparisons were made using log-rank test. A Cox regression analysis was conducted for the PIA2 polymorphism considering age, cardiovascular risk factors, medication use, left ventricular ejection fraction, angiographic characteristics, and

Table 1 Genotype distribution of PIA2 polymorphism in study populations

Genotype	CAD patients	Hypertensive patients	Control population	P
PIA1/A1	70.4	67.8	72	0.79
PIA1/A2	27	29.1	25	0.91
PIA2/A2	2.6	3.1	3	0.81

CAD: Coronary artery disease

interaction of the PIA2 polymorphism in both the study populations. The software used was SPSS 16 (SPSS Inc., Chicago, Illinois).

Results

Frequencies of PIA2 polymorphism in study population

As reported in Table 1, the frequencies of PIA2 polymorphism was similar between study and control group. The genotype distribution was in Hardy-Weinberg equilibrium. The allele frequency for PIA1 and PIA2 was, respectively, 84% and 16% in patients with CAD, 82.3% and 17.7% in hypertensive subjects with cerebrovascular events, and 84.5% and 15.5% in the control healthy group.

Clinical and angiographic characteristics in patients with coronary artery disease

Accordingly to the allelic distribution of the PIA2 allele we divided patients with CAD into 2 groups: group 1 (300 patients, PIA1/PIA1 genotype; 90% male, mean age 60 ± 10 years) and group 2 (100 patients, PIA1/PIA2 and PIA2/PIA2 genotypes; 81% male, mean age 62.1 ± 8.6 years). As reported in tables, no differences were noted between the two groups regarding baseline clinical (table 2) and angiographic (table 3) features.

Table 2 Clinical characteristics of CAD patients

Variable	PIA1 (n = 300)	PIA2 (n = 100)	p Value
Age	60 \pm 10	62.1 \pm 8.6	0.72
Male sex (%)	90	81	0.03
Hypertension (%)	56	57	0.82
Diabetes (%)	29.3	19.4	0.11
Smoking (%)	58.6	53.8	0.45
Dyslipidemia (%)	55.2	53.8	0.81
Obesity (%)	9.5	7.7	0.89
Family history of CAD (%)	38.2	33.4	0.37
Previous AMI (%)	10.9	15.4	0.35
Previous PCI (%)	10.9	15.4	0.35
Previous CABG (%)	9.1	3.8	0.15
LVEF prior to PCI, mean \pm SD	47 \pm 10	51 \pm 8	0.06

PCI: Percutaneous coronary intervention

LVEF: Left ventricular ejection fraction

Table 3 Angiographic characteristics of CAD patients

Variable	PIA1 (n = 300)	PIA2 (n = 100)	p Value
Coronary artery disease (%)			
LAD	61.9	50	0.27
Cx	33.6	29	0.37
Dx	45	50	0.30
Multivessel Disease (%)			
Lesion type, B2/C (%)	78	85	0.55
BMS (%)	74	66	0.56
DES (%)	26	34	0.57
TIMI 3 post PCI (%)	97.5	98	0.89
cTFC post (mean ± SD)	15.10 ± 6	14.25 ± 8	0.76
Lesion length (mm)	15.54 ± 6.59	16.48 ± 8.74	0.13
Preprocedural stenosis (%)	86.55 ± 10.19	85.05 ± 11.48	0.11
Stent/patient (n)	1.08 ± 0.32	1.07 ± 0.26	0.74

BMS: Bare metal stent, Cx: Left circumflex coronary artery, DES: Drug eluting stent, Dx: Right coronary artery, LAD: Left anterior descending coronary artery.

Medication use

There were no differences between groups regarding medication use at the time of PCI and during follow-up time. In particular, at follow-up time both groups were similarly treated, using dual antiplatelet therapy (99% vs. 98% group 2, $p = \text{NS}$), calcium antagonist (19% vs. 18% group 2, $p = \text{NS}$), beta-blockers (45% vs. 47% group 2, $p = \text{NS}$), angiotensin-converting enzyme inhibitors (36% vs. 34% group 2, $p = \text{NS}$), and statins (42% vs. 40% group 2, $p = \text{NS}$).

Long-term follow-up

There were no significant differences between groups regarding MACE incidence during hospitalization. Interestingly, at long-term follow-up, the rates of MACE were significantly higher in PIA2 group compared to PIA1 (43.5% vs 25.8%, $p = 0.018$). In particular, patients with PIA2 allele showed a significant increased rate of cardiac death (14.6% vs 5.3%, $p = 0.025$), AMI (12% vs 4.5%, $p = 0.043$) and new myocardial revascularization (34.8% vs 17.7%, $p = 0.010$). Accordingly, the Kaplan-Meier analysis for event free survival in patients harboring the PIA2 allele (Figure 1) showed worse long-term outcome for these patients ($p = 0.015$). Cox regression analysis identified the presence of PIA2 allele as an independent predictor for cardiac death (OR: 9.594, 95% CI: 2.6 to 35.3, $p = 0.002$) and overall MACE (OR: 1.973, 95% CI: 1.039 to 3.747, $p = 0.036$). There were no interactions noted for this relationship when considering age, sex, risk factors for CAD, multivessel disease, previous myocardial revascularization, number of treated lesions, and basal left ventricular ejection fraction.

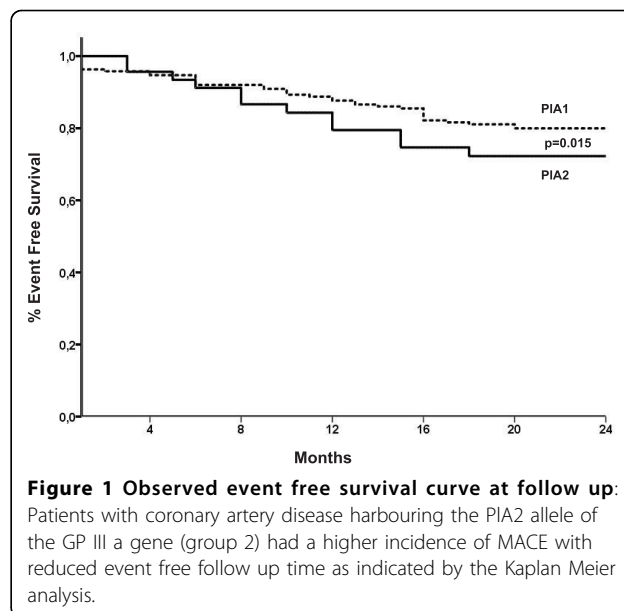


Figure 1 Observed event free survival curve at follow up: Patients with coronary artery disease harbouring the PIA2 allele of the GP III a gene (group 2) had a higher incidence of MACE with reduced event free follow up time as indicated by the Kaplan Meier analysis.

Effect of PIA2 polymorphism on cerebrovascular events in hypertensive patients

To analyze in a different population the impact of this polymorphism on atherothrombotic events we analyzed the impact of PIA2 in hypertensive patients with history of cerebrovascular events according to the level of cerebral damage (TIA or stroke). The characteristics of these patients are depicted in table 4. Both the TIA and stroke groups presented with an elevated cardiovascular risk due to the presence of many risk factors which distribution did not differ between the two groups. Interestingly, PIA2 allele was significantly more represented among patients with stroke than patients with TIA (stroke:46.4%; TIA:17.4%; $p = 0.01$). This polymorphism indeed increased the risk of stroke in this high risk population (OR: 4.1, 95% CI: 1.63-12.4, $p = 0.02$) over TIA. Finally, a multiple regression analysis corrected by common risk factors for cerebrovascular events, showed that PIA2 allele as an independent risk factor for stroke (B:-1.39; Wald: 7.15; $p = 0.001$).

Discussion

The main finding of this study is the relationship between the PIA2 gene variant and the incidence of major adverse cardiovascular events in patients harbouring the PIA2 gene polymorphism. Indeed, in patients with CAD undergoing PCI we found that the presence of PIA2 allele associated with a significantly worse prognosis with a higher incidence of cardiac death, AMI, and new myocardial revascularization. Moreover, in an independent population of hypertensive patients with large vessel atherosclerosis and previous cerebrovascular events, patients harbouring the PIA2 gene polymorphism

Table 4 Characteristics of hypertensive patients

Variable	Hypertensives with TIA (n = 46)	Hypertensives with stroke (n = 28)	P value
Age (years)	62.06 ± 1.63	61.1 ± 2.60	0.77
Male sex (%)	54.3	71.4	0.15
Diabetes (%)	9.7	10.6	0.88
Smoking (%)	55.3	58.1	0.75
Dyslipidemia (%)	51.1	51.6	0.95
SBP (mmHg)	150.08 ± 3.23	147.5 ± 2.88	0.42
DBP (mmHg)	87.94 ± 1.78	88.83 ± 2.16	0.97
LVMI (g/m ²)	127.09 ± 3.64	127.82 ± 2.68	0.98

DBP: Diastolic blood pressure

LVMI: Left Ventricle Mass Index

SBP: Systolic blood pressure

presented with a significantly higher incidence of stroke over TIA. Taken together these data suggest an effect for the PLA2 gene polymorphism in the development of more severe thrombotic complications in high risk patients.

Since the original report from Weiss et al. [8] indicating PLA2 polymorphism as a risk factor for myocardial infarction or unstable angina, several studies have investigated this polymorphism in the effort to discover a novel thrombogenic risk factor but to date results have been inconclusive and often controversial [8,11,22]. The inconsistency of findings in literature can be mostly attributed to differences in the design as well as to the choice of the control group and the endpoint of the studies. Moreover, studies differ in the variation of environmental factors and ethnicity, present biases in the selection of patients and controls and often aim to different clinical endpoints. Since atherosclerosis is a multifactorial disease, it would be too simplistic to explain interindividual variations based on genetic inheritance alone. Indeed several challenges exist in identifying the genetic determinants of such a complex disease including genetic heterogeneity, gene-gene and gene-environment interactions [12]. Furthermore, interaction of multiple genes that are in linkage disequilibrium and simultaneous studies of several genes may reveal associations that at present seem to be weak. Nevertheless, such approaches are costly, and impose the use of large populations and heavy statistic modeling in order to carefully peruse small impact of single gene variants on multifactorial disease [12]. There is still room for candidate gene association study that can be performed in relatively small populations, that are carefully characterized and selected for homogeneity [12]. We also have recently underlined the need for accurately selection of patients in association studies in order to identify the populations in which single gene polymorphisms may be more determinant in complex phenotypes such as atherosclerosis [20,21]. Therefore, since platelets play a major role in the development of

atherosclerotic thrombosis and acute ischemic events, we investigated the role of the PLA2 gene polymorphism in higher risk populations such as patients with severe CAD requiring mechanical revascularization and hypertensive patients with previous cerebrovascular events. Interestingly, in the CAD population, we observed that the presence of PLA2 patients was associated with a 3 times higher risk of death or 2.8 increased risk of AMI. Noteworthy, patients harbouring the PLA2 allele presented an higher risk of needing new revascularization at follow up with 50% of patients undergoing new PCI for the occurrence of a new myocardial infarction. This is consistent with data by Kastrati et al [23] reporting a higher risk of restenosis after coronary stent placement in these patients. Moreover, in an independent population of hypertensive patients with cerebrovascular events, the presence of the PLA2 allele was associated with a 4.1 higher risk to develop stroke rather than TIA. Thus, these data suggest that, in a high risk clinical scenario represented by patients with a greater prevalence of atherothrombotic risk factors, the presence of PLA2 is associated with a more aggressive disease leading to an higher incidence of major ischemic events and to an unfavourable outcome. Our results only apparently differ from the finding observed in a subgroup analysis of the Physicians' health study (PHS) [24] by Ridker et al. [25] which prospectively studied the risk associated with the PLA2 polymorphism for myocardial infarction, stroke or venous thromboses and reported no associations between PLA2 polymorphism and the relative risk to develop any cardiac or cerebro-vascular event. Indeed, as already remarked by previous studies [26,27], the PHS was conducted in a very healthy population, with an event rate 4 times less than general population, and therefore with a very low risk of cardiovascular events. Also, our analysis focused on the outcome and the incidence of MACE in patients that already had a clinical manifestation of the disease, while the PHS aimed to the occurrence of the first event.

Limitations of our study include those inherent to any prospective but observational study. Moreover, since this is an association study, we cannot rule out the presence of a possible linkage disequilibrium with other neighboring genes that might explain the significant association with atherosclerotic phenotype or adverse prognosis.

The study was conducted in patients with severe CAD undergoing PCI while the replication study was performed in hypertensive patients with previous cerebrovascular events; therefore, our findings need to be confirmed in further larger patient populations. Nevertheless, recent studies [20,21] underline the need for selection of patients in association studies in order to identify the populations in which single gene polymorphisms may be more determinant in complex phenotypes such as CAD.

Conclusions and clinical implications

Our study suggests that the PIA2 polymorphism is associated with a more aggressive atherothrombotic disease and adversely affects the prognosis in these high risk patients. Indeed, in patients with severe CAD undergoing PCI the presence of PIA2 allele is associated with increased risk of death, myocardial infarction and new myocardial revascularization. Moreover, high risk hypertension patients harbouring the PIA2 allele show an increased risk to develop severe cerebral damage. Therefore considering the atherothrombotic disease, the PIA2 genotype could be useful to physicians in targeting antithrombotic strategies and therapeutic options. Since atherosclerosis is a multifactorial disease, future studies on interactions between environmental factors, common cardiovascular risk factors and platelet associated genetic determinants are warranted.

All Authors substantially contributed to the production of the manuscript.

FP and GG identified the hypothesis of the study. GG, GS and GI drafted the manuscript. Furthermore, FP was in charge of the percutaneous revascularization procedures, together with GG in patients with coronary artery disease. RDR, RP, SC and VT carried out the molecular genetic studies, performed the statistical analysis, patients' data collection and follow up. MC and BT are respectively, the heads of the Division of Cardiology and Division of Internal Medicine, at our Institution, and they finally approved the submission of the manuscript.

All authors read and approved the final manuscript.

Received: 26 February 2010 Accepted: 16 September 2010
Published: 16 September 2010

References

1. Davi G, Patrono C: Platelet activation and atherothrombosis. *The New England journal of medicine* 2007, **357**(24):2482-2494.

2. Lefkowitz J, Plow EF, Topol EJ: Platelet glycoprotein IIb/IIIa receptors in cardiovascular medicine. *The New England journal of medicine* 1995, **332**(23):1553-1559.
3. Atherosclerosis T, Vascular Biology Italian Study Group: No evidence of association between prothrombotic gene polymorphisms and the development of acute myocardial infarction at a young age. *Circulation* 2003, **107**(8):1117-1122.
4. Payrastra B, Missy K, Trumel C, Bodin S, Plantavid M, Chap H: The integrin alpha IIb/beta 3 in human platelet signal transduction. *Biochemical pharmacology* 2000, **60**(8):1069-1074.
5. Calvete JJ: On the structure and function of platelet integrin alpha IIb beta 3, the fibrinogen receptor. *Proceedings of the Society for Experimental Biology and Medicine Society for Experimental Biology and Medicine (New York, NY)* 1995, **208**(4):346-360.
6. Newman PJ, Derbes RS, Aster RH: The human platelet alloantigens, PIA1 and PIA2, are associated with a leucine33/proline33 amino acid polymorphism in membrane glycoprotein IIIa, and are distinguishable by DNA typing. *The Journal of clinical investigation* 1989, **83**(5):1778-1781.
7. Michelson AD, Furman MI, Goldschmidt-Clermont P, Mascelli MA, Hendrix C, Coleman L, Hamlington J, Barnard MR, Kickler T, Christie DJ, et al: Platelet GP IIIa P1(A) polymorphisms display different sensitivities to agonists. *Circulation* 2000, **101**(9):1013-1018.
8. Weiss EJ, Bray PF, Tayback M, Schulman SP, Kickler TS, Becker LC, Weiss JL, Gerstenblith G, Goldschmidt-Clermont PJ: A polymorphism of a platelet glycoprotein receptor as an inherited risk factor for coronary thrombosis. *The New England journal of medicine* 1996, **334**(17):1090-1094.
9. Mikkelsen J, Perola M, Kauppila LI, Laippala P, Savolainen V, Pajarinen J, Penttila A, Karhunen PJ: The GPIIIa P1(A) polymorphism in the progression of abdominal aortic atherosclerosis. *Atherosclerosis* 1999, **147**(1):55-60.
10. Bojesen SE, Juul K, Schnohr P, Tybjaerg-Hansen A, Nordestgaard BG: Platelet glycoprotein IIb/IIIa P1(A2)/P1(A2) homozygosity associated with risk of ischemic cardiovascular disease and myocardial infarction in young men: the Copenhagen City Heart Study. *Journal of the American College of Cardiology* 2003, **42**(4):661-667.
11. Zhu MM, Weedon J, Clark LT: Meta-analysis of the association of platelet glycoprotein IIIa P1A1/A2 polymorphism with myocardial infarction. *The American journal of cardiology* 2000, **86**(9):1000-1005, A1008.
12. Kullo IJ, Ding K: Mechanisms of disease: The genetic basis of coronary heart disease. *Nature clinical practice* 2007, **4**(10):558-569.
13. De Luca N, Izzo R, Iaccarino G, Malini PL, Morisco C, Rozza F, Iovino GL, Rao MA, Bodenizza C, Lanni F, et al: The use of a telematic connection for the follow-up of hypertensive patients improves the cardiovascular prognosis. *Journal of hypertension* 2005, **23**(7):1417-1423.
14. Smith SC Jr, Dove JT, Jacobs AK, Kennedy JW, Kereiakes D, Kern MJ, Kuntz RE, Popma JJ, Schaff HV, Williams DO, et al: ACC/AHA guidelines for percutaneous coronary intervention (revision of the 1993 PTCA guidelines)-executive summary: a report of the American College of Cardiology/American Heart Association task force on practice guidelines (Committee to revise the 1993 guidelines for percutaneous transluminal coronary angioplasty) endorsed by the Society for Cardiac Angiography and Interventions. *Circulation* 2001, **103**(24):3019-3041.
15. Chesebro JH, Knatterud G, Roberts R, Borer J, Cohen LS, Dalen J, Dodge HT, Francis CK, Hillis D, Ludbrook P, et al: Thrombolysis in Myocardial Infarction (TIMI) Trial, Phase I: A comparison between intravenous tissue plasminogen activator and intravenous streptokinase. Clinical findings through hospital discharge. *Circulation* 1987, **76**(1):142-154.
16. Ellis SG, Vandormael MG, Cowley MJ, DiSciascio G, Deligonou U, Topol EJ, Bulle TM: Coronary morphologic and clinical determinants of procedural outcome with angioplasty for multivessel coronary disease. Implications for patient selection. Multivessel Angioplasty Prognosis Study Group. *Circulation* 1990, **82**(4):1193-1202.
17. Adams H, Adams R, Del Zoppo G, Goldstein LB: Guidelines for the early management of patients with ischemic stroke: 2005 guidelines update a scientific statement from the Stroke Council of the American Heart Association/American Stroke Association. *Stroke; a journal of cerebral circulation* 2005, **36**(4):916-923.
18. Adams HP Jr, Bendixen BH, Kappelle LJ, Biller J, Love BB, Gordon DL, Marsh EE: Classification of subtype of acute ischemic stroke. Definitions for use in a multicenter clinical trial. TOAST. Trial of Org 10172 in Acute Stroke Treatment. *Stroke; a journal of cerebral circulation* 2002, **33**(1):102-108.

19. Easton JD, Albers GW, Caplan LR, Saver JL, Sherman DG: **Discussion: Reconsideration of TIA terminology and definitions.** *Neurology* 2004, **62**(8 Suppl 6):S29-34.
20. Lanni F, Santulli G, Izzo R, Rubattu S, Zanda B, Volpe M, Iaccarino G, Trimarco B: **The PI(A1/A2) polymorphism of glycoprotein IIIa and cerebrovascular events in hypertension: increased risk of ischemic stroke in high-risk patients.** *Journal of hypertension* 2007, **25**(3):551-556.
21. Piscione F, Iaccarino G, Galasso G, Cipolletta E, Rao MA, Brevetti G, Piccolo R, Trimarco B, Chiariello M: **Effects of Ile164 polymorphism of beta2-adrenergic receptor gene on coronary artery disease.** *J Am Coll Cardiol* 2008, **52**(17):1381-1388.
22. Bojesen SE, Juul K, Schnohr P, Tybjaerg-Hansen A, Nordestgaard BG: **Platelet glycoprotein IIb/IIIa PI(A2)/PI(A2) homozygosity associated with risk of ischemic cardiovascular disease and myocardial infarction in young men: the Copenhagen City Heart Study.** *J Am Coll of Cardiol* 2003, **42**(4):661-667.
23. Kastrati A, Schomig A, Seyfarth M, Koch W, Elezi S, Bottiger C, Mehilli J, Schomig K, von Beckerath N: **PIA polymorphism of platelet glycoprotein IIIa and risk of restenosis after coronary stent placement.** *Circulation* 1999, **99**(8):1005-1010.
24. **Final report on the aspirin component of the ongoing Physicians' Health Study. Steering Committee of the Physicians' Health Study Research Group.** *The New England journal of medicine* 1989, **321**(3):129-135.
25. Ridker PM, Hennekens CH, Schmitz C, Stampfer MJ, Lindpaintner K: **PIA1/A2 polymorphism of platelet glycoprotein IIIa and risks of myocardial infarction, stroke, and venous thrombosis.** *Lancet* 1997, **349**(9049):385-388.
26. Goldschmidt-Clermont PJ, Roos CM, Cooke GE: **Platelet PIA2 polymorphism and thromboembolic events: from inherited risk to pharmacogenetics.** *Journal of thrombosis and thrombolysis* 1999, **8**(2):89-103.
27. Mikkelsen J, Perola M, Laippala P, Penttila A, Karhunen PJ: **Glycoprotein IIIa PI(A1/A2) polymorphism and sudden cardiac death.** *J Am Coll Cardiol* 2000, **36**(4):1317-1323.

Pre-publication history

The pre-publication history for this paper can be accessed here:
<http://www.biomedcentral.com/1471-2261/10/41/prepub>

doi:10.1186/1471-2261-10-41

Cite this article as: Galasso *et al.*: The GPIIIA PIA2 polymorphism is associated with an increased risk of cardiovascular adverse events. *BMC Cardiovascular Disorders* 2010 **10**:41.

**Submit your next manuscript to BioMed Central
and take full advantage of:**

- Convenient online submission
- Thorough peer review
- No space constraints or color figure charges
- Immediate publication on acceptance
- Inclusion in PubMed, CAS, Scopus and Google Scholar
- Research which is freely available for redistribution

Submit your manuscript at
www.biomedcentral.com/submit



Letter to the Editor

Advanced algorithms can lead to electrocardiographic misinterpretations

Salvatore Luca D'Ascia¹, Gaetano Santulli¹, Vincenzo Liguori¹, Vittoria Marino¹,
Claudia Arturo¹, Massimo Chiariello¹, Cristoforo D'Ascia^{*,1}

Department of Clinical Medicine, Cardiovascular and Immunologic Sciences, University of Naples "Federico II", Italy

Received 22 June 2008; accepted 26 November 2008

Available online 12 January 2009

Abstract

We observed a patient with syncope, who implanted a pacemaker with advanced algorithms such as “atrial-tachy response” and “dynamic atrio-ventricular delay”. After one year, conventional ECG Holter showed pacemaker malfunction, wrongly attributed to exposure to electromagnetic field. In fact, telemetry revealed an inappropriate programming and solved our case. Holter monitoring is commonly performed in the evaluation of pacemaker malfunction, albeit it remains a quite shallow diagnostic method especially to detect electromagnetic interferences. New algorithms seem important, but it is reasonable to obtain more suitable analytical tools, too.

© 2008 Elsevier Ireland Ltd. All rights reserved.

Keywords: Pacemaker malfunction; Holter monitoring; Electromagnetism; Atrial-tachy response; Atrio-ventricular delay

1. Introduction

It is common knowledge that the presence of electromagnetic interferences is involved in a wide range of devices dysfunction [1–3]. Specific settings of pacemaker (PM) are required in order to reduce interference. However, the interference is identifiable only by endocardial signal (EGM) tracing with a typical morphology that could be lacking when the interference is present exclusively in the electronic circuit. Moreover, PM malfunction could be present only when the subject is exposed to electromagnetic field. New generation algorithms offer tailored program settings, albeit both devices' reduced memory and few number of telemetric controls often require a traditional 24 h ECG Holter recording system [4] at follow-up.

* Corresponding author. Department of Clinical Medicine, Cardiovascular and Immunologic Sciences, Via Sergio Pansini, 5-Ed. 2; 80131 Naples, Italy. Tel./fax: +39 081 7463075.

E-mail address: gaetanosantulli@libero.it (C. D'Ascia).

¹ Postal Address: Dipartimento di Medicina Clinica, Scienze Cardiovascolari ed Immunologiche, Università degli Studi di Napoli "Federico II". Via Pansini no. 5, Ed. 2; 80131 Naples, Italy.

2. Clinical case

A 70 years old woman was admitted to our hospital because of a syncope. The ECG revealed a second degree type 2 atrioventricular block. The woman was not affected by documented hypertension, coronary artery disease or diabetes evaluated by standard methods. Subsequently, a dual chamber device “Discovery 2” DDD Guidant with bipolar endocardial catheters (all parameters are depicted in Table 1) was implanted [5]. No adverse events took place during surgical intervention or hospitalization. In order to assess device function during daily activities, the patient underwent Holter monitoring, performed 1 year after implantation.

The patient lived in a house placed near a mobile phone radio antenna and consequently probably subjected to an intensive electromagnetic field. This fact was not known at the moment of implantation.

Holter analysis showed both atrial tachyarrhythmia and atrial fibrillation. In the first case, an inappropriate ventricular tracking not stopped by atrial-tachy response (ATR) algorithm occurred (Fig. 1A); in the second case, an atrial undersensing determined a useless DDD stimulation with frequent fusions (Fig. 1B).

Table 1
Setting parameters of pacemaker device.

Mode: DDD	
Electro catheter configuration: bipolar	
Ventricular and atrial sensing and output: standard	
Ventricular	Atrial
Impedance: 800 Ω	Impedance: 796 Ω
Amplitude: 7 mV	Amplitude: 3.1 mV
Threshold: 0.8 V at 0.5 ms; 3 mV at 0.5 ms	Threshold: 0.6 V at 0.5 ms; 2.6 mV at 0.5 ms
Lower rate: 60 bpm	
Frequency hysteresis: OFF	
AV delay: <i>DYNAMIC</i> (80 ms at max rate–150 ms at minimum rate)	
Maximum tracking rate (MTR): 120 bpm	
Atrial-tachy response (ATR): on	

Besides, the atrio-ventricular delay (AVD) programmed in *DYNAMIC* mode, was shorter than the expected one. We highlight that the *DYNAMIC* AVD provides a physiologic replay of the cardiac frequency variation, so that the AVD used at 60 bpm (lower ratio) is 150 ms (high), while at 100 bpm the AVD is 80 ms (low), with a linear correlation for the intermediate frequencies. Anyway, Holter documented cardiac cycles at 60 bpm in which AVD was shorter than expected.

3. Discussion

How to explain PM malfunction? The first hypothesis was an abnormality linked to patient's exposure to electromagnetic interferences [1,4–6]. Pacing, sensing and impedances tested by telemetry were found to be in normal range (Table 1), with no matching with the observed abnormalities.

The second hypothesis was that the device had been reprogrammed by other physicians in another medical center. Indeed, the patient referred about several previous cardiologic visits, but she was not informed about re-programming and did not exhibit any documentation. Our interpretation of Holter monitoring [4,6] was that PM had been re-programmed in the ATR *OFF* mode. This fact was then confirmed by telemetric interrogation.

About the variability of AVD, we saw that this phenomenon used to happen always after a cycle preceding the maximum tracking rate (MTR), most likely a premature atrial contraction triggered to the ventricle. The presence of this dependence from the preceding cycle has been confirmed by device producers. Analysis of a particular Holter strip confirmed our theory: in fact, ECG showed a cycle at MTR followed by stimulation at lower rate. The first beat at lower rate is at AVD of 80 ms, while the subsequent beats are at AVD of 150 ms, related to the previous long cycle (Fig. 1C).

4. Conclusions

The present case-report highlights that PM settings have both electrophysiological and clinical relevance [5]. ATR and

DYNAMIC-AVD are advanced algorithms of a considerable clinical impact albeit an adequate knowledge is the fundamental premise for their use. The risk of electromagnetic interference, permanent or intermittent, needs to be checked in any case, possibly in the same setting where the interference seems to be present [5,6]. Nevertheless, because of the

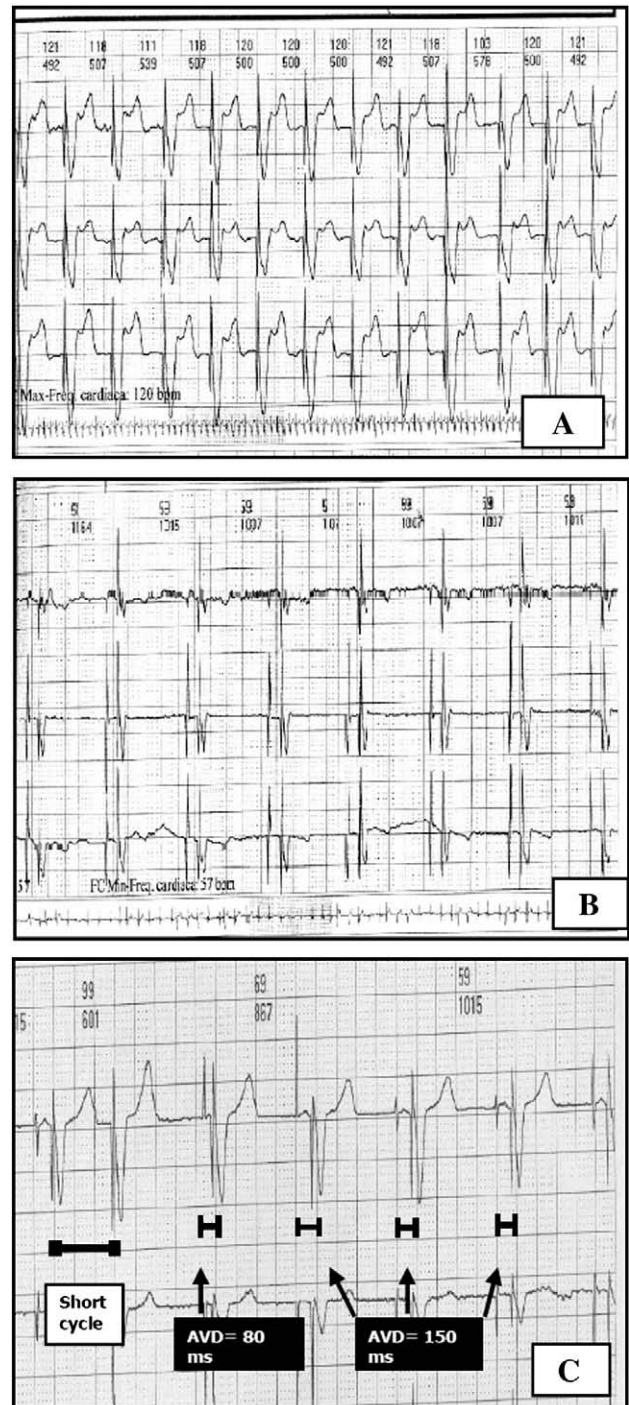


Fig. 1. (A) Missed intervention of ATR algorithm: AF triggered in Ventricle. (B) Inadequate DDD stimulation due to atrial undersensing. (C) Dynamic AV delay previous-cycle-dependent.

underlined problem, it should be desirable to plan an increased number of telemetric controls, also using on-line systems. From a technical point of view, we evidence that these devices don't keep either the date of the last programming change or the operator that reprogrammed the device, but there is only the most recent interrogation date. Therefore, it would be preferable to have in all devices a list of programming changes, with the possibility to identify any operator. In this way, interpretation of PM behavior could become easier, enabling a reliable assessment of the appropriateness of special pacing algorithms, in order to improve the detection of PM dysfunctions due to inappropriate programming [4]. In fact, with increasing automation, analysis of the ambulatory tracing becomes very difficult without access to the internal operation of the PM.

Acknowledgement

The authors of this manuscript have certified that they comply with the Principles of Ethical Publishing in the *International Journal of Cardiology* [7].

References

- [1] Chongtham DS, Bahl A, Kumar RM, Talwar KK. Inappropriate shock delivery by implantable cardioverter defibrillator due to electrical interference with washing machine. *Int J Cardiol* 2007;118:e44.
- [2] Thaker JP, Patel MB, Jongnarangsin K, Liepa VV, Thakur RK. Electromagnetic interference with pacemakers caused by portable media players. *Heart Rhythm* 2008;5:538.
- [3] Trigano A, Blandeau O, Dale C, Wong MF, Wiart J. Risk of cellular phone interference with an implantable loop recorder. *Int J Cardiol* 2007;116:126.
- [4] Nowak B, Henry S, Mols R, Maertens S, Coenen M, Meyer J. Holter recordings with continuous marker annotation to evaluate pacemaker function. *Ann Noninvasive Electrocardiol* 2002;7:22.
- [5] Vardas PE, Auricchio A, Blanc JJ, et al. Guidelines for cardiac pacing and cardiac resynchronization therapy. The Task Force for Cardiac Pacing and Cardiac Resynchronization Therapy of the European Society of Cardiology. Developed in collaboration with the European Heart Rhythm Association. *Europace* 2007;9:959.
- [6] Sweesy MW. Understanding electromagnetic interference. *Heart Rhythm* 2004;1:523.
- [7] Coats AJ. Ethical authorship and publishing. *Int J Cardiol* 2009;131:149–50.

Intracardiac Injection of AdGRK5-NT Reduces Left Ventricular Hypertrophy by Inhibiting NF- κ B-Dependent Hypertrophic Gene Expression

Daniela Sorriento, Gaetano Santulli, Anna Fusco, Antonio Anastasio, Bruno Trimarco, Guido Iaccarino

Abstract—Several studies underline the role of the transcription factor NF- κ B in the development of left cardiac hypertrophy (LVH). We have demonstrated recently that the RGS homology domain within the amino terminus of GRK5 (GRK5-NT) is able to inhibit NF- κ B transcription activity and its associated phenotypes. The aim of this study was to evaluate the ability of GRK5-NT to regulate LVH through the inhibition of NF- κ B both in vitro and in vivo. In cardiomyoblasts, GRK5-NT inhibits phenylephrine-induced transcription of both NF- κ B and atrial natriuretic factor promoters, assessed by luciferase assay, thus confirming a role for this protein in the regulation of cardiomyocyte hypertrophy. In vivo, we explored 2 rat models of LVH, the spontaneously hypertensive rat and the normotensive Wistar Kyoto rat exposed to chronic administration of phenylephrine. Intracardiac injection of an adenovirus encoding for GRK5-NT reduces cardiac mass in spontaneously hypertensive rats and prevents the development of phenylephrine-induced LVH in Wistar Kyoto rats. This associates with inhibition of NF- κ B signaling (assessed by NF- κ B levels), transcriptional activity and phenotypes (fibrosis and apoptosis). Such phenomenon is independent from hemodynamic changes, because adenovirus encoding for GRK5-NT did not reduce blood pressure levels in spontaneously hypertensive rats or in Wistar Kyoto rats. In conclusion, our study supports the regulation of LVH based on the GRK5-NT inhibition of the NF- κ B transduction signaling. (*Hypertension*. 2010;56:696-704.)

Key Words: cardiac hypertrophy ■ intracardiac injection ■ spontaneously hypertensive rats ■ NF- κ B ■ transcription factors

NF- κ B is an ubiquitously expressed transcription factor that modulates the expression of genes involved in the regulation of cell functions, such as survival, apoptosis, growth, division, innate immunity, differentiation, and cellular responses to stress, hypoxia, and ischemia.¹⁻⁴ The classic cellular model in which this factor is studied is the immune system for its central role in cytokine production.^{4,5} It has been reported recently that NF- κ B is relevant in the development of left ventricular hypertrophy (LVH) and remodeling through mechanisms independent from inflammation. NF- κ B mediates hypertrophic growth of cardiomyocytes in response to G protein-coupled receptor agonists, including norepinephrine, endothelin 1, and angiotensin II.^{6,7} Also, NF- κ B inhibition attenuates LVH in different animal models of disease.^{8,9} This evidence suggests that NF- κ B blockade may be an effective strategy to inhibit LVH and remodeling. The family of G protein-coupled receptor kinases (GRKs) and, in particular GRK2 and GRK5, possesses the ability to bind both NF- κ B and its inhibitor, I κ B α .^{10,11} In particular,

GRK5, by means of its RGS homology (RH) domain within the amino terminus, interacts with I κ B α leading to the stabilization and accumulation of the I κ B α /NF- κ B complex in the nucleus and, consequently, to the inhibition of NF- κ B transcriptional activity.¹¹ This feature of the RH domain of GRK5 leads to the hypothesis that the use of peptides that are designed and engineered on this sequence of the kinase may induce NF- κ B inhibition. When applied to cardiac myocytes, this strategy could efficiently reduce hypertrophic responses. To test this hypothesis, we evaluated whether an adenovirus that encodes for the RH domain within the amino terminal of GRK5 (AdGRK5-NT) is able to regulate hypertrophic responses of the cardiac myocyte, both in vitro and in vivo, by means of its ability to inhibit NF- κ B transcription activity.

Methods

Cell Culture

A cell line of cardiac myoblasts (H9C2) was maintained in culture in DMEM supplemented with 10% FBS at 37°C in 95% air-5% CO₂.

Received May 4, 2010; first decision May 26, 2010; revision accepted June 29, 2010.

From the Department of Clinical Medicine, Cardiovascular and Immunologic Sciences, "Federico II University," Naples, Italy.

D.S. and G.S. are joint first authors with equal contributions to this work.

D.S. and G.S. participate in the PhD Program "Clinical Pathophysiology and Experimental Medicine"; A.F. participates in the PhD Program "Model Organisms in Biomedical and Veterinary Research" of the Federico II University. Author contributions are as follows: D.S., G.S., and G.I. conceived the research; D.S., G.S., A.F., and A.A. performed experiments; G.S. and G.I. analyzed the data; D.S., G.S., G.I., and B.T. drafted the article.

Correspondence to Guido Iaccarino, Dipartimento di Medicina Clinica, Scienze Cardiovascolari ed Immunologiche, Università degli Studi di Napoli "Federico II," via Pansini 5; Edificio 2, 80131 Naples, Italy. E-mail guiaccar@unina.it

© 2010 American Heart Association, Inc.

Hypertension is available at <http://hyper.ahajournals.org>

DOI: 10.1161/HYPERTENSIONAHA.110.155960

Luciferase Assay

Cells were transfected with plasmid expression vectors containing the luciferase reporter gene linked to 5 repeats of an NF- κ B binding site (κ B-Luc) or atrial natriuretic factor (ANF) promoter and infected with 10^{10} pfu/mL of an adenovirus encoding the amino-terminal region of GRK5 (AdGRK5-NT) that comprises the RH domain. AdGRK5-NT was a kind gift of Prof Walter J. Koch (Thomas Jefferson University).¹² Transient transfection was performed using the Lipofectamine 2000 (Invitrogen) according to the manufacturer's instruction. Cells were stimulated with the alpha 1 adrenergic receptor agonist phenylephrine (PE; 10^{-7} M) for 24 hours. Lysates were analyzed using the luciferase assay system with reporter lysis buffer from Promega and measured by liquid scintillation. Luciferase activity was normalized against the coexpressed β -galactosidase activity to overcome variations in transfection efficiency between samples.

In Vivo Study

Experiments were carried out in accordance with the Federico II University Ethical committee on 12-week-old normotensive Wistar Kyoto (WKY; $n=13$, subdivided as follows: untreated $n=4$, PE $n=3$, PE+AdLac-Z $n=3$, and PE+AdGRK5-NT $n=3$) and spontaneously hypertensive (SHR; $n=12$, subdivided as follows: untreated $n=3$, AdLac-Z $n=3$, and AdGRK5-NT $n=6$) male rats (Charles River, Calco, LC, Italy), which had access to water and food ad libitum. The animals were anesthetized by vaporized isoflurane (4%). After the induction of anesthesia, rats were orotracheally intubated, the inhaled concentration of isoflurane was reduced to 1.8%, and lungs were mechanically ventilated (New England Medical Instruments Scientific, Inc) as described previously.¹³ The chest was opened under sterile conditions through a right parasternal minithoracotomy to expose the heart. Then, we performed 4 injections (50 μ L each) of AdGRK5-NT (10^{10} pfu/mL) or AdLac-Z (10^{10} pfu/mL), as control, into the cardiac wall (anterior, lateral, posterior, and apical). Finally, the chest wall was quickly closed in layers using 3-0 silk suture, and animals were observed and monitored until recovery. In the WKY group, we implanted under the skin a miniosmotic pump (ALZET 2004) releasing PE (100 mg/kg).¹⁴

Echocardiography

Transthoracic echocardiography was performed at days 0, 7, 14, and 28 after surgery using a dedicated small-animal high-resolution imaging system (VeVo 770, Visualsonics, Inc) equipped with a 17.5-MHz transducer (RMV-716). The rats were anesthetized by isoflurane (4%) inhalation and maintained by mask ventilation (isoflurane 2%). The chest was shaved with a depilatory cream (Veet, Reckitt-Benckiser).¹⁵ Left ventricular (LV) end-diastolic and LV end-systolic diameters (LVEDD and LVESD, respectively) were measured at the level of the papillary muscles from the parasternal short-axis view as recommended.¹⁶ Intraventricular septal (IVS) and LV posterior wall thickness (PW) were measured at end diastole. LV fractional shortening (LVFS) was calculated as follows: $LVFS = (LVEDD - LVESD) / LVEDD \times 100$. LV ejection fraction (LVEF) was calculated using a built-in software for the VeVo770.¹³ LV mass (LVM) was calculated according to the following formula, representing the M-mode cubic method: $LVM = 1.05 \times [(IVS + LVEDD + LVPW)^3 - (LVEDD)^3]$; LVM was corrected by body weight. All of the measurements were averaged on 5 consecutive cardiac cycles and analyzed by 2 experienced investigators blinded to treatment (G.S. and A.A.).

Blood Pressure Measurement and Evaluation of Cardiac Performance

Blood pressure (BP) was measured as described previously,^{17,18} and the record of both systolic (SBP) and diastolic (DBP) BPs was taken using a pressure transducer catheter (Mikro-Tip, Millar Instruments, Inc). The catheters already placed in the ascending aorta were then advanced further into LV to record the maximal and minimal first derivatives of pressure over time (dP/dt maximum and dP/dt minimum), as indices of global cardiac contractility and relaxation.¹⁹ To include the effects of differences of SBP on cardiac contractility, we

also corrected dP/dt maximum by peak systolic pressure (dP/dt maximum/SBP), as described previously.²⁰ These maneuvers were performed at week 4 after surgery.

Histology

Four weeks after AdGRK5-NT or AdLac-Z intracardiac injection, the hearts were immersion fixed in 10% buffered paraformaldehyde. The tissues were embedded in paraffin, cut at 5 μ m, and processed. For Masson's trichrome staining of collagen fibers, slides were stained with Weigert hematoxylin (Sigma-Aldrich) for 10 minutes, rinsed in PBS (Invitrogen), and then stained with Biebrich scarlet-acid fuchsin (Sigma-Aldrich) for 5 minutes. Slides were rinsed in PBS and stained with phosphomolybdic/phosphotungstic acid solution (Sigma-Aldrich) for 5 minutes, then stained with light green (Sigma-Aldrich) for 5 minutes. Slides were rinsed in distilled water, dehydrated with 95% and absolute alcohol, and a coverslip was placed. To evaluate adenovirus expression, paraffined sections were analyzed directly at fluorescent microscopy or the green fluorescent protein (GFP) tag was evaluated by immunohistochemistry, as previously described.¹² For the analysis of cardiomyocytes size, Masson's trichrome staining sections were used.²¹ The areas (squared micrometers) of 100 cardiac myocytes per heart were measured with the public domain Java image processing program ImageJ.²²

Western Blot

The experiments were performed as described previously.¹¹ The antibodies anti-I κ B α , actin, and histone 3 were from Santa Cruz Biotechnology, Inc; anticaspase 3, NF- κ B, p-NF κ B (p65), and phospho-cAMP responsive element binding (p-CREB) antibodies were from Cell Signaling Technology. Densitometric analysis was performed using Image Quant software (Molecular Dynamics, Inc). Blots from 3 independent experiments were quantified and corrected for appropriate loading control. Densitometric analysis was adapted to fit a graph scale between 0 and 10 000 arbitrary densitometric units (ADUs). Results are reported as mean \pm SEM.

Real-Time PCR

Total RNA was isolated using TRIzol reagent (Invitrogen) and cDNA was synthesized by means of a Thermo-Script RT-PCR System (Invitrogen), following the manufacturer's instruction. After reverse transcription, real-time quantitative PCR was performed with the SYBR Green real-time PCR master mix kit (Applied Biosystems) and quantified by built-in SYBR Green Analysis (Applied Biosystem) on a StepOne instrument (Applied Biosystem). Primers for gene analysis were as follows: ANF: forward 5'cgtgccccgaccacgccagcatggctccc3', reverse 5'ggctccgaggccagcagcagagcctca3'; tumor necrosis factor alpha (TNF- α): forward 5'caggagaaagtcagcctct3', reverse 5'cgataaagggtcagagtaat3'; and 18S: forward 5'gtaaccctggaaccatt3', reverse 5'catccaatcgtagtagc3'.

Electrophoretic Mobility-Shift Assay

Nuclear proteins were isolated from heart samples, and NF- κ B binding activity was examined by electrophoretic mobility-shift assay, as described previously.¹¹ For the competition, assay nuclear extracts were incubated with a 50-fold excess of unlabeled oligos for 20 minutes before adding the labeled oligo. Electrophoretic mobility-shift assay for organic cation transporter 1 (OCT-1) binding was performed as a loading control (5'tgtcaatgcaaacctctctct3').

Statistical Analysis

For each parameter we compared the values observed in the AdGRK5-NT-treated SHRs ($n=6$) with a control SHR group, which was composed of untreated ($n=3$) and AdLacZ-treated ($n=3$) SHRs. This was possible because within these groups there was no statistical difference. For the same reason, in WKY rats we compared the effect of PE between AdGRK5-NT-treated rats ($n=3$) with a control WKY PE group, composed of PE-treated ($n=3$) and PE/AdLac-Z-treated ($n=3$) rats. Both SHRs and PE-treated WKY rats were compared with untreated WKY rats ($n=4$). All values are

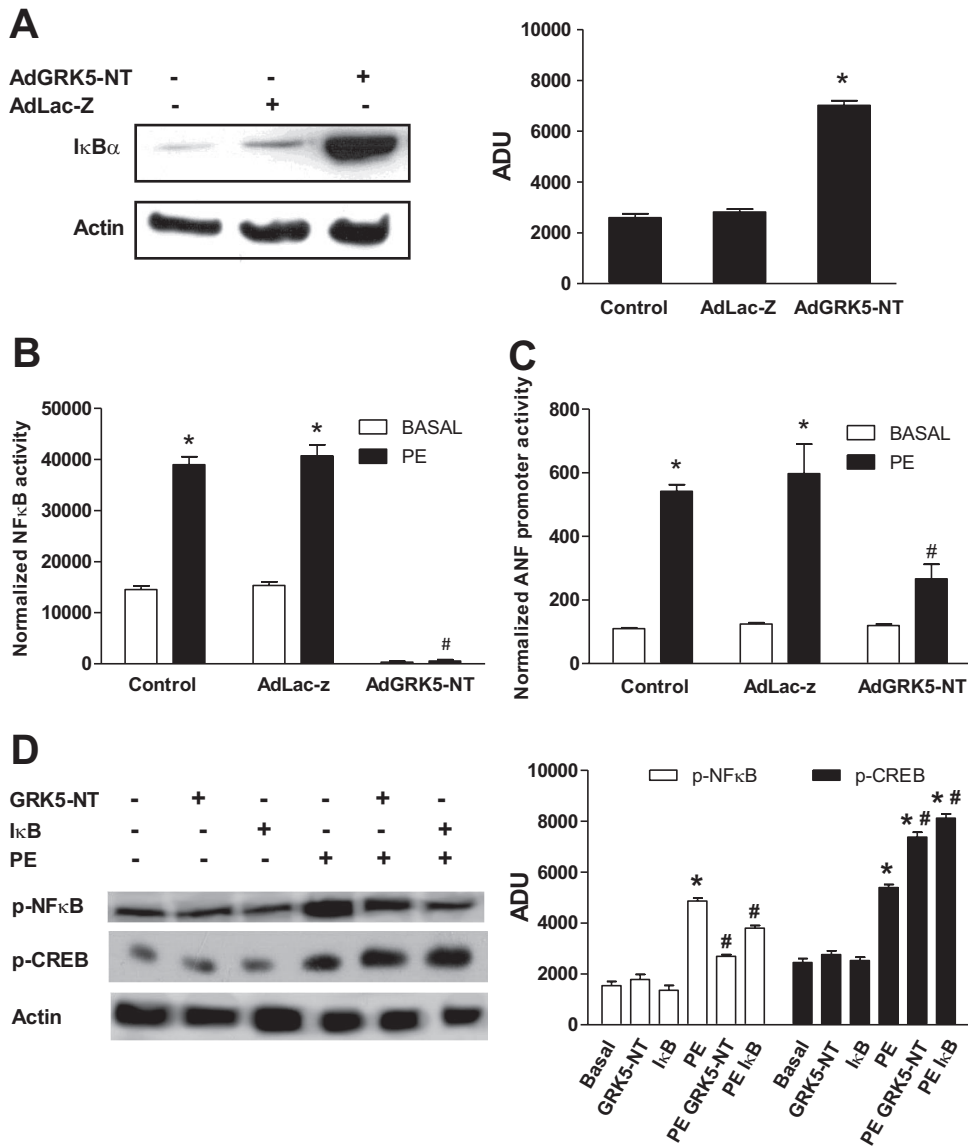


Figure 1. The effect of AdGRK5-NT on hypertrophy in vitro. A, In H9C2 cardiomyoblasts, GRK5-NT overexpression was induced by adenovirus-mediated gene transfer (AdGRK5-NT), and total IκBα levels were analyzed by Western blot. GRK5-NT causes an increase of IκBα levels. AdLac-Z and noninfected cells were used as controls. The graph shows densitometric analysis after normalization according to Methods from 3 independent experiments expressed in ADUs; * $P < 0.05$ vs control. B, H9C2s were infected with AdGRK5-NT and stimulated with PE. NF-κB activity was evaluated by luciferase assay and normalized according to the Methods section. PE increases NF-κB activity, and AdGRK5-NT inhibits this activity both in basal condition and after PE stimulation (* $P < 0.05$ vs basal, # $P < 0.05$ vs control). Results are expressed as mean ± SEM from 5 independent experiments. C, H9C2s were infected with AdGRK5-NT and stimulated with PE. ANF promoter activity was evaluated by luciferase assay and normalized as indicated in the Methods section. PE induces ANF promoter activity, and AdGRK5-NT inhibits such response (* $P < 0.05$ vs Basal, # $P < 0.05$ vs Control). Results are expressed as mean ± SEM from 5 independent experiments. D, H9C2s were transfected with either GRK5-NT or IκB and stimulated with PE. Control cells were transfected with an empty plasmid. p65 and CREB phosphorylations were evaluated by Western blot. Overexpression of either GRK5-NT or IκB inhibits NF-κB but not CREB activation. Actin was used as loading control. The graph shows the densitometric analysis after normalization according to methods of 3 independent experiments (* $P < 0.05$ vs basal, # $P < 0.05$ vs PE).

presented as mean ± SEM. Two-way ANOVA was performed to compare the different parameters between the different groups. A P value < 0.05 was considered to be significant. Statistics were computed with GraphPad Prism version 5.01 (GraphPad Software).

Results

In Vitro Study

We evaluated in vitro the effect of GRK5-NT, comprising the RH domain, on the regulation of NF-κB signaling and transcriptional activity. In H9C2 cardiomyoblasts, AdGRK5-NT

caused an increase of total IκBα levels (Figure 1A), analyzed by Western blot, as described previously in other cellular types.^{11,12} The effect of GRK5-NT on NF-κB activity was evaluated by luciferase assay. PE increased NF-κB transcription activity, and the overexpression of GRK5-NT reduced such effect both in basal conditions and after PE stimulation (Figure 1B), suggesting that NF-κB is induced by hypertrophic stimuli in cardiac cells and that GRK5-NT is able to inhibit such phenomenon. To assess the ability of GRK5-NT

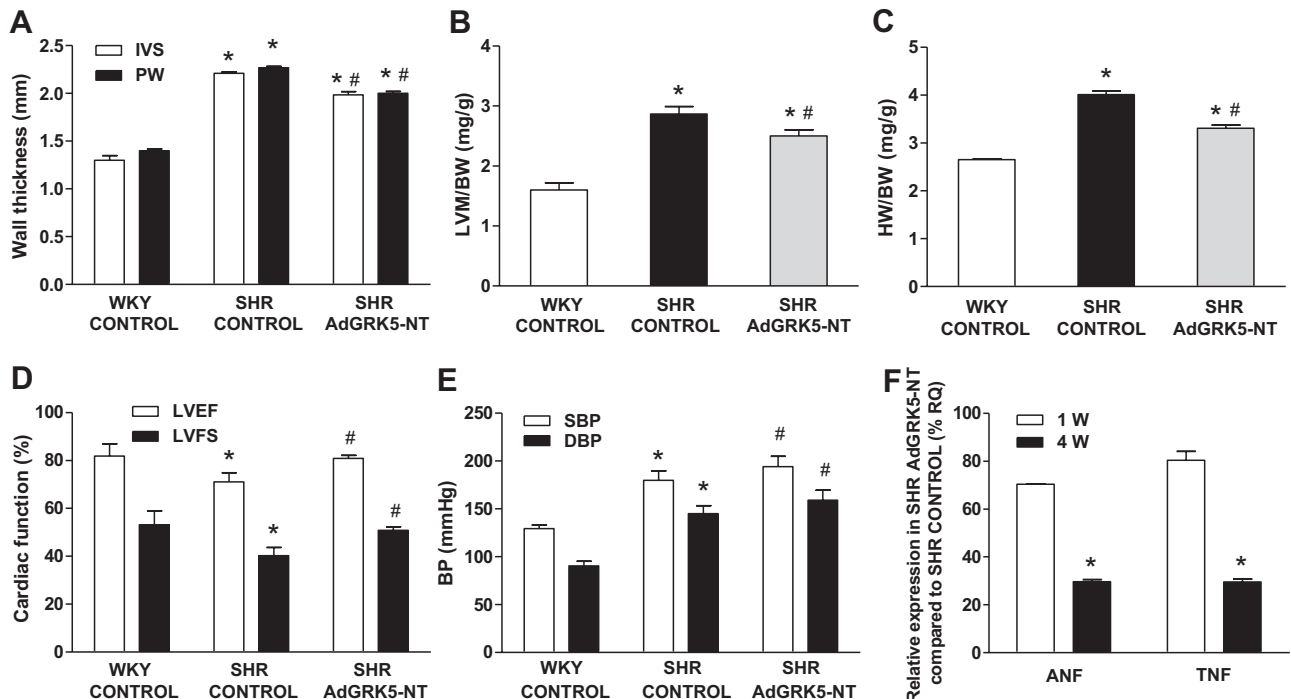


Figure 2. The effect of intracardiac injection of AdGRK5-NT in vivo in SHR. A through C, Cardiac hypertrophy was evaluated by echocardiography in 4 untreated WKY rats, 6 AdGRK5-NT SHR, and 6 control SHR, as indicated in the Methods section. Four weeks after injection, a reduction of IVS and PW (A), LVM/BW ratio (B), and HW/BW ratio (C) was found in AdGRK5-NT versus SHR control hearts ($P < 0.05$ vs WKY; $\#P < 0.05$ vs SHR control). D, Interestingly, LVFS and LVEF were also ameliorated in SHR by AdGRK5-NT as compared with SHR control ($*P < 0.05$ vs WKY; $\#P < 0.05$ vs SHR control). E, To exclude the involvement of BP values in GRK5-NT-dependent regulation of cardiac hypertrophy, we assessed in treated rats SBP and DBP values. AdGRK5-NT-treated rats had higher SBP and DBP than SHR controls ($*P < 0.05$ vs WKY; $\#P < 0.05$ vs SHR control). F, The ability of AdGRK5-NT to reduce LVH was further confirmed on myocardial samples by a reduction of ANF and TNF- α gene expression evaluated by real-time PCR. The values found in AdGRK5-NT-treated LVs were corrected by those found in the SHR control and expressed as the percentage of SHR control at 1 week and 4 weeks from starting treatment ($*P < 0.05$ vs 1 week). Results are expressed as mean \pm SEM from 3 to 5 independent experiments.

to modulate hypertrophy in vitro, we performed an ANF promoter-driven luciferase assay. Figure 1C shows that GRK5-NT overexpression inhibits PE-induced ANF promoter activity. These in vitro data suggest that GRK5-NT can regulate the expression of hypertrophic genes by modulating NF- κ B activity. To evaluate whether GRK5-NT effect is selective for NF- κ B signaling, we assessed its ability to regulate an NF- κ B-independent transcription factor, CREB, by Western blot. We overexpressed in cardiomyoblasts GRK5-NT or the main inhibitor of NF- κ B, I κ B, by transient transfection. Control cells were transfected with an empty plasmid. The overexpression of either GRK5-NT or I κ B inhibited NF- κ B phosphorylation but did not affect CREB activation both in basal condition and after stimulation with PE (Figure 1D). These results indicate that GRK5-NT selectively inhibits NF- κ B signaling and does not affect the signaling of other transcription factors.

In Vivo Study in SHR

Echocardiographic Parameters

To confirm the role of GRK5-NT in the regulation of LVH, we analyzed in vivo the SHR, an animal model of hypertension-induced LVH. AdGRK5-NT or AdLac-Z was injected in the cardiac wall of the SHR. LVH was evaluated weekly for 4 weeks by echocardiography. AdGRK5-NT treatment efficiently reduced IVS and PW thickness (Figure

2A), LVM/body weight (BW; Figure 2B) and the heart weight (HW)/BW ratio (Figure 2C). Cardiac function assessed by ultrasound changed accordingly. Indeed, LV ejection fraction and LVFS, which are depressed in the SHR control group with respect to the WKY rat, returned to the levels of normotensive rats in the AdGRK5-NT-treated SHR (Figure 2D). To rule out changes in hemodynamics as a possible mechanism of regulation of LVH, we measured BP in rats at 4 weeks. BP was slightly but significantly increased in AdGRK5-NT-treated rats with respect to controls (Figure 2E). This phenomenon might be attributed to an amelioration of LV dysfunction observed by cardiac ultrasounds and also

Table. Cardiac Contractility Assessed In Vivo

Group	dP/dt Maximum	dP/dt Minimum	dP/dt Maximum/SBP
WKY control (n=4)	+7989 \pm 486	-6728 \pm 452	59.35 \pm 9.84
SHR control (n=6)	+4187 \pm 296*	-4761 \pm 398*	24.02 \pm 5.08*
SHR AdGRK5-NT (n=6)	+7543 \pm 683†	-6754 \pm 554†	41.87 \pm 8.13†

Cardiac contractility was assessed by intra-LV positioning through the carotid artery of a pressure transducer catheter. WKY control indicates untreated WKY rats; SHR control, SHR control group; SHR AdGRK5-NT, SHR hearts infected with the adenovirus encoding for the amino-terminus region of GRK5. Data are mean \pm SEM.

* $P < 0.05$ vs WKY.

† $P < 0.05$ vs SHR control.

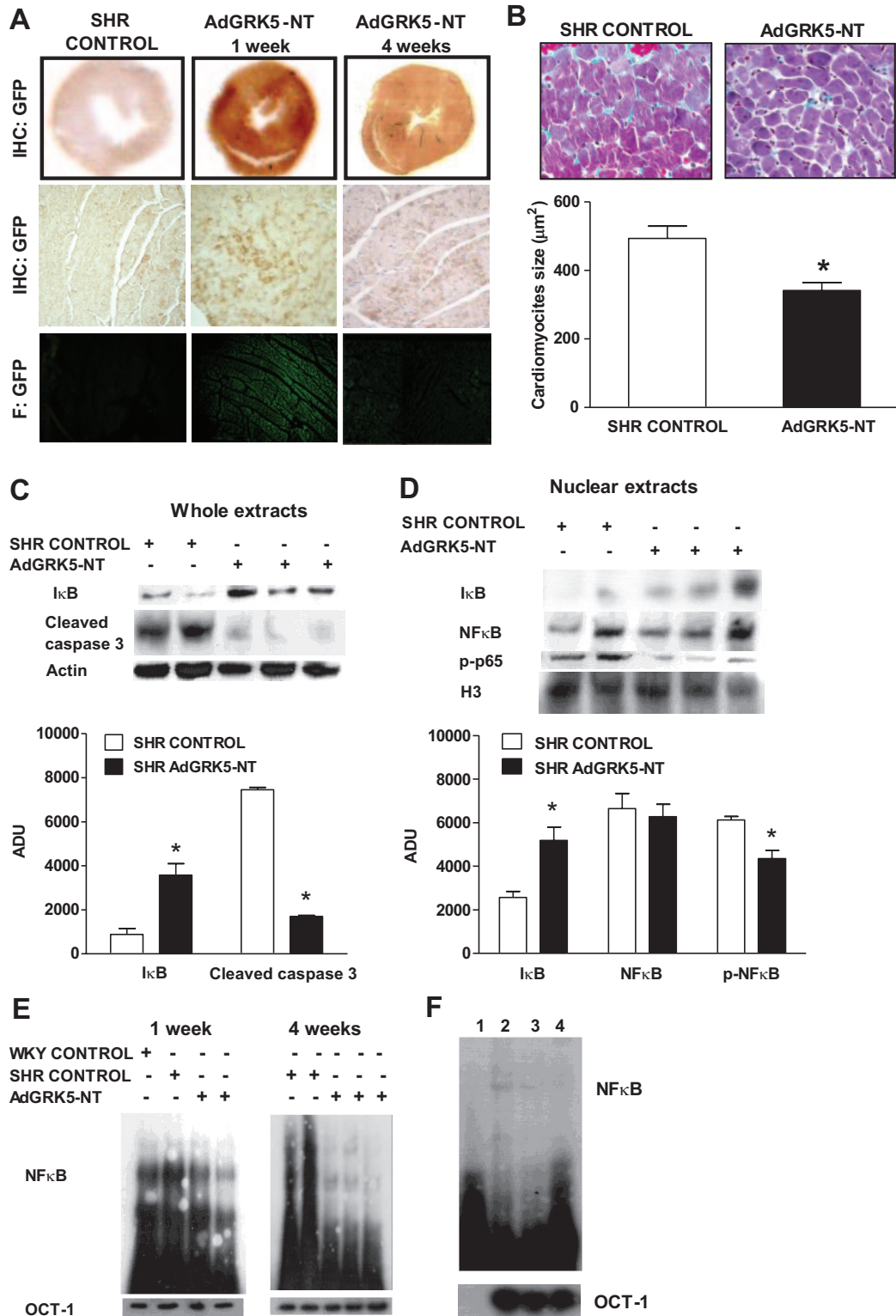


Figure 3. Evaluation of AdGRK5-NT treatment on NF-κB signaling. A, AdGRK5-NT expression in treated hearts was evaluated by GFP expression by both immunohistochemistry (IHC) and fluorescence (F) 1 week and 4 weeks from injection. In the top lane, IHC shows that GFP is homogeneously diffused in the whole heart at 1 week, and its expression is decreased but still present at 4 weeks from intracardiac injection. In the middle lane, panels show an upper magnification of IHC. In the bottom lane, panels show that also by fluorescence the distribution of the GFP localizes to the cardiac myocytes after 1 week and 4 weeks. Images are representative of 3 independent experiments. B, Paraffin-embedded sections of control and treated hearts were stained by trichrome staining to evaluate collagen fibers. AdGRK5-NT treatment reduces fibrosis compared with SHR control. Cardiomyocytes size was measured by means of ImageJ software, and means of areas are showed in the histogram (* $P < 0.05$ vs SHR control). Images are representative of 3 independent experiments. C, In LV whole extracts, IκBα and cleaved caspase 3 levels were evaluated by Western blot. Four weeks after injection, AdGRK5-NT treatment increases the levels of IκBα and reduces apoptosis with respect to controls (* $P < 0.05$ vs SHR control).

confirmed by invasive hemodynamics, which showed the hastening of both systolic and diastolic performance: indeed, both positive and negative dP/dt were ameliorated by AdGRK5-NT (Table). Biochemical analysis confirmed the reduction of LVH. We evaluated the expression of the hypertrophy marker gene ANF and the inflammation marker gene TNF- α by means of real-time PCR in rat hearts. After 1 week, ANF expression was significantly reduced in AdGRK5-NT-treated hearts, and after 4 weeks a further reduction was observed (Figure 2F). A similar pattern is shown for the TNF- α gene expression (Figure 2F).

Histological Analysis

At 1 or 4 weeks from injection, hearts were harvested, and AdGRK5-NT expression was assessed by histological analysis. GRK5-NT was homogeneously expressed in the heart at 1 week and, although decreased, was still expressed at 4 weeks from injection as assessed by both immunohistochemistry and fluorescence analysis (Figure 3A). LVH caused by chronic hypertension is accompanied by 2 key pathological processes, myocyte hypertrophy, because of increased cell size, and fibrosis. Thus, to confirm the inhibitory effect of GRK5-NT on LVH, we analyzed cardiomyocyte size and fibrosis by immunohistochemistry. Both myocyte size and collagen fiber staining were reduced in AdGRK5-NT versus SHR control hearts (Figure 3B).

NF- κ B Signaling

We have shown previously that GRK5-NT causes cellular and nuclear accumulation of the negative regulator of NF- κ B signaling, I κ B.¹¹ To verify the ability of AdGRK5-NT to induce the same phenomenon also in the hypertrophic SHR heart, we analyzed I κ B α levels both in whole and nuclear extracts by Western blot. AdGRK5-NT increased cellular (Figure 3C) and nuclear (Figure 3D) I κ B α levels with respect to the SHR control group. The regulation of apoptosis is an event under the control of NF- κ B activity. Although NF- κ B is commonly found to be cytoprotective, there are a number of instances, depending on stimuli and cell context, where it is proapoptotic. LVH is such an example.²³ Thus, we evaluated apoptosis in hypertrophic hearts by analyzing cleaved caspase 3 levels. In agreement with the inhibition of NF- κ B, we found that AdGRK5-NT reduced apoptosis in hypertrophic SHR hearts (Figure 3C). To demonstrate that I κ B accumulation results in the inhibition of NF- κ B, we assessed NF- κ B nuclear localization by Western blot. NF- κ B levels in the nucleus were increased both in SHR control and AdGRK5-NT hearts, but the activated form of NF- κ B (phosphorylated p65) was reduced only in the latter, suggesting that NF- κ B accumulates in the nucleus with I κ B α but cannot activate gene transcription. To confirm such a result, we

evaluated NF- κ B transcriptional activity by electrophoretic mobility-shift assay. NF- κ B activity was enhanced in hypertrophic SHR hearts with respect to nonhypertrophic WKY rats. AdGRK5-NT, on the contrary, reduces NF- κ B activity at 1 week from starting treatment, and prolonged treatments further decreased such activity (Figure 3E). To assess the specificity of NF- κ B binding, a competition assay was performed. The DNA binding of NF- κ B was reduced by 10-fold excess of unlabeled oligos, and it was completely inhibited by 20-fold excess (Figure 3F).

In Vivo Study in WKY Rats

We then verified whether AdGRK5-NT was able to prevent the development of LVH. To this aim, we chronically (14 days) injected PE in WKY rats infected previously with AdGRK5-NT (n=3) or AdLac-Z (n=3) in the left ventricle. As a control we used untreated WKY rats (n=4). Cardiac remodeling was evaluated by echocardiographic analysis once a week for 2 weeks. AdGRK5-NT significantly prevented the development of PE-induced LVH, because we found a smaller increase of IVS (Figure 4A), LVM/BW (Figure 4B), and HW/BW (Figure 4C). This finding is associated with a reduction of ANF gene expression, evaluated by real-time PCR (Figure 4D).

Discussion

In the present study we offer the compelling evidence that the RH domain within GRK5-NT inhibits LVH in 2 animal models of the disease. This effect is attributed to the sterical inhibition of NF- κ B activity in the cardiac myocyte through means of the stabilization of I κ B α . Indeed, GRK5-NT contains the kinase RH domain, which is sufficient for GRK5-NT effects¹² but lacks both the catalytic domain and the nuclear localization sequence of GRK5. Thus, this mutant cannot participate in the regulation of hypertrophy that depends on GRK5-mediated phosphorylative events.²⁴ Rather, we show NF- κ B inhibition induced by I κ B α accumulation in cardiac myocytes, a mechanism demonstrated previously in other cell types.^{11,12} In the in vivo study, we used a genetic model of LVH, the SHR, in which LVH is sustained by high BP levels. It has been described that the inhibition of NF- κ B reduces LVH in SHRs in a BP-independent manner.²⁵ Indeed, the antihypertensive drug hydralazine has no effect on cardiac mass or NF- κ B activity in hypertrophic SHRs.²⁵ On the contrary, the pharmacological inhibition of NF- κ B with pyrrolidine dithiocarbamate or the treatment with an angiotensin-converting enzyme inhibitor (captopril) significantly reduces heart size and inhibits NF- κ B activity.²⁵ Our present data are, therefore, in agreement with the literature, because we found that GRK5-NT is able to inhibit NF- κ B activity

Figure 3 (Continued). Graph summarizes normalized ADUs from 3 independent experiments. D, In nuclear extracts, 4 weeks after injection AdGRK5-NT causes accumulation of I κ B α . NF- κ B levels in the nucleus are increased both in controls and treated hearts, but the phosphorylated, active form of p65 is reduced in GRK5-NT-treated hearts (* P <0.05 vs SHR control). Histone 3 (H3) was used as loading control. Graph summarizes normalized ADUs from 3 independent experiments. E, NF- κ B activity was evaluated by electrophoretic mobility-shift assay in control and treated hearts. NF- κ B activity is enhanced in hypertrophic SHR hearts with respect to nonhypertrophic WKY rats; GRK5-NT treatment reduces such activity in a time-dependent manner. Organic cation transporter 1 was used as the loading control. Images are representative of 3 independent experiments. F, A competition assay was performed adding unlabeled oligos. A 10-fold excess of unlabeled oligos reduced and a 20-fold excess completely inhibited binding of NF- κ B. Lane (Ln) 1, empty; Ln 2, no unlabeled oligos; Ln 3, 10-fold excess of unlabeled oligos; Ln 4, 20-fold excess of unlabeled oligo. Images are representative of 3 independent experiments.

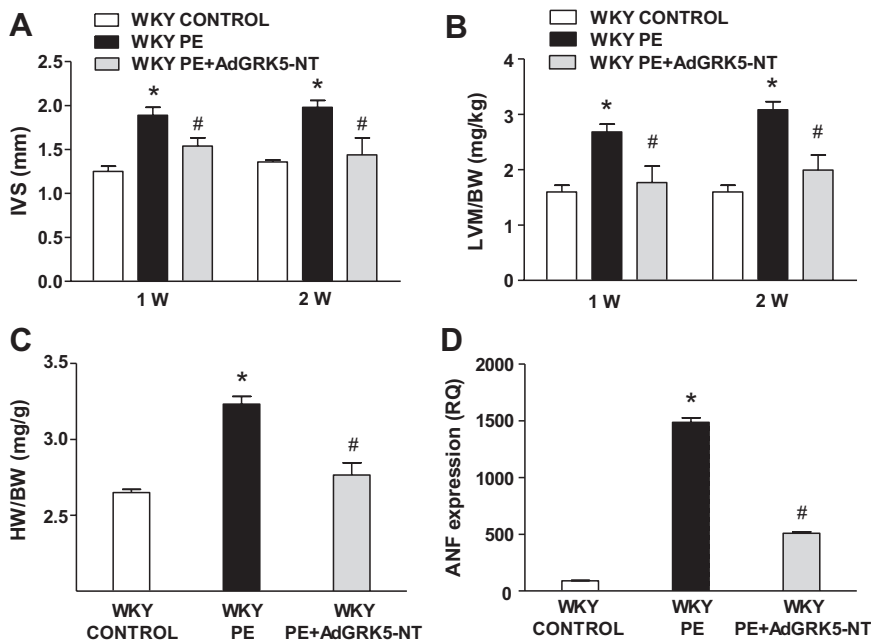


Figure 4. The effect of AdGRK5-NT treatment on PE-induced cardiac hypertrophy was evaluated in WKY rats. We studied a group of WKY PE+AdGRK5-NT-treated rats ($n=3$) and a group of WKY PE-treated rats ($n=6$), as indicated in the Methods section. As control we used untreated WKY ($n=4$). After 2 weeks, AdGRK5-NT treatment causes a reduction of IVS (A), LVM/BW ratio (B), and HW/BW ratio (C). Accordingly, we found a reduction of ANF gene expression evaluated by real-time PCR (D) (* $P<0.05$ vs WKY control; # $P<0.05$ vs WKY PE).

and, consequently, to reduce LVH without reducing BP levels. Indeed, GRK5-NT effect on LVH in SHR does not associate with a reduction but rather causes a slight increase of BP levels. Although we do not have a direct proof of it, we believe that the increased BP is the result of the ameliorated cardiac contractility, as shown by dP/dt maximum and LV ejection fraction, which occurs without modification of total peripheral resistance.^{26–28} Total peripheral resistances are increased by the hypertensive status and are a hallmark of SHRs, and our treatment, being localized in the heart, cannot affect them. Therefore, increased systolic function in the presence of unchanged total peripheral resistances, results in increased systolic BP. In turn, the ameliorated cardiac contractility can be the result of reduced cardiac fibrosis and hastened diastolic dysfunction typical of the SHR.^{19,28} As a consequence, GRK5-NT-induced inhibition of LVH does not depend on systemic hemodynamics but rather is an effect of myocyte biology and intracellular signal transduction. We also performed a confirmatory *in vivo* study in a different animal model, the WKY rats, in which LVH was induced pharmacologically by means of chronic PE administration. This model differs from the SHR because it is not genetically determined, and the phenotype is acutely induced by treatment. Also in this model, AdGRK5-NT is able to reduce the development of LVH by inhibiting NF- κ B activity. Thus, our data demonstrate that GRK5-NT exerts its effect on cardiac LVH independently from the animal model and that NF- κ B activation is an intrinsic determinant of the cardiac hypertrophic response. We also showed that GRK5-NT inhibition of LVH is attributed to the inhibition of apoptosis and fibrosis that characterize the hypertrophic phenotype. This could appear in contrast with our previous data, when we demonstrated that GRK5-NT-dependent inhibition of NF κ B causes an increase of apoptosis both in endothelial and tumor cells.^{11,12} In fact, NF- κ B has contradictory effects on apoptosis and cell survival that largely depend on cell type.²⁹ In

particular, NF- κ B is antiapoptotic in tumor cells³⁰ and proapoptotic in cardiac cells.²³ Therefore, the different reported effects of GRK5-NT on apoptosis can be ascribed to differences in cell types.²⁹

LVH is a complex event that depends on the activation of different signaling pathways.³¹ Several mechanisms are involved in this response, including cardiomyocyte stretching, as well as circulating neurohormones, such as catecholamines, endothelin 1, angiotensin II, insulin and growth factors, and cytokines released locally by the myocardial cells.^{32–34} These, in turn, activate second messengers that regulate nuclear transcription factors activity (NF- κ B, CREB, NFAT, and GATA-4) modifying the expression of hypertrophic genes.^{35,36} Our data support the relevance of NF- κ B to the hypertrophic phenotype. This further underlines the general application of GRK5-NT treatment versus a transduction signaling that is involved not only in LVH but also in other physiological and pathological conditions in different tissues. From our data, we cannot exclude the possibility that GRK5-NT could have multiple cellular targets and that its effect on LVH could also involve other signaling pathways.³⁷ We, therefore, tested the effects of GRK5-NT on CREB, a transcription factor activated by cAMP signaling that is involved in the development of LVH by enhancing the expression of pivotal genes for efficient oxidative capacity and resistance to apoptosis.³⁸ Because AdGRK5-NT does not change on CREB activation, we can rule out that the effect on NF- κ B is attributable to a nonspecific inhibition of nuclear transcriptional activity. Rather, AdGRK5-NT is selective in its inhibition of NF- κ B.

For the *in vivo* study, we used the intracardiac injection of the adenovirus AdGRK5-NT. We opted for adenovirus-mediated gene delivery to obtain GRK5-NT expression in the heart, because the adenovirus homogeneously diffuses throughout the treated tissue, also far from directly injected sites,³⁹ and is maintained for as long as 30 days.⁴⁰ One way

of directly obtaining cardiac delivery is the intracoronary way,¹³ but it causes high mortality and is not easily achievable in small animals, such as the rat. Otherwise, the systemic administration through the intravenous route does not guarantee a good expression of a protein in the heart, because, in large part, the adenovirus targets other organs and tissues. Moreover, systemic treatment could be toxic for animals. The advantage of the intracardiac injection directly into the wall is that this maneuver is less toxic for the whole body and leads to a selective localization of the adenovirus throughout the heart to obtain a specific overexpression of the encoded protein in the cardiac tissue.

In conclusion, our study demonstrates the ability of GRK5-NT to reduce myocardial NF- κ B activity and LVH. Moreover, our data suggest the efficiency of such a mechanism of regulation of LVH based on the inhibition of a specific transduction signaling that is independent from BP overload, the main stimulus for LVH.

Perspectives

Our data suggest NF- κ B as a target for LVH. This inhibition could be used in combination with BP-lowering strategies to better achieve the target of organ protection in hypertensive states. Furthermore, it is possible that, in other conditions with reduced cardiac performance, such as heart failure, it may be useful to increase cardiac contractility and reduce adverse remodeling. Further studies need to confirm this hypothesis.

Acknowledgments

We thank Walter J. Koch (Thomas Jefferson University) for providing the AdGRK5-NT.

Sources of Funding

This work was funded by grants from Ministero Istruzione, Università e Ricerca Scientifica (MIUR; 20074MSWYW_003), granted to G.I., and Agenzia Italiana del Farmaco (AIFA; FARM5STRH9), granted to B.T.

Disclosures

None.

References

- Akira S, Uematsu S, Takeuchi O. Pathogen recognition and innate immunity. *Cell*. 2006;124:783–801.
- Baldwin AS Jr. Series introduction: the transcription factor NF- κ B and human disease. *J Clin Invest*. 2001;107:3–6.
- Karin M, Cao Y, Greten FR, Li ZW. NF- κ B in cancer: from innocent bystander to major culprit. *Nat Rev Cancer*. 2002;2:301–310.
- Li Q, Verma IM. NF- κ B regulation in the immune system. *Nat Rev Immunol*. 2002;2:725–734.
- Cao S, Zhang X, Edwards JP, Mosser DM. NF- κ B1 (p50) homodimers differentially regulate pro- and anti-inflammatory cytokines in macrophages. *J Biol Chem*. 2006;281:26041–26050.
- Purcell NH, Tang G, Yu C, Mercurio F, DiDonato JA, Lin A. Activation of NF- κ B is required for hypertrophic growth of primary rat neonatal ventricular cardiomyocytes. *Proc Natl Acad Sci U S A*. 2001;98:6668–6673.
- Hirota S, Otsu K, Nishida K, Higuchi Y, Morita T, Nakayama H, Yamaguchi O, Mano T, Matsumura Y, Ueno H, Tada M, Hori M. Involvement of nuclear factor- κ B and apoptosis signal-regulating kinase 1 in g-protein-coupled receptor agonist-induced cardiomyocyte hypertrophy. *Circulation*. 2002;105:509–515.
- Li Y, Ha T, Gao X, Kelley J, Williams DL, Browder IW, Kao RL, Li C. NF- κ B activation is required for the development of cardiac hypertrophy in vivo. *Am J Physiol Heart Circ Physiol*. 2004;287:H1712–H1720.
- Kawano S, Kubota T, Monden Y, Kawamura N, Tsutsui H, Takeshita A, Sunagawa K. Blockade of NF- κ B ameliorates myocardial hypertrophy in response to chronic infusion of angiotensin II. *Cardiovasc Res*. 2005;67:689–698.
- Parameswaran N, Pao CS, Leonhard KS, Kang DS, Kratz M, Ley SC, Benovic JL. Arrestin-2 and G protein-coupled receptor kinase 5 interact with NF κ B1 p105 and negatively regulate lipopolysaccharide-stimulated ERK1/2 activation in macrophages. *J Biol Chem*. 2006;281:34159–34170.
- Sorriento D, Ciccarelli M, Santulli G, Campanile A, Altobelli GG, Cimini V, Galasso G, Astone D, Piscione F, Pastore L, Trimarco B, Iaccarino G. The G-protein-coupled receptor kinase 5 inhibits NF κ B transcriptional activity by inducing nuclear accumulation of I κ B α . *Proc Natl Acad Sci U S A*. 2008;105:17818–17823.
- Sorriento D, Campanile A, Santulli G, Leggiero E, Pastore L, Trimarco B, Iaccarino G. A new synthetic protein, Tat-rh, inhibits tumor growth through the regulation of NF κ B activity. *Mol Cancer*. 2009;8:97.
- Pleger ST, Remppis A, Heidt B, Volkers M, Chuprun JK, Kuhn M, Zhou RH, Gao E, Szabo G, Weichenhan D, Muller OJ, Eckhart AD, Katus HA, Koch WJ, Most P. S100a1 gene therapy preserves in vivo cardiac function after myocardial infarction. *Mol Ther*. 2005;12:1120–1129.
- Iaccarino G, Keys JR, Rapacciuolo A, Shotwell KF, Lefkowitz RJ, Rockman HA, Koch WJ. Regulation of myocardial β arct1 expression in catecholamine-induced cardiac hypertrophy in transgenic mice overexpressing α 1B-adrenergic receptors. *J Am Coll Cardiol*. 2001;38:534–540.
- Santulli G, Ciccarelli M, Palumbo G, Campanile A, Galasso G, Ziaco B, Altobelli GG, Cimini V, Piscione F, D'Andrea LD, Pedone C, Trimarco B, Iaccarino G. In vivo properties of the proangiogenic peptide QK. *J Transl Med*. 2009;7:41.
- Watson LE, Sheth M, Denyer RF, Dostal DE. Baseline echocardiographic values for adult male rats. *J Am Soc Echocardiogr*. 2004;17:161–167.
- Ciccarelli M, Santulli G, Campanile A, Galasso G, Cervero P, Altobelli GG, Cimini V, Pastore L, Piscione F, Trimarco B, Iaccarino G. Endothelial α 1-adrenoceptors regulate neo-angiogenesis. *Br J Pharmacol*. 2008;153:936–946.
- Oriente F, Iovino S, Cassese A, Romano C, Miele C, Troncone G, Balletta M, Perfetti A, Santulli G, Iaccarino G, Valentino R, Beguinot F, Formisano P. Overproduction of phosphoprotein enriched in diabetes (ped) induces mesangial expansion and upregulates protein kinase C- β activity and TGF- β 1 expression. *Diabetologia*. 2009;52:2642–2652.
- Ogata T, Miyachi T, Sakai S, Takashi M, Irukayama-Tomobe Y, Yamaguchi I. Myocardial fibrosis and diastolic dysfunction in deoxycorticosterone acetate-salt hypertensive rats is ameliorated by the peroxisome proliferator-activated receptor- α activator fenofibrate, partly by suppressing inflammatory responses associated with the nuclear factor- κ B pathway. *J Am Coll Cardiol*. 2004;43:1481–1488.
- Schellings MW, Baumann M, van Leeuwen RE, Duisters RF, Janssen SH, Schroe B, Peutz-Kootstra CJ, Heymans S, Pinto YM. Imatinib attenuates end-organ damage in hypertensive homozygous tgr(mren2)27 rats. *Hypertension*. 2006;47:467–474.
- Santulli G, Cipolletta E, Campanile A, Maione S, Trimarco V, Marino M, Trimarco B, Illario M, Iaccarino G. Deletion of the camk4 gene in mice determines a hypertensive phenotype. *Circulation*. 2009;120:S613–S613.
- Abramoff MD, Magelhaes PJ, Ram SJ. Image processing with ImageJ. *Biophotonics Int*. 2004;11:36–42.
- Wang S, Kotamraju S, Konorev E, Kalivendi S, Joseph J, Kalyanaraman B. Activation of nuclear factor- κ B during doxorubicin-induced apoptosis in endothelial cells and myocytes is pro-apoptotic: the role of hydrogen peroxide. *Biochem J*. 2002;367:729–740.
- Martini JS, Raake P, Vinge LE, DeGeorge BR Jr, Chuprun JK, Harris DM, Gao E, Eckhart AD, Pitcher JA, Koch WJ. Uncovering G protein-coupled receptor kinase-5 as a histone deacetylase kinase in the nucleus of cardiomyocytes. *Proc Natl Acad Sci U S A*. 2008;105:12457–12462.
- Gupta S, Young D, Sen S. Inhibition of NF- κ B induces regression of cardiac hypertrophy, independent of blood pressure control, in spontaneously hypertensive rats. *Am J Physiol Heart Circ Physiol*. 2005;289:H20–H29.
- Bing OH, Brooks WW, Robinson KG, Slawsky MT, Hayes JA, Litwin SE, Sen S, Conrad CH. The spontaneously hypertensive rat as a model of the transition from compensated left ventricular hypertrophy to failure. *J Mol Cell Cardiol*. 1995;27:383–396.
- Capasso JM, Palackal T, Olivetti G, Anversa P. Left ventricular failure induced by long-term hypertension in rats. *Circ Res*. 1990;66:1400–1412.

28. Ayobe MH, Tarazi RC. Reversal of changes in myocardial β -receptors and inotropic responsiveness with regression of cardiac hypertrophy in renal hypertensive rats (RHR). *Circ Res*. 1984;54:125–134.
29. Barkett M, Gilmore TD. Control of apoptosis by rel/NF- κ B transcription factors. *Oncogene*. 1999;18:6910–6924.
30. Pacifico F, Leonardi A. NF- κ B in solid tumors. *Biochem Pharmacol*. 2006;72:1142–1152.
31. Dorn GW II. The fuzzy logic of physiological cardiac hypertrophy. *Hypertension*. 2007;49:962–970.
32. Dash R, Schmidt AG, Pathak A, Gerst MJ, Biniakiewicz D, Kadambi VJ, Hoit BD, Abraham WT, Kranias EG. Differential regulation of p38 mitogen-activated protein kinase mediates gender-dependent catecholamine-induced hypertrophy. *Cardiovasc Res*. 2003;57:704–714.
33. Harada K, Komuro I, Shiojima I, Hayashi D, Kudoh S, Mizuno T, Kijima K, Matsubara H, Sugaya T, Murakami K, Yazaki Y. Pressure overload induces cardiac hypertrophy in angiotensin II type 1a receptor knockout mice. *Circulation*. 1998;97:1952–1959.
34. Aikawa R, Nagai T, Tanaka M, Zou Y, Ishihara T, Takano H, Hasegawa H, Akazawa H, Mizukami M, Nagai R, Komuro I. Reactive oxygen species in mechanical stress-induced cardiac hypertrophy. *Biochem Biophys Res Commun*. 2001;289:901–907.
35. De Windt LJ, Lim HW, Bueno OF, Liang Q, Delling U, Braz JC, Glascock BJ, Kimball TF, del Monte F, Hajjar RJ, Molkentin JD. Targeted inhibition of calcineurin attenuates cardiac hypertrophy in vivo. *Proc Natl Acad Sci U S A*. 2001;98:3322–3327.
36. Liang Q, Molkentin JD. Divergent signaling pathways converge on gata4 to regulate cardiac hypertrophic gene expression. *J Mol Cell Cardiol*. 2002;34:611–616.
37. Dorn GW II, Force T. Protein kinase cascades in the regulation of cardiac hypertrophy. *J Clin Invest*. 2005;115:527–537.
38. Sands WA, Palmer TM. Regulating gene transcription in response to cyclic amp elevation. *Cell Signal*. 2008;20:460–466.
39. Cowen RL, Williams JC, Emery S, Blakey D, Darling JL, Lowenstein PR, Castro MG. Adenovirus vector-mediated delivery of the prodrug-converting enzyme carboxypeptidase g2 in a secreted or gpi-anchored form: high-level expression of this active conditional cytotoxic enzyme at the plasma membrane. *Cancer Gene Ther*. 2002;9:897–907.
40. Leor J, Quinones MJ, Patterson M, Kedes L, Kloner RA. Adenovirus-mediated gene transfer into infarcted myocardium: feasibility, timing, and location of expression. *J Mol Cell Cardiol*. 1996;28:2057–2067.